GEOCHEMICAL AND PETROLOGIC SYSTEMATICS IN LAVAS FROM HALEAKALA VOLCANO, EAST MAUI: IMPLICATIONS FOR THE EVOLUTION OF HAWAIIAN MANTLE

by

Chu-Yung Chen

B.Sc. National Taiwan University
(1977)

Submitted to the Department of Earth
and Planetary Sciences in Partial Fulfillment
of the Requirements of the Degree of

DOCTORATE IN PHILOSOPHY

at the

MASSACHUSETTS INSTITUTE OF TECHNOLOGY

September 1982

© Massachusetts Institute of Technology 1982

Signature of Author . . . . . .
Department of Earth and Planetary Sciences

Certified by . . . . . .
F.A. Frey
Thesis Supervisor

Accepted by . . . . . .
T. Madden
Chairman, Department Committee

WITHDRAWN FROM MIT LIBRARIES

Archives
MASSACHUSETTS INSTITUTE OF TECHNOLOGY
MAR 1 1983
LIBRARIES

GEOCHEMICAL AND PETROLOGIC SYSTEMATICS IN LAVAS FROM HALEAKALA VOLCANO, EAST MAUI: IMPLICATIONS FOR THE EVOLUTION OF HAWAIIAN MANTLE

by

Chu-Yung Chen

Submitted to the Department of Earth and Planetary Sciences
on September 17, 1982 in partial fulfillment of the
requirements of the Degree of Doctor of Philosophy

ABSTRACT

Haleakala volcano on East Maui, Hawaii, consists of a tholeiitic basalt shield which grades into a younger alkalic series that was followed by a post-erosional alkalic series. Fresh, stratigraphically controlled samples from the three volcanic series were analyzed for major element abundances, Sr and Nd isotopic ratios and trace element (K, Rb, Sr, Ba, Th, Ta, Nb, REE, Hf, Zr, Sc, V, Cr, Co, Ni and Zn) abundances. These samples include tholeiites, transitional basalts, alkalic basalts, ankaramites, hawaiites and mugearites which range widely in abundances of major elements, trace elements and isotopic ratios. Most of the variations among tholeiites can be explained by olivine±clinopyroxene fractionation and different degrees of partial melting. Olivine composition and Ni abundance in one tholeiite which contains 16.6% MgO suggest that this tholeiite could be close to a primary melt in equilibrium with mantle olivine with composition of Fo_{90}. Isotopic ratios, incompatible trace element abundances, compatible element abundances and major element abundances indicate that hawaiites and mugearites can be derived from their stratigraphically associated alkalic basalts by fractionation of abundant clinopyroxene and plagioclase and minor amounts of olivine and magnetite. Olivine and clinopyroxene compositions suggest a cumulative origin for ankaramites.

Isotopic ratios and incompatible element abundance ratios (e.g., Ba/La, Nb/La, La/Ce, La/Sm) vary systematically with age. The youngest series (post-erosional alkalics) has the highest Rb/Sr, Ba/La, Nb/La, La/Ce and $^{143}Nd/^{144}Nd$ ratios but the lowest $^{87}Sr/^{86}Sr$ ratios whereas the oldest series (dominantly tholeiitic basalts) has the lowest Rb/Sr, Ba/La, Nb/La, La/Ce and $^{143}Nd/^{144}Nd$ ratios but the highest $^{87}Sr/^{86}Sr$ ratios. The post-erosional basalts have La/Ce and La/Sm ratios much higher than chondrites whereas these ratios in the tholeiites are similar to those in chondrites. All the Haleakala samples fall in the $^{143}Nd/^{144}Nd$-$^{87}Sr/^{86}Sr$ mantle array with ratios of the post-erosional basalts overlapping the MORB field and ratios in the tholeiites lying closer to estimated bulk earth ratios. The most striking feature of the trace element and isotopic data is the inverse correlations between isotopic ratios and parent/daughter abundance ratios in the Sr and Nd systems. These inverse correlation trends are opposite to the well-known "mantle isochron" established by

oceanic basalts. Decoupling of isotopic ratios with parent/daughter abundance ratios is common in Hawaiian basalts. For example, basalts from other Hawaiian volcanoes such as Loihi seamount, East Molokai volcano and Koolau volcano also show this phenomenon.

A mixing model is proposed to explain the contrasting isotopic and trace element characteristics in Hawaiian basalts. The mixing end-members are proposed to be primitive mantle plumes and incipient melts (IM) derived by small degrees (0.1%-1%) of melting of a MORB-source. Peridotites with compositions similar to a MORB source are presumed to be the wall-rocks for the ascending mantle plume which induces melting in its wall rocks. The mixing process may be IM mixed with mantle plumes to form the sources of Hawaiian basalts, or, mixing of IM with melts derived by large degrees (12%-16%) melting of mantle plumes. The contribution of the plume material to the basalts decreases as Hawaiian volcanoes evolve and the basalts become more enriched in incompatible trace elements but less radiogenic in $^{87}Sr/^{86}Sr$ ratios. Quantitative calculations show that this model accurately predicts the observed isotopic ratios and incompatible trace element abundances in representative samples from the three Haleakala volcanic series. An important implication of this model is that the inferred degrees of melting for the mixing components require that the lower lithosphere and much of the asthenosphere beneath Hawaiian volcanoes is involved in creating these volcanoes. Both the MORB reservoir and primitive mantle components required in the proposed mixing model may be abundant in the Earth's mantle, thus this model may be applicable for other oceanic and continental areas where alkalic basalts have lower $^{87}Sr/^{86}Sr$ and higher $^{143}Nd/^{144}Nd$ than geographically associated tholeiites.

Thesis Supervisor: F. A. Frey, Professor of Geochemistry

Acknowledgements

First of all, I would like to express my deep gratitude to my advisor, Fred Frey, for his continuous advice and support. His enthusiasm towards petrology and geochemistry has been a great source of inspiration throughout my graduate years at M.I.T. I would also like to thank him and Mike Garcia (University of Hawaii) for initiating my interest in studying the Haleakala volcano.

I benefited from numerous discussions with Stan Hart, Tim Grove, Mike Garcia, Nobu Shimizu, David Kohlstedt, and many of my graduate student colleagues. Their constructive comments on my thesis are appreciated.

G. Thompson (Woods Hole Oceanographic Institution) made the shatter box, XRF equipment and CHN analyzer in his laboratory available to me. So did M. Rhodes (University of Massachusetts) with his XRF equipment. In addition, this thesis would not have reached its present stage without the mass spectrometer in the laboratories of Stan Hart.

Special thanks to M.I.T. Campus police for their escort services during all those late night sample changes. Dorothy Frank patiently spent weekends and nights typing my thesis over many times. Cathy and Tom Sando and Peter Molnar provided shelter during the last three weeks of this thesis writing.

Last but not least, I would like to thank my family in Taiwan and my husband, Wang-Ping, for consistent support and encouragement throughout all the years.

Abstract 2

Acknowledgements 4

Introduction 10

Chapter 1: Major and compatible trace element geochemistry of the Haleakala volcanic series: the role of crystal fractionation 13

1. Introduction 14
2. Nomenclature 15
3. Sampling 17
4. Analytical Techniques 18
5. Results 19
6. Discussion
   6-1 Effects of late-stage alteration on major element and transition metal abundances 22
   6-2 Comparison of major element compositions of the three Haleakala volcanic series 23
   6-3 Evaluation of fractionation process 26
   6-4 Comparison of Haleakala basalts with other Hawaiian basalts, mid-ocean ridge basalts and chondrites 46
7. Summary of Conclusions 47

Tables 50

Figures 78

Chapter 2: $^{87}Sr/^{86}Sr$ and $^{143}Nd/^{144}Nd$ systematics of the Haleakala volcanic series 114

Abstract 115

1. Introduction 115
2. Analytical techniques 116
3. Results 117
4. Discussion
   4-1 Correlation of parent/daughter abundance ratios and isotopic ratios 119
   4-2 The mantle array 122
   4-3 Systematic $^{87}Sr/^{86}Sr$ and $^{143}Nd/^{144}Nd$ variations with time of eruption 124
   4-4 Comparison with other Hawaiian volcanoes 125
5. Summary and Conclusions 128

Tables 130

Figures 133

Chapter 3:	Trace element geochemistry of the Haleakala volcanic series	142
	1. Introduction	143
	2. Analytical techniques	144
	3. Results	145
	3-1 Trace element abundance variations	145
	3-2 Ratios of trace element abundances	150
	4. Discussion	
	4-1 Effects of alteration on trace element abundances	152
	4-2 Source heterogeneity of the Haleakala basalts	153
	4-3 Evaluation of partial melting and fractionation processes	158
	4-4 Systematic variations in trace element abundance ratios as a function of stratigraphy	165
	4-5 Comparison of Haleakala basalts with modern Hawaiian basalts, mid-ocean ridge basalts and chondrites	168
	5. Summary of conclusions	169
	Tables	172
	Figures	182
Chapter 4:	Origin of Hawaiian tholeiites and alkalic basalts - geochemical evidence for contaminated mantle plumes	244
	1. Introduction	245
	2. Alternative mantle models for the origin of Hawaiian tholeiites and alkalic basalts	248
	2-1 Metasomatic model	248
	2-2 Mixing model	259
	3. Discussion	269
	4. Conclusions	276
	Tables	277
	Figures	284
	References	309
Appendix 1		334
Appendix 2		338

Figures

1-1: Location of Maui in the Hawaiian island chain 81

1-2: Core logs of drill hole 65 and hole 85 82

1-3: $Na_2O + K_2O$ versus SiO_2 for Haleakala basalts 83

1-4: Variations of major oxides (a) SiO_2, (b) Al_2O_3, (c) FeO, (d) CaO, (e) Na_2O, (f) K_2O, (g) TiO_2, (h) P_2O_5 with MgO of Haleakala basalts 84

1-5: Variations of (a) Sc, (b) V, (c) Cr, (d) Co, (e) Ni, (f) Zn as a function of MgO contents in Haleakala samples 92

1-6: Variations of major oxide (a) SiO_2, (b) Al_2O_3, (c) FeO, (d) MgO, (e) CaO, (f) Na_2O, (g) KgO, (h) TiO_2 (i) P_2O_5 and (j) oxide abundance ratio K_2O/P_2O_5 in Haleakala samples as a function of depth 98

1-7: (a) plag-qtz-oliv (b) cpx-oliv-qtz ternary diagrams for Honomanu samples 108

1-8: Variation of CaO/MgO ratios as a function of MgO content in Haleakala basalt 110

1-9: Variation of Al_2O_3/CaO ratios as a function of MgO content in Haleakala basalt 111

1-10: plag-oliv-cpx ternary diagram for alkalic Kula samples 112

1-11: Correlation of P_2O_5 abundances with Ce abundances in Haleakala samples 113

2-1: $^{87}Sr/^{86}Sr$ versus Rb/Sr diagram for the Haleakala samples 136

2-2: $^{143}Nd/^{144}Nd$ versus Sm/Nd for the Haleakala samples 137

2-3: $^{143}Nd/^{144}Nd$ and $^{87}Sr/^{86}Sr$ correlation diagram 138

2-4: Correlation of $^{87}Sr/^{86}Sr$ ratios with stratigraphic sequences 139

2-5: Correlation of $^{143}Nd/^{144}Nd$ ratios with stratigraphic sequences 140

2-6: $^{87}Sr/^{86}Sr$ ratios plotted as a function of distance from Kilauea volcano 141

3-1:	Variations of trace element abundances (K, Rb, Ba, Th, Ta, Nb, Sr, Ce, Yb, La) in Haleakala volcanic series	186
3-2:	Chondrite-normalized REE abundances in Haleakala volcanic series	195
3-3:	Zr, Hf variations in Haleakala samples	202
3-4:	Variations of trace element abundance ratios with La abundances in Haleakala volcanic series	205
3-5:	Enriched factors of La/Ce, Ba/La and La by partial melting process	219
3-6:	Variation of Nd/Sm ratios with Mg-numbers in the Haleakala volcanic series	220
3-7:	Correlations of trace element abundance ratios (Ba/La, Rb/La, Nb/La and La/Ce) with $^{87}Sr/^{86}Sr$ ratios in the Haleakala volcanic series	221
3-8:	Variations of La/Ce, Ba/La, La/Sm, La/Eu, La/Yb with Mg-numbers in the Haleakala volcanic series	225
3-9:	Correlations of trace element abundance ratios in Haleakala volcanic series with stratigraphic sequences	230
4-1:	$^{87}Sr/^{86}Sr$ versus Rb/Sr for Haleakala samples	290
4-2:	$^{143}Nd/^{144}Nd$ versus Sm/Nd for Haleakala samples	291
4-3:	$^{143}Nd/^{144}Nd$ evolution diagram for the sources of Haleakala basalts (Case 2)	292
4-4:	(a) $^{143}Nd/^{144}Nd$, (b) $^{87}Sr/^{86}Sr$ evolution diagram for the sources of Haleakala basalts (Case 3)	293
4-5:	(a) Ba/La versus Ce/La, (b) Th/La versus Ce/La and (c) Nb/La versus Ce/La for samples from Haleakala	295
4-6:	La/Ce versus $^{87}Sr/^{86}Sr$ for samples from Haleakala	298
4-7:	$^{143}Nd/^{144}Nd$ versus $^{87}Sr/^{86}Sr$ for MORB, Haleakala basalts and bulk earth	299
4-8:	Mixing curves for various curvature coefficient r	300
4-9:	Trace element variation diagram for MORBs and the estimated MORBs source normalized to primitive mantle compositions	301

4-10: La/Ce versus $^{87}Sr/^{86}Sr$ ratios with mixing lines for Haleakala samples 302

4-11: Variation of $^{87}Sr/^{86}Sr$ ratios with depth 303

4-12: Variation of La/Ce ratios with depth 304

4-13: Trace element variation diagram for the calculated Haleakala sources normalized to primitive mantle compositions 305

4-14: Comparisons of calculated and measured trace element abundances and $^{143}Nd/^{144}Nd$ ratios in C122, H65-4 and H65-11 306

4-15: Comparison of the calculated and measured trace element distribution patterns for C122, H65-4 and H65-11 307

4-16: La/Ce versus $^{87}Sr/^{86}Sr$ for Hawaiian basalts 308

Introduction

Recent studies of Hawaiian basalts show that each Hawaiian volcano may have distinct geochemical characteristics which require distinct mantle source compositions (e.g., Leeman et al., 1977; Tatsumoto, 1978; Leeman et al., 1980; Lanphere et al., 1980). Since the linear Hawaiian seamount chain is a well-known example of migrating hot spot volcanism (e.g. Wilson, 1963a; Morgan, 1971; Clague and Jarrard, 1973; Molnar and Atwater, 1973; Crough et al., 1980), an understanding of the nature and extent of source heterogeneity may provide constraints on the relative importance of mantle sources (e.g., lithosphere, asthenosphere or lower mantle) and elucidate mantle processes related to hot spot volcanism.

Previous studies of Hawaiian volcanoes were focussed on the tholeiitic-shield building series. For example, tholeiites from Kilauea, Mauna Loa and Kohala volcanoes have been extensively studied (e.g., Wright, 1971; Leeman et al., 1977, 1980; Hofmann et al., 1978b, Feigenson et al., 1982). These studies led to a conclusion that tholeiites from a single volcano can be derived from a compositionally homogeneous mantle source. However, when lavas from different volcanoes are compared, e.g. recent Kilauea tholeiites vs. Mauna Loa tholeiites, different mantle source compositions are required (e.g. Leeman et al., 1977). Clague and Beeson (1980) and Feigenson et al., (1982) studied the transition between tholeiites and alkalic basalts from East Molokai and Kohala volcano, respectively. They concluded that, except for small variations in phlogopite content, tholeiites and alkalic basalts from single volcanos can be derived from a homogeneous mantle source.

However, the samples studied from Kilauea, Mauna Loa, East Molokai and Kohala encompass only a small time fraction of the eruptive history of Hawaiian volcanoes. When lavas from single volcanoes with considerable differences in eruption age are compared, for example tholeiites and post-erosional basalts from Koolau volcano on Oahu, compositionally distinct mantle sources are required (e.g., Lanphere and Dalrymple, 1980; Clague and Frey, 1982). Moreover, based on major element compositions, Easton and Garcia (1980) suggested that some prehistoric Kilauea tholeiites are distinct from recent Kilauea tholeiites. Trace element abundances (Chen and Frey, unpublished data) and Sr isotopic ratios (Easton, personal communication) also suggest that the mantle sources for some prehistoric and recent Kilauea tholeiites are distinct. Thus, the geochemical differences in lavas from different Hawaiian volcanoes may be due to lateral heterogeneity of the Hawaiian mantle and/or due to comparisons of different evolutional stages of each volcano.

Systematic studies of stratigraphically controlled samples from a mature Hawaiian volcano can provide constraints on the compositional evolution of Hawaiian mantle. None of the previous studies included stratigraphically controlled samples which encompass a major time fraction of the eruption history of a mature Hawaiian volcano. Obtaining samples encompassing a major time fraction of a Hawaiian volcano is difficult because older lavas are deeply buried and when exposed on seacliffs they are commonly highly altered. In order to develop ground-water resources on Maui many drill holes (up to 300 meters) were made on the northeastern slope of Haleakala, East Maui. These drill cores encompass a major time fraction of the alkalic series (Kula) and the post-erosional series (Hana) of Haleakala volcano. This thesis presents isotopic ratios ($^{87}Sr/^{86}Sr$ and

$^{143}Nd/^{144}Nd$) and major and trace element abundances (Sc, V, Cr, Co, Ni, Zn, Ba, Rb, Th, Ta, Nb, Sr, REE, Hf and Zr) in these fresh, stratigraphically controlled alkalic drill core samples and in tholeiitic samples collected from the northeast coast of Haleakala volcano.

The objectives of this thesis are: (1) to document variations in major and trace element abundances and isotopic ratios in Haleakala lavas as a function of age and to compare these variations with geochemical variations in lavas from other Hawaiian volcanoes, (2) to evaluate the role of crystal fractionation and partial melting in generating the Haleakala lavas, (3) to characterize the nature and evolution of the mantle sources of these Haleakala basalts, and (4) to propose and evaluate possible processes which create compositional heterogeneity in Hawaiian mantle. Four chapters are included in this thesis. Major element and transition metal (Sc, V, Cr, Co, Ni and Zn) abundances of the Haleakala samples are presented in Chapter 1. Since the abundances of major elements and transition metals are very sensitive to crystal fractionation, their abundances are used to evaluate the role of crystal fractionation in generating Haleakala lavas. Sr and Nd isotopic ratios of Haleakala lavas and Sr isotopic ratios of other Hawaiian lavas such as those from Loihi seamount and Kilauea, Kohala, East Molokai and Koolau volcanoes are discussed in Chapter 2. Trace element abundances and their abundance ratios in the Haleakala samples are presented in Chapter 3 and are used to evaluate source heterogeneity, partial melting, crystal fractionation and alteration processes. Based on these major element, isotopic and trace element abundances possible mantle processes which generated these Hawaiian basalts are proposed and evaluated in Chapter 4.

CHAPTER 1

MAJOR AND COMPATIBLE TRACE ELEMENT GEOCHEMISTRY OF THE HALEAKALA VOLCANIC SERIES: THE ROLE OF CRYSTAL FRACTIONATION

1. Introduction

The island of Maui located northwest of the island of Hawaii is the second largest island in the Hawaiian chain (Fig. 1-1). Haleakala volcano constitutes the eastern part of this island and consists of three volcanic series: the Honomanu volcanic series, the Kula volcanic series and the Hana volcanic series (Stearns and Macdonald, 1942). The Honomanu volcanic series is the main shield-building volcanic series, consisting primarily of tholeiites and picrites, but some transitional basalts and alkalic basalts are interbedded with tholeiites at the top of the series (Macdonald and Katsura, 1964). The Kula volcanic series overlies the Honomanu volcanic series and forms an alkalic capping series, consisting mainly of alkalic basalts, hawaiites and mugearites. Two samples, one from near the base and one from a considerably higher section of the Kula volcanic series were dated at 0.84 m.y. and 0.45 m.y. by the K-Ar method (McDougall, 1964), indicating that the Kula volcanic activity may have lasted 0.4 million years. The Hana volcanic series is the youngest volcanic series and is separated from the Kula volcanic series by profound erosional unconformities (Stearns and Macdonald, 1942). This post-erosional series consists mainly of alkalic basalts, ankaramites and hawaiites (e.g. Macdonald and Powers, 1968). The most recent eruption of the Hana volcanic series was around 1790 (Oostdam, 1965).

The purpose of this chapter is to document and interpret the major element abundances of samples from the three Haleakala volcanic series. Major element abundances of melts are easily changed by crystal fractionation, thus their abundances will be used to evaluate the role of crystal fractionation in generating Haleakala basalts. Because transition metals such as Sc, V, Cr, Co and Ni have mineral/liquid partition

coefficients exceeding unity for at least one phase such as olivine, pyroxene and garnet, their abundance in melts are sensitive to fractionation of mafic minerals (e.g. Gast, 1968; Frey et al., 1978). Based on the mineral/liquid partition coefficients (e.g. Frey et al., 1978), fractionation of olivine would decrease the abundances of Ni, Co and Cr but increase the abundances of Sc and V in the melt. On the other hand, fractionation of clinopyroxene would decrease the abundances of Ni, Co, Cr, and Sc in the melt. Thus, the abundances of these transition metals will be used to evaluate the fractionation models based on major element compositions.

2. Nomenclature

The nomenclature used in this study follows the chemical classification of Irvine and Baragar (1971) but also takes into account the mineralogy for samples plotting close to boundary lines which divide rock types. An alkali vs. silica diagram is used to distinguish tholeiitic rocks from alkalic rocks using the boundary line proposed by Macdonald and Katsura (1964). The tholeiitic rocks are subdivided to tholeiite and picrite according to modal content of olivine in the rocks. The division between tholeiites and picrites is set at 25% modal olivine (Macdonald and Katsura, 1964). The term "tholeiite" is used as a general term for tholeiitic samples with less than 25% modal olivine. The alkalic rocks are subdivided to ankaramite, alkalic basalt, hawaiite, mugearite and nephelinite according to the normative color index and normative plagioclase compositions (Irvine and Baragar, 1971). This nomenclature scheme is based on chemical compositions and the compositions of Hawaiian basalts were important data used in establishing the boundaries for various rock types (Irvine and Baragar, 1971). The tholeiitic samples generally

contain pigeonite as the groundmass pyroxene and normally do not contain olivine in the groundmass. On the other hand, the alkalic rocks contain olivine in the groundmass but no pigeonite in the groundmass. However, samples which plot close to the dividing line between tholeiitic rocks and alkalic rocks sometimes contain both olivine and pigeonite in the groundmass (Keil et al., 1972; Fodor et al., 1975, 1977). These samples are called "transitional basalts".

Macdonald (1949) proposed 5% normative nepheline as a division line between alkalic basalt and basanitoid if there is no modal nepheline in the rocks. However, the normative nepheline is very sensitive to Na_2O contents which are sensitive to late-stage alteration. Since there is no difference in mineralogical assemblage between alkalic basalt and basanitoid, this arbitrary 5% normative nepheline boundary will not be used. The term "alkalic basalt" will be used as a general term to include both alkalic basalt and basanitoid as defined by Macdonald (1949). The alkalic basalts from Kula and Hana volcanic series range in normative nepheline content from 0-7% and 5-10%, respectively. A Fortran IV program modified after Smith and Stupak (1978) has been written for the chemical classification of Irvine and Baragar (1971).

Most of the samples studied are from drill cores drilled by East Maui Irrigation Co. about forty years ago in the Nahiku area. The drilling record, geology of the Nahiku area and brief descriptions of the cores are found in Stearns and Macdonald (1942). They suggested that some lower sections of the cores are lavas of the Honomanu volcanic series. However, major element analyses show that all the samples from the drill cores are alkalic samples. Since there is no apparent erosional break between the dominantly tholeiitic Honomanu volcanic series and alkalic Kula volcanic

series (Macdonald and Katsura, 1964) and alkalic basalts are interbedded with tholeiites at the end of the Honomanu volcanic series, it is not possible to determine if the cores penetrated into the Honomanu volcanic series. In this study, alkalic basalt erupted at the end of the shield building stage will be classified within the dominantly tholeiitic Honomanu series only if it is interbedded with tholeiites and transitional basalts. Since there are no tholeiites or transitional basalts in the drill cores, the lower section of the drill cores will be classified as Kula volcanic series rather than Honomanu volcanic series. The boundary between the alkalic Kula volcanic series and post-erosional Hana volcanic series is adopted from Stearns and Macdonald (1942) which is marked by a soil formation (e.g., at a depth of about 65 meters in Hole 85) recorded in most of the drilled cores. However, it should be noted that local erosional breaks marked by soil, or soft, highly altered basalts occur within the Kula volcanic series in several drill cores. The extent and frequency of the erosional breaks increase upwards in the cores (Fig. 1-2).

3. Sampling

All studied samples of the alkalic Kula series and the post-erosional Hana series are from drill holes which lie on the northeastern slope of Haleakala volcano (Fig. 1). About a hundred samples were selected from five drill holes (Hole 62, 65, 83, 85 and 99) which contain long sections of cores (up to 300 meters in depth). Samples were selected in an attempt to include all rock types and to span the entire stratigraphic sequence in the cores. Based on major element analyses and sample freshness, a subset of about 30 drill-core samples, mostly less fractionated alkalic basalts and only a few fractionated hawaiites and mugearites were selected for isotopic and trace element analyses. Brief petrographic descriptions of

these samples are listed in Appendix 1. In this subset of samples, the Kula basalts are mainly from drill hole 85 and the Hana basalts are mainly from hole 65. Although it would be best to have Kula and Hana samples from the same cores, the "freshness" criteria required sampling from two cores. However, these two holes are only 500 meters apart (Stearns and MacDonald, 1942) and can be correlated very well using major element compositions, mineral assemblages and textures of the samples. The core logs of hole 65 and 85 are shown in Figure 1-2. A few samples from more distant holes (Hole 62 and Hole 83) are also included in the subset of samples to test if the geochemical variations shown by samples from Hole 65 and 85 are representative.

Samples of the Honomanu series were collected along the east coast (HO-1, HO-2) and west coast (HO-3, HO-4, HO-5) of the Honomanu Bay (Fig. 1-1) and selected from Macdonald's C-series collection (C121, C122, C123, C124, C125, C126) which were collected along the road above the bay.

4. Analytical Techniques

Each sample was crushed to small fragments using either a hydraulic rock splitter or a hammer. When a hammer was used, the sample was wrapped with clean cloth to avoid metal contamination and then cleaned in an ultrasonic bath with distilled water in order to remove superficial contamination. The rock fragments were then crushed to powder (about 100 to 200 grams) using an agate container in a shatter box and then shaken in an automatic shaker for at least half an hour to homogenize the rock powder.

Major element analyses of the tholeiites and drill-core samples (~100 samples) were analyzed at the Woods Hole Oceanographic Institute (WHOI) by X-ray fluorescence (XRF) using methods described by Schroeder *et al.*

(1980). A duplicate major element analysis was made for 38 samples using the XRF facility at the University of Massachusetts. Table 1 summarizs major element abundances for USGS standard rock BCR-1 and BHVO-1 analyzed in the two laboratories. The major element abundances for BHVO-1 reported by Flanagan et al. (1976) are also shown in Table 1 for comparison. Precision estimated from replicate analyses of BHVO-1 is better than 1% for SiO_2, Al_2O_3, Fe_2O_3 (or FeO), CaO, K_2O, and TiO_2, 2% for MgO and 5% for Na_2O and P_2O_5 for both laboratories. Na_2O abundances were also determined by instrumental neutron activation analyses (INAA) and K_2O abundances were determined by isotope dilution (I.D.) method (Hart and Brooks, 1976) at M.I.T. The precisions for Na_2O by INAA and K_2O by ID are estimated to be better than 2% and 0.2% from replicate analyses of a sample (H85-8).

The abundances of transition metals were determined by INAA at M.I.T. (Sc, Cr, Co) and by XRF at the Univ. of Massachusetts (V, Cr, Ni, Zn). In addition to synthetic standards, BCR-1 was included in each set of analyses by XRF and sample H85-8 was included in each set of analyses by INAA in order to evaluate analytical precisions. Accuracy and precision of the transition metal abundances can be evaluated from the analyses of standard rocks (BCR-1, BHVO-1) and H85-8 (Table 2).

The H_2O^+ and CO_2 contents of the samples were analyzed by a CHN analyzer (Peskin Elmer) at WHOI. Duplicate analyses of three samples are listed in Table 3.

5. Results

(a) Major element abundances

Major element compositions of samples analyzed at WHOI are in Appendix 2 and those analyzed at the Unversity of Massachusetts are in Table 4A.

Abundances of Na_2O determined by INAA, K_2O by I.D. and H_2O^+, and CO_2 by CNH elemental analyzer are also in Table 4A.

If the data obtained at U. Mass. are recalculated with Fe_2O_3 content to FeO and then normalized to 100%, the abundances of SiO_2, Al_2O_3, CaO, Na_2O, K_2O and TiO_2 determined at WHOI and the University of Massachusetts agree within experimental uncertainties except for one sample (C123) (Appendix 2, Table 4A). However, abundances of MgO and FeO are systematically different between the two laboratories; specifically, MgO values generally are higher and FeO values generally lower for analyses done at the University of Massachusetts. However, the relative deviations for MgO and FeO contents for all duplicate analyses except C123, are less than 5%. (Table 1, Table 4A, Appendix 2). The average renormalized FeO content for BHVO-1 determined at the University of Massachusetts and WHOI is 0.5 wt% and 1.0 wt%, respectively, higher than the average value reported by Flanagan et al. (1976) (Table 1). The average renormalized MgO content for BHVO-1 determined at the University of Massachusetts agrees (±1%) with the value reported by Flanagan et al. (1976). The MgO value for BHVO-1 determined at WHOI is slightly lower (5%) (Table 1). The agreement of P_2O_5 abundances for samples analyzed in the two laboratories is very poor; however P_2O_5 abundances of BCR-1 and BHVO-1 determined at the University of Massachusetts agree very well with the values reported in the literature (e.g. Flanagan et al., 1976; Sun et al., 1979; Feigenson et al., 1982).

Table 4B lists the renormalized (to 100%) major element compositions where SiO_2, Al_2O_3, FeO, MgO, CaO, TiO_2, P_2O_5, and MnO contents are from analyses by XRF at the University of Massachusetts, Na_2O contents are from analyses by INAA and K_2O contents are analyses by I.D. at MIT. This data

set is the preferred data set and will be used in the discussion. The Mg-numbers in Table 4A and CIPW norms list in Table 4B are calculated assuming a molar ratio of $Fe_2O_3/(Fe_2O_3 + FeO) = 0.10$. This is the ratio of least oxidized Hawaiian samples reported in the literature (Macdonald and Katsuro, 1964; Macdonald and Powers, 1968, Wright, 1971) and will be used in all the Mg-number calculations.

Haleakala samples vary widely in major element compositions (Table 4B) with SiO_2 contents varying from 43.9% to 52.9%, MgO contents vary from 2.8 % to 17.6%, K_2O contents vary from 0.14% to 2.29%, P_2O_5 contents vary from 0.16% to 0.99% and Mg-numbers from 35 to 73. These samples include tholeiites, transitional basalts and alkalic basalt from Honomanu volcanic series, alkalic basalts, hawaiites and mugearites from Kula volcanc series and alkalic basalts, ankaramites and hawaiite from Hana volcanic series (Table 4A and Fig. 1-3). Major element abundances of these Haleakala samples are plotted as a function of MgO contents in Figures 1-4 (a to h).

(b) Transition metal abundances (Sc, V, Cr, Co, Ni and Zn)

Abundances of transition metals in Haleakala basalts are in Table 5. The Cr abundances were determined by XRF and INAA (Table 5). The agreement is usually better than 20% for the samples with Cr abundances greater than 10 ppm. For some of the samples with Cr abundances less than 10 ppm, XRF analyses did not give reasonable results (negative values). The Cr values determined by INAA are used in the discussion. These Haleakala samples range widely in Sc (3.6-33.7 ppm), V (34-401 ppm), Cr (5-804 ppm) Co (9.9-76.9 ppm) and Ni (4-703 ppm) abundances, but abundances of Zn vary in a narrower range (93-138 ppm). Abundances of these transition metals are plotted as a function of MgO contents in Figures 1-5 (a to f).

6. Discussion

6-1 Effects of late-stage alteration on major element and transition metal abundances

Most of the drill core samples are very fresh in thin section except samples H85-13, H85-15, H85-21, H65-9 and H65-13. Alteration of these 5 alkalic samples is indicated by slightly altered glass (H85-13) or slightly to moderate iddingsitized rims on olivines (H85-15, H85-21, H65-9 and H65-13). H_2O contents of these slightly altered alkalic samples range from 0.44% to 0.85% compared to 0.17% to 0.63% of fresh samples. The best samples to evaluate alteration effects on major element and transition metal abundances are samples with varying degrees of alteration from the same lava flow or same batch of melts. H65-4 (fresh) and H85-21 (altered); H65-8, H65-10 (fresh) and H65-9 (altered); H65-14 (fresh) and H65-13 (altered) are three groups of samples with these features. Based on isotopic ratios (Chapter 2), highly incompatible element abundance ratios (Chapter 3) and stratigraphic positions (Fig. 1-2), each group of samples are probably from the same lava flow or the same batch of melts. In each case, the altered samples have lower Na_2O and K_2O but higher H_2O than their fresh counterpart (Table 4A). However, other major element abundances and transition metal abundances in altered samples are within the experimental uncertainty of the data for fresh samples (Table 4A and Table 5). Apparently only alkalis (Na_2O and K_2O) were lost during alteration of the alkalic samples.

The tholeiites (except C122) appear less fresh in thin section than alkalic samples. HO-1, HO-5 and C121 contain slightly altered glass and moderately iddingsitized rims on olivine. HO-3 and HO-4 contain very thin iddingsite rims on olivine. C122 is very fresh in thin section and

contains less H_2O than the other tholeiites except HO-4 (Table 4A). The alkali contents in these tholeiites do not correlate well with H_2O contents. However, the alkali abundances in the samples reflect the integrated effects of source composition, the melting process, fractionation processes and alteration processes. Judging from trace element abundance ratios (Chapter 3) and Mg-numbers (Table 4A) these tholeiites are likely to represent melts of at least two different degrees of melting and various degrees of crystal fractionation, thus alkalis abundances do not correlate well with H_2O contents as expected. The K_2O content in the fresh tholeiite (C122) and less altered tholeiite (HO-3) are among the high end of the tholeiites (Table 4A). Based on the alteration effects in alkalic samples discussed above, alkali abundances in the altered tholeiites were probably lowered by alteration. Alteration effects on element abundances will be further discussed in Chapter 3.

Previous studies of interaction between seawater and basalts at low temperatures (e.g., Moore, 1966; Hart, 1970; Hart and Nawalk, 1970; Thompson, 1973) indicated that submarine alteration increased H_2O and K_2O contents in basalts probably because the clay minerals formed in ocean floor basalts are a sink for alkalis. However, in Haleakala samples the alkalis apparently were leached from the basalts by groundwater and rainfall. A similar conclusion was reached for Kohala basalts by Feigenson et al. (1982). The only alteration products observed in Haleakala samples are slightly altered glass and/or iddingsite rims on olivine. Apparently, compositional changes during alteration of Hawaiian basalts differ from those caused by alteration of seafloor basalts.

6-2 Comparison of major element compositions of the three Haleakala volcanic series

Major element abundances of these Haleakala samples vary randomly with stratigraphic level (Fig. 1-6a to i). However, if hawaiites and mugearites are excluded, the younger basalts have lower SiO_2 contents than the older basalts (Fig. 1-6a), e.g., the tholeiites have higher SiO_2 contents but lower FeO, Na_2O, K_2O, TiO_2, P_2O_5 contents than the alkalic basalts (Fig. 1-4 and Fig. 1-6). The transitional basalts have SiO_2, Na_2O, K_2O and P_2O_5 contents similar to the tholeiites (Fig. 1-4). At the same MgO content, the alkalic basalt (C124) from the Honomanu volcanic series has higher SiO_2 content than alkalic basalts from Kula and Hana volcanic series (Fig. 1-4a). Also, alkalic basalts from the post-erosional Hana volcanic series generally have lower SiO_2 contents than those from the Kula volcanic series (Figs. 1-4a and 1-6a). However, these post-erosional basalts are not as SiO_2-undersaturated as post-erosional basalts from other Hawaiian islands such as those from the Honolulu volcanic series on the island of Oahu and the Koloa volcanic series on Kauai (e.g. Macdonald and Katsura, 1964; Macdonald and Powers, 1968; Jackson and Wright, 1970; Kay and Gast, 1973). Also, the post-erosional series in Haleakala volcano is separated from alkalic Kula series by a shorter erosional period than the post-erosional series mentioned above (Macdonald and Powers, 1968).

FeO contents of the alkalic basalts from the Kula and Hana volcanic series vary in a narrow range (13.5 to 14.1) except for three Kula alkalic basalts (H85-1, 14.6%, H85-14, 12.4%, and H85-15, 12.2%) (Figs. 1-4 and 1-6c) which will be discussed later. The alkalic basalt from the Honomanu volcanic series (C124) is slightly lower in FeO content (13.15%) than those from the alkalic Kula volcanic series and post-erosional Hana volcanic

series (Fig. 1-6c). The tholeiites have lower FeO content (12.3% to 13.0%) than the alkalic basalts (Fig. 1-4c and Fig. 1-6c). Higher FeO contents of Kula and Hana basalts relative to the Honomanu basalts requires that the Kula and Hana basalts were derived by smaller degrees of melting than Honomanu basalts and/or the source of the Kula and Hana basalts contained higher FeO content than the source of the Honomanu basalts (Langmuir and Hanson, 1980).

Figure 1-6j shows the variations of K_2O/P_2O_5 ratios vs. depth for the Haleakala samples. The K_2O/P_2O_5 ratios of samples from the Hana volcanic series and Kula volcanic series generally are higher than those from the Honomanu volcanic series. Tholeiitic samples from the Honomanu volcanic series have a wide range in K_2O/P_2O_5 ratios (0.54 to 1.63). Such variations of K_2O/P_2O_5 ratios could reflect source heterogeneity, different degrees of partial melting and alteration effects. However, isotopic ratios (Chapter 2) and abundance ratios of incompatible trace elements (e.g. La/Ce, Nb/ La, Chapter 3) suggest that these tholeiites could have been derived from the same mantle source; consequently, the wide variation of K_2O/P_2O_5 ratios in the tholeiites is likely due to alteration. Altered alkalic basalts (e.g. H85-21, H65-9, H65-13) clearly have lower K_2O/P_2O_5 ratios when compared to fresh samples from similar depths (Fig. 1-6j). When only fresh samples are considered, the K_2O/P_2O_5 ratios increase slightly up the stratigraphic sequences (Fig. 1-6j); that is, fresh tholeiite has K_2O/P_2O_5 ratio of 1.63; the oldest alkalic basalt of the Kula volcanic series (H85-1) has K_2O/P_2O_5 ratio of 1.75; other fresh alkalic basalts from the Kula volcanic series average K_2O/P_2O_5 ratio is 2.17 ± 0.13; and the alkalic basalts and ankaramite from the Hana volcanic series average K_2O/P_2O_5 ratio is 2.33 ± 0.06. This K_2O/P_2O_5 trend suggests that the

sources of the younger basalts are more enriched in K_2O relative to P_2O_5 than the sources of the older basalts and/or the degrees of partial melting decrease through time.

6-3 Evaluation of fractionation process

The most intensively studied Hawaiian volcano is Kilauea and there is abundant petrologic and geochemical evidence that crystal fractionation and magma mixing are important processes controlling the major element compositions of Kilauea lavas, especially those erupted along rift zones distant from the summit (e.g. Wright, 1971; Wright and Fiske, 1971). Beeson (1976) and Clague and Beeson (1980) who studied East Molokai volcano also concluded that the lavas have undergone shallow fractionation and possibly high-pressure fractionation. It is very likely that similar processes affected the Haleakala samples obtained from the northeastern flank of the volcano; consequently, it is important to evaluate these processes in Haleakala volcano.

(a) The Honomanu volcanic series

Samples from the Honomanu volcanic series include 7 tholeiites (HO-1, HO-3, HO-4, HO-5, C121, C122, C123), 2 transitional basalts (C125, C126) and 1 alkalic basalt (C-124) (Fig. 1-3). Based on the oxide-MgO variation diagrams (Fig. 1-4a to h), Pl-Qtz-Ol (Fig. 1-7a) and Cpx-Ol-Qtz (Fig. 1-7b) ternary diagrams, these samples are divided into three groups. The first group contains only C122 which is an olivine-rich (~20%) tholeiite. This tholeiite contains higher SiO_2 but lower Al_2O_3, Na_2O, TiO_2, P_2O_5 abundances than the rest of the tholeiites (Fig. 1-4). Ratios of incompatible trace element abundances suggest that this sample was derived by a higher degree of partial melting than the other tholeiites (Chapter 3). The second group includes the other six tholeiites (HO-1, HO-3, HO-4, HO-5, C121, C123) and

the two transitional basalts (C125, C126). The third group contains only the alkalic basalt (C124).

Olivine and very rare clinopyroxene are phenocryst phases in samples with MgO content greater than 9% (HO-3, HO-4, HO-5, C121, C122, C123). Plagioclase, rare olivine and rare clinopyroxene are the phenocryst phases for samples with MgO content less than 9% (HO-1, C124, C125, C126). Olivine in six tholeiites (HO-1, HO-4, HO-5, C121, C122, C123) were analyzed for major element compositions (Garcia, written communication). Olivine crystals with subgrain boundaries occur in three tholeiites (HO-4, HO-5 and C123). Subgrain boundaries in olivine are generally considered as a deformation or recrystallization feature in response to stress (e.g. Nicolas and Poirier, 1976; Goetze, 1978), thus these olivine crystals probably are not directly crystallized from the host magmas and are likely to be xenocrysts. These xenocrystic olivines are euhedral, very large in size (1-7 mm) and have normal zonation with compositions of $Fo_{89.1}$ in the cores and Fo_{80} (C123) to Fo_{78} (HO-5) on the edges. Similar forsterite content in the core ($Fo_{89.9}$) of olivine from C123 was reported by Fodor et al., 1977. CaO contents in these xenocrystic olivines range from 0.17% to 0.27% which is very similar to the CaO contents in the olivine phenocrysts (0.18% to 0.29%, Garcia, personal communication) and these CaO contents in olivines are consistent with the olivine compositions crystallized from basaltic liquids (e.g., Watson, 1979). CaO contents of olivine in gabbros and peridotites are generally lower than 0.1% (e.g., Simkin and Smith, 1970; Finnerty, 1977), therefore the xenocrystic olivines in the Haleakala tholeiites are not likely from disaggregated xenoliths. Instead, they probably formed as phenocrysts in older lavas. Their compositions indicate that the olivine in the mantle residue of the

Haleakala tholeiites must have composition $\geq Fo_{90}$. Olivine of similar forsterite composition (Fo_{85-92}) is very common in ultramafic nodules included within Hawaiian basalts and peridotites (e.g. Ross et al., 1954; White, 1966; Kuno, 1969).

C122: This sample has a MgO content of 16.61% and Mg-number of 73. A melt with this Mg-number can be in equilibrium with olivine composition of Fo_{90} if the FeO-MgO exchange reaction distribution coefficient, K_D, between olivine and melt is 0.30 which is within the range (0.28-0.36) reported in the literature (Roeder and Emslie, 1970; Arndt, 1977; Bickle et al., 1977; Irvine, 1977; Langmuir and Hanson, 1980). As discussed above, Fo_{89-90} olivine xenocrysts occur in several Haleakala tholeiites and Fo_{85-92} olivine is common in mantle xenoliths included within Hawaiian alkalic basalts. Consequently, the source for Hawaiian basalt may contain olivine with composition around Fo_{90} and sample C122 may have a composition similar to a primary melt.

The olivine composition in this sample C122 can be used to evaluate if this rock represents a near primary melt. Most of the olivine phenocrysts in this sample are small, ranging from 0.7 mm to 1.0 mm and are uniform in composition ($Fo_{83.7}$ to $Fo_{82.3}$) except near their rims which are Fe-rich (Fo_{78} to Fo_{74}). Xenocrystic olivine is absent in this sample. The nearly constant composition of the olivines (except the rims) indicate that olivine formed under near-equilibrium conditions. If closed system equilibrium crystallization is assumed, olivine phenocrysts of $Fo_{83.7}$ are in equilibrium with the residual melt formed after 22 wt% olivine ($Fo_{83.7}$) crystallized from a melt equal to C122 in composition assuming K_D equal to 0.30 (Table 6). Variations in assumed $Fe^{3+}/(Fe^{2+}+Fe^{3+})$ ratio(r) in the lava do not strongly affect this calculated result. For example, if r is

assumed to be 0.18 which is the ratio of the least oxidized Haleakala samples (Macdonald and Katsuro, 1964; Macdonald and Powers, 1968), the mg-number in C-122 would then be 75. Lavas with this Mg-number can be in equilibrium with Fo_{90} mantle olivine if K_D = 0.32 which is also within the range reported in the literature. With this K_D (0.32) and r(0.18), olivine phenocrysts ($Fo_{83.7}$) are in equilibrium with the residual melt formed after 22% of olivine crystallized from a melt with C122 composition. C122 contains about 20 volume % olivine phenocrysts which is close to the calculated amount of olivine fractionation. Thus, the FeO and MgO contents of the bulk rock, the FeO and MgO content of the olivine phenocrysts and the quantity of the olivine phenocrysts in C122 are consistent with the hypothesis that the bulk composition of C122 is close to a primary melt formed by melting a mantle containing olivine of Fo_{90}.

C122 contains 703 ppm Ni (Table 5) and olivine phenocrysts in this sample contain about 2400 ppm Ni (0.31 wt% NiO, Garcia, written communication). From mass balance calculations, the residual liquid remaining after 22% equilibrium crystallization of the olivine phenocrysts is calculated to contain 224 ppm Ni (Table 6). The partition coefficient of Ni between olivine ($Fo_{83.7}$, 2400 ppm Ni) and this residual liquid (MgO = 10.13%, 224 ppm Ni) is calculated to be 11 which is close to the partition coefficient (D=13) calculated from the equation D = (124/MgO -0.9) reported by Hart and Davis (1978). If the same equation (Hart and Davis, 1978) is used, a primitive melt with 16.61% MgO and 703 ppm Ni (C122) should have been in equilibrium with mantle olivine with Ni content of 4615 ppm which is close to the highest Ni content in xenocrystic olivines ($Fo_{89.1}$ and 0.60% NiO ≈ 4700 ppm Ni) included in other Haleakala tholeiites (Garcia, written communication). Thus, the Ni content of sample C122 is also

consistent with the hypothesis that C122 is close to a primary melt which equilibrated with mantle olivine of Fo_{90}.

Finally Al_2O_3/CaO ratio of C122 (1.3) is near the chondritic ratio (1.1) which suggests that the residual mantle contained mainly of olivine and orthopyroxene (Clague and Frey, 1982).

HO-1, HO-3, HO-4, HO-5, C121, C123, C125, C126: This group includes 6 tholeiites (HO-1 to C123) and 2 transitional basalts (C125, C126). The tholeiites have MgO content from 8.61 wt% (HO-1) to 17.63 wt% (C123b) and Mg-number from 57 to 73 (Table 4A, 4B). The FeO contents of these tholeiites are quite constant (12.31% to 12.97%) (Fig. 1-4c), but Al_2O_3 and CaO contents increase with decreasing MgO contents (Fig. 1-4b, 1-4d). Ratios of CaO/MgO systematically increase with decreasing MgO contents (Fig. 1-8). These trends suggest that olivine is the dominate phase which has been fractionated. On the Cpx-Ol-Qtz and Pl-Qtz-Ol projection diagrams (Fig. 1-7a,b) these tholeiites do not fall on 1 bar cotectic lines (Walker et al., 1979), instead they form linear trends which project to the olivine apex. These trends also suggest that olivine is the main phase which has been added to or subtracted from the melts. The two transitional basalts (C125, C126) fall along the same trends.

The Al_2O_3/CaO ratio is quite constant (1.3) exept for C123 (1.5) and HO-1 (1.6) (Fig. 1-9). The Al_2O_3/CaO ratios range from 0.13 to 0.16 for clinopyroxenes and from 1.86 to 2.35 for plagioclase from Haleakala tholeiites (Keil et al., 1972; Fodor et al., 1975). Thus, fractionation of clinopyroxene increases Al_2O_3/CaO ratios in the residual melts but fractionation of plagioclase decreases the Al_2O_3/CaO ratio of such melts. The higher Al_2O_3/CaO ratios in HO-1 and C123 suggests that clinopyroxene has been fractionated from these two samples.

Olivines in these tholeiites have a variety of textures and compositions (Garcia, written communication):

HO-1: Olivines in this sample are euhedral with a small range of forsterite contents in their cores ($Fo_{77.6}$ to $Fo_{78.3}$). Rims of the olivine grains are iddingsitized.

HO-4: Three types of olivine phenocyrsts occur: the first type are rounded grains with $Fo_{87.3}$ to $Fo_{87.4}$ in the cores and Fo_{83} to Fo_{79} at the rims; the second type range from euhedral to embayed grains with a narrow range of composition ($Fo_{82.3}$ to $Fo_{83.1}$) in the cores and Fo_{76} to Fo_{78} at the rims; the third type are rare large olivines with subgrain boundaries.

HO-5: Two types of olivine grains occur: the first type are large, euhedral olivines with subgrain boundaries and with Fo_{89} in the cores and Fo_{78} at the rims; the second type are small euhedral olivine phenocrysts with $Fo_{83.3}$ to Fo_{81} in the cores and Fo_{82} to Fo_{75} at the rims.

C121: Most of the olivine crystals are euhedral. The olivine crystals have uniform core compositions but iron content increases rapidly at rim. The core compositions vary from Fo_{81} for a large grain (0.6 mm) to Fo_{76} for a small grain (0.25 mm). One elongate olivine grain is zoned with a gradational change from Fo_{80} in the core to Fo_{73} at rim.

C123: Three types of olivines occur: the first types are large (0.7 mm to 5 mm) grains as in HO-5 with Fo_{89} in the cores and Fo_{80} at rims and with subgrain boundaries; the second type are large (~0.6 mm), zoned olivine phenocrysts ranging from Fo_{85} in the cores to Fo_{68} at the rims; the third type is small euhedral olivine with $Fo_{74.1}$ in the cores and Fo_{67} at the rims.

As discussed above, the large olivines with subgrain boundaries in samples C123, HO-4 and HO-5 are likely xenocrystic olivine of cumulate origin. Excluding such xenocrystic olivine, the general characteristics of olivine phenocrysts in these tholeiites are: (1) All olivine phenocrysts show small extents of normal zoning, with higher forsterite content from the cores to near the rims and lower forsterite content at the rims. (2) For samples with two types of olivine phenocrysts (HO-4, C121, C123), the larger olivine phenocrysts are more strongly zoned and their cores have higher forsterite content than the cores of smaller grains. (3) The rims of the larger crystals have forsterite contents similar to the cores or rims of the smaller crystals. These data are consistent with multi-stage crystallization; that is the crystallization process occurred in incremental steps rather than complete equilibrium crystallization or Rayleigh fractional crystallization.

The extents of fractionation for C121 and HO-1 which do not contain xenocrystic olivines can be estimated. C121 contains 9.56% MgO with a Mg number of 60 and Al_2O_3/CaO ratio of 1.3. As discussed before, olivine is the dominant phase which has been fractionated from this sample. Since the crystallization process could be intermediate between equilibrium crystallization and fractional crystallization, the amount of olivine fractionation was calculated for two cases: (1) fractional crystallization, (2) equilibrium crystallization.

For the case of fractional crystallization, the equations for calculation of primitive melts proposed by Irvine (1977) are used. This approach requires an estimate of the olivine composition in the mantle residue and the FeO-MgO exchange reaction distribution coefficient (K_D) between olivine and melt. The values (Fo_{90} and $K_D = 0.30$) used in the

discussion of C122 were used. The amount of olivine needed to fractionate from the primitive melt to derive C121 is calculated to be 20%. The calculated composition of primitive melt is listed in Table 7 as L_1. For the case of equilibrium fractionation, the composition of the fractionated olivine and the content of at least one oxide of the parental liquid have to be estimated. The composition of the fractionated olivine is taken to be the same as the core of the phenocryst olivine ($Fo_{81.1}$). The MgO content of the parental melt is assumed to be the same as C122 which may be close to a primary melt. Hanson and Langmuir (1978) and Langmuir and Hanson (1980) showed that for isothermal melting the MgO content of primary melts is not sensitive to the MgO content of the parent and the degree of partial melting as long as olivine remains in the residue. Therefore, the assumption that the parental melt for C121 had a similar MgO content as sample C122 is reasonable if the two tholeiitic melts were derived at similar temperature. Trace element abundances suggest that the degree of melting for these two samples may differ by only a factor of 1.3 (Chapter 3). Therefore, melting temperatures between these tholeiites could be similar. The parental melt composition calculated assuming equilibrium olivine fractionation is listed in Table 7 as L_2. To derive C121, 21% of olivine ($Fo_{81.1}$) must fractionate from L_2.

Since the actual fractionation process could be step-wise fractionation, the parental melt for C121 which equilibrated with mantle olivine of Fo_{90} should have a composition intermediate between L_1 and L_2. The calculated amounts of olivine needed to fractionate from the calculated parental melts to derive C121 are quite close (20% vs. 21%) for the two cases considered. Moreover, the MgO content (16.44%) of the primary liquid (L_1) calculated by assuming fractional crystallization is very close to

that in C122 (16.61%). However L_1 and L_2 have lower SiO_2 but higher Al_2O_3, CaO, TiO_2 and P_2O_5 contents than C122. Isotopic ratios and incompatible trace element abundances suggest that C121 and C122 could be derived from the same mantle source but that C121 was derived by a slightly lower degree of partial melting than C122 (Chapters 2 and 3). The higher abundances of TiO_2 and P_2O_5 in the parental melt for C121 are consistent with this parent being a melt derived by a smaller degree of partial melting than C122. The low K_2O content in the calculated parental liquid (L_1 or L_2) is due to low K_2O content in C121 which is most likely due to alteration. Lower SiO_2 but higher Al_2O_3 and CaO contents in a melt derived by smaller degree of melting require that clinopyroxene and garnet and/or olivine preferentially contribute to the melt, and/or that residual orthopyroxene increases as clinopyroxene melts incongruently. This is consistent with the reaction relationships of olivine and clinopyroxene with orthopyroxene, garnet and melt in the presence of CO_2 as proposed by Brey and Green (1977), Brey (1978), Eggler (1978) and Frey et al. (1978). The FeO content of parental melt of C121 should lie between L_1 and L_2 (Table 7) which is higher than that of C122. This is also consistent with C121 being derived by smaller degree of partial melting than C122 (Hanson and Langmuir, 1978; Langmuir and Hanson, 1980).

Sample HO-1 has a high Al_2O_3/CaO ratio (1.6) and low abundances of Ni, Co, Cr, Sc, V (Table 5 and Figs. 1-5a to e) indicating that both olivine and clinopyroxene were fractionated. The least-square regression program of Wright and Doherty (1970) was used to estimate the extent and proportion of olivine and clinopyroxene fractionation. Average composition of L_1 and L_2 (Table 7) was used as the parental liquid for HO-1. Olivine with composition of Fo_{81} and clinopyroxene with Mg-number of 81.6 were used in

the calculation (Table 7). Olivine and clinopyroxene compositions were chosen based on Fe-Mg exchange distribution coefficients (K_D) between olivine/melt, clinopyroxene/melt and olivine/clinopyroxene (e.g., Roeder and Emslie, 1970; Frey and Prinz, 1978; Grove and Bence, 1979) so that they are close to the olivine and clinopyroxene composition that can be in equilibrium with HO-1 (Mg-number = 57). The best-fit solution of the parental liquid is listed in Table 7 as L_3. About 20% olivine and 11% clinopyroxene are required to fractionate from this parental liquid to derive HO-1. In addition to olivine and clinopyroxene, abundant plagioclase phenocrysts occur in HO-1; therefore, the average plagioclase phenocryst composition (An72) in Haleakala tholeiites (Keil et al., 1972) was also included in the least-squares regression calculation. The calculated proportions of fractionated minerals are: 11.30% clinopyroxene + 20.73% olivine + 1.37% plagioclase with HO-1 representing 66.61% of the parental liquid which is very similar to the result calculated with only olivine and clinopyroxene as the fractionating phases.

Figures 1-5 (a to f) show that the Sc, V, and Zn abundances increase while Cr, Co and Ni abundances decrease rapidly with decreasing MgO contents. These transition metal abundances were used to test fractionation models for C121 and HO-1 based on major element compositions. Since abundances of transition metals (Sc, V, Cr, Co, Ni and Zn) in the liquids are not very sensitive to various degrees of partial melting (e.g. Gast, 1968), such abundances in the parental liquid for C121 and HO-1 were assumed to be the same as in C122 which may be close to a primary melt. The abundances of these transition metals in the differentiated melts are calculated using the partition coefficients listed in Table 9 and the mineral proportions estimated from the major element models. Table 10

shows that the calculated abundances of Sc, V, Cr, Co, Ni and Zn are in good agreement with the measured abundances in C121 and HO-1 and support the fractionation model based on major element compositions. These variations in transition metal abundance also indicate that olivine was the dominate fractionating phase.

Samples HO-4, HO-5, and C123 contain olivine xenocrysts; consequently degrees of fractionation required to generate their compositions are difficult to estimate. HO-4 and HO-5 have Al_2O_3/CaO ratios similar to C121 and C122, thus it is quite likely that olivine was the dominate fractionating phase. C123 has high Al_2O_3/CaO (1.5), a low Sc content (Table 5 and Fig. 1-5a) and the composition of small euhedral olivine phenocrysts in C123 is more iron-rich than in the other tholeiites. Apparently C123 is a more differentiated sample that has fractionated both olivine and clinopyroxene.

The high MgO content of C123 may be due to accumulation of xenocrystic olivines. Replicate major element analyses show poor agreement (1 analysis at WHOI, 4 analyses at University of Massachusetts, Table 8). The MgO content of these 5 analyses ranges from 15.67% to 17.63%. The differences between these analyses can be reduced to within the analytical errors if olivine is added or subtracted from the analyses. For example, about 6% of $Fo_{89.1}$ (composition of xenocrystic olivine) is required to change MgO content from 15.67% to 17.63%. Apparently the rock powder of this sample is not homogeneous although each sample was shaken in a mechanical shaker for more than 30 minutes. The average of the four analyses determined in University of Massachusetts is listed in Table 4 as C123b. The major element data for HO-4, HO-5 and C123 are consistent with extensive

crystallization and loss of olivine±clinopyroxene, yet these samples contain xenocrystic olivines. Apparently, the xenocrystic olivine was incorporated subsequent to the crystal fractionation, perhaps during a rapid ascent to the surface.

C124: This sample plots in the alkalic basalt field on a $Na_2O + K_2O$ vs. SiO_2 diagram (Fig. 1-3), contains olivine in the groundmass (Fodor et al., 1977) and the interstitial plagioclase ranges from oligoclase to anorthoclase and sanidine (Keil et al., 1972). These are characteristics of alkalic basalts. This sample does not lie in the same field as the tholeiites on the plag-qtz-ol and cpx-ol-qtz projection diagrams (Fig. 1-7a,b). Isotopic ratios and incompatible element ratios (Chapter 2 and 3) suggest that this sample can be derived from a similar source as the tholeiites but by smaller degree of melting than the tholeiites. Al_2O_3/Ca ratio in this sample is 1.4 which is slightly higher than C122 (1.3) suggesting that minor amounts of clinopyroxene may have fractionated from this sample.

(b) The Kula volcanic series

Samples from the Kula volcanic series include 12 alkalic basalts, 3 hawaiites and 3 mugearites (Appendix 2 and Table 4). On the basis of core stratigraphy the eruption sequence is alkalic basalts followed by hawaiites and mugearites (Fig. 1-2). There are at least four sequences of alkalic basalts - hawaiites (± mugearites) in a 300 meter core (Hole 85, Fig. 1-2). Thin soil or highly altered basalts often occur between alkalic basalts and hawaiites or mugearites and among alkalic basalts (Fig. 1-2). The thickness of the soil generally increases up the stratigraphic section (Fig. 1-2).

Samples from this volcanic series are generally less mafic than samples from the Honomanu volcanic series. For example, the MgO content of the Kula volcanic series range from 2.5% to 8.5% (Table 4), and the Mg-number ranges from 35 to 56. Samples H85-21 and H65-4 which have MgO contents of 8.5% and 8.3%, respectively, are the two most MgO-rich samples from the Kula volcanic series. Based on their stratigraphic positions, isotopic ratios, trace element abundances and major element abundances, these two samples are probably from the same lava flow although H85-21 is more altered than H65-4.

These two samples have Mg-number of 54 (Table 4A). Melts with this Mg-number would be in equilibrium with olivine with composition of Fo_{80} if $K_D = 0.30$ (e.g., Roeder and Emslie, 1970). Based on ultramafic inclusions in Hawaiian basalts, the Hawaiian mantle olivine compositions generally are estimated to be around Fo_{85} to Fo_{92} (e.g., Ross et al., 1954; White, 1966; Kuno, 1969), thus these two most-mafic Kula alkalic samples are probably not primary melts and have undergone crystal fractionation. Since element abundances in the melts will be changed by crystal fractionation, it is important to estimate the approximate degree of crystal fractionation. Both olivine and clinopyroxene phenocrysts occur in these two samples, however their low Al_2O_3/CaO ratio (1.3) and a high Sc content (31 ppm) suggest that clinopyroxene was not significantly fractionated from their parental liquid. Therefore, olivine is the most likely phase which has been fractionated. Hanson and Langmuir (1978) showed that for near isothermal partial melting, the MgO abundance in primary melts is not very sensitive to source compositions and degrees of partial melting. Thus, to a first approximation, the parental liquid of H65-4 is assumed to contain 16.6% (same as C122) MgO and equilibrium fractionation of olivine is assumed.

Under these assumptions 24.4% of olivine (Fo_{80}) is calculated to fractionate from parental liquid with such MgO content (16.61%) to derive H65-4 (Table 11). The olivine composition (Fo_{80}) used in this calculation is taken from an olivine phenocryst in alkalic basalt from the Hana series; this forsterite content would be in equilibrium with a melt having the bulk rock composition of H85-21 and H65-4 assuming K_D = 0.30. The abundances of transition metals (Sc, V, Co, Ni and Zn) in the parental liquid of H65-4 (Table 11) are calculated assuming equilibrium fractionation and using the partition coefficients listed in Table 9. The calculated Sc abundance in the parental liquid is 25.3 ppm which is very close to that in C122 (25.8 ppm). The Ni abundance in the parental liquid for these alkalic basalts is calculated to be 455 ppm which is lower than that in C122 (703 ppm). Perhaps, the parental liquid of H65-4 and H85-21 was derived by smaller degrees of partial melting than C122 and/or the amount of olivine fractionation from the parental liquid of H65-4 and H85-21 was slightly higher than the calculated amount (24.4%). If the latter case is true, 4% of olivine fractionation would decrease the Ni abundance in the liquid from 703 ppm to 455 ppm.

Isotopic ratios and highly incompatible element abundance ratios (Chapters 2 and 3) suggest that the less mafic alkalic basalts, hawaiites and mugearites can be derived from the same mantle source as their stratigraphically associated more mafic alkalic basalts. The alkalic basalts generally contain plagioclase, olivine and clinopyroxene phenocrysts. Some of the hawaiites contain plagioclase microphenocrysts but most of the hawaiites and mugearites are aphyric. In Figure 1-10, major element abundances (analyses determined at WHOI) of the Kula alkalic samples are projected from nepheline (ne) onto plagioclase (plag), olivine

(oliv) and clinopyroxene (cpx) plane to compare with the low pressure (1 bar) fractionation experimental data of Walker et al., 1979 project from silica onto the same plane. Although the Kula alkalic samples and the tholeiitic glass from Walker et al.'s (1979) experiments lie on the opposite side of a thermal divide, the Kula alkalic samples form a trend very close to the line defined by plagioclase + low-Ca-pyroxene + high-Ca-pyroxene saturated liquids. The excess alkali components in the alkali samples would increase the olivine primary phase field and decrease the orthopyroxene primary phase field (Presnall et al., 1978). Thus, the trend in the Kula alkalic series suggests that hawaiites and mugearites may be derived by low pressure fractionation of plagioclase, clinopyroxene and olivine from alkalic basalts.

In these less-mafic alkalic samples, Al_2O_3/CaO and CaO/MgO ratios increase while CaO, FeO, TiO2, Sc, V, Cr, Co, and Ni abundances decrease as MgO content decreases (Fig. 1-4, 1-5, 1-8, 1-9) which are consistent with plagioclase, clinopyroxene, olivine and magnetite fractionation from their parental liquids. A least square regression program by Wright and Doherty (1970) was used to estimate the extent of and proportion of olivine, clinopyroxene, plagioclase and magnetite fractionation from alkalic basalts to derive these less mafic alkalic samples. Three parent-daughter pairs (H65-4 vs. H85-22, H85-10 vs. H85-11 and H85-23 vs. H85-24) were selected for fractionation calculations. These samples were selected because there is no erosional break between the proposed daughter and parent (Fig. 1-2) and their isotopic ratios and incompatible trace element abundances (Chapter 2 and 3) indicate that the proposed parent-daughter samples could have been derived from same mantle source. The fractionation calculations are in Tables 12, 13 and 14. The olivine composition in the input data was

calculated from the bulk rock Mg-number and assuming FeO-MgO exchange reaction coefficient, K_D, between olivine and liquid is equal to 0.30. The clinopyroxene composition in the input data is the average clinopyroxene of Kula volcanic series taken from Fodor et al. (1975). The plagioclase phenocryst compositions of the Kula volcanic series range from An_{70} to An_{85} (Keil et al., 1972). This range (An_{70} to An_{85}) was used for the plagioclase input data. The magnetite composition was calculated assuming an ulvospinel content of 70 mole % and that the Al_2O_3 content is 3% (Fodor and Keil, 1972; 1980).

P_2O_5 abundances in the Haleakala samples correlate positively with abundances of highly incompatible trace elements such as Ce (Fig. 1-11) which suggests that apatite is not a fractionating phase, thus P_2O_5 behaves as an incompatible element during fractionation. The abundances of P_2O_5 in the daughter and parent were also used to estimate the extent of fractionation (Tables 12, 13 and 14) assuming equilibrium fractionation and the bulk distribution coefficient ($\overline{D}_{P_2O_5}$) is zero. The amount of residual liquid estimated by the two methods are very similar (Table 12, 13 and 14).

The least squares regression method shows that the major element composition of the hawaiite (H85-11) can be derived by fractionation of about 22% clinopyroxene, 15% plagioclase and minor magnetite from an alkalic basalt (H85-10) (Table 12). The major element composition of the mugearite (H85-24) can be derived by fractionation of about 23% plagioclase, 21% clinopyroxene, 10% magnetite and minor olivine from an alkalic basalt (H85-23) (Table 13) and the less-mafic alkalic basalt (H85-22) can be derived by fractionation of about 5% olivine, 10% clinopyroxene, 5% plagioclase and 2% magnetite from an alkalic basalt

(H65-4) (Table 14).

The abundances of transition metals (Sc, V, Co, Ni) in the residual liquids were calculated using the abundances in the parental liquids (H85-10 H85-23, and H65-4), the percentages of mineral fractionated determined from least-squares fitting of major element contents and assuming equilibrium fractionation using the partition coefficients in Table 9. The results (Table 15) agree very well with the measured abundances of Sc, V, Co and Ni in H85-11, H85-24 and H85-22. Thus both major element compositions and transition metal abundances are consistent with a hypothesis that hawaiite, mugearite and less-mafic alkalic basalt are residual melts by fractionation of olivine, clinopyroxene, plagioclase and magnetite, from more mafic alkalic basalts. Based on major and trace element abundances in lavas from East Molokai volcano, Clague and Beeson (1980) also concluded that hawaiites can be derived from alkalic basalts by fractionating olivine, clinopyroxene, plagioclase and titanomagnetite. Based on these calculations, the sequence of fractionating phases is: olivine followed by clinopyroxene, and plagioclase, and finally magnetite.

The three alkalic basalts with anomalous FeO contents (Fig. 1-4c) may also reflect fractionation effects. Sample H85-1 is a highly fractionated sample (Mg-number of 42) and the slightly higher FeO content (14.6%) is likely due to clinopyroxene and plagioclase fractionation. Samples H85-14 and H85-15 are the two alkalic basalts with low FeO content (12.4% and 12.2%). These are the only basalt samples containing magnetite phenocrysts; therefore, the low FeO content of these two samples may be due to magnetite fractionation. On V vs. MgO plot (Fig. 1-5b), these samples fall below the trends established by other alkalic basalts, thus V abundances are consistent with magnetite loss from these two alkalic

basalts (Leeman et al., 1978). Among the Kula basalts, sample H85-15 has the lowest TiO_2 and contents (Figs. 1-4h and 1-5b); therefore, this sample may have lost more magnetite than H85-14.

(c) The Hana volcanic series

Samples from the Hana volcanic series include 7 alkalic basalts (H62-47, H65-8, H65-9, H65-10, H62-48, H65-1, H62-49), 2 ankaramites (H65-13, H65-14) and 1 hawaiite (H62-52). The MgO content and Mg-number of the alkalic basalts and ankaramites vary in a small range (7.8% to 9.9%, and 52 to 59, respectively). The hawaiite has a lower MgO content (6.2%) and lower Mg-number (46) than the alkalic basalts and ankaramites. Among the alkalic basalts, H65-8, H65-9, H65-10 and H62-48 have very similar major element compositions (Table 4) and transition metal abundances (Table 5). The two ankaramites (H65-13, H65-14) also are very similar in major element compositions and transition metal abundances.

The ankaramites contain abundant ($\gtrsim$25%) (clinopyroxene + olivine) phenocrysts whereas the alkalic basalts contain about 5% to 6% olivine phenocrysts and about 1% to 2% clinopyroxene phenocrysts except H62-49 which contains about 20% (olivine + clinopyroxene), thus it is transition between alkalic basalt and ankaramite. Most of the clinopyroxene in H62-49 show subgrain boundaries, thus they are likely xenocrysts. The olivine and clinopyroxene crystals in H65-10, H65-11 (alkalic basalts) and H65-14 (ankaramite) were analyzed for major element compositions (Garcia, written communications). In H65-10, two types of olivine phenocrysts are found. The first type is moderate (0.3 mm) to large (0.6 mm), euhedral phenocrysts with Fo_{82} to Fo_{84} in the core and Fo_{78} to Fo_{72} at the rims. The second type is small to moderate size, euhedral olivine phenocrysts with Fo_{78} to Fo_{79} in the cores and Fo_{75} to Fo_{76} at the rims. Like the olivine

phenocrysts from the Honomanu volcanic series, the forsterite contents of the phenocrysts seem to correlate with grain size and the rim compositions of larger grains overlap with the compositions of the cores or rims of smaller grains. Also, the larger olivine phenocrysts show stronger zonation than the smaller olivine phenocrysts. Consequently, the compositions and textures of these olivine phenocrysts indicate that the larger phenocrysts crystallized earlier.

Olivine phenocrysts in H65-11 are similar to those in H65-10 but they have a narrower range of core composition. The forsterite contents of olivine phenocrysts in H65-11 vary from Fo_{79} to Fo_{83} in the cores and Fo_{70} to Fo_{80} at the rims. The clinopyroxene phenocrysts in H65-11 are not zoned, and the Mg-number of the clinopyroxene phenocrysts ranges from 73 to 75 which is lower than the Mg-number of the olivine cores but similar to the rims of olivine phenocrysts. Based on the FeO-MgO exchange distribution coefficients for olivine/melt and clinopyroxene melt (e.g. Roeder and Emslie, 1970, Grove and Bence, 1979), the clinopyroxene phenocrysts probably crystallized contemporaneous with growth of the olivine rims. This alkalic basalt (H65-11) has Al_2O_3/CaO ratio of 1.33 which is similar to that of the most primitive tholeiite C122. This Al_2O_3/CaO ratio and the composition of olivine and clinopyroxene phenocrysts in H65-11 suggest that clinopyroxene was not significantly fractionated from the parental liquid of H65-11. To a first approximation, the parental liquid of H65-11 is assumed to have 16.61% MgO as was assumed for Kula alkalic basalt, and if equilibrium fractionation of olivine is assumed, about 21% olivine (Fo_{83}) fractionation is required to derive H65-11 (Table 16). The calculated, parental liquid compositions of H65-11 and H65-4 are very similar in major element abundances (Table 16).

The abundances of transition metals in the parental liquid were calculated using the abundances in H65-11, assuming equilibrium fractionation and using the partition coefficients in Table 9 and the amount of olivine fractionation estimated from major element compositions (Table 16). The calculated abundances of Sc (23.6 ppm), V (261 ppm), Co (68 to 139 ppm) Ni (496 ppm) and Zn (108 ppm) in the parental liquid of H65-11 are very similar to the calculated abundances of parental liquid of the alkalic basalt from the Kula volcanic series (H65-4) except for Cr abundances and are within the range of compositions commonly estimated for primitive liquids (e.g. Frey et al., 1978; Allegre et al., 1977).

The olivine and clinopyroxene crystals in ankaramite (H65-14) are not strongly zoned but they require a complicated history. Two types of olivine crystals occur in H65-14. Small euhedral olivine (~0.2 mm) have nearly constant forsterite content in their cores (Fo_{78} to Fo_{79}) and lower forsterite content in their rims (Fo_{76}); whereas, the large euhedral olivines (0.8 mm to 1.3 mm) have uniform forsterite content in their cores (Fo_{76}) but show slight reverse zonation to Fo_{77} to Fo_{78} within 20-50 μ of their rims and then forsterite content decreases at the rims ($Fo_{76.7}$). Clinopyroxene in this sample also shows slight reverse zonation, the Mg-number of a large clinopyroxene varies from 73 in the core to 75 at the rim.

The slight reverse zonation of olivine and clinopyroxene may reflect mixing of two magmas. Based on the FeO-MgO exchange distribution coefficient, K_D, between olivine and melt, the difference between the reverse zoned olivine (Fo_{76} in the core, $Fo_{77.5}$ near the rim) can be reconciled if the core of the olivine was crystallized from a liquid which had undergone 1-2% more olivine fractionation than the liquid in which

the rim of the olivine crystallized. Therefore, the two magmas may have had very similar Mg/Fe^{2+} ratios. Alternatively, the reverse zonation could have resulted from crystal settling; that is the core of the large clinopyroxene and olivine crystallized in a slightly more differentiated liquid and settled in to a slightly less differentiated liquid. The rims of the large clinopyroxene and olivine and the small olivine phenocryst were crystallized from the less differentiated liquid. It is likely that much of the clinopyroxene and olivine in this ankaramite are cumulate in origin. Evidence for clinopyroxene accumulation is the relatively high Sc content (33 ppm, Table 5), the low Al_2O_3/CaO ratio (1.1, Figure 1-9), the higher Mg-number in the bulk rock but lower Mg-number in clinopyroxene and olivine than that of the Hana alkalic basalts and the reverse zonation of clinopyroxene and olivine.

The hawaiite (H62-52) contains rare olivine and rare clinopyroxene microphenocrysts. This Hana hawaiite contains 6.07% MgO which is slightly higher than the MgO content (≤5%) in the Kula hawaiites. However, in major oxide vs. MgO (Figs. 1-4a to h) and transition metal vs. MgO plots (Figs. 1-5a to f), the Hana hawaiite fall in the same trends as the Kula hawaiites and suggest that these hawaiites are possibly derived by a similar process.

6-4 Comparison of Haleakala basalts with other Hawaiian basalts, mid-ocean ridge basalts and chondrites

When compared to olivine-controlled tholeiites from 1959 Kilauea eruptions and historical Mauna Loa eruptions (Wright, 1971), C122 has SiO_2, CaO, K_2O, TiO_2, and P_2O_5 contents very similar to historical Mauna Loa lavas but the rest of the tholeiites have SiO_2, TiO_2 and P_2O_5 contents similar to the recent Kilauea lavas (Fig. 1-4a to h). All these Haleakala tholeiites have higher FeO content than the average recent Kilauea lavas and average historic Mauna Loa lavas (Fig. 1-4c). The renormalized FeO

content for BHVO-1 determined at the University of Massachusetts (11.22%) is about the same as the FeO content (11.26%) of recent Kilauea lavas reported by Wright (1971), so the difference in FeO content among these Hawaiian tholeiites is not due to interlaboratory analytical error. However, the FeO contents in Kilauea and Mauna Loa tholeiites have wider ranges than the other major oxides especially in the prehistoric Kilauea and Mauna Loa tholeiites (Fig. 1-4c, data from Wright, 1971 and Easton and Garcia, 1980). The upper range of FeO content in these prehistoric Kilauea and Mauna Loa tholeiites is similar to that in the Haleakala tholeiites. Wide abundance variations of FeO contents in Prehistoric Kilauea and Mauna Loa tholeiites may result from heterogeneous FeO contents in the mantle sources and/or variations in degrees of partial melting (Langmuir and Hanson, 1980).

The least fractionated Haleakala tholeiite (C122) and alkalic basalts (H65-4 and H65-11) have Al_2O_3/CaO, Al_2O_3/TiO_2 and CaO/TiO_2 ratios very similar to basalts from modern Hawaiian volcanoes such as Kilauea and Mauna Loa (Table 17). The Al_2O_3/CaO ratio of the Hawaiian basalts is very similar to that of mid-ocean ridge basalt (MORB) and chondrites (Table 17). However, Al_2O_3/TiO_2 and CaO/TiO_2 ratios of the Hawaiian basalts are much lower than those of MORB and chondrites (Table 17). Lower ratios of Al_2O_3/TiO_2 and CaO/TiO_2 in Hawaiian basalts require that the sources of the Hawaiian basalts are more enriched in TiO_2 content relative to Al_2O_3 and CaO contents than chondrites. K_2O/P_2O_5 ratio of a fresh Haleakala tholeiite (C122) is similar to the K_2O/P_2O_5 ratio of historic Mauna Loa tholeiites but slightly smaller than that of recent Kilauea tholeiites (Table 17). The K_2O/P_2O_5 ratios of the Haleakala alkalic basalts are higher than Haleakala, Mauna Loa and Kilaeua tholeiites. The K_2O/P_2O_5

ratios of all these Hawaiian tholeiites and alkalic basalts are much higher than that of chondrites and slightly higher than MORB (Table 17). Higher ratios of K_2O/P_2O_5 in Hawaiian basalts require enrichment of K_2O relative to P_2O_5 in the source of Hawaiian basalts.

7. Summary of Conclusions

(1) Based on field observations, the eruption sequence for Haleakala volcano is tholeiitic Honomanu series followed by alkalic Kula series and finally post-erosional, alkalic Hana series. On the basis of core stratigraphy, the eruption sequence for the alkalic Kula and Hana series is alkalic basalts or ankaramites followed by hawaiites and mugearites (Fig. 1-2). There are at least four sequences in the Kula and Hana series (Fig. 1-2).

(2) Major element abundance ratios such as Al_2O_3/CaO, Al_2O_3/TiO_2 and CaO/TiO_2 in the Haleakala tholeiites are similar to other Hawaiian tholeiites such as Kilauea and Mauna Loa tholeiites. However, the post-erosional Haleakala basalts are less undersaturated than post-erosional basalts from other Hawaiian volcanoes such as those from Honolulu volcanics on the island of Oahu and Koloa volcanics on Kauai.

(3) The Haleakala samples show wide range variations in major and compatible element contents.

(4) FeO, K_2O, TiO_2, P_2O_5 abundances and K_2O/P_2O_5 ratios increase but SiO_2 abundances decrease up the stratigraphic section for the fresh, least fractionated samples. These trends are not caused by fractionation and probably reflect changing source compositions and/or a decrease in degree of melting with time (e.g. Clague and Beeson, 1980; Feigenson et al., 1982).

(5) Late stage alteration has removed alkalis such as K and Na. However, the other major element and compatible element abundances are not obviously affected by alteration.

(6) Most major and compatible element variations within tholeiites can be explained by fractionation of olivine±clinopyroxene and by different degrees of partial melting.

(7) Xenocrystic olivines with Fo_{89-90} occur in some of the tholeiites. High CaO contents (0.17%-0.27%) in these xenocrystic olivines suggest a cumulate origin for such olivines. Therefore, the source of the Haleakala tholeiites must have olivine with forsterite content ≥90 mole %.

(8) A parental melt containing 16.6% MgO is proposed for the tholeiites which is similar to those proposed for Kilauea tholeiites (13%-22%) and Mauna Loa tholeiites (14%-21%) (Wright, 1981). Mg-number of the proposed parental melt is 73 which can be in equilibrium with mantle olivine composition of Fo_{90} if $K_D = 0.30$ (e.g. Roeder and Emslie, 1970).

(9) Major element and transition metal (Sc, V, Co and Ni) abundances in the less-mafic alkalic basalts, hawaiites and mugearites suggest that these low MgO samples can be derived from stratigraphically associated more-mafic alkalic basalts by fractionation of olivine, clinopyroxene, plagioclase and magnetite. For the alkalic basalts with Mg-number close to 55, olivine is the dominate fractionating phase.

(10) Clinopyroxenes and olivines in one ankaramite show slight reverse zoning suggesting that the clinopyroxenes and olivines were crystallized in more than one magma. Magma mixing or cumulate origin for ankaramites is suggested. However, olivine and clinopyroxene in tholeiites and alkalic basalts do not show such reverse zoning. Thus, there is no strong evidence for mixing in tholeiites and alkalic basalts.

Table 1 Major Element Compositions for Standard Rocks, BCR-1 and BHVO-1

	BCR-1[1]	BCR-1[2]	BHVO-1[3] (6)*	BHVO-1[1] (4)*	BHVO-1[2] (4)*	Relative Deviation[4] BCR-1	Relative Deviation[4] BHVO-1
SiO_2	55.37	54.2	49.90±0.17	49.98±0.14	49.57±0.49	-0.2%	+0.8%
Al_2O_3	13.83	13.55	13.89±0.10	13.89±0.06	13.66±0.14	-0.07%	0
Fe_2O_3	-	13.43	11.94±0.03	-	12.34±0.06	-	-
FeO	12.30	-	-	11.84±0.04	-	+0.2%	-4%
MgO	3.52	3.43	7.35±0.05	7.02±0.06	7.18±0.11	-0.6%	+4%
CaO	7.03	7.00	11.41±0.03	11.87±0.03	11.37±0.07	+1.4%	-2%
Na_2O	3.33	3.20	2.21±0.09	2.20±0.16	2.25±0.17	-2.1%	+3%
K_2O	1.73	1.70	0.55±0.01	0.52±0.01	0.53±0.01	0	+2%
TiO_2	2.24	2.23	2.66±0.03	2.89±0.01	2.77±0.01	1.3%	-2%
P_2O_5	0.37	0.37	0.28±0.01	0.15±0.01	0.27±0.01	2.7%	+78%
MnO	0.18	0.19	0.16±0.01	-	0.17±0.01	-	-

[1] Average values of replicate analyses at Woods Hole Oceanographic Institution

[2] Average values of replicate analyses at University of Massachusetts

[3] Flanagan et al. (1976)

[4] Relative deviations are calculated as: [(average value analyzed in U. Mass)/(average value analyzed in W.H.O.I.)]-1 after converting total iron as FeO and renormalizing the total to 100%.

* Values in parentheses are number of analyses. BCR-1 is used as a standard for analyses at WHOI. BCR-1 values determined at U. of Massachusetts are average of replicate analyses during calibration period.

Table 2 Transition Metal Abundances of Standard Rock BCR-1, BHVO-1 and H85-8

	BCR-1		BHVO-1		H85-8
	(1)	(3)	(1)	(4)	(1)**
Sc	33	33	33	31	26.7±0.7
Cr	13	17	295	315	136±5
Co	38	38	46	45	50.6±0.9
	(2)*	(3)	(2)	(4)	
V	368±6	399	289	296	
Cr	9±3	17	289	315	
Ni	10.4±0.4	16	119	114	
Zn	151±3	120	112	103	

(1) Determined by INAA method, this study

(2) Determined by XRF method, this study

(3) Flanagan (1973)

(4) Flanagan (1976)

* Average of 10 analyses, errors are 1σ.

** Average of 5 analyses, errors are 1σ.

Table 3 Duplicate Analyses of H_2O^+ and CO_2 Contents (wt%) in Haleakala Basalts

	H85-8	H65-4	H85-21
H_2O^+	0.27	0.21	0.89
	0.22	0.20	0.79
CO_2	0.33	0.20	0.27
	0.11	0.20	0.11

Table 4A: Major element abundances (wt%) of Haleakala volcanic series[1]

Rock[2]	HO-1	HO-3	HO-4	HO-5	C-121	C-122	C-123B	C-124	c-125	C-126
type	Th	Th	Th	Th	Th	Th	Th	AB	Tran	Tran
depth[3]	>300	>300	>300	>300	>300	>300	>300	>300	>300	>300
SiO_2	46.47	47.70	47.10	47.13	47.66	48.05	45.67	46.61	46.86	47.53
Al_2O_3	15.20	13.03	13.72	13.80	13.45	9.89	11.33	14.37	14.25	14.24
Fe_2O_3	14.21	13.80	13.49	13.83	13.54	13.44	13.69	14.27	14.88	13.75
MgO	8.49	10.44	9.68	9.96	9.41	16.31	17.22	5.62	6.72	8.44
CaO	9.70	10.15	10.42	9.93	10.53	7.77	7.67	10.27	10.57	9.81
Na_2O	2.34	2.02	2.45	2.28	2.30	1.53	1.77	3.44	2.10	2.49
K_2O	0.26	0.30	0.15	0.16	0.19	0.26	0.14	0.64	0.34	0.44
TiO_2	2.85	2.52	2.65	2.63	2.52	1.83	2.16	3.72	3.30	2.83
P_2O_5	0.30	0.24	0.26	0.27	0.25	0.16	0.23	0.42	0.32	0.31
MnO	0.19	0.19	0.18	0.19	0.19	0.17	0.17	0.18	0.19	0.17
total	100.00	100.39	100.09	100.18	100.03	99.41	100.12	99.47	99.53	100.01
H_2O	1.13	0.59	0.46	0.79	0.87	0.55	0.77	(0.96)	(2.03)	(0.60)
CO_2	0.37	0.41	0.40	0.40	0.17	0.20	0.23	-	-	-
Na_2O^4	2.33	2.02	2.35	2.22	2.10	1.67	1.95	2.99	-	2.64
K_2O^4	0.25	0.30	0.14	0.15	0.15	0.26	0.15	-	-	-
Mg[5]#	56.8	62.5	61.2	61.3	60.5	72.8	73.5	46.4	49.8	57.5

Table 4A: (continued)

	H85-1	H85-7	H85-8	H85-10	H85-11	H85-12	H85-13	H85-14	H85-15	H85-16
Rock type	AB	AB	AB	AB	ha	AB	AB	AB	AB	ha
depth	300	261	255	249	245	240	229	228	198	189
SiO_2	45.87	44.94	44.97	45.18	45.16	45.57	45.76	45.61	45.17	49.09
Al_2O_3	13.81	14.54	14.56	14.54	15.62	14.74	14.64	15.61	15.27	17.29
Fe_2O_3	15.94	15.00	14.68	14.85	15.04	14.96	15.26	13.58	13.31	12.56
MgO	5.19	5.90	5.92	6.28	4.95	5.18	4.67	6.44	7.56	4.34
CaO	9.51	11.07	11.35	11.17	8.60	10.09	10.09	10.73	11.02	7.31
Na_2O	3.41	3.20	2.74	2.48	3.70	3.29	3.12	2.77	2.38	4.33
K_2O	1.09	0.99	0.91	0.89	1.51	1.23	1.16	1.02	0.88	1.54
TiO_2	4.84	3.63	3.55	3.53	4.30	4.03	4.29	3.41	3.10	3.14
P_2O_5	0.56	0.45	0.42	0.43	0.71	0.56	0.55	0.44	0.38	0.68
MnO	0.20	0.20	0.20	0.20	0.21	0.22	0.22	0.20	0.18	0.23
total	100.43	99.92	99.28	99.55	99.79	99.85	99.75	99.82	99.24	100.53
H_2O	0.63	0.37	0.25	0.45	0.44	0.53	0.60	0.48	0.58	-
CO_2	0.55	0.71	0.22	0.39	0.53	0.46	0.60	0.64	0.67	-
Na_2O	3.03	2.87	2.91	2.78	3.68	3.30	3.13	2.99	2.67	4.21
K_2O	0.98	0.89	0.93	0.85	1.51	1.16	1.16	1.04	0.87	1.53
Mg#	41.7	46.4	47.0	48.2	42.0	43.2	40.2	51.1	55.6	43.2

Table 4A: (continued)

	H85-21	H65-4	H85-22	H85-23	H85-24	H85-25	H85-31	H85-33
Rock type	AB	AB	AB	AB	Mu	Mu	Mu	ha
depth	164	(164)	161	157	155	154	110	82
SiO_2	43.90	44.04	44.30	44.14	51.02	51.19	52.47	45.97
Al_2O_3	14.55	14.28	15.87	15.70	17.62	17.72	17.74	16.83
Fe_2O_3	15.45	15.38	15.23	15.24	10.52	10.59	10.25	13.42
MgO	8.40	8.23	5.65	5.78	2.76	2.88	2.49	4.68
CaO	11.35	11.04	10.61	10.64	6.55	6.66	5.83	8.62
Na_2O	1.90	2.74	3.46	3.41	5.46	5.31	6.10	4.27
K_2O	0.76	0.86	1.04	1.01	2.17	2.17	2.30	1.40
TiO_2	3.23	3.12	3.66	3.65	2.24	2.30	2.02	4.03
P_2O_5	0.41	0.39	0.46	0.45	0.94	0.98	0.84	0.62
MnO	0.22	0.20	0.22	0.23	0.26	0.24	0.28	0.24
total	100.16	100.28	100.49	100.26	99.54	100.06	100.31	100.09
H_2O	0.85	0.21	0.26	0.54	-	-	-	-
CO_2	0.20	0.20	0.30	0.87	-	-	-	-
Na_2O	1.97	2.94	3.37	3.38	5.34	5.05	5.96	4.21
K_2O	0.76	0.87	1.04	1.03	1.94	2.17	2.27	1.41
Mg#	54.5	54.1	44.9	45.5	36.6	37.4	34.8	43.4

Table 4A: (continued)

Rock type[2]	H62-47 AB	H65-8 AB	H65-9 AB	H65-10 AB	H62-48 AB	H65-11 AB	H62-49 AB	H62-52 ha	H65-13 ank	H65-14 ank
depth[3]	(70)	64	62	60	(60)	58	(50)	(25)	3	2
SiO_2	44.07	43.58	43.69	43.60	44.23	44.51	44.43	43.19	43.57	43.66
Al_2O_3	14.57	14.25	14.34	14.26	14.05	14.14	13.63	15.40	13.17	13.13
Fe_2O_3	15.17	15.37	15.34	15.38	15.26	15.43	15.25	15.54	14.89	14.84
MgO	7.61	8.34	8.34	8.35	8.28	8.89	9.41	6.07	9.67	9.75
CaO	10.26	10.57	10.79	10.60	10.51	10.61	11.18	10.26	12.23	12.12
Na_2O	3.40	3.02	2.88	3.20	3.13	2.88	2.69	3.69	1.99	2.50
K_2O	0.96	0.91	0.86	0.92	0.87	0.81	0.73	1.40	0.75	0.86
TiO_2	3.19	3.05	3.02	3.05	3.04	2.99	2.88	3.63	2.91	2.97
P_2O_5	0.41	0.39	0.39	0.39	0.35	0.35	0.31	0.56	0.37	0.37
MnO	0.18	0.19	0.18	0.19	0.18	0.20	0.19	0.23	0.21	0.21
total	99.80	99.65	99.83	99.94	99.92	100.80	100.71	99.96	99.76	100.40
H_2O	0.25	0.10	0.44	0.17	0.18	0.33	0.24	-	0.63	0.34
CO_2	0.42	0.22	0.22	0.17	0.21	0.18	0.26	-	0.47	0.40
Na_2O[4]	3.25	3.42	2.91	3.25	3.14	2.86	2.67	3.75	2.14	2.57
K_2O[4]	0.97	0.93	0.86	0.93	0.87	0.82	-	1.37	0.75	0.86
Mg#[5]	52.5	54.4	54.5	54.4	54.4	55.9	57.6	46.2	58.8	59.4

[1] Major element abundances determined at U. of Massachusetts by XRF method. H_2O and CO_2 abundances determined at W.H.O.I using CHN analyzer except those in the parentheses which were taken from MacDonald and Katsura (1964).

[2] Th = Tholeiites. Picr = Picrites. Tran = Transitional basalt. AB = Alkalic basalt. ha = hawaiite, Mu = mugearite. Ank = ankaramite.

[3] "depths" list in this table are meters below the ground surface of drill Hole 85. Depths in the parentheses are adjusted depths according to drill core correlations which are based on mineralogy, textures and major element compositions of the samples. The depths of Honomanu basalts are estimated to be greater than those at the bottom of the drill cores according to field observations.

[4] Na_2O determined by INAA, K_2O determined by I.D. at M.I.T.

[5] $Mg\# = 100(Mg/Mg + Fe^{2})$ assuming $Fe^{3+}/ (Fe^{3+} + Fe^{2+}) = 0.10$.

Table 4B: Normalized[1] Major Element Compositions and C.I.P.W. Norms[2] of Haleakala Volcanic Series

Rock type*	Th	Th	Th	Th	Th	Th	Th	AB	tran	tran
Depth(m)*	>300	>300	>300	>300	>300	>300	>300	>300	>300	>300
	ho-1	ho-3	ho-4	ho-5	c121	c122	c123b	c124	c125	c126
sio2	47.15	48.18	47.75	47.74	48.41	48.93	46.19	47.73	47.80	48.12
al2o3	15.42	13.16	13.91	13.98	13.66	10.07	11.46	14.71	14.54	14.42
feo	12.97	12.54	12.31	12.61	12.38	12.31	12.46	13.15	13.66	12.53
mgo	8.61	10.54	9.81	10.09	9.56	16.61	17.42	5.75	6.86	8.54
cao	9.84	10.25	10.56	10.06	10.70	7.91	7.76	10.52	10.78	9.93
na2o	2.36	2.04	2.38	2.25	2.13	1.70	1.97	3.06	2.14	2.67
k2o	0.25	0.30	0.14	0.15	0.15	0.26	0.15	0.66	0.35	0.45
tio2	2.89	2.55	2.69	2.66	2.56	1.86	2.18	3.81	3.37	2.86
p2o5	0.30	0.24	0.26	0.27	0.25	0.16	0.23	0.43	0.32	0.31
mno	0.19	0.19	0.18	0.19	0.19	0.17	0.17	0.18	0.19	0.17
c.i.p.w.norms										
or	1.50	1.79	0.84	0.90	0.90	1.56	0.90	3.87	2.05	2.63
ab	19.97	17.24	20.13	19.00	18.02	14.37	16.67	25.87	18.10	22.58
an	30.67	25.82	26.80	27.56	27.22	19.04	21.94	24.44	28.98	25.99
diwo	6.72	9.76	9.94	8.55	10.07	7.97	6.25	10.38	9.34	8.84
dien	3.75	5.83	5.88	5.05	5.87	5.31	4.23	5.10	4.74	4.99
difs	2.71	3.42	3.56	3.08	3.73	2.08	1.55	5.08	4.38	3.48
hyen	8.59	11.61	7.65	10.28	11.84	19.38	8.35	2.36	10.80	6.57
hyfs	6.21	6.81	4.64	6.27	7.52	7.58	3.06	2.35	10.00	4.59
fo	6.37	6.15	7.62	6.84	4.25	11.64	21.54	4.80	1.06	6.79
fa	5.07	3.98	5.09	4.59	2.98	5.02	8.69	5.26	1.08	5.23
mt	2.07	2.00	1.96	2.01	1.97	1.96	1.98	2.09	2.18	1.99
il	5.48	4.83	5.10	5.05	4.86	3.53	4.14	7.22	6.38	5.43
ap	0.70	0.56	0.61	0.63	0.59	0.38	0.54	0.99	0.73	0.73

Table 4B(continue)

Rock type	AB	AB	AB	AB	ha	AB	AB	AB	AB	ha
Depth	300	261	255	249	245	240	229	228	198	189
	h85-1	h85-7	h85-8	h85-10	h85-11	h85-12	h85-13	h85-14	h85-15	h85-16
sio2	46.65	45.86	46.24	45.95	45.96	46.23	46.58	46.22	46.00	49.58
al2o3	14.04	14.84	14.97	14.79	15.90	14.95	14.90	15.82	15.55	17.43
feo	14.59	13.77	13.58	13.59	13.77	13.66	13.98	12.38	12.20	11.39
mgo	5.28	6.02	6.09	6.39	5.04	5.25	4.75	6.53	7.70	4.37
cao	9.67	11.30	11.67	11.36	8.75	10.24	10.27	10.87	11.22	7.37
na2o	3.08	2.93	2.22	2.83	3.74	3.35	3.19	3.03	2.72	4.24
k2o	1.00	0.91	0.96	0.86	1.54	1.18	1.18	1.05	0.89	1.54
tio2	4.92	3.70	3.65	3.59	4.38	4.36	4.37	3.46	3.16	3.16
p2o5	0.57	0.46	0.43	0.44	0.72	0.57	0.56	0.45	0.39	0.69
mno	0.20	0.20	0.20	0.20	0.21	0.22	0.22	0.20	0.18	0.23
c.i.p.w.norms										
or	5.88	5.36	5.64	5.10	9.07	6.94	6.97	6.22	5.23	9.10
ab	26.03	19.32	18.76	19.33	23.73	22.75	24.44	19.51	17.98	35.63
an	21.51	24.62	28.01	25.07	21.99	22.26	22.84	26.41	27.57	23.92
ne	0.00	2.94	0.00	2.47	4.28	2.99	1.34	3.30	2.71	0.12
diwo	9.47	11.83	11.26	11.84	6.95	10.33	10.18	10.25	10.65	3.39
dien	4.42	5.74	5.52	5.90	3.22	4.90	4.53	5.40	5.94	1.56
difs	4.94	5.90	5.54	5.69	3.67	5.29	5.61	4.54	4.29	1.80
hyen	1.76	0.00	1.50	0.00	0.00	0.00	0.00	0.00	0.00	0.00
hyfs	1.96	0.00	1.51	0.00	0.00	0.00	0.00	0.00	0.00	0.00
fo	4.87	6.47	5.69	6.99	6.52	5.73	5.11	7.59	9.26	6.53
fa	5.99	7.33	6.29	7.42	8.20	6.82	6.96	7.03	7.37	8.32
mt	2.32	2.19	2.16	2.16	2.19	2.17	2.23	1.97	1.94	1.81
il	9.33	7.03	6.92	6.81	8.30	8.27	8.28	6.55	5.99	6.00
ap	1.32	1.06	1.00	1.01	1.67	1.31	1.30	1.03	0.90	1.59

Table 4B(continue)

Rock type	AB	AB	AB	AB	Mu	Mu	Mu	ha
Depth	164	(164)	161	157	155	154	110	82
	h85-21	h65-4	h85-22	h85-23	h85-24	h85-25	h85-31	h85-33
sio2	44.48	44.51	44.80	44.72	51.99	51.86	52.94	46.58
al2o3	14.74	14.43	16.05	15.91	17.96	17.95	17.90	17.05
feo	14.09	13.99	13.86	13.89	9.65	9.65	9.30	12.24
mgo	8.51	8.32	5.71	5.86	2.81	2.92	2.51	4.74
cao	11.50	11.16	10.73	10.78	6.67	6.75	5.88	8.74
na2o	2.00	2.97	3.41	3.42	5.44	5.12	6.01	4.27
k2o	0.77	0.88	1.05	1.04	1.98	2.20	2.29	1.43
tio2	3.27	3.15	3.70	3.70	2.28	2.33	2.04	4.08
p2o5	0.42	0.39	0.47	0.46	0.96	0.99	0.85	0.63
mno	0.22	0.20	0.22	0.23	0.26	0.24	0.28	0.24
c.i.p.w.norms								
or	4.54	5.19	6.21	6.16	11.67	12.98	13.52	8.43
ab	14.83	12.56	16.05	15.50	40.29	39.11	41.00	24.58
an	28.95	23.41	25.35	24.91	18.71	19.50	15.07	23.13
ne	1.10	6.79	6.90	7.27	3.09	2.24	5.32	6.21
diwo	10.57	12.23	10.34	10.65	3.39	3.11	3.57	6.70
dien	5.72	6.56	4.88	5.07	1.31	1.23	1.31	3.22
difs	4.48	5.27	5.33	5.43	2.12	1.91	2.34	3.38
fo	10.82	9.90	6.54	6.65	3.98	4.22	3.46	6.01
fa	9.35	8.78	7.88	7.85	7.09	7.20	6.82	6.95
mt	2.24	2.23	2.21	2.21	1.54	1.54	1.48	1.95
il	6.21	5.98	7.02	7.01	4.33	4.42	3.87	7.75
ap	0.96	0.91	1.08	1.05	2.22	2.30	1.96	1.45

Table 4B(continue)

Rock type	AB	AB	AB	AB	AB	AB	AB	ha	ank	ank
Depth	(70)	64	62	60	(60)	58	(50)	(25)	3	2
	h62-47	h65-8	h65-9	h65-10	h6248	h65-11	h62-49	h62-52	h65-13	h65-14
sio2	44.90	44.22	44.44	44.28	44.96	44.85	44.81	43.87	44.27	44.10
al2o3	14.84	14.46	14.59	14.48	14.28	14.25	13.75	15.64	13.38	13.26
feo	13.91	14.03	14.04	14.06	13.96	13.99	13.84	14.20	13.61	13.49
mgo	7.75	8.46	8.48	8.48	8.42	8.96	9.49	6.17	9.83	9.85
cao	10.45	10.73	10.97	10.77	10.68	10.69	11.28	10.42	12.43	12.24
na2o	3.31	3.47	2.96	3.30	3.19	2.88	2.69	3.81	2.17	2.60
k2o	0.99	0.94	0.87	0.94	0.88	0.83	0.74	1.39	0.76	0.87
tio2	3.25	3.09	3.07	3.10	3.09	3.01	2.90	3.69	2.96	3.00
p2o5	0.42	0.40	0.40	0.40	0.36	0.35	0.31	0.57	0.38	0.37
mno	0.18	0.19	0.18	0.19	0.18	0.20	0.19	0.23	0.21	0.21
c.i.p.w.norms										
or	5.83	5.57	5.16	5.57	5.22	4.87	4.34	8.21	4.50	5.13
ab	14.87	11.04	12.65	11.51	14.19	14.39	12.85	10.97	9.29	7.57
an	22.69	21.06	23.89	21.88	22.00	23.46	23.21	21.44	24.47	21.94
ne	7.10	9.90	6.69	8.87	6.92	5.39	5.36	11.49	4.92	7.78
diwo	11.01	12.31	11.64	12.05	11.94	11.35	12.78	11.05	14.46	15.14
dien	5.78	6.62	6.26	6.48	6.42	6.22	7.16	5.31	8.28	8.72
difs	4.90	5.29	5.00	5.17	5.12	4.71	5.10	5.57	5.55	5.74
fo	9.46	10.11	10.40	10.24	10.17	11.25	11.52	7.02	11.32	11.05
fa	8.84	8.90	9.15	9.01	8.94	9.39	9.05	8.13	8.36	8.01
mt	2.21	2.23	2.24	2.24	2.22	2.23	2.20	2.26	2.17	2.15
il	6.16	5.87	5.82	5.87	5.86	5.71	5.51	6.99	5.61	5.69
ap	0.97	0.92	0.92	0.92	0.82	0.82	0.72	1.32	0.87	0.86

1:SiO_2,Al_2O_3,MgO,CaO,TiO_2,P_2O_5,MnO and iron contents are from analyses by XRF at the University of Massachusetts. The total iron content is recalculated to FeO. Na_2O and K_2O contents are from analyses by INAA and I.D. ,respectively, at MIT. The total has been renormalized to 100%.

2:C.I.P.W. norms are calculated assuming $Fe_2O_3/(Fe_2O_3+FeO)=0.10$.

*: same as in Table 4A

Table 5: Transition metal abundances (ppm) of Haleakala volcanic series

	HO-1	HO-3	HO-4	HO-5	C-121	C-122	C-123	C-124	C-126
Rock type	Th	Th	Th	Th	Th	Picr	Picr	AB	Tran.
Sc (1)*	27.9	28.2	30.1	29.8	30.4	25.8	22.7	28.9	25.6
V (2)	259.	262.	274.	251.	286.	205.	205.	-	-
Cr (1)	253.	490.	439.	428.	523.	804.	582.	105	238
Cr (2)	235.	478.	392.	381.	526.	791.	498.	-	-
Co (1)	59.1	66.5	58.0	57.5	58.7	76.9	77.4	45.6	55.4
Ni (2)	226.	360.	281.	288.	210.	703.	542.	-	-
Zn (2)	124.	127.	120.	117.	121.	115.	122.	-	-

* the number in the parentheses indicate: (1) determined by INAA method (2) by XRF method.

Table 5 (continued)

Rock type	H85-1 AB	H85-2 ha	H85-7 AB	H85-8 AB	H85-9 AB	H85-10 AB	H85-11 ha	H85-12 AB	H62-2 AB	H85-13 AB
Sc	28.1	21.2	26.8	26.7	27.6	26.8	21.7	24.3	21.9	21.2
V	360.	285.	347.	363.	401.	362.	243.	315.	320.	323.
Cr	30.	11.	79.	136.	119.	120.	14.	31.	48.	4.
Cr	21.	-	77.	114.	116.	98.	3.	16.	39.	-
Co	46.7	40.9	53.5	50.6	52.7	53.1	46.4	45.	46.1	39.5
Ni	51.	23.9	82.	84.	86.	97.	32.	35.	51.	8.
Zn	138.	122.	119.	124.	121.	125.	134.	112.	125.	144.

Table 5 (continued)

	H85-14	H85-15	H85-16	H85-21	H65-4	H85-22	H62-14	H85-23	H85-24	H85-25
Rock type	AB	AB	ha	AB	AB	AB	AB	AB	Mu	Mu
Sc	23.2	24.6	10.7	31.1	31.	21.	29.6	20.3	5.6	5.6
V	301.	240.	121.	361.	346.	343.	362.	358.	55.	54.
Cr	229.	327.	9.	171.	167.	26.	89.	25.	5.	3.
Cr	197.	248.	-	167.	156.	23.	77.	20.	-	-
Co	48.2	54.8	23.0	61.3	61.7	47.2	58.6	48.4	14.5	15.
Ni	93.	124.	4.5	111.	109.	31.	67.	33.	4.6	5.1
Zn	115.	93.	106.	117.	110.	118.	122.	124.	120.	118.

Table 5 (continued)

	H85-31	H85-33	H62-47	H65-8	H65-9	H65-10	H62-48	H65-11	H62-49
Rock type	Mu	ha	AB	AB	AB	AB	AB	AB	AB
Sc	3.6	11.9	25.4	26.6	26.9	26.6	26.2	28.1	28.2
V	34.	168.	325.	344.	331.	331.	337.	324.	348.
Cr	5.	5.	200.	257.	258.	246.	271.	289.	333.
Cr	-	-	161.	230.	234.	229.	247.	254.	318.
Co	9.9	29.6	57.2	60.6	61.4	60.4	59.9	63.9	61.8
Ni	4.4	9.3	91.9	126.	130.	123.	137.	139.	174.
Zn	136.	111.	107.	109.	111.	116.	114.	109.	116.

Table 5 (continued)

Rock type	H62-52 ha	H65-13 ank	H65-14 ank
Sc	17.6	33.7	32.8
V	304.	336.	339.
Cr	70.	382.	367.
Cr	47.	321.	336.
Co	50.4	63.3	62.8
Ni	33.	110.	109.
Zn	124.	103.	101.

Table 6 Major Element Compositions of C122, Olivine Phenocryst and Calculated Residual Melt

	C122	olivine*	L^R
SiO_2	48.93	39.3	51.59
Al_2O_3	10.07	-	12.89
FeO	12.31	15.5	11.39
MgO	16.61	44.5	8.73
CaO	7.91	-	10.13
Na_2O	1.70	-	2.18
K_2O	0.26	-	0.33
TiO_2	1.86	-	2.40
P_2O_5	0.16	-	0.20
MnO	0.17	-	0.16
total	100.00	99.3	100.00
Ni(ppm)	703	2400	224
F	1.00	-	0.78
Mg#	72.8	83.7	60.4

L^R is the calculated residual liquid after 22% of olivine with composition of $Fo_{83.7}$ has been fractionated from C122. This residual liquid can be in equilibrium with olivine ($Fo_{83.7}$) if $K_D = 0.30$

* Composition of olivine phenocryst in C122 (Garcia, written communication)

Table 7 Major Element Composition of C122 olivine, clinopyroxene in C121 and the Calculated Parental Liquid Composition for C121 and HO-1

	C122	L_1	L_2	L_3	ol	cpx	r*
SiO_2	48.93	46.93	46.39	46.07	38.7	52.6	0.59
Al_2O_3	10.07	11.16	10.78	10.94	-	3.2	0.03
FeO	12.31	12.40	13.53	13.24	17.8	6.7	-0.27
MgO	16.61	16.44	16.61	16.44	42.9	16.7	0.08
CaO	7.91	8.75	8.45	8.96	-	19.6	-0.36
Na_2O	1.70	1.74	1.68	1.65	-	0.25	0.06
K_2O	0.26	0.12	0.12	0.18	-	-	-0.06
TiO_2	1.86	2.10	2.02	2.08	-	0.87	-0.02
P_2O_5	0.16	0.20	0.20	0.21	-	-	-0.01
MnO	0.17	0.16	0.20	0.20	0.25	0.12	-0.02
Mg#	72.8	72.4	70.9	71.1	81.1	81.2	Σr^2=.57

L_1: Calculated composition of primitive melt which was in equilibrium with mantle residue with olivine composition of Fo_{90} and K_D = 0.30. C121 can be derived from this primitive melt by fractional crystallization of 20% olivine. Equations by Irvine (1977) are used.

L_2: Composition of parental melt calculated by assuming equilibrium crystallization of olivine ($Fo_{81.1}$) and assuming the parental melt has 16.61% MgO. 21% olivine ($Fo_{81.1}$) must to fractionate from this parental melt to derive C121.

L_3: Calculated parental primitive melt composition by least-square regression of HO-1, olivine ($Fo_{81.1}$), clinopyroxene (Mg-number = 81.6) and average of (L_1 + L_2) using computer program by Wright and Doherty (1970). L_3 = 68.55% (HO-1) + 20.16% (olivine) + 11.30% (clinopyroxene).

ol, cpx: olivine and clinopyroxene in C121. The olivine composition was determined by Garcia (written communication). The composition of clinopyroxene was taken from Fodor et al. (1975).

* Residuals: observed values (in this case: $\frac{L_1+L_2}{2}$) - calculated values (L3).

Table 8 Replicate Major Element Analyses of C123

	1	2	3	4	5	6	AV*
SiO_2	46.62	45.85	45.56	45.73	45.55	44.63	45.67
Al_2O_3	12.03	11.39	11.07	11.48	11.38	12.66	11.33
Fe_2O_3	-	13.73	13.80	13.59	13.64	2.75	13.69
FeO	13.11	-	-	-	-	9.77	-
MgO	15.67	17.30	17.63	16.85	17.10	17.01	17.22
CaO	8.06	7.67	7.52	7.79	7.70	7.84	7.67
Na_2O	1.65	1.74	1.64	1.80	1.88	1.73	1.77
K_2O	0.15	0.14	0.13	0.14	0.15	0.20	0.14
TiO_2	2.34	2.16	2.13	2.19	2.17	1.83	2.16
P_2O_5	0.40	0.23	0.22	0.24	0.24	0.21	0.23
MnO	-	0.17	0.18	0.16	0.17	0.17	0.17
total	100.03	100.36	99.88	99.98	99.96	98.80	100.05

1: Analyses from WHOI

2,3,4,5: Analyses from U. of Mass. 2 and 3,4 and 5 are two sets of duplicated analyses

6: Analyses reported by MacDonald and Katsura (1964)

* Average of 4 analyses from U. of Mass.

Table 9 Partition Coefficients of Transition Metals Between Mineral and Melt

	ol	cpx	pl	mt
Sc	0.25	3.1	0.04	5
V	0.09	0.8	0.01	10-63
Cr	3	15	0.01	-
Co	1.3-6.5	1	0.05	6-16
Ni	*	2	0.04	19
Zn	0.95	-	-	4

Partition coefficients summary from Gunn (1971), Frey et al. (1978) and Clague et al., 1981

* $D^{ol/l}_{Ni}$ = (124/MgO)- 0.9 (Hart and Davis, 1978)

Table 10 Comparison of Calculated and Measured Transition Metal Abundances in C121 and HO-1

	C121		HO-1	
	calculated	measured	calculated	measured
Sc	30.4	30.4	28.0	27.9
V	256	286	258	259
Cr	574	523	269	253
Co	36.6+-72.5	58.7	36.5+-72.5	59.1
Ni*	218	210	188	226
Zn	116	121	-	124

*Partition coefficient of Ni between olivine and liquid is calculated using the MgO content of the sample and the equation given by Hart and Davis (1978)

+Calculated from higher $D_{Co}^{ol/l}$ in Table 9.

Table 11 Composition of H65-4, Olivine Phenocrysts and Calculated Parental Liquid

	Differentiated H65-4	Olivine $Fo_{80.6}$	Parent (calculated)
SiO_2	44.51	39.3	43.24
Al_2O_3	14.43	-	10.91
FeO	13.99	18.1	14.99
MgO	8.32	42.3	16.61
CaO	11.16	-	8.44
NA_2O	2.97	-	2.25
K_2O	0.88	-	0.67
TiO_2	3.15	-	2.38
P_2O_5	0.39	-	0.29
MnO	0.20	0.28	0.22
*Fℓ	0.756		1.00
Sc	31.0		25.3
V	346		269
Cr	167		248
Co	61.7		66.2^{+}-144.5
Ni	109		455
Zn	110		109

$^{+}$ Calculated from higher $D_{Co}^{ol/l}$ in Table 9.

* Amount of residual liquid

Table 12 Fractionation Solution for Deriving a Hawaiite (H85-11) From an Akalic Basalt (H85-10)

	ol	cpx	plag.	Mt	H85-11	H85-10	Calculated parent	r*
SiO_2	37.80	50.70	51.30	0.00	45.96	45.95	45.78	0.17
Al_2O_3	0.00	3.30	30.70	3.00	15.89	14.79	14.74	0.05
FeO	24.30	10.00	0.53	72.13	13.77	13.49	13.52	-0.03
MgO	36.60	14.50	0.00	0.00	5.04	6.39	6.37	0.02
CaO	0.00	19.00	14.00	0.00	8.75	11.36	11.32	0.04
Na_2O	0.00	0.30	3.20	0.00	3.74	2.83	2.73	0.10
K_2O	0.00	0.00	0.13	0.00	1.54	0.86	0.92	0.06
TiO_2	0.00	1.50	0.00	24.87	4.38	3.59	3.93	-0.34
P_2O_5	0.00	0.00	0.00	0.00	0.72	0.44	0.42	0.02
MnO	0.00	0.00	0.00	0.00	0.21	0.20	0.13	0.07
Solution[1]	0.83%	21.60%	15.11%	4.24%	58.24%	100%		Σr^2= 0.17
F[2]					61.1%	100%		

1: Using least-squares regression program by Wright and Doherty (1970)

2: F is the amount of residual liquid calculated from P_2O_5 content in the parent and daughter using equilibrium crystallization equation:

$$C^{\ell}/Co = \frac{1}{F+D(1-F)} \text{ assuming } D = 0$$

* residuals = observed values (H85-10) - calculated values (calculated parent)

Table 13 Fractionation Solution For Deriving a Mugearite (H85-24) From An Alkalic Basalt (H85-23)

	ol	cpx	plag.	Mt	H85-24	H85-23	Calculated parent	r*
SiO_2	39.20	50.70	46.80	0.00	51.99	44.72	45.03	-0.33
Al_2O_3	0.00	3.30	32.50	3.00	17.96	15.91	16.04	-0.13
FeO	18.00	10.00	0.66	72.13	9.65	13.89	14.02	-0.13
MgO	42.00	14.50	0.00	0.00	2.81	5.86	5.91	-0.05
CaO	0.00	19.00	17.50	0.00	6.67	10.78	10.84	-0.06
Na_2O	0.00	0.30	1.70	0.00	5.44	3.42	2.77	0.65
K_2O	0.00	0.00	0.10	24.87	1.98	1.04	0.87	0.17
TiO_2	0.00	1.50	0.00	0.00	2.28	3.70	3.69	0.01
P_2O_5	0.00	0.00	0.00	0.00	0.96	0.46	0.41	0.05
MnO	0.00	0.00	0.00	0.00	0.26	0.23	0.12	-
Solution[1]	3.94%	21.11%	22.80%	9.63%	42.54%	100%		Σr^2 = 0.60
F[2]					47.92%	100%		

[1] Using least squares regression program by Wright and Doherty (1970)

[2] F = P_2O_5 in the parent/P_2O_5 in the daughter

* residuals = observed values (H85-23) - calculated values (calculated parent)

Table 14 Fractionation Solution for Deriving an Alkalic Basalt (H85-22) From a More-Mafic Alkalic Basalt (H65-4)

	ol	cpx	plag	Mt	H85-22	H65-4	Calculated parent	r*
SiO_2	39.3	50.70	46.80	0.00	44.80	44.51	44.48	0.33
Al_2O_3	0.00	3.30	32.50	3.00	16.05	14.43	14.42	0.01
FeO	18.10	10.00	0.66	72.13	13.86	13.99	14.03	-0.04
MgO	42.30	14.50	0.00	0.00	5.71	8.32	8.26	0.06
CaO	0.00	19.00	17.50	0.00	10.73	11.16	11.15	0.01
Na_2O	0.00	0.30	1.70	0.00	3.41	2.97	2.78	0.19
K_2O	0.00	0.00	0.10	0.00	1.05	0.88	0.83	0.05
TiO_2	0.00	1.50	0.00	24.87	3.70	3.15	3.44	-0.29
P_2O_5	0.00	0.00	0.00	0.00	0.47	0.39	0.37	0.02
MnO	0.00	0.00	0.00	0.00	0.22	0.20	0.18	0.02
Solution[1]	5.45%	10.23%	4.61%	1.62%	78.11%			Σr^2 = 0.13
F[2]					83.0%			

[1] Using least squares regression program by Wright and Doherty (1970)

[2] F = P_2O_5 in the parent/P_2O_5 in the daughter

* residuals = observed values (H65-4) - calculated values (calculated parent)

Table 15 Comparison of Calculated and Measured Abundances of Sc, V, Co and Ni in H85-11, H85-24 and H85-22

	H85-11 hawaiite	calc.*	H85-24 (mugearite)	calc.*	H85-22 alkalic basalt	calc.*
Sc	21.7	18.2	6	13	21	25
V	243	106^{+}-306	55	54^{+}-229	343	183^{+}-336
Co	46.4	34.5^{+}-49.6	14.5	19.8^{+}-25.8	47.2	41.2^{+}-58.6
Ni	32	50	5	7	31	44

*: The abundances of Sc, V, Co, Ni are calculated using the abundances in their parent (H85-10, H85-23 and H65-4, respectively), the percentages of mineral fractionated calculated by major element compositions (Tables 12, 13 and 14) and assuming equilibrium fractionation using the partition coefficients in Table 9.

+: Using high partition in Table 9.

Table 16 Composition of H65-11, Olivine Phenocryst and Its Calculated Parental Liquid

	Differentiated H65-11	Olivine $Fo_{83.4}$	Calculated* parent for H65-11 Hana	Calculated** parent for H65-4 Kula
SiO_2	44.85	39.6	43.72	43.24
Al_2O_3	14.25	-	11.19	10.91
FeO	13.99	15.8	14.38	14.99
MgO	8.96	44.6	16.61	16.61
CaO	10.69	-	8.40	8.44
Na_2O	2.88	-	2.26	2.25
K_2O	0.83	-	0.65	0.67
TiO_2	3.01	-	2.36	2.38
P_2O_5	0.35	-	0.27	0.29
MnO	0.20	0.10	0.18	0.22
F^{ℓ}	0.79		1.00	1.00
Sc	28.1		23.6	25.3
V	324		261	269
Cr	289		413	248
Co	63.9		68.0^{+}-139	66.2^{+}-144.5
Ni	139		496	455
Zn	109		108	109

* Parental liquid composition calculated assuming olivine equilibrium fractionation and assuming the parental liquid contains 16.61% MgO. 21% of olivine need to fractionate from this parental liquid to derived H65-11

** from Table 11

$^{+}$ Calculated from high partition coefficient in Table 9

Table 17 Comparison of Haleakala Basalts With Other Hawaiian Basalts, Mid-ocean Ridge Basalts and Chondrites

	C122+	H65-4+	H65-11+	KL[1]	ML[1]	MORB[2]	Chond.[3]
Al_2O_3/CaO	1.3	1.3	1.3	1.2	1.3	1.2	1.1
Al_2O_3/TiO_2	5.4	4.6	4.7	5.0	6.8	20	20.4
CaO/TiO_2	4.3	3.5	3.6	4.2	5.1	17	17
K_2O/P_2O_5	1.63	2.26	2.37	2.14	1.76	1.4	0.3-0.5

[1] Data from Wright 1971. KL: 1959 Kilauea lavas. ML: historic Mauna Loa lavas

[2] Data from Sun et al., 1979

[3] From Clague and Frey, 1978

[+] C122, H65-4, H65-11 are the three least fractionated samples from the Honomanu volcanic series, Kula volcanic series and Hana volcanic series, respectively

Figure Captions:

Figure 1-1: Location of Maui in the Hawaiian island chain

▤: drill hole locality, Nahiku area

▨: Honomanu Bay

Figure 1-2: Core logs of drill hole 65 and hole 85. In each drill hole, the samples are numbered in an incremental manner so that the older sample in the drill hole would have smaller number than the younger sample. For example, H85-1 is the oldest sample (on the very bottom of the core) in drill hole 85 and H85-2 is the sample right above H85-1. Sample numbers are listed on the right side (hole 85) and left side (hole 65) of the core logs.

Figure 1-3: $Na_2O + K_2O$ versus SiO_2 for Haleakala basalts.

□: Tholeiites from Honomanu volcanic series

■: Transitional basalts and alkalic basalt from Honomanu volcanic series

Δ: Alkalic basalts from Kula volcanic series

⊙: Hawaiites and mugearites from Kula volcanic series

*: Alkalic basalts and ankaramites from Hana volcanic series

●: Hawaiite from Hana volcanic series

Figure 1-4: Variations of major oxides (a) SiO_2, (b) Al_2O_3, (c) FeO, (d) CaO, (e) Na_2O, (f) K_2O, (g) TiO_2, (h) P_2O_5 with MgO of Haleakala basalts. Symbols as in figure 1-3.

The olivine-controlled lines of 1959 Kilauea tholeiites (KL, dash line) and historic Mauna Loa tholeiites (ML, solid line) from Wright (1971) are also included for comparison. The ranges of FeO vs. MgO variations for prehistoric Kilauea tholeiites (circled by dash lines)

and prehistoric Mauna Loa tholeiites (circled by solid lines) are also shown in (c).

Figure 1-5: Variation of (a) Sc, (b) V, (c) Cr, (d) Co, (e) Ni, (f) Zn as a function of MgO contents in Haleakala samples. Symbols as in figure 1-3.

Figure 1-6: Variation of major oxide (a) SiO_2, (b) Al_2O_3, (c) FeO, (d) MgO, (e) CaO, (f) Na_2O, (g) K_2O, (h) TiO_2, (i) P_2O_5 and (j) oxide abundance ratio K_2O/P_2O_5 in Haleakala samples as a function of depth. Symbols as in figure 1-3. The altered samples are circled in (j).

Figure 1-7: Samples from Honomanu volcanic series plotted in terms of (a) their normative plagioclase, quartz and olivine contents (b) their normative clinopyroxene, olivine and quartz contents. Major element compositions of the samples are plotted in these projections using molecular proportions calculated according to the following:

plagioclase = $Al_2O_3 + Na_2O + K_2O$

clinopyroxene = $CaO - Al_2O_3 + Na_2O + K_2O - 3.33\ P_2O_5$

olivine = $(FeO + MgO + MnO + Al_2O_3 - CaO - Na_2O - K_2O - Fe_2O_3 - TiO_2 + 3.33\ P_2O_5)/2$

quartz = $SiO_2 - (Al_2O_3 + FeO + MnO + MgO + MnO + 3CaO + 11Na_2O + 11K_2O - TiO_2 - Fe_2O_3 - 10P_2O_5)/2$ assuming FeO = 90 mole % of total iron. Proportions of diopside, olivine and silica are then normalized to the sum of (a) plagioclase, quartz and olivine and (b) clinopyroxene, olivine and quartz and plotted on a molecular basis.

□:tholeiites

■:transitional basalts and alkalic basalt

Dashed lines are 1 bar cotectic lines from experimental data by Walker

et al. (1979). Sample HO-1, C121, C122, C123 and C124 are marked by 1, 121, 122, 123 and 124.

Figure 1-8: Variation of CaO/MgO ratios as a function of MgO content in Haleakala basalt. Symbols as in figure 1-3.

Figure 1-9: Variation of Al_2O_3/CaO ratios as a function of MgO content in Haleakala basalt. Symbols as in figure 1-3. Samples H85-10, 11, 22, 23, 24 are marked by 10, 11, 22, 23 and 24.

Figure 1-10: Alkalic samples from Kula volcanic series projected from nepheline (Ne) onto plagioclase (plag), olivine (oliv) and clinopyroxene (cpx) plane (data from analyses determined at WHOI). Dashed line is a (plagioclase + pyroxene) cotectic line from low pressure (1 bar) fractionation experiment by Walker et al. (1979). The experimental data were projected from silica onto the plag-oliv-cpx plane. The projection scheme is calculated according to the following formulae:

plagioclase = $Al_2O_3 + K_2O + Na_2O$

clinopyroxene = $CaO - Al_2O_3 + K_2O + Na_2O - 3.33\ P_2O_5$

olivine = $(FeO + MgO + MnO - Fe_2O_3 - TiO_2 + Al_2O_3$
$- CaO - K_2O - Na_2O + 3.33\ P_2O_5)/2$

silica = $SiO_2 - (Al_2O_3 + FeO + MgO + MnO + 3CaO + 11Na_2O + 11K_2O -$
$- 10P_2O_5 - TiO_2 - Fe_2O_3)/2$

The Fe_2O_3/total Fe is assumed to be 0.1. If silica is negative, then nepheline = -(1/2) silica, plagioclase = $(Al_2O_3 + K_2O + Na_2O)$ - nepheline. Proportions of plag, oliv and cpx are then normalized to a total of 100% and plotted on a molecular basis.

Figure 1-11: Correlation of P_2O_5 abundances with Ce abundances in Haleakala samples. Symbols as in figure 1-3. Ce abundances are from Chapter 3.

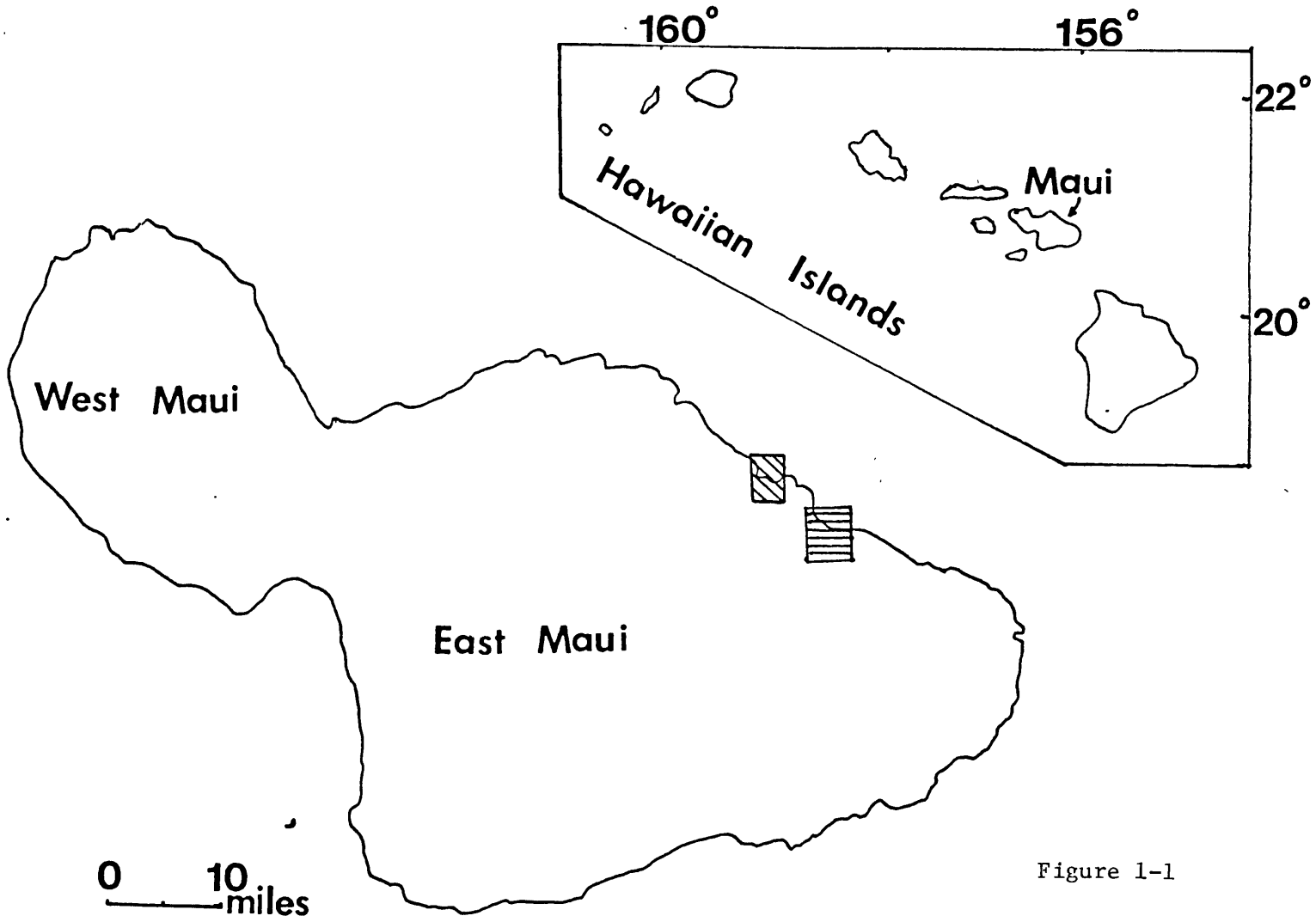

160°
156°
22°
20°
Hawaiian Islands
Maui
West Maui
East Maui
0 10 miles

Figure 1-1

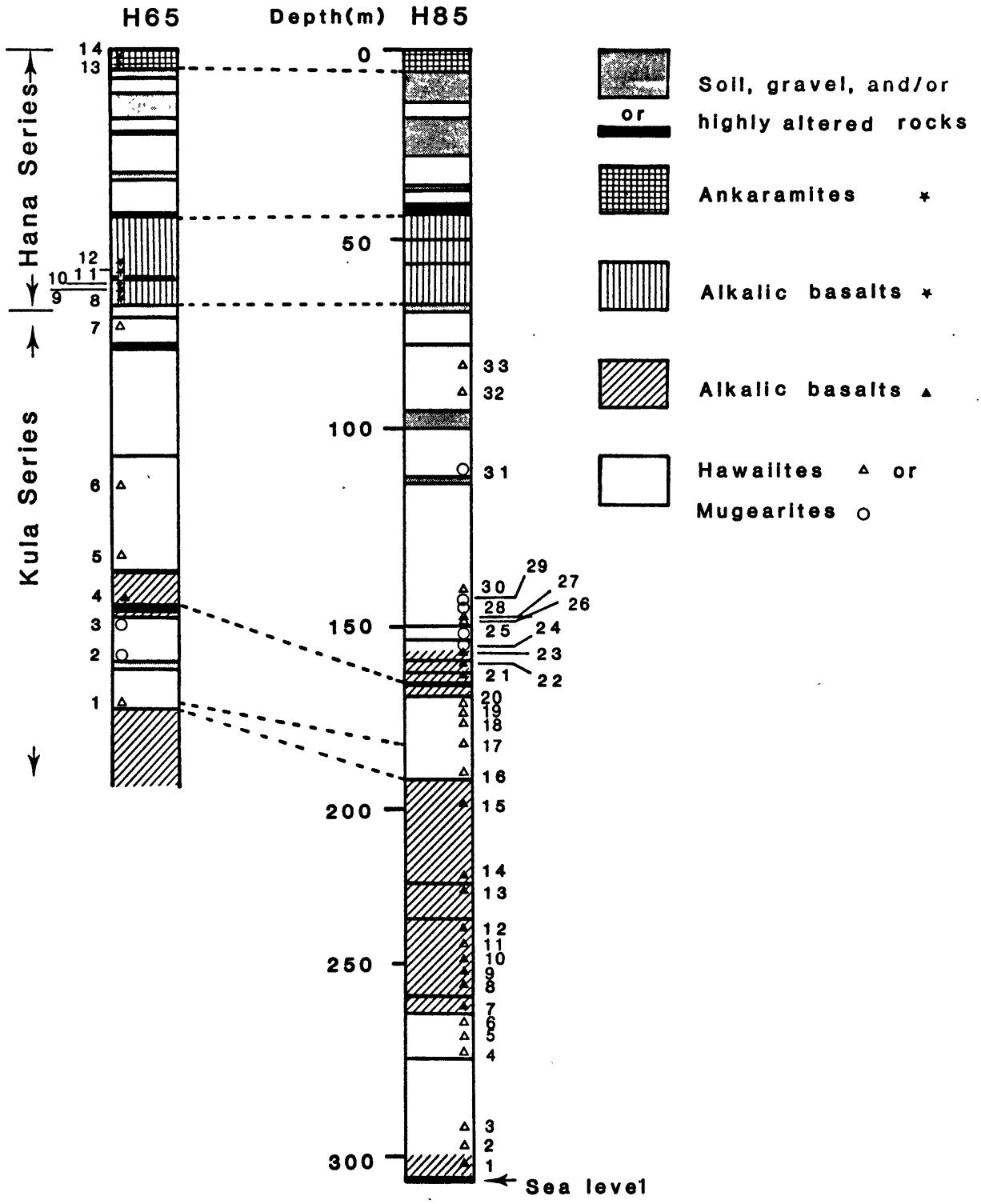

H65
Depth(m)
H85
Hana Series
Kula Series
Soil, gravel, and/or
or
highly altered rocks
Ankaramites
Alkalic basalts
Alkalic basalts
Hawaiites or
Mugearites
0
50
100
150
200
250
300
Sea level

Figure 1-2

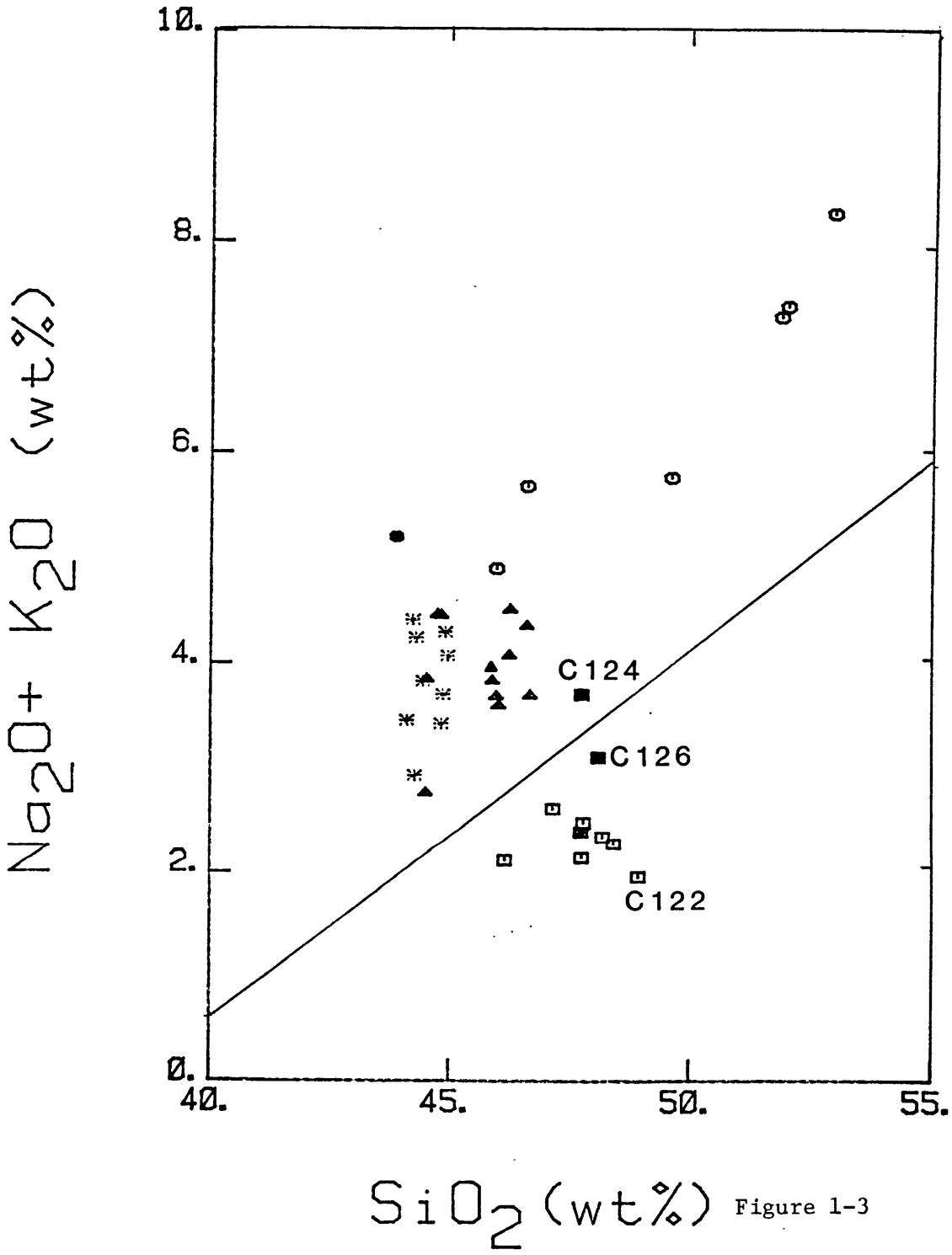


Figure 1-3

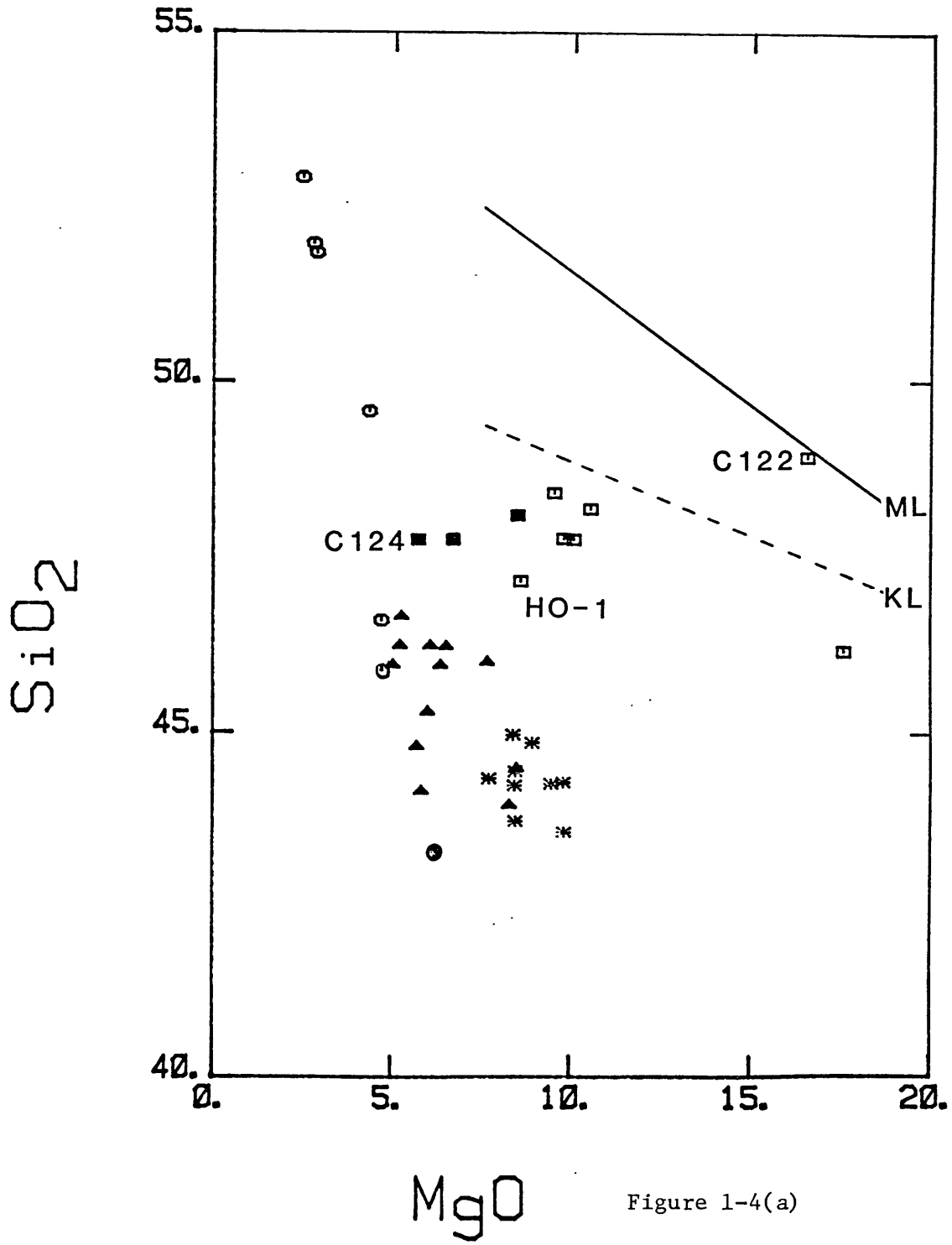


Figure 1-4(a)

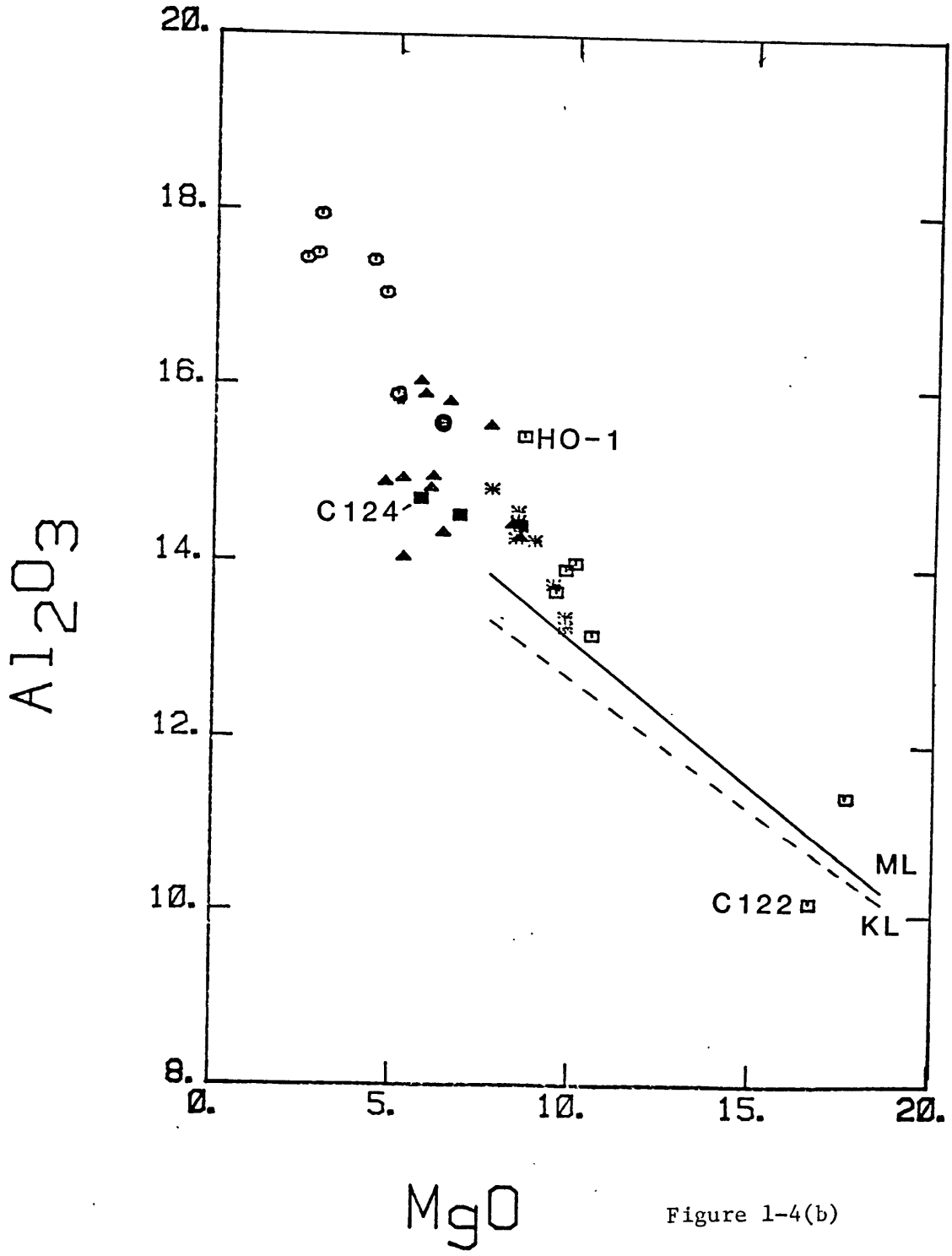


Figure 1-4(b)

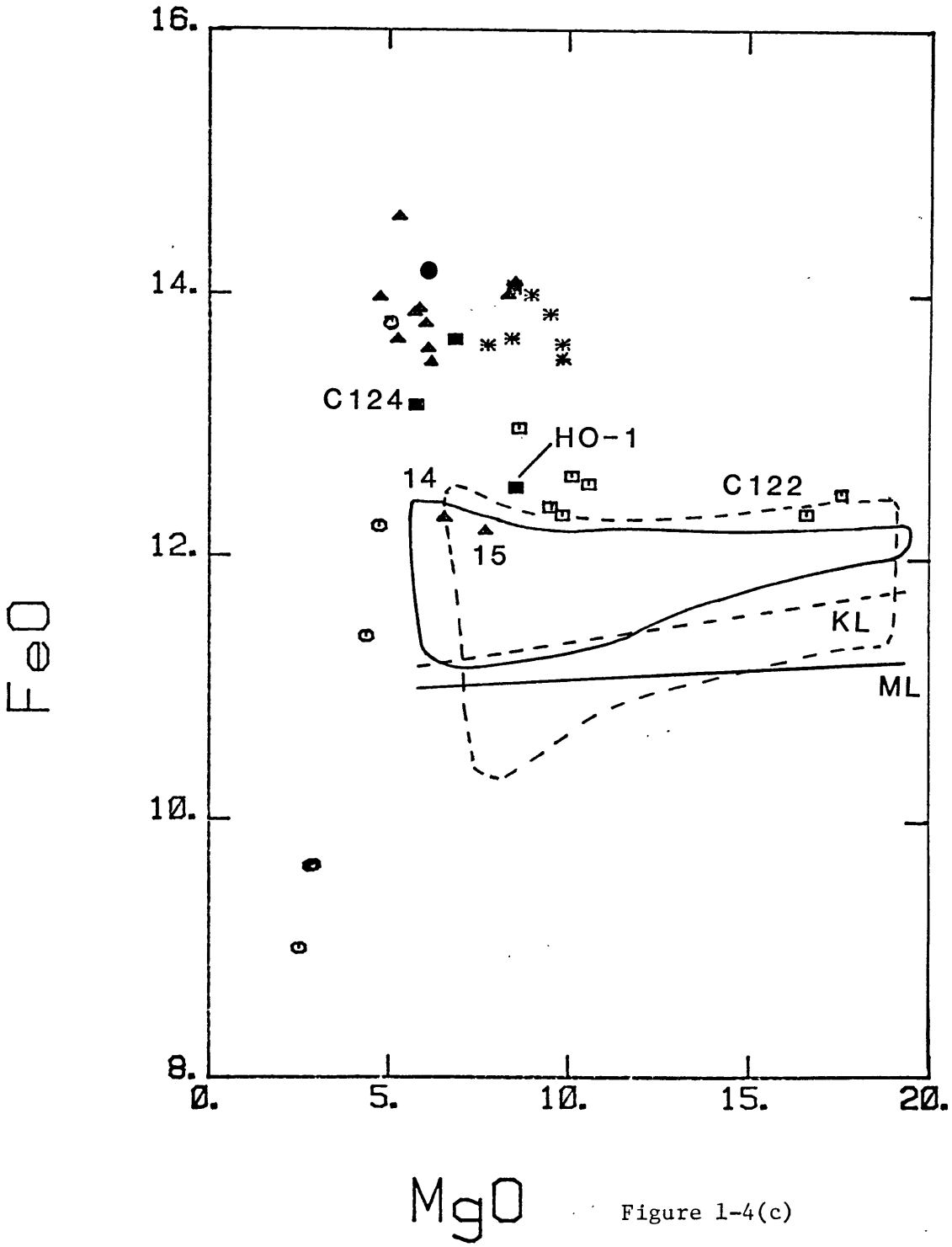


Figure 1-4(c)

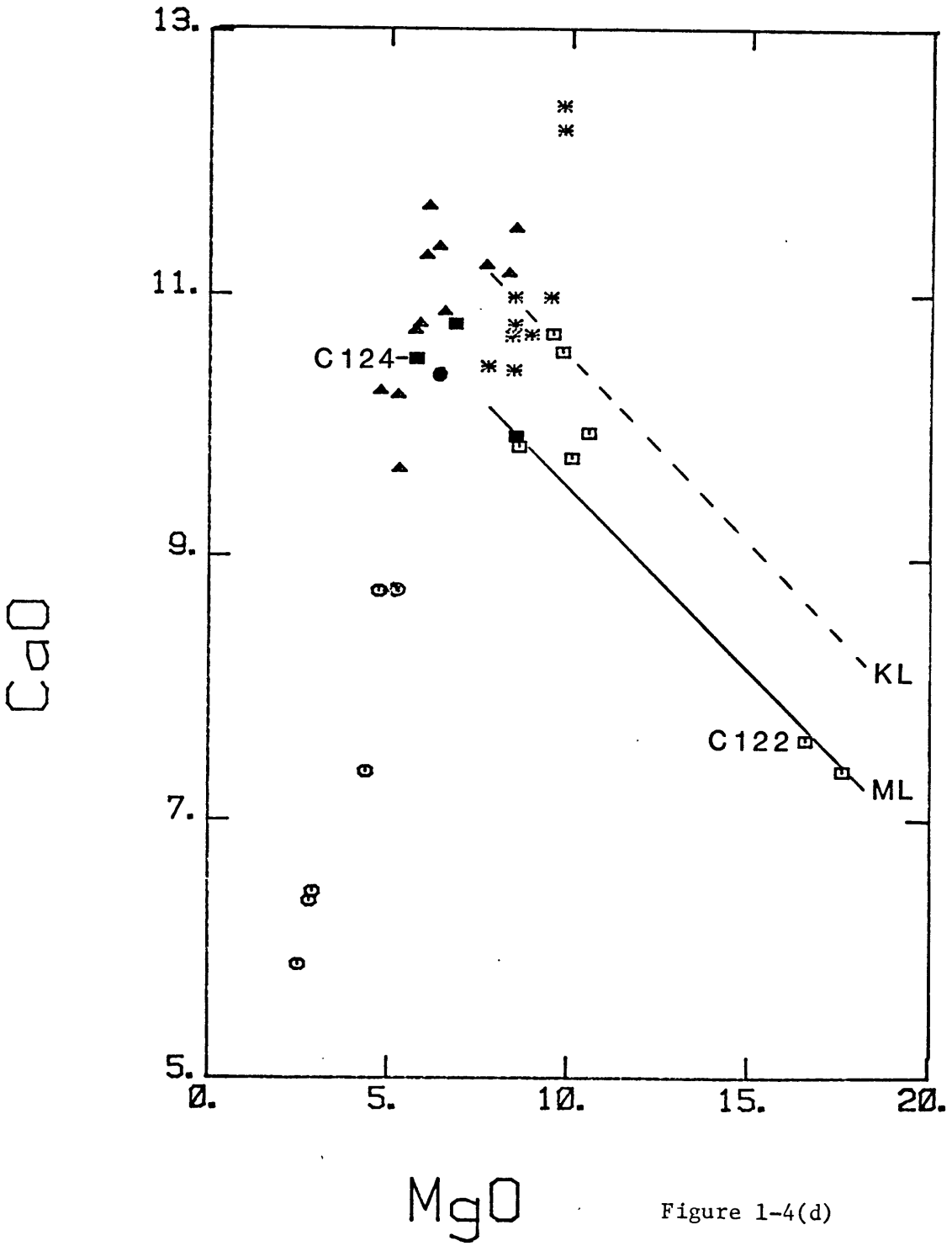


Figure 1-4(d)

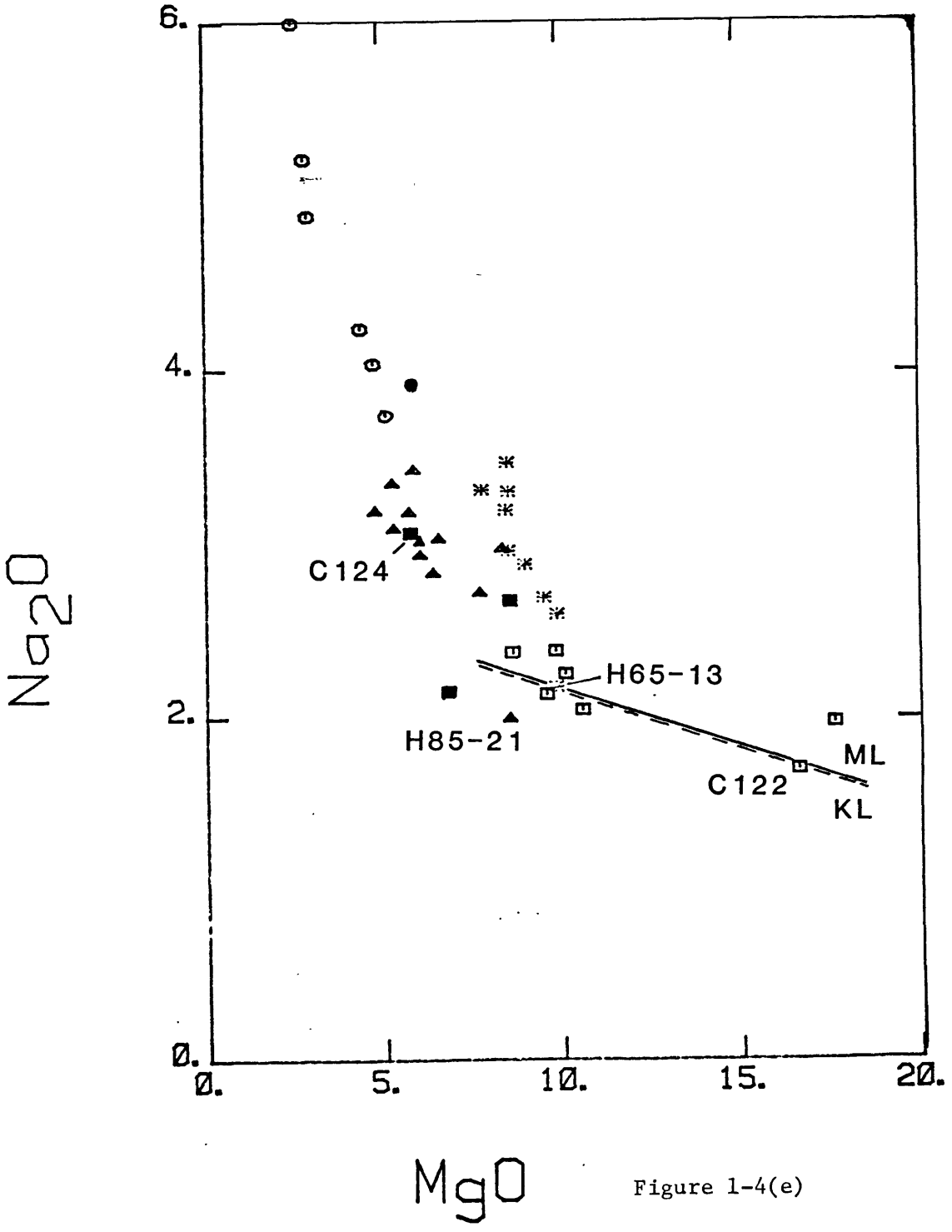


Figure 1-4(e)

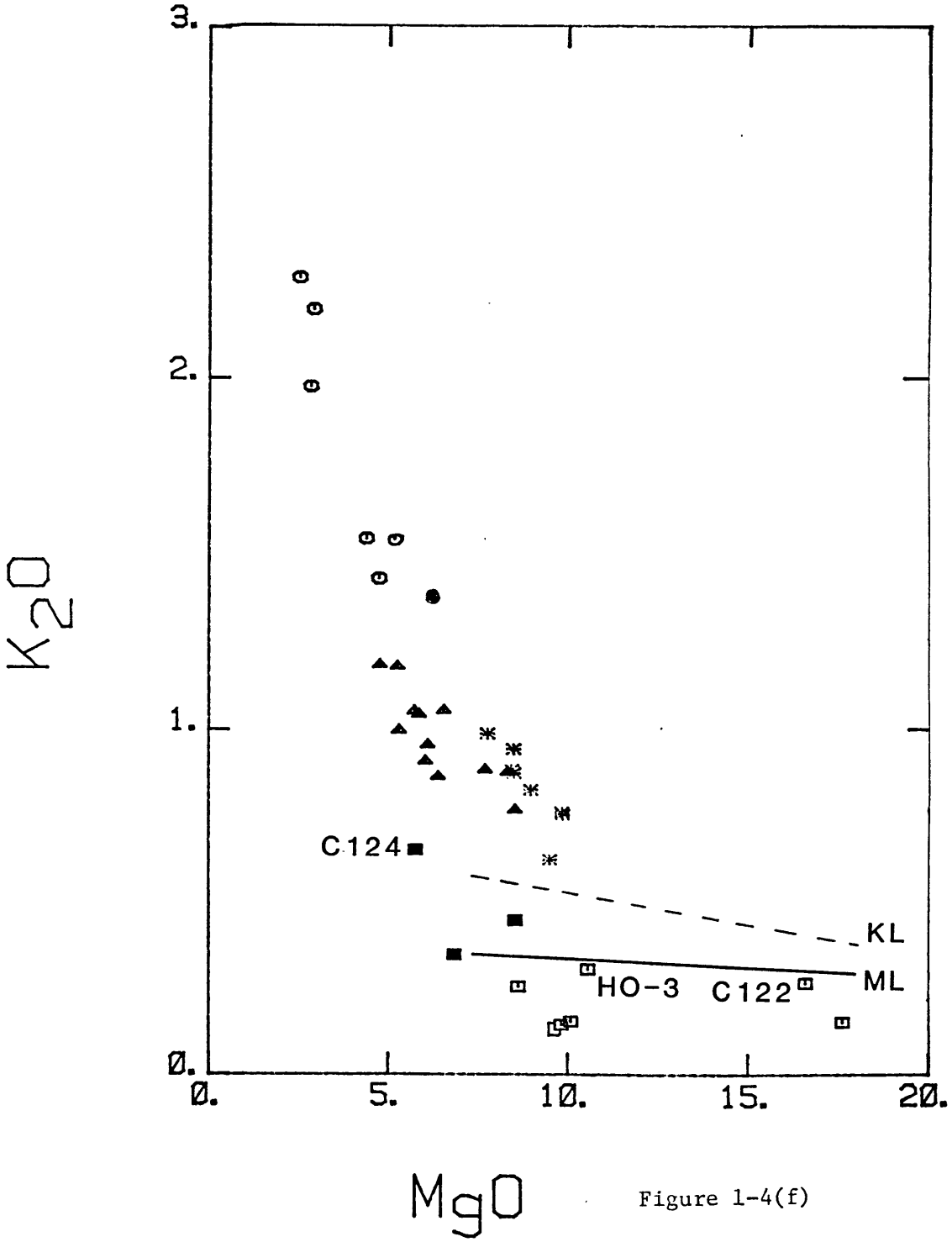


Figure 1-4(f)

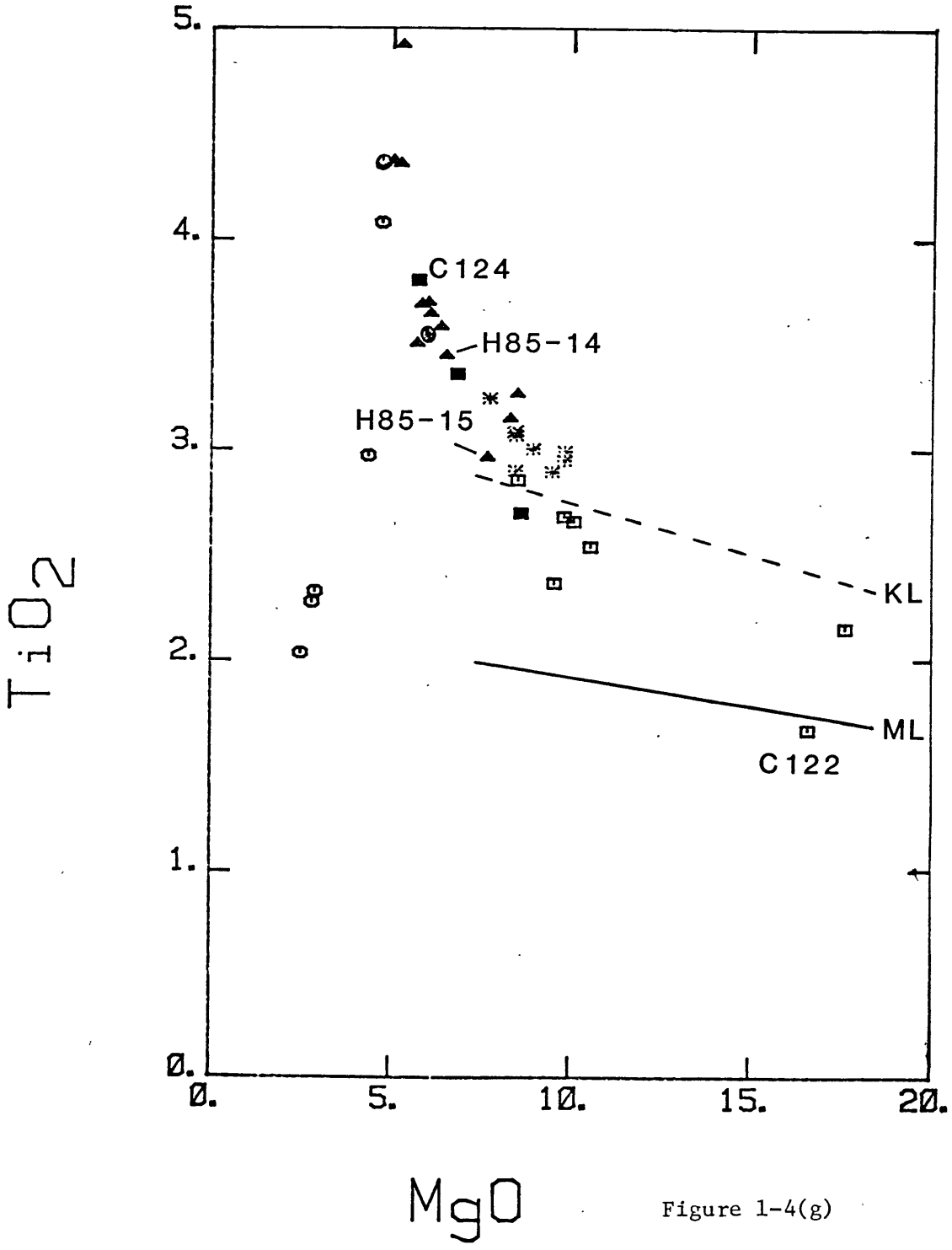


Figure 1-4(g)

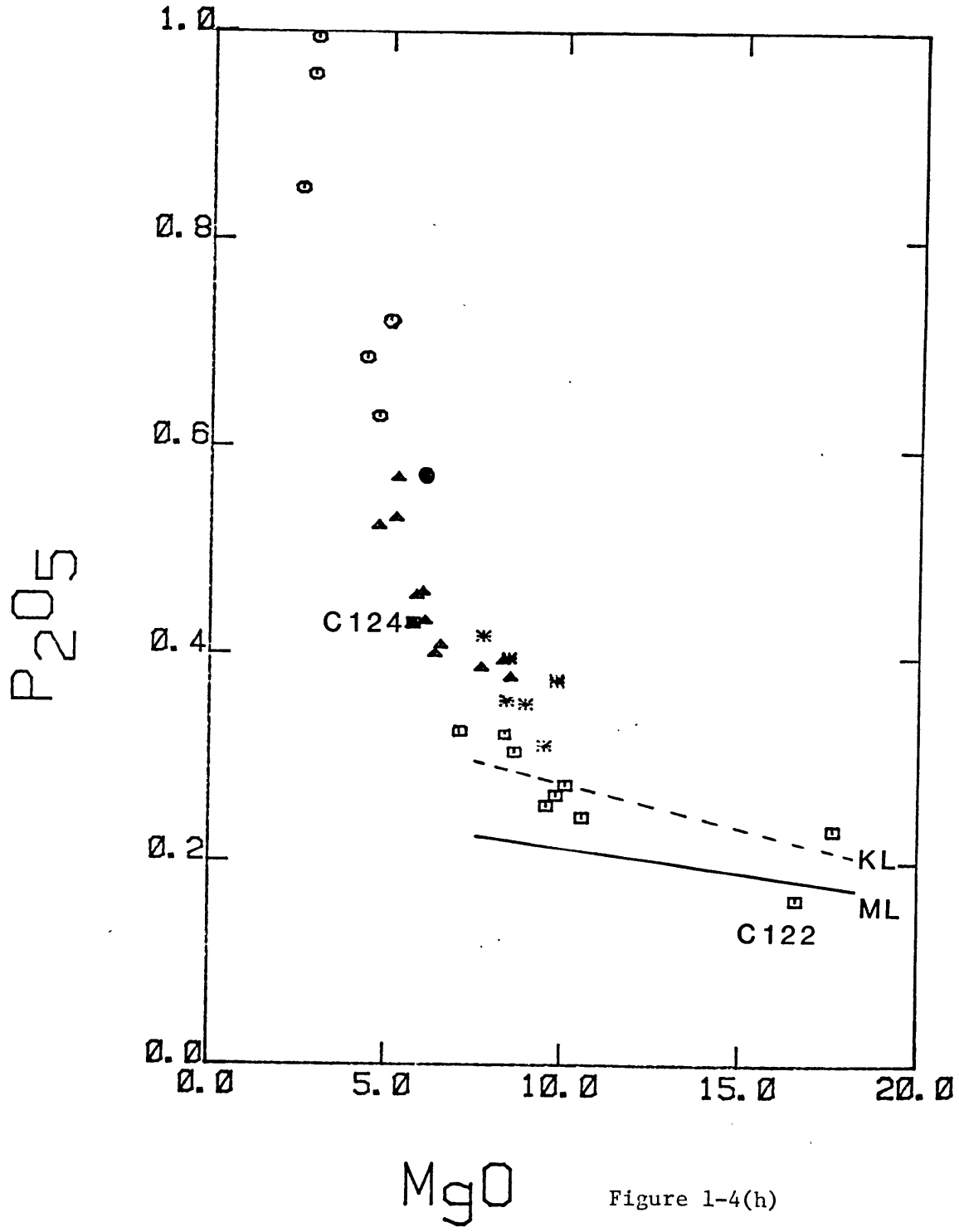


Figure 1-4(h)

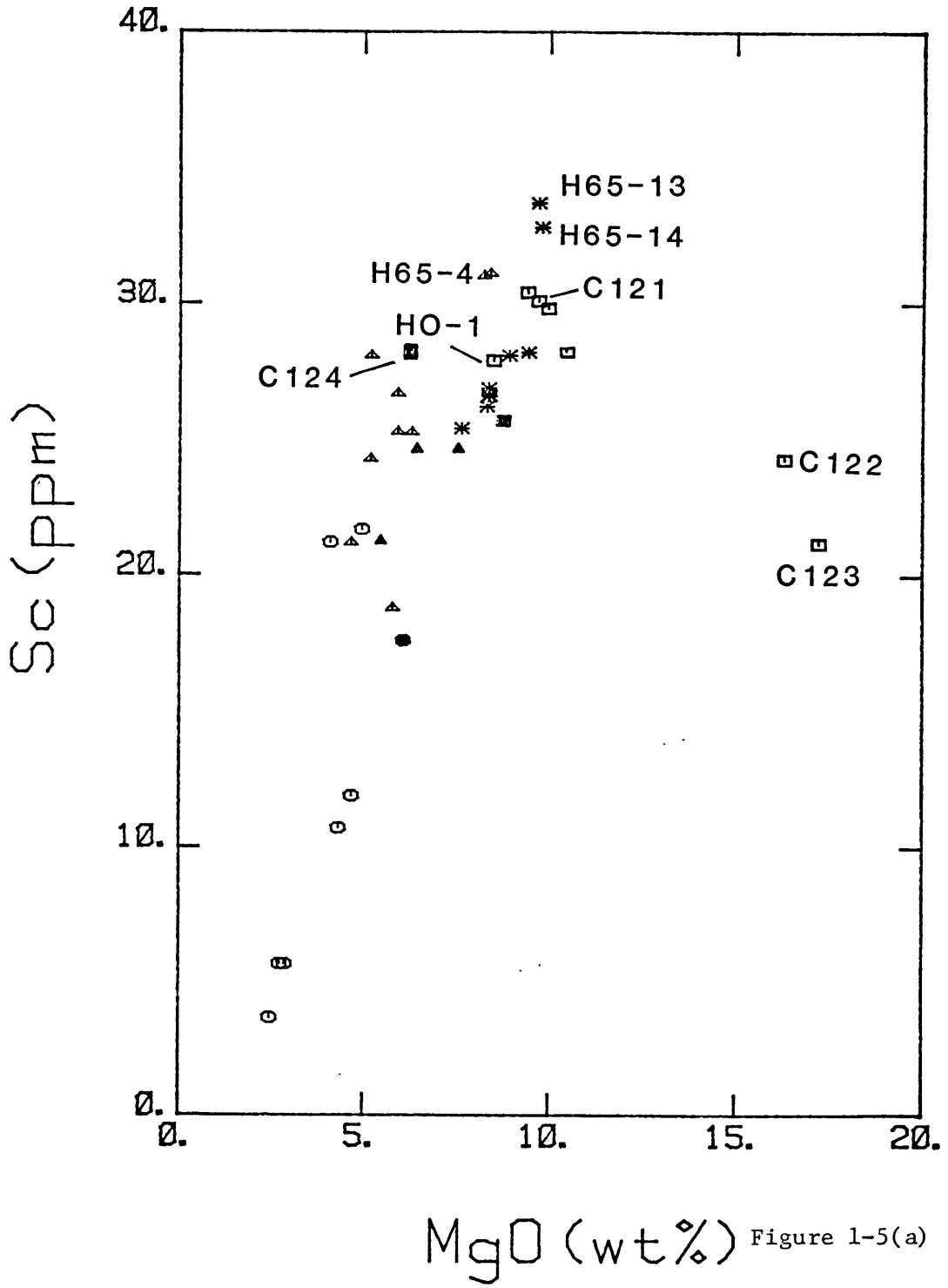

40.
30.
20.
10.
0.
0.
5.
10.
15.
20.
Sc (ppm)
MgO (wt%)
H65-13
H65-14
H65-4
C121
HO-1
C124
C122
C123

Figure 1-5(a)

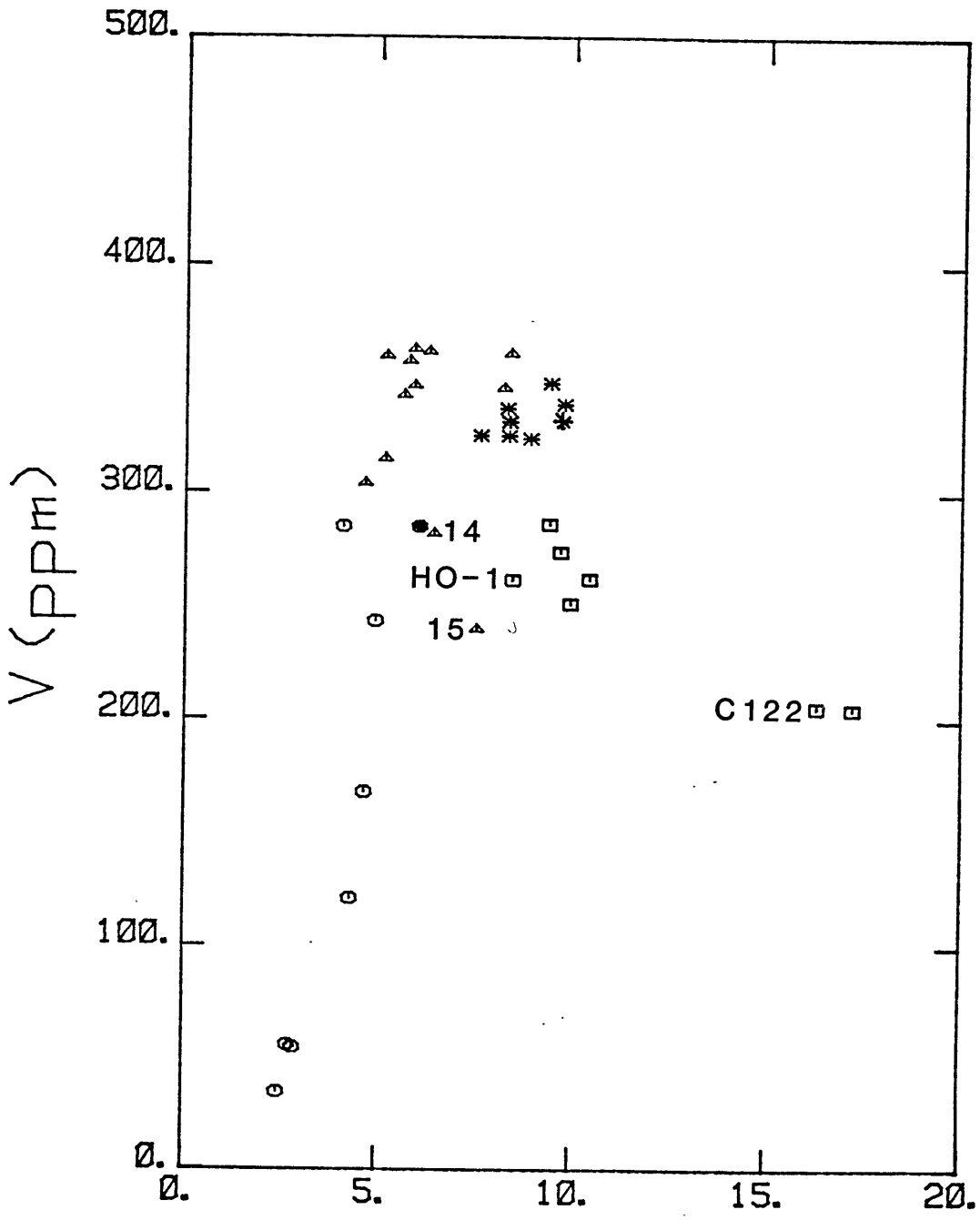


Figure 1-5(b)

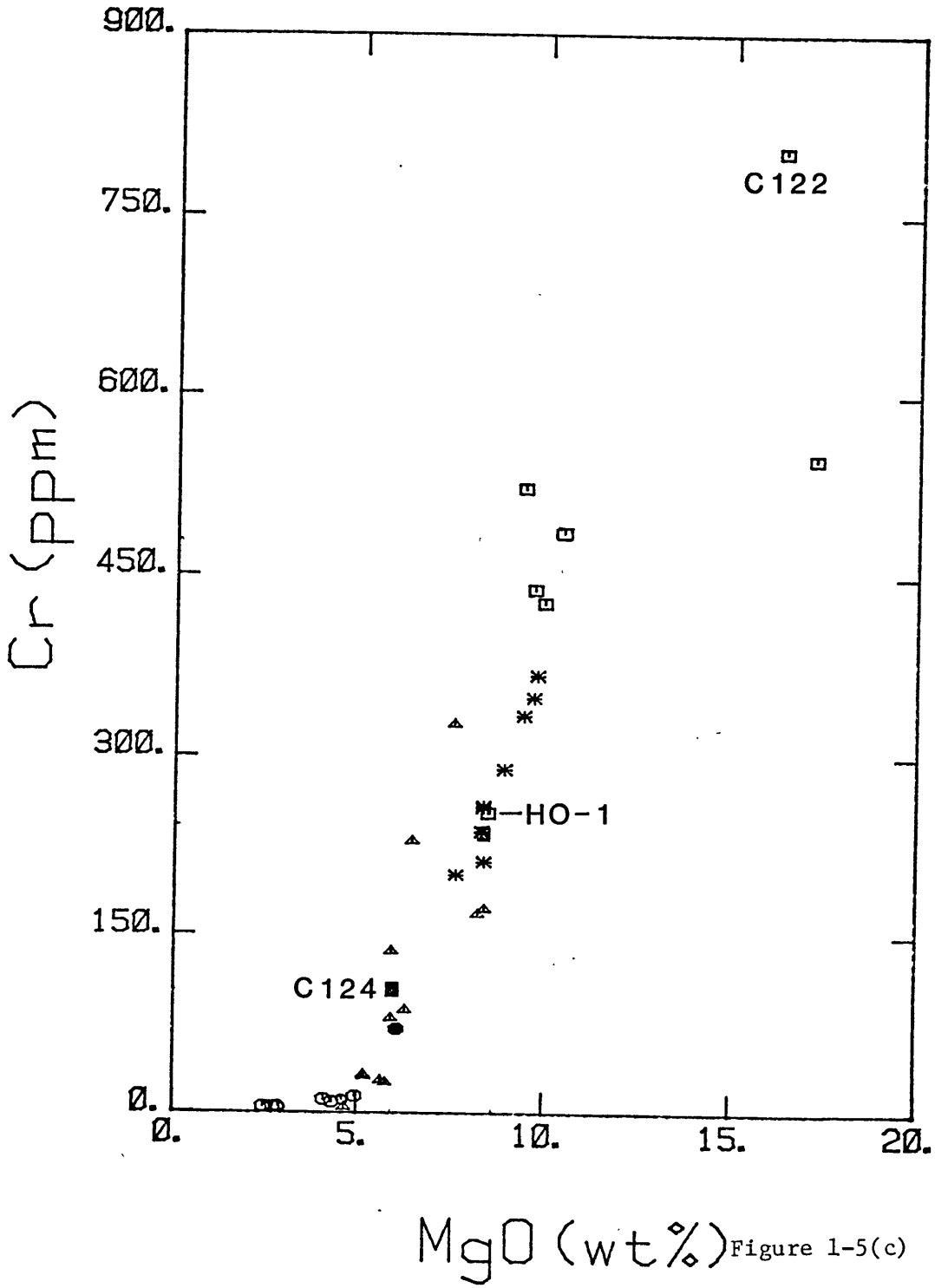


Figure 1-5(c)

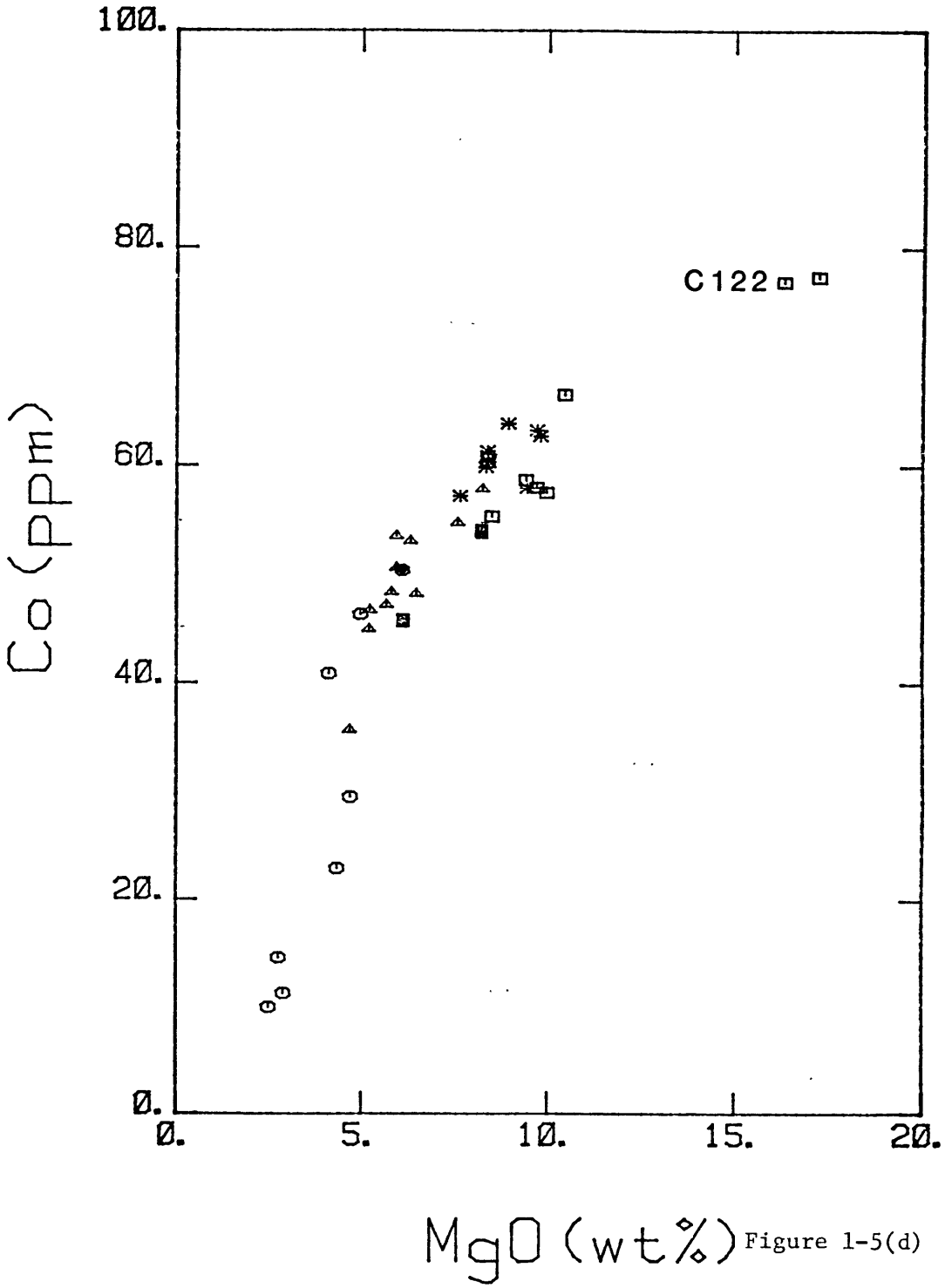


Figure 1-5(d)

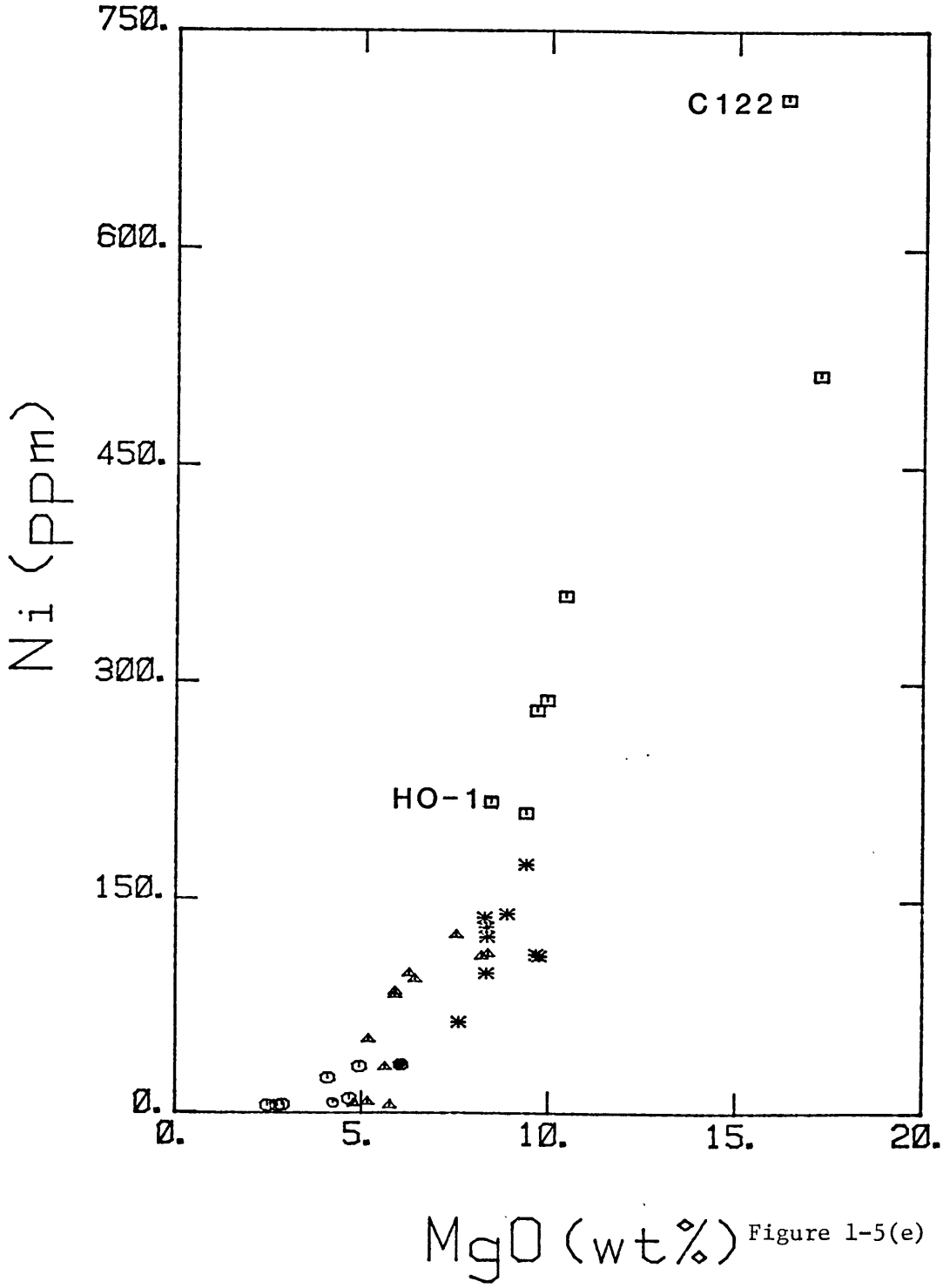


Figure 1-5(e)

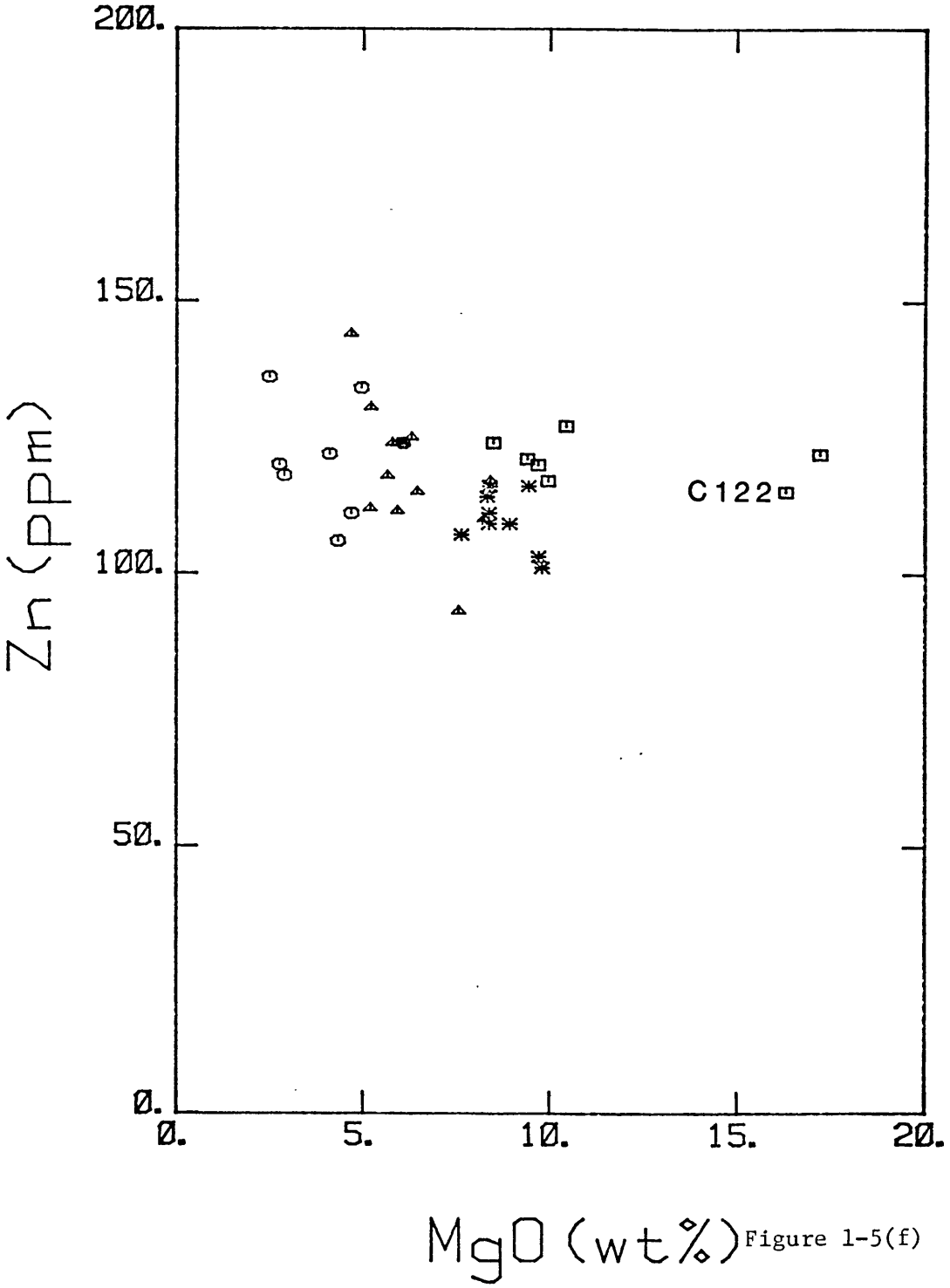


Figure 1-5(f)

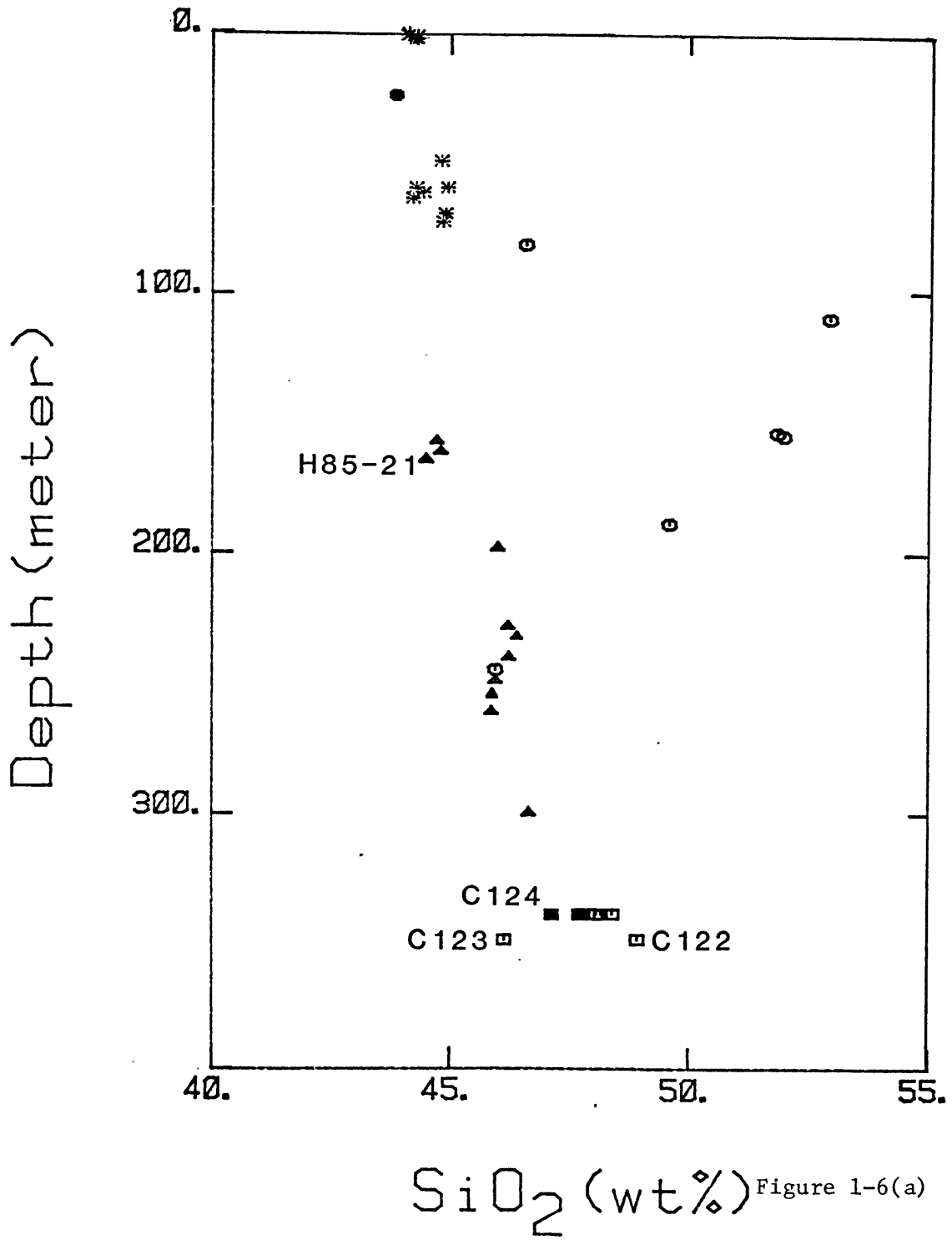

0.
100.
200.
300.
Depth (meter)
H85-21
C124
C123
C122
40.
45.
50.
55.
SiO2 (wt%)

Figure 1-6(a)

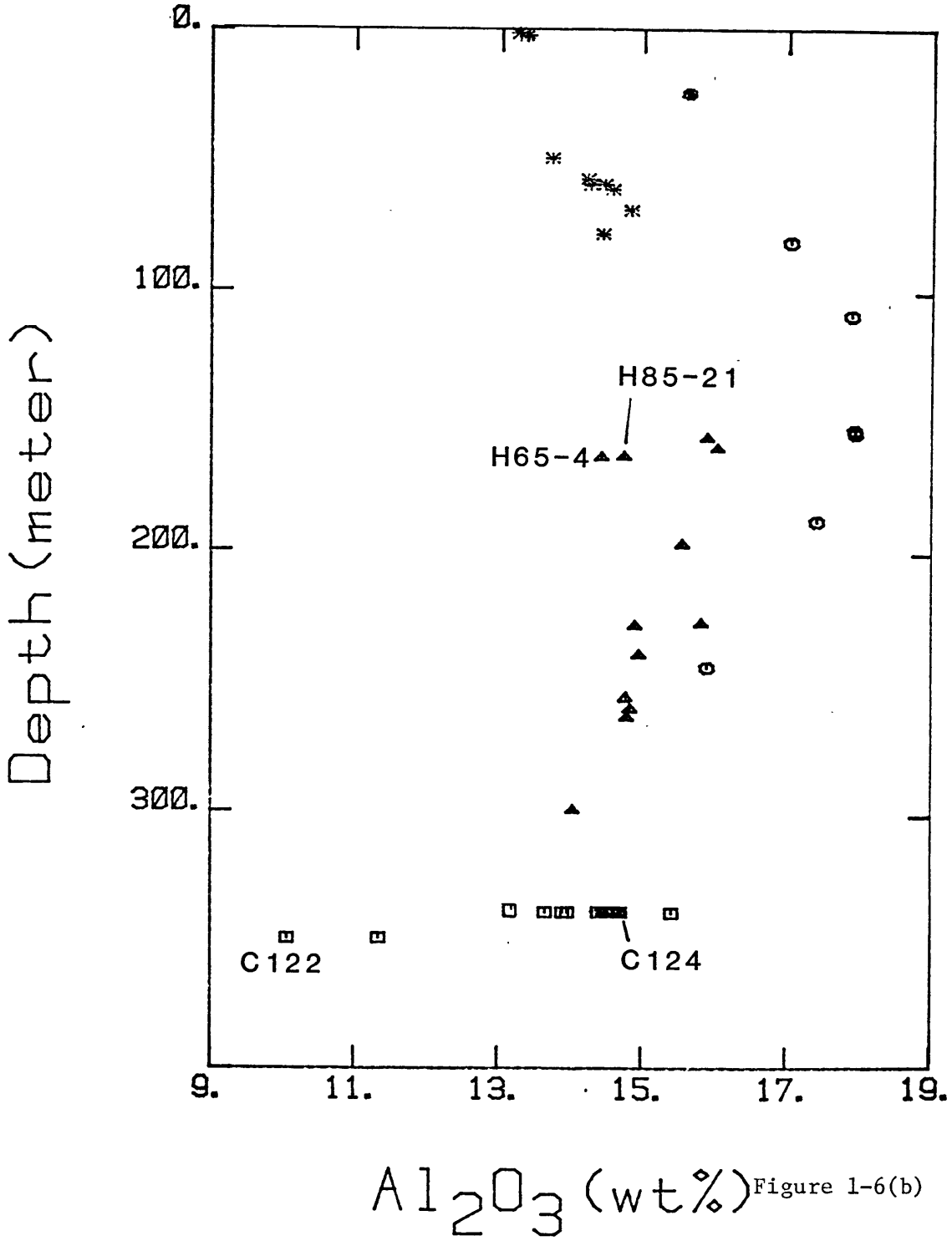

0.
100.
200.
300.
Depth (meter)
H85-21
H65-4
C122
C124
9.
11.
13.
15.
17.
19.
Al2O3 (wt%)

Figure 1-6(b)

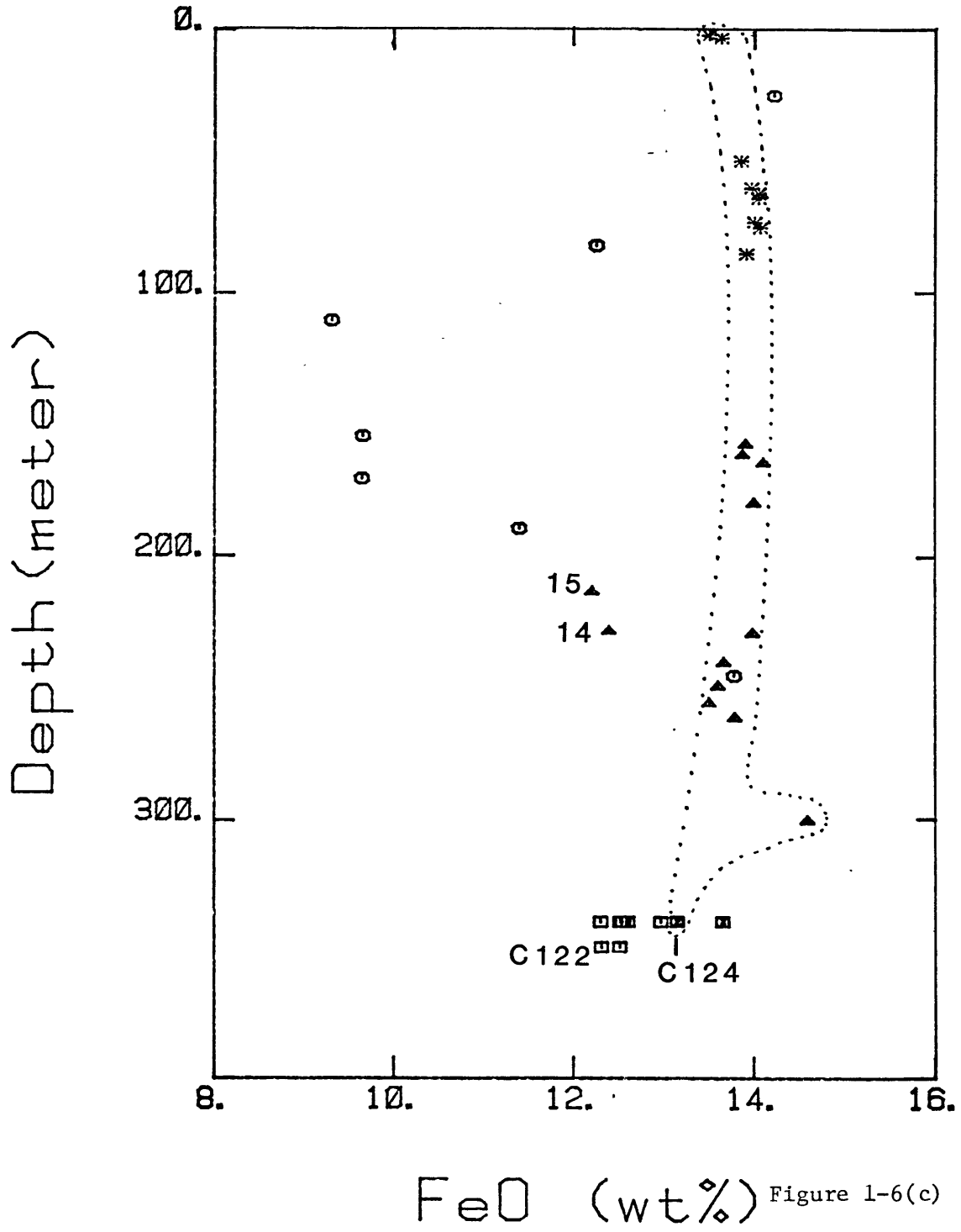


Figure 1-6(c)

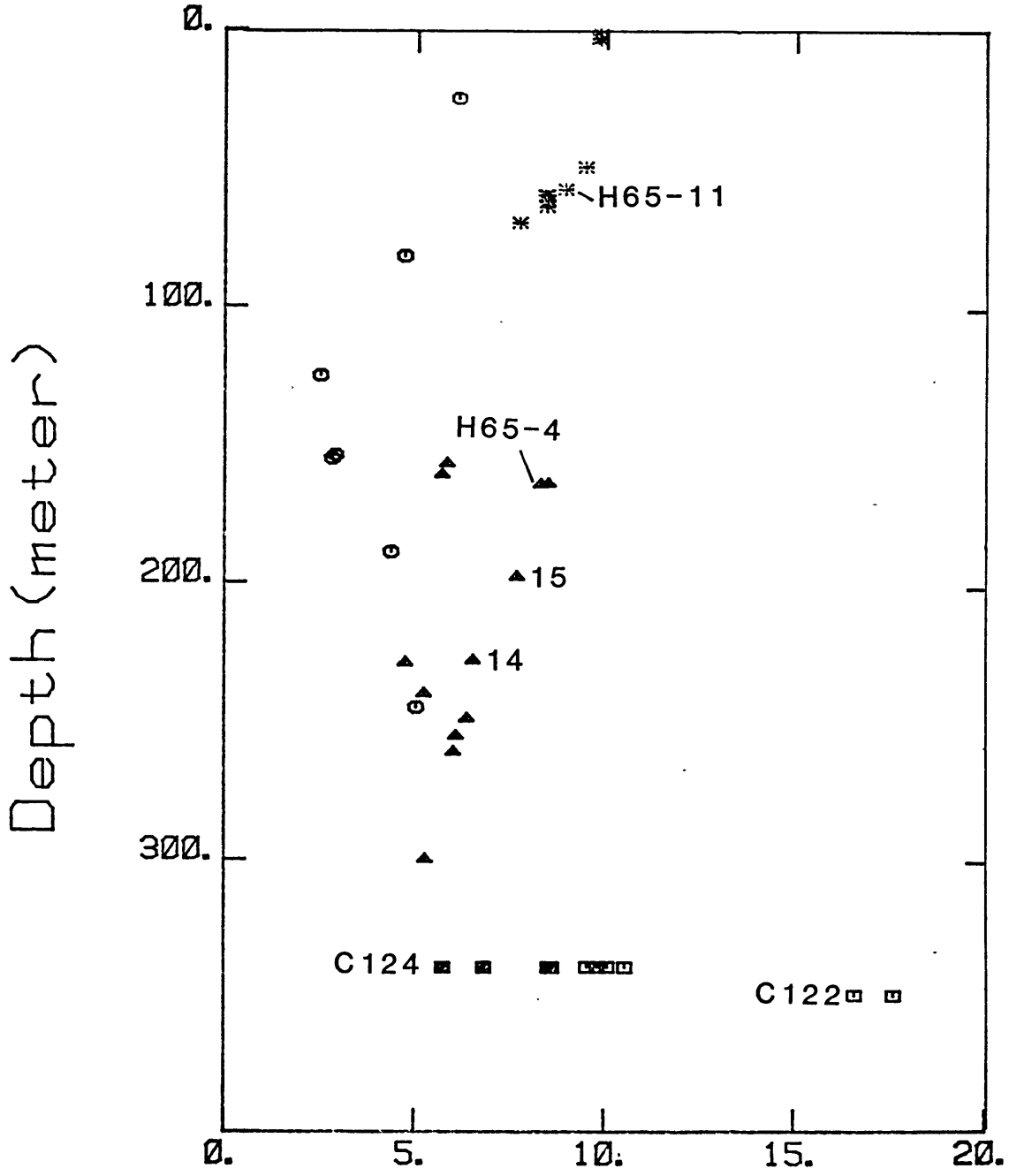

0.
100.
200.
300.
Depth (meter)
H65-11
H65-4
15
14
C124
C122
0.
5.
10.
15.
20.
MgO (wt%)

Figure 1-6(d)

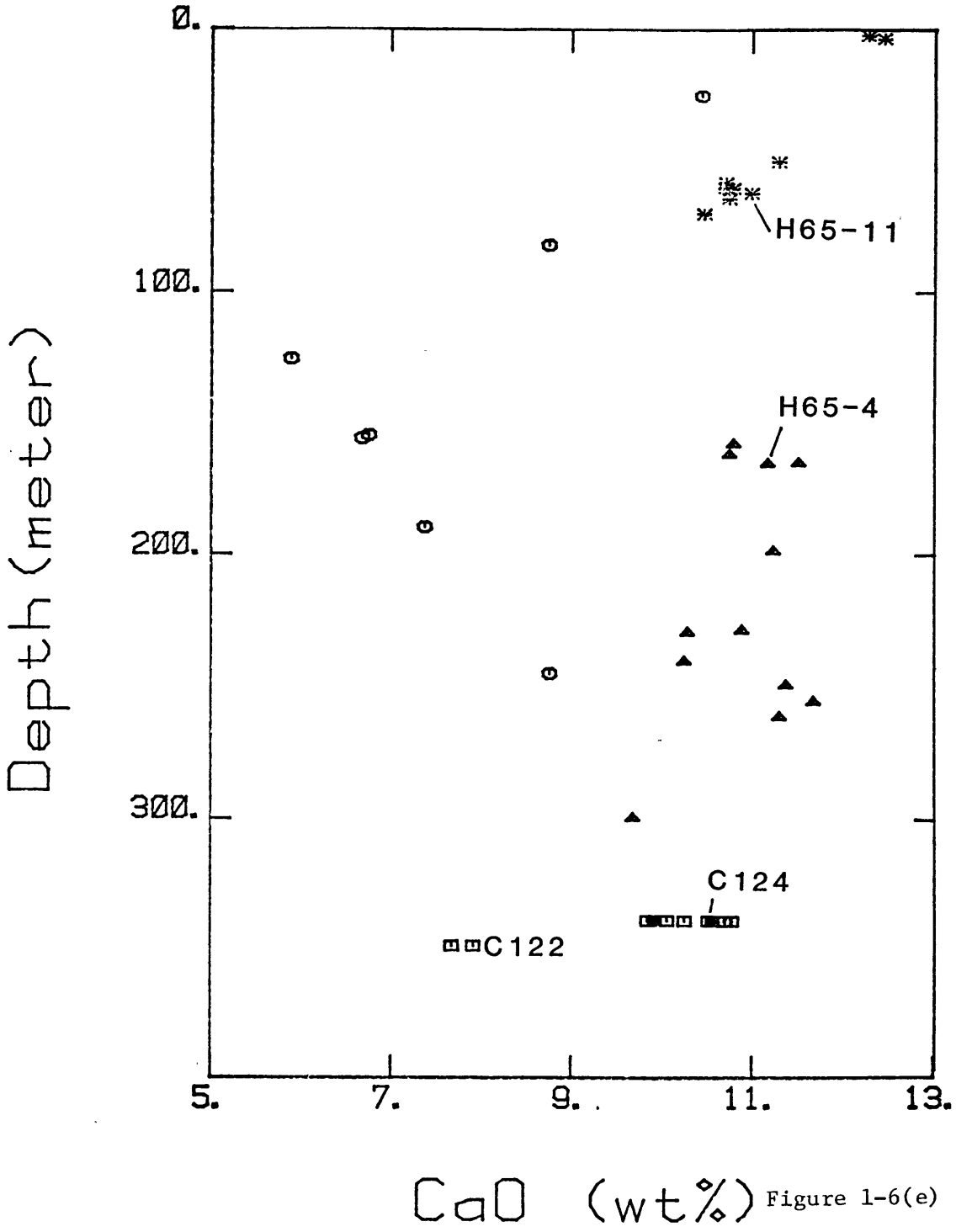


Figure 1-6(e)

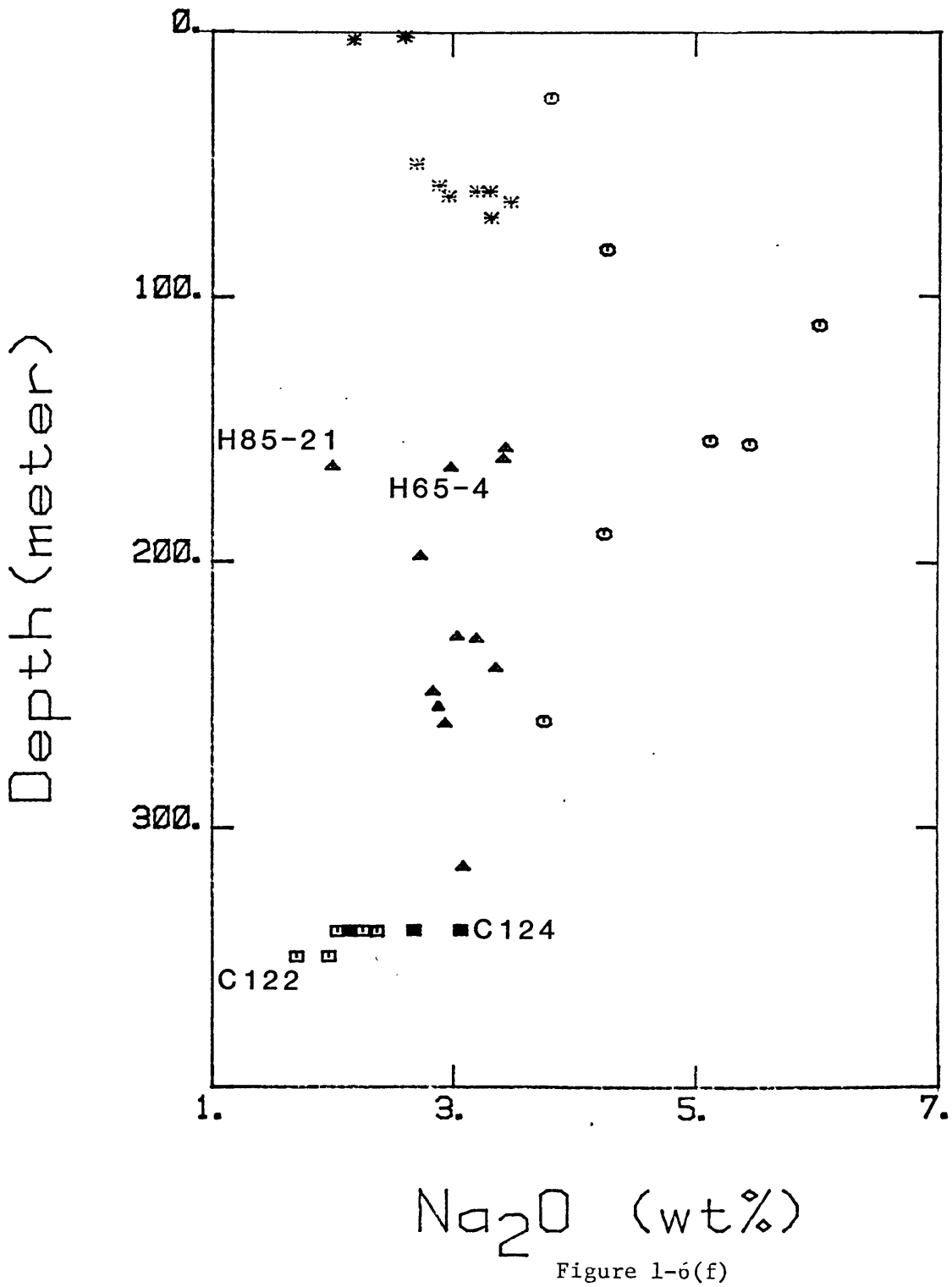


Figure 1-6(f)

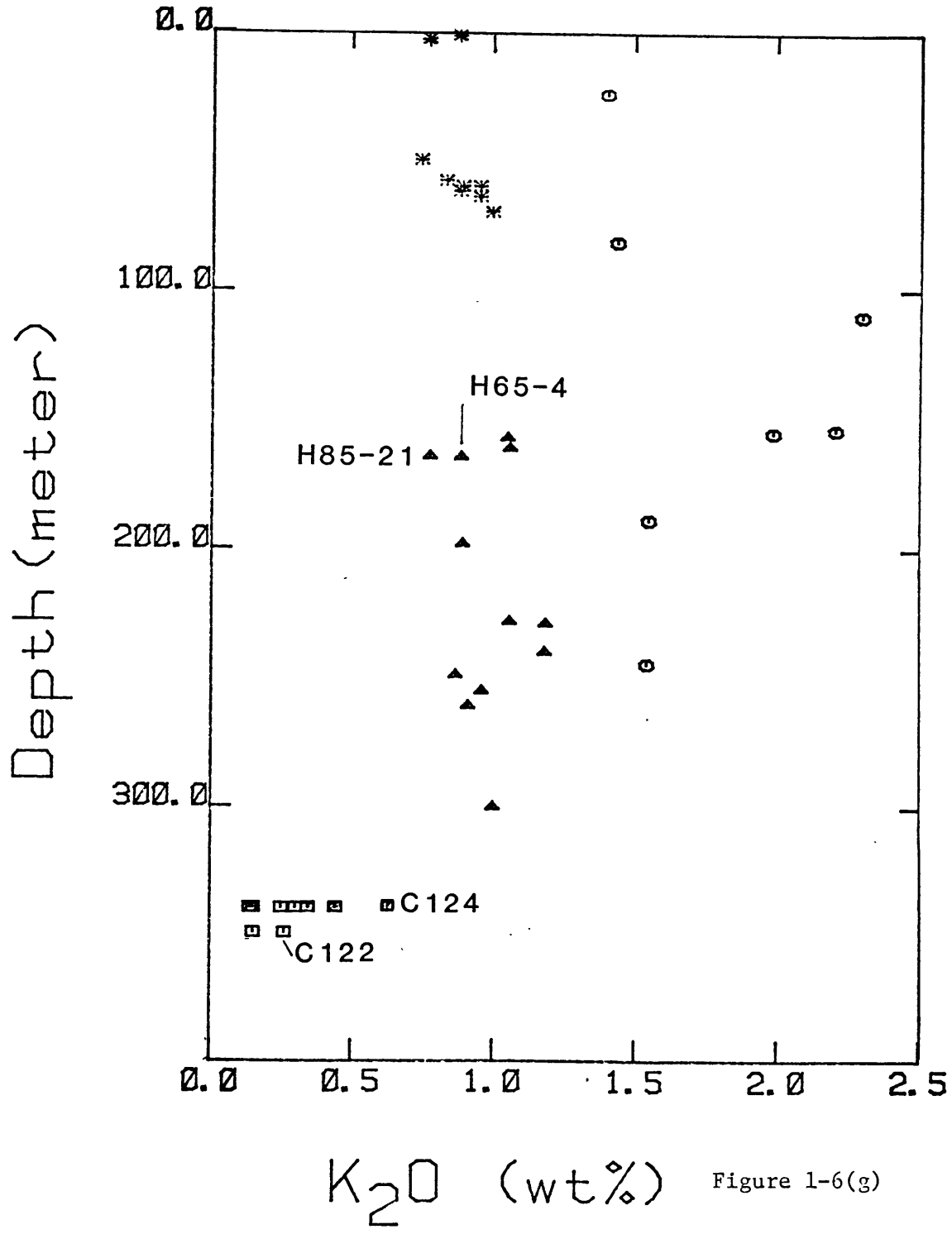

0.0
100.0
200.0
300.0
Depth(meter)
H65-4
H85-21
C124
C122
0.0
0.5
1.0
1.5
2.0
2.5
K2O (wt%)

Figure 1-6(g)

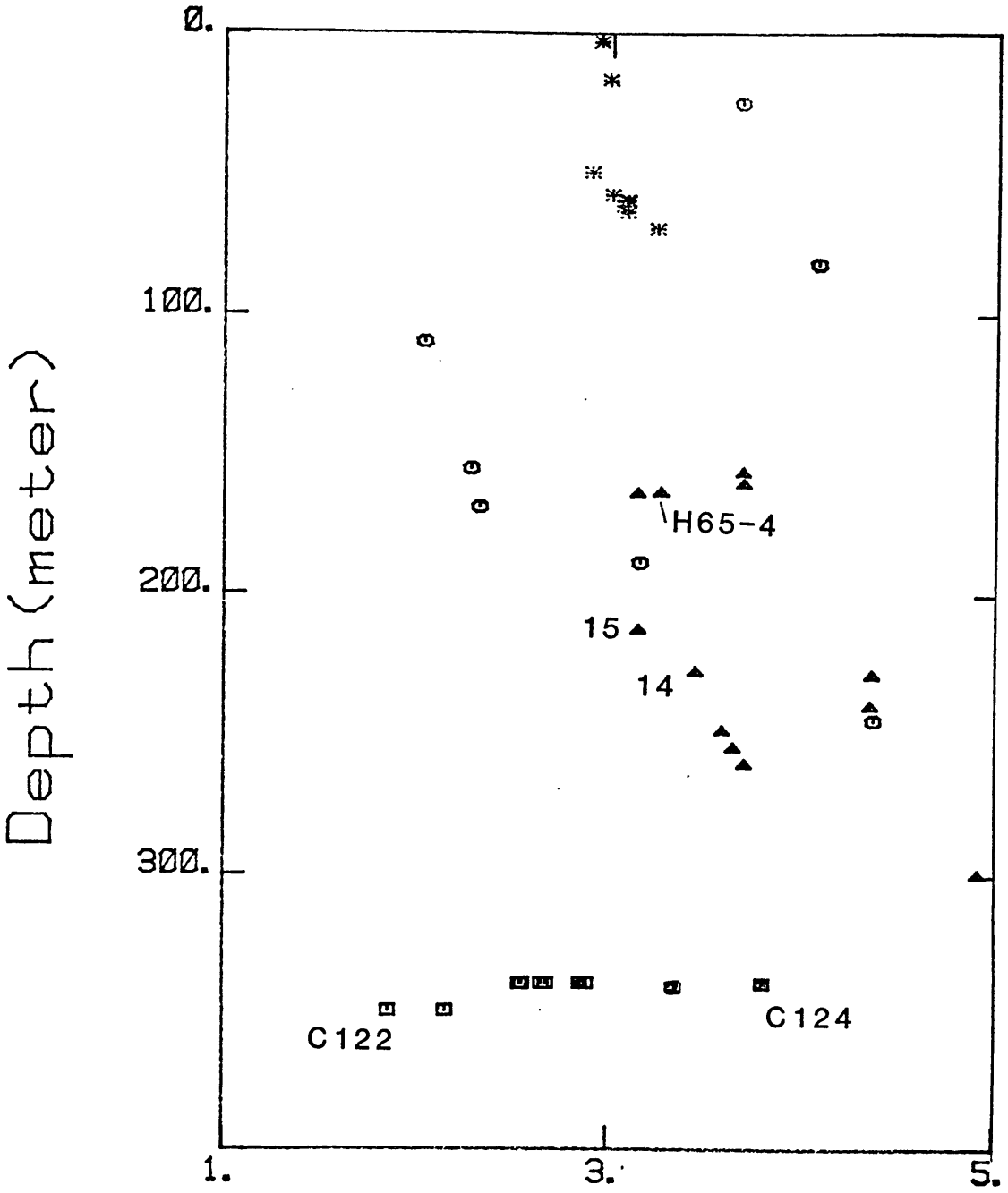


Figure 1-6(h)

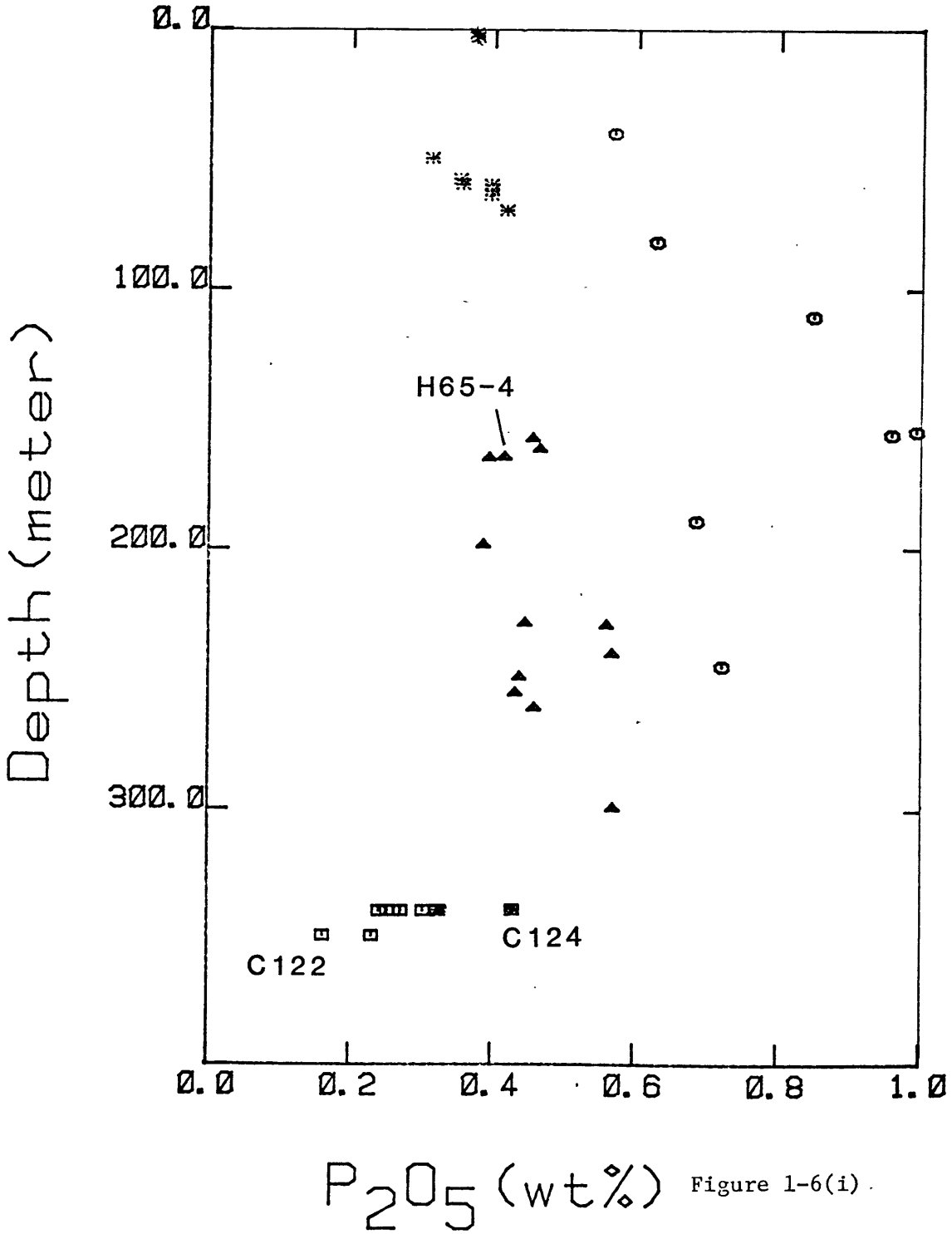

0.0
100.0
200.0
300.0
Depth (meter)
H65-4
C122
C124
0.0
0.2
0.4
0.6
0.8
1.0
P2O5 (wt%)

Figure 1-6(i)

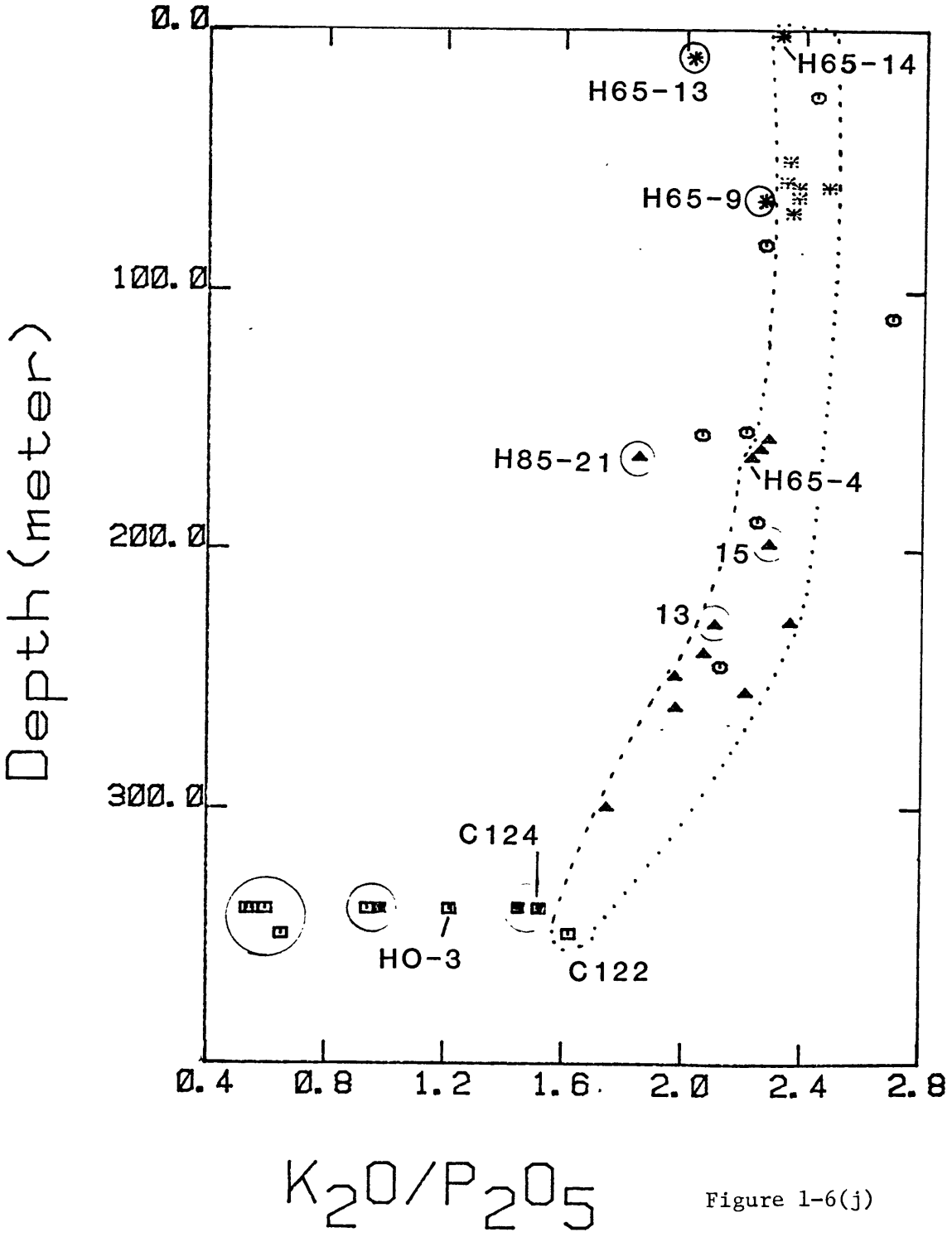

0.0
100.0
200.0
300.0
Depth (meter)
H65-13
H65-14
H65-9
H85-21
H65-4
15
13
C124
HO-3
C122
0.4
0.8
1.2
1.6
2.0
2.4
2.8
K2O/P2O5

Figure 1-6(j)

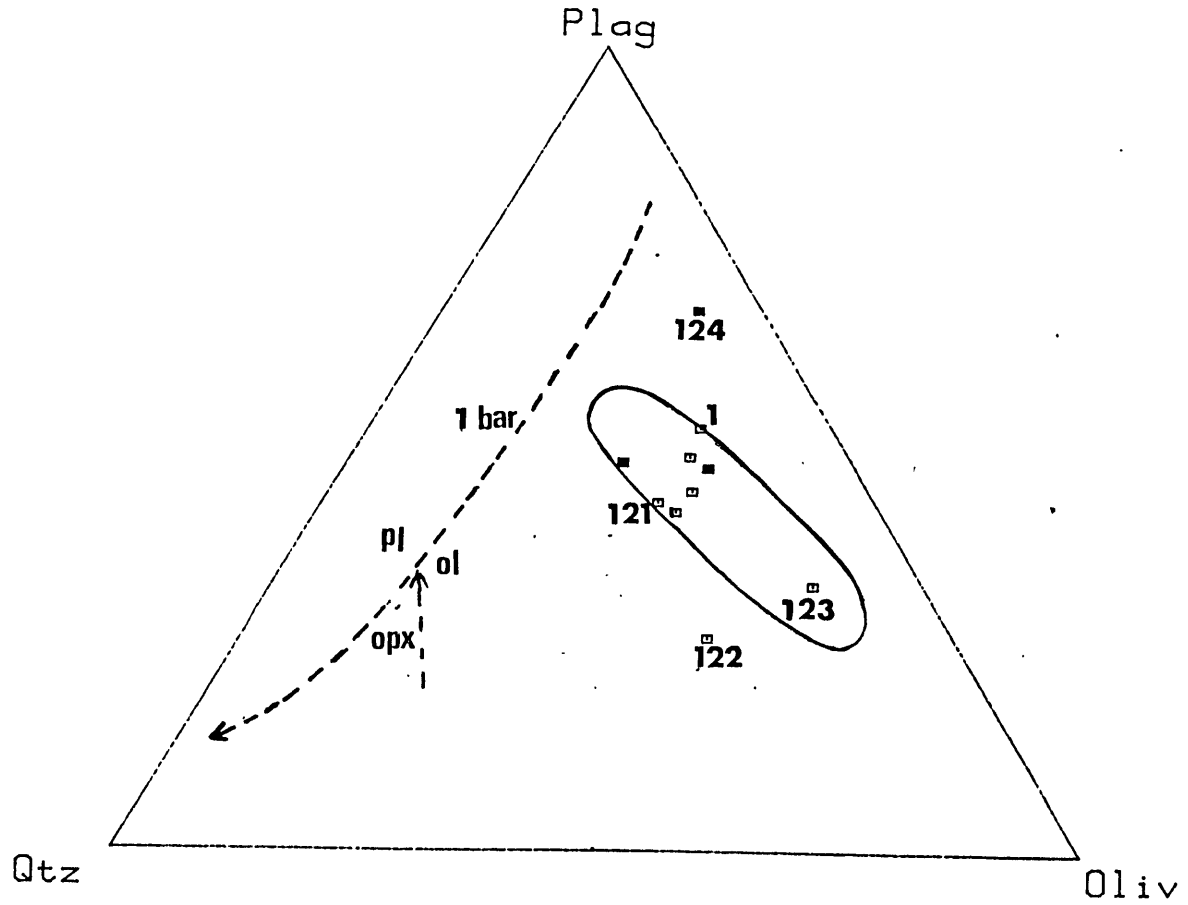


Figure 1-7(a)

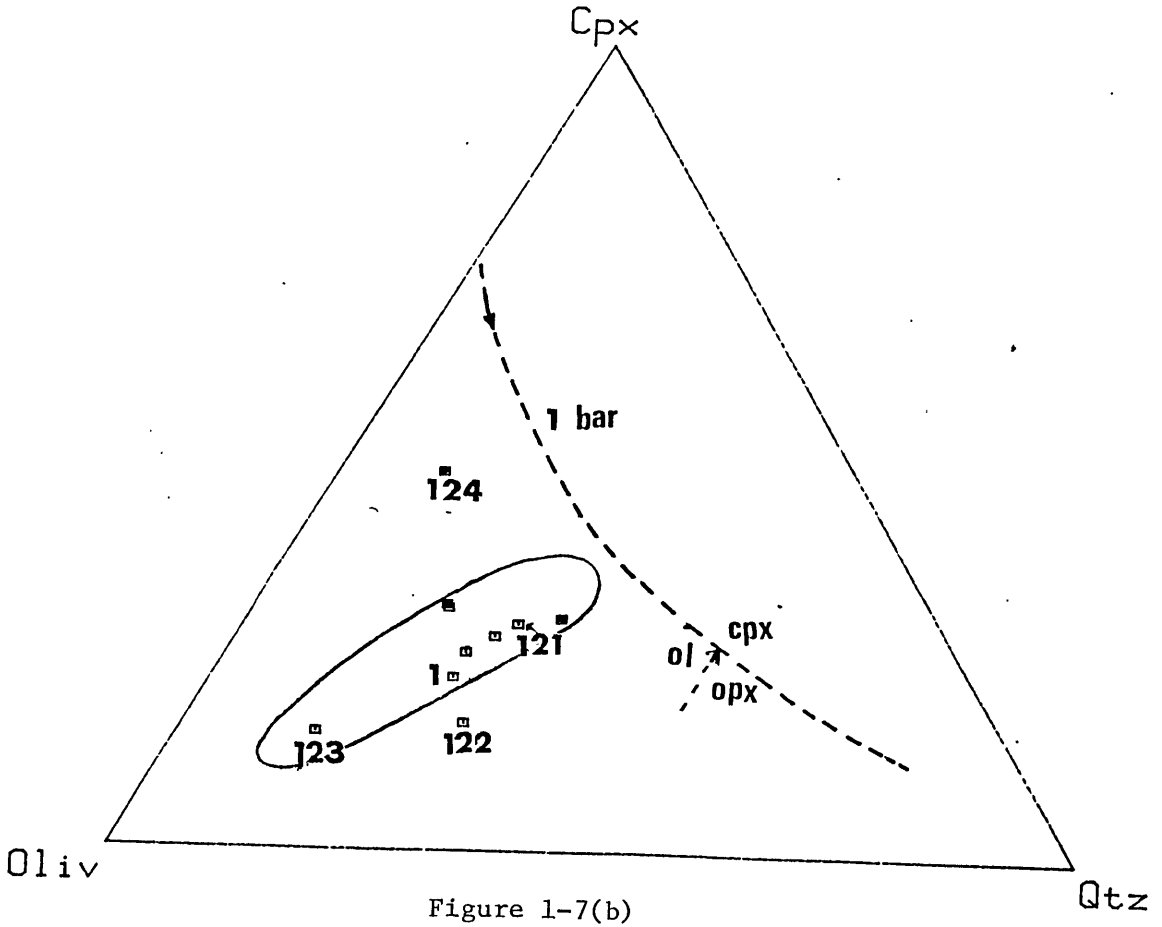


Figure 1-7(b)

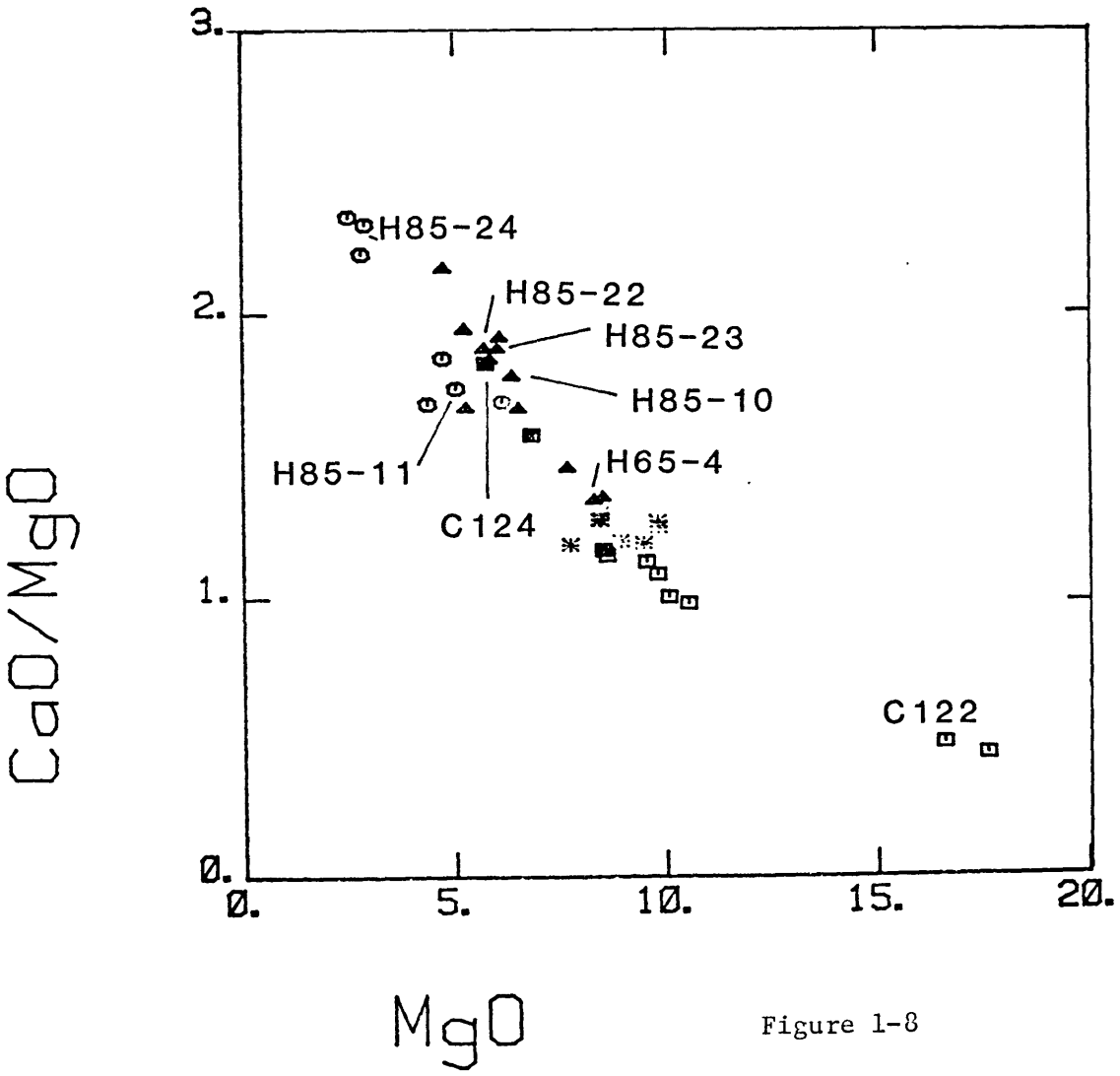

3.
2.
1.
0.
0.
5.
10.
15.
20.
CaO/MgO
MgO
H85-24
H85-22
H85-23
H85-10
H85-11
H65-4
C124
C122

Figure 1-8

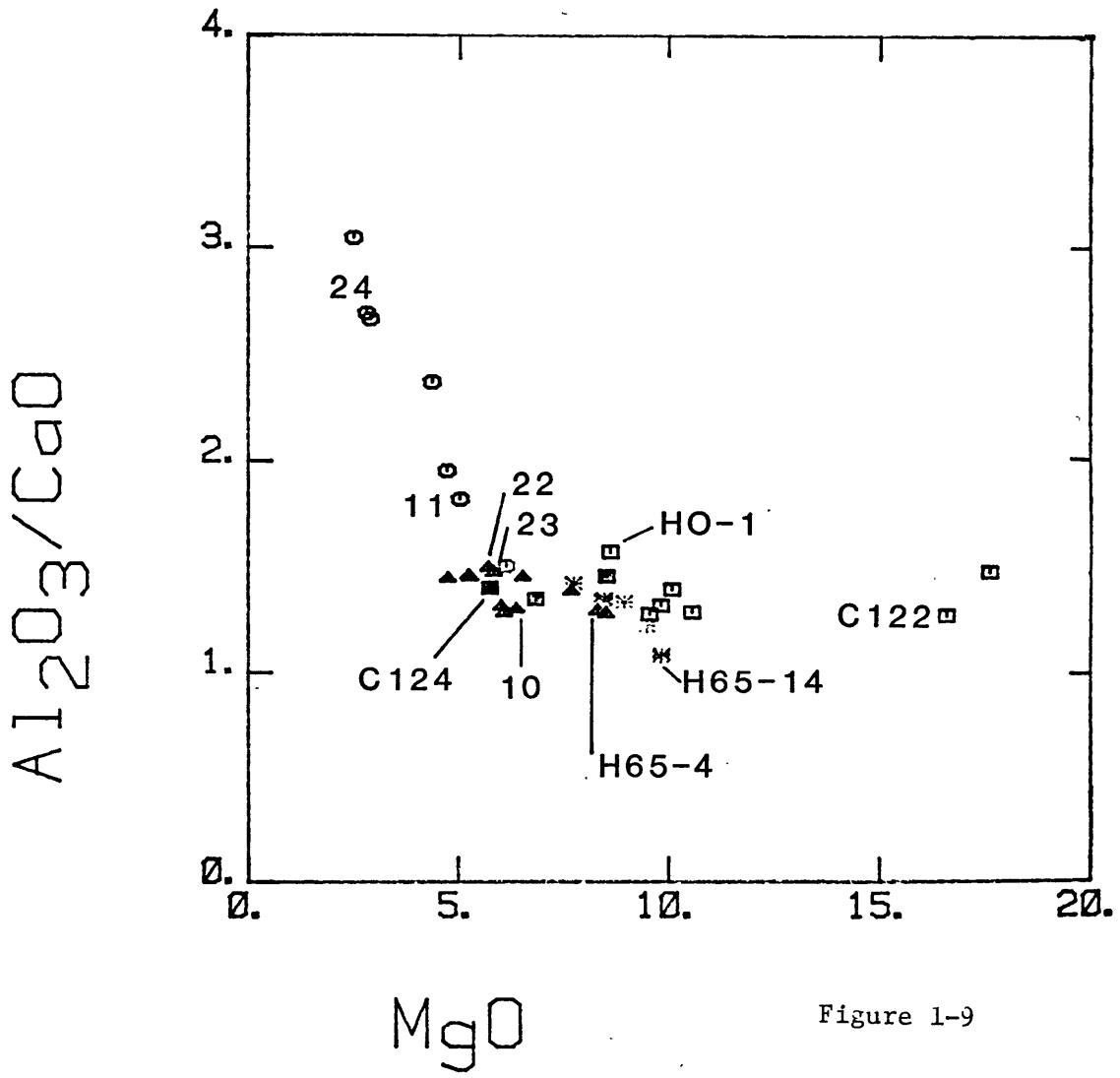

4.
3.
2.
1.
0.
0.
5.
10.
15.
20.
Al2O3/CaO
MgO
24
11
22
23
HO-1
C122
C124
10
H65-14
H65-4

Figure 1-9

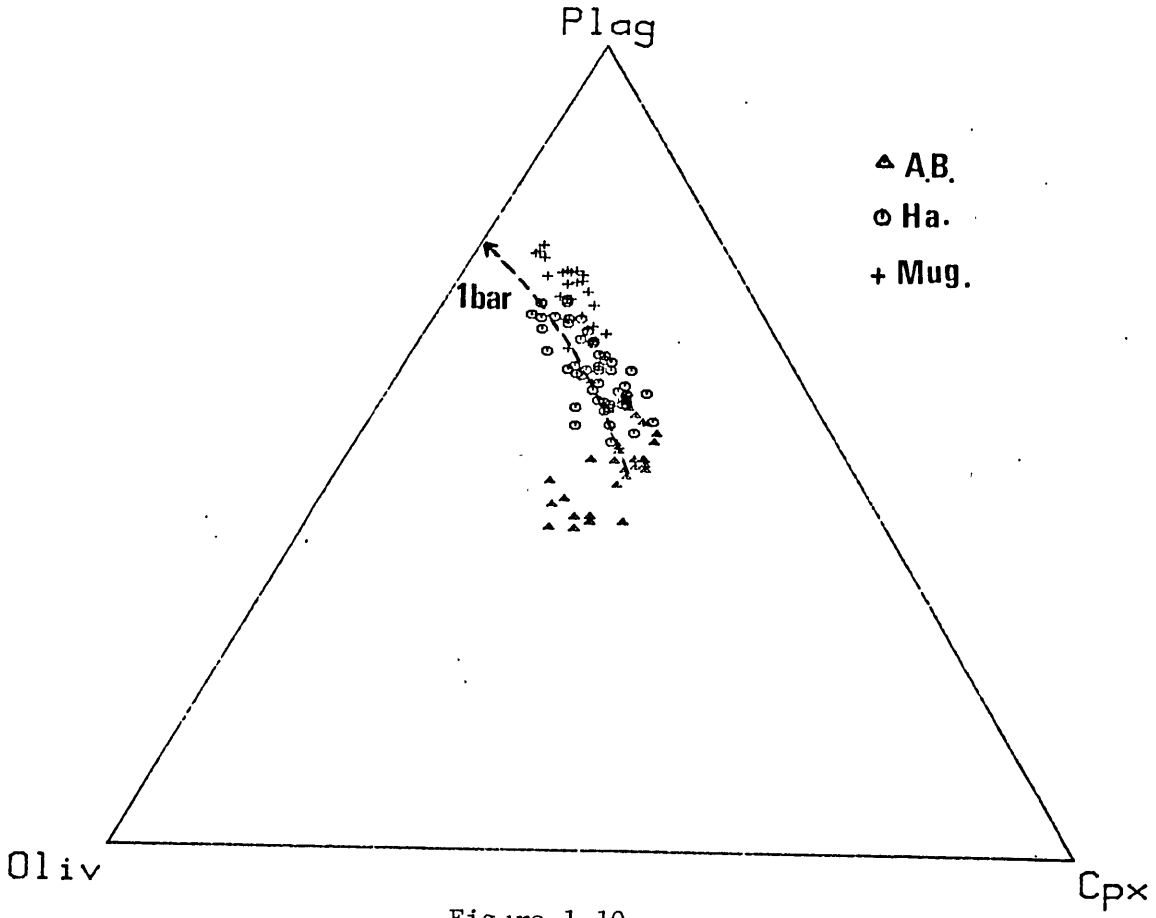


Figure 1-10

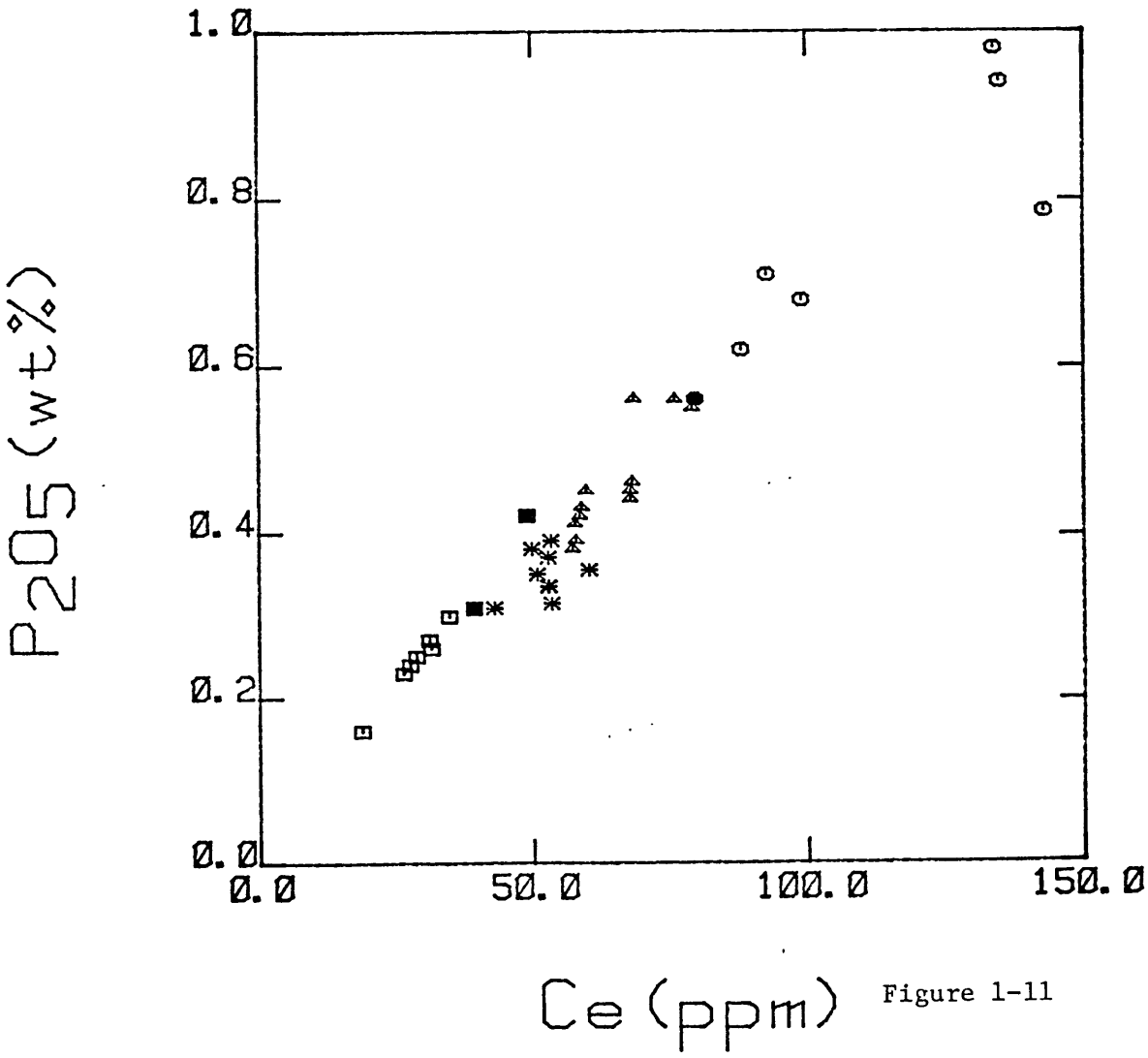


Figure 1-11

CHAPTER 2

$^{87}Sr/^{86}Sr$ AND $^{143}Nd/^{144}Nd$ SYSTEMATICS OF THE HALEAKALA VOLCANIC SERIES

Abstract. Ratios of $^{87}Sr/^{86}Sr$ (0.70306 to 0.70387) and $^{143}Nd/^{144}Nd$ ratios (0.51313 to 0.51291) range widely in samples from the Haleakala volcanic series, but they lie within the Nd-Sr mantle array. Both $^{87}Sr/^{86}Sr$ and $^{143}Nd/^{144}Nd$ ratios vary systematically with time, with older lavas being more radiogenic in $^{87}Sr/^{86}Sr$ but less radiogenic in $^{143}Nd/^{144}Nd$ than the younger lavas. Rb/Sr ratios correlate negatively with $^{87}Sr/^{86}Sr$ ratios and Sm/Nd ratios correlate negatively with $^{143}Nd/^{144}Nd$ ratios for these Haleakala samples. Recent mixing of sources in the mantle is proposed to explain these negative correlations. Compilation of $^{87}Sr/^{86}Sr$ and $^{143}Nd/^{144}Nd$ data suggest that Hawaiian volcanoes such as Loihi, Kilauea, Kohala, East Molokai, Koolau and the Haleakala volcano have very similar isotopic variations with time. The previously observed difference in isotopic ratios among the Hawaiian volcanoes are likely due to the difference in their evolutional stages.

1 Introduction

Previous studies of Hawaiian basalts showed that each Hawaiian volcano may have distinct geochemical characteristics which require different source composition and/or different generation processes (e.g. Macdonald and Katsura, 1964; Macdonald, 1968; Jackson, 1968; Wright, 1971; Clague, 1974; Tatsumoto, 1978; Leeman et al., 1980; Lanphere and Dalrymple, 1980). However, a homogeneous source composition was proposed for some single volcanos such as Kilauea (Hofmann et al., 1978b; Hofmann and Wright, 1979), Molokai (Clague and Beeson, 1980) and Kohala (Feigenson et al., 1982). Since isotopic ratios are difficult to change by partial melting or fractionation processes, they provide the most important evidence for evaluating the source homogeneity or heterogeneity for lavas from a single volcano.

In this study, I analyzed Rb-Sr and Sm-Nd isotopic compositions for 45 samples from the three Haleakala volcanic series: the tholeiitic Honomanu volcanic series, the alkalic Kula volcanic series and the post-erosional Hana volcanic series. Samples of the Kula and Hana volcanic series are from drill cores and have very good stratigraphic control. The objectives of this study are (1) to characterize the Sr and Nd isotopic compositions of the Haleakala volcanic series; (2) to characterize the correlations between parent/daughter abundance variations and isotopic variations; (3) to determine if the Haleakala tholeiites and alkalic basalts can be derived from the same source; (4) to compare the isotopic characteristics of several Hawaiian volcanoes.

2 Analytical Techniques

Abundances of Rb and Sr were determined by isotope dilution method and ratios of $^{87}Sr/^{86}Sr$ and $^{143}Nd/^{144}Nd$ were determined by mass spectrometry at M.I.T. The Rb-Sr procedure has been described by Hart and Brooks (1977). The Nd-Sm procedure is modified after the technique of Richard (Richard et al., 1976) and has been described by Zindler (1980). The blanks are about 0.1 ng for Rb and 1 ng for Sr. Intra-run precision (2σ) for $^{87}Sr/^{86}Sr$ and $^{143}Nd/^{144}Nd$ measurements is generally better than 0.005%. During the period of this study, 4 runs of Eimer and Amend $SrCO_3$ standard average to $0.70780\pm0.00005(2\sigma)$ in $^{87}Sr/^{86}Sr$ ratios. The $^{87}Sr/^{86}Sr$ ratios reported here have been adjusted so that the Eimer and Amend $SrCO_3$ standard will yield a value of 0.70800. Three runs of BCR-1 yield 0.51265 ± 0.00003 (2σ) in $^{143}Nd/^{144}Nd$ ratio. Duplicate analyses of $^{87}Sr/^{86}Sr$ and $^{143}Nd/^{144}Nd$ have been done for a few samples in the beginning and at the end of this study to check if there is any systematic analytical error due to machine drift.

No systematic error was observed (Table 1). One sample (C-123) has been run using both spiked and unspiked method to check the effect of the Rb-Sr spike on the $^{87}Sr/^{86}Sr$ ratios. The two measurements agree very well (Table 2). Based on duplicate analyses of a sample (H85-8) the precision (2σ) for Rb, Sr abundance is estimated to be better than 1%. The Nd and Sm abundances are determined by Instrumental Neutron Activation (INAA) method at M.I.T. Based on 5 replicate analyses of H85-8 the precision (2σ) is estimated to be better than 5% for Nd and 2% for Sm (Chapter 3). H_2O and CO_2 contents in these Haleakala basalts were determined by CHN analyses at Woods Hole Oceanographic Institution (Chapter 1).

3 Results

(a) Abundances of Rb and Sr and Sr isotopic ratios

The Haleakala basalts range widely in Sr isotopic ratios (0.70306 to 0.70387) and in Rb/Sr ratios (0.001 to 0.057), and the three volcanic series have distinct isotopic compositions (Table 2). The $^{87}Sr/^{86}Sr$ ratios for eight tholeiites range from 0.70373 to 0.70387 with a mean value of 0.70382 and two standard deviations (2σ) of 0.00008. The range of $^{87}Sr/^{86}Sr$ variation for these tholeiites is slightly larger than the analytical errors at the 95% confidence level (2σ), but is within the analytical errors at the 99.7% confidence level (3σ).

However, Rb/Sr ratios for these tholeiites range widely (from 0.001 to 0.020). A similar wide range of Rb/Sr ratios has been observed in other Hawaiian tholeiites such as those from Koolau volcano, Oahu and Kohala volcano, Island of Hawaii (Lanphere and Dalrymple, 1980; Feigenson, et al., 1982).

The two transitional basalts (C125 and C126) have the same $^{87}Sr/^{86}Sr$ ratios as the tholeiites (Table 2). The alkalic basalt (C124) from the

Honomanu volcanic series has $^{87}Sr/^{86}Sr$ ratio slightly lower (but within 3σ analytical error) than the average tholeiites (Table 2). Haleakala tholeiites with very low Rb/Sr ratios have low Rb(<1 ppm) concentrations (Table 2). These samples also have extremely high K/Rb ratios (>2000, Chapter 3). The two tholeiites with high Rb/Sr ratios contain greater than 4 ppm Rb and have relatively lower H_2O content than the other tholeiites (Table 2); consequently, they are probably more representative of the magmatic compositions. Tholeiites with low Rb content, low Rb/Sr ratio and high K/Rb contain altered glass and iddingsitized rims on olivine crystals (Chapters 1 and 3).

The alkalic basalts (18 samples) from the Kula volcanic series range in $^{87}Sr/^{86}Sr$ ratios from 0.70317 to 0.70346 with a mean value of 0.70335 and 2σ of 0.00014. The range in Rb/Sr ratios is from 0.022 to 0.033. The hawaiites and mugearites (6 samples) from the Kula volcanic series have $^{87}Sr/^{86}Sr$ ratios ranging from 0.70318 to 0.70347 which is similar to that of the alkalic basalts. However, the Rb/Sr ratios (0.029 to 0.057) for hawaiites and mugearites are higher than those of the alkalic basalts.

Ten samples of alkalic basalts, ankaramite, and hawaiites from the post-erosional Hana volcanic series range in $^{87}Sr/^{86}Sr$ ratios from 0.70306 to 0.70326, with a mean value of 0.70319 and 2σ of 0.00012. The Rb/Sr ratios range from 0.029 to 0.036. Variations of the Sr isotopic ratios in both the Kula volcanic series and the Hana volcanic series are much larger than the analytical errors and reflect isotopic heterogeneity for these lavas.

(b) Abundances of Nd and Sm and Nd isotopic ratios

Table 3 summarizes the results of Nd and Sm abundances and $^{143}Nd/^{144}Nd$ measurements. The $^{143}Nd/^{144}Nd$ ratios vary from 0.51291 to 0.51311 and the

Sm/Nd ratios vary from 0.303 to 0.182 for the three Haleakala volcanic series (Table 3). Eight tholeiites from the Honomanu volcanic series range in $^{143}Nd/^{144}Nd$ from 0.51291 to 0.51298, with a mean value of 0.51293 and 2σ of 0.00005. The Sm/Nd ratios for the tholeiites are quite constant (0.265 to 0.280) except for sample C-122 (0.303). The transitional basalts and alkalic basalt from the Honomanu volcanic series have similar range of $^{143}Nd/^{144}Nd$ and Sm/Nd ratios (Table 3).

The alkalic basalts from the Kula volcanic series have higher $^{143}Nd/^{144}Nd$ ratios (0.51297 to 0.51309) and lower Sm/Nd ratios (0.213 to 0.246) than the tholeiites. As in the $^{87}Sr/^{86}Sr$ and Rb/Sr ratios, the hawaiites and mugearites span the same range in $^{143}Nd/^{144}Nd$ ratios as those of the alkalic basalts, but they have lower Sm/Nd ratios (0.188 to 0.233).

For the Hana volcanic series, 9 samples have $^{143}Nd/^{144}Nd$ ratios ranging from 0.51306 to 0.51313 and Sm/Nd ratios ranging from 0.229 to 0.245.

Variations of $^{143}Nd/^{144}Nd$ ratios within the Honomanu volcanic series and within the Hana volcanic series are slightly larger than analytical errors at the 95% confidence level (2σ), but are within the analytical errors at the 99.7% confidence level (3σ). Variations of $^{143}Nd/^{144}Nd$ ratios within the Kula volcanic series are larger than 3σ analytical errors.

4 Discussion

4-1 Correlation of parent/daughter abundance ratios and isotopic ratios

If the altered tholeiites and highly fractionated hawaiites and mugearites are excluded, the Haleakala samples show a negative correlation between Rb/Sr ratios and $^{87}Sr/^{86}Sr$ ratios (Fig. 2-1). The alkalic basalts have higher Rb/Sr ratios but lower $^{87}Sr/^{86}Sr$ ratios than the tholeiites. This negative correlation trend is opposite to the well-known Rb-Sr "mantle

isochron" established by oceanic samples when average Rb/Sr ratios and average $^{87}Sr/^{86}Sr$ ratios for individual ocean basins and oceanic islands are compared (Brooks et al., 1976; Duncan and Compston, 1976; Hedge, 1978; Hart and Brooks 1980). Negative correlation between Rb/Sr ratios and $^{87}Sr/^{86}Sr$ ratios is not unique to the Haleakala volcanic series, samples from other Hawaiian volcanoes such as Loihi seamount (Frey and Clague, 1982; Lanphere, 1982) and from other oceanic islands such as Canary Islands, Jan Mayen, Cape Verde Islands (Bence, 1966; Lussiaa-Berdon-Polve and Vidal, 1973; Klerkx et al., 1974; O'Nions and Pankhurst, 1974; Brooks et al., 1976) also show a negative correlation between Rb/Sr ratios and $^{87}Sr/^{86}Sr$ ratios for each island.

The hawaiites and mugearites have Sr and Nd isotopic ratios similar to those of alkalic basalts but have higher Rb/Sr and lower Sm/Nd ratios than the alkalic basalts. Since clinopyroxene and plagioclase are the major phases which have been fractionated from the alkalic basalts to derive the hawaiites and mugearites (Chapter 1), higher Rb/Sr ratios for the hawaiites and mugearites are expected. For example, an alkalic basalt H85-23 has the same Sr and Nd isotopic ratios as a mugearite H85-24. By using clinopyroxene, plagioclase, olivine and magnetite fractionation proportions calculated from major element compositions (Chapter 1, Table 3) and partition coefficients for Rb and Sr from the literature (Philpotts and Schnetzler, 1970; Hart and Brooks, 1974; Shimizu, 1974; Arth, 1976) fractionation of H85-23 to H85-24 would increase the Rb/Sr ratio by factors of 1.46 to 2.06, depending on whether low or high values of partition coefficients are used. Increase of the Rb/Sr ratio by a factor of 1.46 would increase the Rb/Sr ratio of H85-23 (0.030) to that of the H85-24 (0.044). Similarly, the lower Sm/Nd ratio of the hawaiites and mugearites

are due to fractionation of abundant clinopyroxene from the alkalic basalts (Chapter 3). For tholeiites and alkalic basalts, olivine is the dominant fractionating phase (Chapter 1), thus fractional crystallization is relatively ineffective in changing the Rb/Sr and Sm/Nd ratios of these basalts (Gast, 1968).

Brooks et al. (1976) noticed the higher Rb/Sr ratios in alkalic basalts compared to tholeiites for samples from Hawaiian islands as well as other oceanic islands and they proposed that the difference in Rb/Sr ratios between tholeiites and alkalic basalts is due to the melting process. Specifically, they suggested that the alkalic basalts were derived by smaller degrees of melting with amphibole as residual phase in the source region, or the melts re-equilibrated with amphibole-bearing mantle at a shallow depth (Brooks et al., 1976; Hart and Brooks, 1980). However, this explanation cannot adequately explain the heterogeneous isotopic ratios among the Honomanu tholeiites, Kula alkalic basalts and Hana alkalic basalts (Fig. 2-1) or the factor of 1.6 variation in Rb/Sr among the alkalic basalts. The different $^{87}Sr/^{86}Sr$ and Rb/Sr ratios and inverse trend (Fig. 2-1) in the Haleakala volcanic series must be due to processes other than partial melting and fractionation.

Other possible explanations for the Rb-Sr variations are (1) contamination and (2) source heterogeneity.

Sediments are ruled out as a possible contaminating source because of their high Rb/Sr and high $^{87}Sr/^{86}Sr$ ratios (Dasch, 1969; Biscaye and Dasch, 1971; Church, 1971). Since all the Haleakala samples plot inside the "mantle array" (Figs. 2-3), significant contamination from seawater is also unlikely (Hawkesworth et al., 1977; DePaolo and Wasserburg, 1977). A contamination processs involving carbonates has been proposed (Brooks et

al., 1976), but the limited data for carbonates shows that $^{87}Sr/^{86}Sr$ ratios for carbonates are about the same as seawater (0.709) with Rb/Sr ratio of 0.005 and Sr abundance as high as 2000 ppm (Dasch, 1969). The two least-fractionated tholeiites have Sr abundance of 207 ppm and 307 ppm. If carbonate contamination were responsible for the negative Rb/Sr - $^{87}Sr/^{86}Sr$ correlation, the basaltic Sr abundances should be the upper limit of the magmatic compositions. It would take only 1% to 2% of carbonates with a $^{87}Sr/^{86}Sr$ ratio of 0.709 and Sr abundance 7 to 10 times of the basalts to change the $^{87}Sr/^{86}Sr$ ratio of the basalt from the lowest observed value of 0.70306 to the highest value of 0.70387. However, 1% to 2% carbonate contamination only changes the Rb/Sr ratio by about 2% which is much smaller than the observed Rb/Sr variations of the fresh samples (Table 2). Lack of correlation between $^{87}Sr/^{86}Sr$ ratio and CO_2 content also argues against carbonate contamination as the cause of the negative Rb/Sr -$^{87}Sr/^{86}Sr$ correlation. Furthermore, the non-linear trend of $^{143}Nd/^{144}Nd$ vs. Sm/Nd (Fig. 2.2) is not consistent with two component mixing. This is also confirmed by trace element abundance variations (Chapter 3).

Therefore, the Rb/Sr-$^{87}Sr/^{86}Sr$, and Sm/Nd-$^{143}Nd/^{144}Nd$ variations must reflect source heterogeneity. Negative correlation between isotopic ratios and parent/daughter abundance ratios (Fig. 2-1 and 2-2) cannot reflect a long-term history of the Haleakala source and must be due to recent processes in the mantle. Possible processes which will produce such mantle sources will be discussed in Chapter 4.

4-2 The Mantle Array

Previous isotopic studies have documented a negative Sr-Nd correlation trend for oceanic basalts and continental basalts and defined the trend as a "mantle array" (DePaolo and Wasserburg, 1976a,b; O'Nions et al., 1977;

Hawkesworth et al., 1977; Hart and Brooks, 1980; Dosso and Murthy, 1980). O'Nions et al. (1977) noticed an exception for Hawaiian basalts and concluded that the negative correlation does not pertain to the Hawaiian samples. However, in this study, all the samples from the three Haleakala volcanic series fall into the mantle array (Fig. 2-3).

A negative Sr-Nd correlation has also been observed in other Hawaiian volcanic series such as Loihi seamount (Staudigel et al., 1981), the post-erosional Honolulu Volcanics and the Koolau tholeiites (Roden et al., 1981). Data for the Haleakala samples, the Loihi samples and data from O'Nions et al. (1977) are plotted in Figure 2-3 for comparison. In general, there is a negative correlation between $^{87}Sr/^{86}Sr$ and $^{143}Nd/^{144}Nd$. However one sample, a tholeiite (T-10) from Mauna Loa, has a typical $^{143}Nd/^{144}Nd$ ratio (0.51288±2) while the $^{87}Sr/^{86}Sr$ ratio (0.70331) (O'Nions et al., 1977) is much lower than other Hawaiian tholeiites. The reason for the abnormal $^{87}Sr/^{86}Sr$ ratio of this sample is unknown. However, another tholeiite from Mauna Loa (HA-5) reported by O'Nions et al. (1977) has $^{143}Nd/^{144}Nd$ of (0.51289±3) and $^{87}Sr/^{86}Sr$ ratio of 0.70380 which plots in the mantle array along with other Hawaiian samples (Fig. 2-3).

Models such as sequential partial melting and remixing events in the mantle (Allegre et al., 1980), two-stage enriched and depleted events in the mantle (Anderson, 1982), mixing of MORB type depleted mantle with sediments or altered oceanic crust (Hofmann and White, 1982), mixing of MORB-type source with melts from enriched mantle source, mixing of magmas from enriched and depleted mantle reservoirs (Anderson, 1982), and mixing of three components (Zindler et al., 1982) have been proposed to explain the observed Nd-Sr mantle array. However, a wide variety of samples plot within the mantle array; e.g., ultramafic nodules which have undergone

mantle metasomatic events (e.g., Menzies and Murthy, 1980a, Chen and Frey, 1980), basalts from the Hawaiian Islands, Canary Islands, Cape Verde Islands which all have negative correlations between Rb/Sr ratios and Sr isotopic ratios; and basalts from Kerguelen Island, and Samoa Island which have positive correlations between Rb/Sr ratios and Sr isotopic ratios (Brooks et al. 1976). Apparently, the inverse trend between $^{143}Nd/^{144}Nd$ and $^{87}Sr/^{86}Sr$ reflects the covariation of Rb/Sr and Nd/Sm ratios during petrogenic process. However, the diverse geochemical characteristics of the samples in the mantle array cannot result from only one of the models mentioned above, and a combination of models is necessary.

4-3 Systematic $^{87}Sr/^{86}Sr$ and $^{143}Nd/^{144}Nd$ variations with time of eruption

The alkalic basalts in this study are from drill cores (Chapter 1); consequently, we have very good stratigraphic control for these samples. However, the drill cores do not contain tholeiites, but the stratigraphic position of the tholeiites is below the alkalic series based on field relationships. K-Ar dating yielded ages of 0.84 m.y. and 0.45 m.y. for samples from the basal and upper sections, respectively, of the Kula volcanic series (McDougall, 1964). Age corrections in the initial $^{87}Sr/^{86}Sr$ ratios and $^{143}Nd/^{144}Nd$ ratios are negligible (less than 1×10^{-5}) for these young basalts. In Figure 2-4, $^{87}Sr/^{86}Sr$ ratios are shown versus stratigraphic sequence for the Haleakala samples. The average $^{87}Sr/^{86}Sr$ ratio of the tholeiites is plotted at an arbitrary depth greater than 300 meters which is the depth at the bottom of the drill cores. The data show a general trend of decreasing $^{87}Sr/^{86}Sr$ ratio up the stratigraphic section. This trend, with minor local fluctuations, seems to be more or less continuous for those samples with good stratigraphic control (Fig. 2-4).

The samples from different drill cores fall on the same trend when the "depth" of each sample is adjusted according to the core logs and core correlations (Chapter 1). The $^{143}Nd/^{144}Nd$ trend (Fig. 2-5) is not as obvious as the $^{87}Sr/^{86}Sr$ trend because of smaller range of $^{143}Nd/^{144}Nd$ variations. However, the direction of $^{143}Nd/^{144}Nd$ variation is consistent with the $^{87}Sr/^{86}Sr$ variation. Moreover, hawaiites, mugearites, ankaramites and alkalic basalts fall in the same isotopic variation trends (Figs. 2-4 and 2-5). The systematic decrease in $^{87}Sr/^{86}Sr$ ratios and increase in $^{143}Nd/^{144}Nd$ ratios of these Haleakala volcanic series requires that partial melting involves sources with lower $^{87}Sr/^{86}Sr$ ratios and higher $^{143}Nd/^{144}Nd$ ratios as the volcano evolved.

4-4 Comparison with other Hawaiian volcanoes

Both homogeneous and heterogeneous mantle sources have been proposed for individual Hawaiian volcanic series (e.g. Hart, 1973; O'Nions et al., 1977; Hofmann et al.,1978b; Lanphere et al., 1980; Lanphere and Dalrymple, 1980, Staudigel et al., 1981; Feigenson et al., 1982). Hart (1973) studied four dredged tholeiites which span about 4000 meters in depth from the east Kilauea rift and reported homogeneous $^{87}Sr/^{86}Sr$ ratios (0.70357±10 to 0.70364±10) for these tholeiites. It is suggested that these samples may come from the same flow (Hart, personal communication). Hofmann et al. (1978b) also reported constant $^{87}Sr/^{86}Sr$ ratios (0.70348-0.70360) for the Mauna Ulu eruption of the Kilauea volcano from 1968 to 1974. Feigenson et al. (1982) reported similar $^{87}Sr/^{86}Sr$ ratios (0.70358±8) for tholeiites and transitional basalts from Kohala volcano. However, for the same volcano (Kohala) Lanphere (1982) found significant $^{87}Sr/^{86}Sr$ differences between 2 tholeiites (average 0.70371±25) and 2 alkalic basalts (average 0.70344±4). Lanphere et al. (1980) also found isotopic difference between the

tholeiitic series and alkalic series for other Hawaiian-Emperor volcanoes such as Waianae volcano on Oahu, Midway Island, Koko seamount and Suiko seamount. Unfortunately, the number of samples from any single volcano was too small to make definitive conclusions. An unambiguous demonstration of isotopically heterogeneous mantle sources involved in a single volcano results from the significant isotopic difference between the post-erosional Honolulu Volcanics and the underlying tholeiitic Koolau Volcanics on the island of Oahu (Lanphere and Dalrymple, 1980; Roden et al., 1981).

The gradational changes in $^{87}Sr/^{86}Sr$ and $^{143}Nd/^{144}Nd$ ratios with eruption time in the Haleakala volcanic series and similar results for the East Molokai volcanic series (Clague, personal communication) lead us to suspect that previous reports of isotopic homogeneity within a single Hawaiian volcano results from studying samples of similar age and/or lower analytical precision. A compilation of recent $^{87}Sr/^{86}Sr$ measurements of Hawaiian basalts (Hart, 1973; O'Nions et al., 1977; Hofmann et al., 1978b; Lanphere et al., 1980; Lanphere and Dalrymple, 1980; Staudigel et al., 1981; Feigenson et al., 1982; DePaolo and Wasserberg, 1976b; Clague, personal communication; and this study) is shown in Figure 2-6. This diagram includes only volcanoes with data for more than three samples in each volcanic series. The distance from Kilauea for each volcano is taken from Dalrymple et al. (1980). The diagram shows that $^{87}Sr/^{86}Sr$ ranges widely in samples from each volcano and even within each volcanic series (dashed lines, Fig. 2-6).

Since the data are compiled from various sources with different analytical precision, it is important to evaluate if the observed range of $^{87}Sr/^{86}Sr$ ratios is caused by analytical uncertainties or by true variations of $^{87}Sr/^{86}Sr$ among the samples. It is difficult to do an

interlaboratory comparison unless measurements are done on the same sample. Fortunately interlaboratory errors for $^{87}Sr/^{86}Sr$ ratios are minimized by adjusting the measured $^{87}Sr/^{86}Sr$ values so that the $^{87}Sr/^{86}Sr$ ratio for Eimer and Amend $SrCO_3$ standard is 0.70800. To distinguish the possible real $^{87}Sr/^{86}Sr$ spread among the samples from the $^{87}Sr/^{86}Sr$ spread caused by analytical uncertainty, we plot for each volcanic series the range of $^{87}Sr/^{86}Sr$ ratios (Fig. 2-6, solid lines) defined by the maximum measured $^{87}Sr/^{86}Sr$ -2σ and the minimum measured $^{87}Sr/^{86}Sr$ $+ 2\sigma$. This approach of substracting 2σ from the maximum measured value and adding 2σ to the minimum measured value defines the minimum range in $^{87}Sr/^{86}Sr$ ratios at the 95% confidence level. After this treatment, a substantial range in $^{87}Sr/^{86}Sr$ ratios still exists and suggests that there are real $^{87}Sr/^{86}Sr$ variations within each volcano and within each volcanic series. This observation confirms the conclusions based on Haleakala data that the sources for Hawaiian basalts are isotopically heterogeneous even within single volcanoes. Not only are the sources for tholeiites and alkalic basalts different, but the sources for tholeiites or alkalic basalts from the same volcano can also be isotopically heterogeneous.

In general, older lavas have higher $^{87}Sr/^{86}Sr$ ratios than younger lavas (Loihi seamount is an exception which will be discussed). For example, the best stratigraphic control exists for Haleakala (Fig. 2-4) and East Molokai volcanoes (Clague, personal communication) and in each case $^{87}Sr/^{86}Sr$ ratios increase with increasing depth. Also, the two high $^{87}Sr/^{86}Sr$ samples reported for Kilauea volcano are from a prehistoric eruption and a 1790 eruption. A trace element study of the oldest exposed Kilauea tholeiites, the Hilina formation, shows that some prehistoric Kilauea lavas are distinct from the recently erupted lavas (Chen,

unpublished data). Sr isotopic study also shows that some Hilina basalts have higher $^{87}Sr/^{86}Sr$ ratios than the recent Kilauea lavas (Easton, personal communication).

Alkalic basalts generally have lower $^{87}Sr/^{86}Sr$ ratios than the tholeiites (Fig. 2-6) and samples from the post-erosional series have lower $^{87}Sr/^{86}Sr$ ratios than the samples from the alkalic series. The widest range of $^{87}Sr/^{86}Sr$ variations are observed in samples from Haleakala volcano on East Maui, and Koolau volcano on Oahu, both volcanoes have developed a post-erosional series.

At Loihi seamount, tholeiites apparently erupted later than the alkalic basalts (Moore et al., 1982), but they generally have higher $^{87}Sr/^{86}Sr$ ratios than the alkalic basalts (Fig. 2-6). This suggests that $^{87}Sr/^{86}Sr$ variations are not only correlated with the evolutional stage of the volcano but are also correlated with basalt type. This observation is very important to the origin of Hawaiian tholeiites and alkalic basalts and will be discussed further in Chapter 4.

5 Summary and Conclusion

(1) The $^{87}Sr/^{86}Sr$ ratios and $^{143}Nd/^{144}Nd$ ratios vary systematically with age for samples from the three Haleakala volcanic series. The data suggest that partial melting involves sources with lower $^{87}Sr/^{86}Sr$ ratios and hgher $^{143}Nd/^{144}Nd$ ratios as the volcano evolved from tholeiitic shield building to the post-erosional alkalic series.

(2) Variations of $^{87}Sr/^{86}Sr$ ratios and $^{143}Nd/^{144}Nd$ ratios correlate with age and with basalt type. Tholeiites generally have higher $^{87}Sr/^{86}Sr$ ratios and lower $^{143}Nd/^{144}Nd$ ratios than the alkalic basalts in the Hawaiian volcanos which have been studied in detail (e.g. Loihi seamount, Kohala volcano, East Molokai volcano, Haleakala volcano and Koolau

volcano). Samples from the post-erosional series have even lower $^{87}Sr/^{86}Sr$ and higher $^{143}Nd/^{144}Nd$ ratios than samples from the alkalic series.

(3) Hawaiian samples have a negative correlation between $^{143}Nd/^{144}Nd$ and $^{87}Sr/^{86}Sr$ ratios and they fall inside the "mantle array". However, Hawaiian samples are more radiogenic in $^{87}Sr/^{86}Sr$ ratios than the mid-ocean ridge basalts but are less radiogenic in $^{87}Sr/^{86}Sr$ ratios than the primitive mantle.

(4) Among Haleakala samples there are negative correlations between parent/daughter abundance ratios (Rb/Sr and Sm/Nd) and isotopic ratios ($^{87}Sr/^{86}Sr$ and $^{143}Nd/^{144}Nd$). Contamination of a basaltic magma by seawater, sediments or carbonates are not consistent with these correlations, but recent mixing of at least two sources can explain these negative correlations.

TABLE 1. Duplicate Analyses of 87Sr/86Sr and $^{143}Nd/^{144}Nd$ Ratios

Sample	$^{87}Sr/^{86}Sr$	2σ	Sample	$^{143}Nd/^{144}Nd$	2σ
C123	0.70382	4	HO-2	0.51292	2
	0.70383	3		0.51291	2
H85-8	0.70339	3	C121	0.51298	2
	0.70333	3		0.51292	3
H85-23	0.70319	3	H85-14	0.51302	2
	0.70317	3		0.51307	2
H65-4	0.70336	3	H85-23	0.51301	2
	0.70332	3		0.51297	2
H65-14	0.70319	4	H65-4	0.51301	1
	0.70317	3		0.51302	2
E&A	0.70778	5	BCR-1	0.51264	2
	0.70779	4		0.51267	2
	0.70784	3		0.51263	3
	0.70779	3			

TABLE 2. Rb, Sr and Sr Isotopic Ratios

	Sample	Rock Type	Rb (ppm)	Sr (ppm)	Rb/Sr	$^{87}Sr/^{86}Sr$	2σ ($1x10^{-5}$)	depth+ (m)	H_2O (wt%)	CO_2 (wt%)
	BHVO-1	Th	9.10	397	0.023	.70339	4			
Honomanu series	HO-1	Th	0.82	353	0.002	.70379	4	>300	1.13	0.37
	HO-2	Th	1.49	327	0.005	.70387	4	>300	2.13	0.42
	HO-3	Th	4.39	322	0.014	.70385	4	>300	0.59	0.41
	HO-4	Th	0.44	343	0.001	.70384	3	>300	0.46	0.40
	HO-5	Th	0.51	324	0.002	.70373	5	>300	0.79	0.40
	C-121	Th	0.50	336	0.001	.70382	3	>300	0.87	0.47
	C-122	Th	4.11	207	0.020	.70387	4	>300	0.55	0.20
	C-123	Th	0.55	308	0.002	.70382	3	>300	0.77	0.43
						**.70383	3			
	C-124	AB	-	-	-	.70372	5	>300	-	-
	C-125	Trans.B	-	-	-	.70385	5	>300	-	-
	C-126	Trans.B	-	-	-	.70384	3	>300	-	-
Kula series	H85-1	AB	19.00	580	0.033	.70344	3	300	0.63	0.55
	H85-2	ha	21.71	752	0.029	.70347	4	299	-	-
	H85-7	AB	18.08	649	0.028	.70346	3	261	0.37	0.71
	H85-8	AB	18.28	690	0.026	*.70336	6	255	0.27	0.33
	H85-9	AB	17.16	769	0.022	.70339	4	252	0.42	0.55
	H85-10	AB	17.35	688	0.025	.70336	5	249	0.45	0.39
	H85-11	ha	30.06	930	0.032	.70338	3	245	0.44	0.53
	H85-12	AB	22.92	719	0.032	.70340	3	240	0.53	0.46
	H85-13	AB	18.52	733	0.025	.70333	4	229	0.60	0.60
	H85-14	AB	20.68	743	0.028	.70338	3	228	0.48	0.64
	H85-15	AB	16.51	724	0.023	.70335	3	198	0.58	0.67
	H85-16	ha	30.67	974	0.031	.70330	3	189	-	-
	H85-21	AB	17.23	653	0.026	.70334	4	164	0.89	0.27
	H85-22	AB	23.48	754	0.031	.70333	3	161	0.26	0.30
	H85-23	AB	23.76	790	0.030	*.70318	2	157	0.54	0.87
	H85-24	Mu	44.36	1006	0.044	.70321	4	155	-	-
	H85-25	Mu	49.00	1012	0.048	.70328	4	154	-	-
	H85-31	Mu	52.75	919	0.057	.70334	3	110	-	-
	H85-33	ha	30.42	913	0.033	.70318	4	82	-	-
	H62-2	AB	23.62	725	0.033	.70334	4	~240+	0.33	0.44
	H62-14	AB	23.08	689	0.033	.70332	4	~160+	0.52	0.50
	H83-1	AB	16.31	591	0.028	.70338	4	~250+	0.45	0.29
	H83-7	AB	19.64	616	0.032	.70331	4	164+	0.22	0.35
	H65-4	AB	19.86	616	0.032	*.70334	3	164+	0.21	0.20
Hana series	H65-8	AB	21.73	603	0.036	.70319	4	64	0.10	0.22
	H65-9	AB	18.41	626	0.029	.70322	4	62	0.44	0.22
	H65-10	AB	21.69	608	0.036	.70325	4	60	0.17	0.17
	H65-11	AB	18.83	582	0.032	.70314	4	58	0.33	0.18
	H65-13	AnK	16.99	561	0.030	.70311	4	3	0.63	0.47
	H65-14	AnK	20.15	565	0.036	*.70318	2	2	0.34	0.40
	H62-47	AB	22.45	649	0.035	.70306	3	~70+	0.25	0.42
	H62-48	AB	20.15	583	0.035	.70322	4	~60+	0.18	0.21
	H62-49	AB	17.85	511	0.035	.70321	3	~50+	0.24	0.26
	H62-52	ha	32.99	908	0.036	.70326	3	~25+	-	-

* average of duplicate analyses
** unspiked
+ Meters beneath ground surface.
Samples other than from Holes 65 and 85 are adjusted based on core logs and stratigraphic correlation (Chapter 1).

TABLE 3. Nd, Sm and Nd Isotropic Ratios

	Sample	Nd	Sm	Sm/Nd	$^{143}Nd/^{144}Nd$	2σ ($1x10^{-5}$)
	BCR-1	26.7	6.54	.245	+.51265	3
	BHVO-1	23.6	6.11	.259	.51301	2
Honomanu series	HO-1	21.8	6.08	.279	.51292	2
	HO-2	-	-	-	*.51292	2
	HO-3	18.5	5.06	.274	.51295	3
	HO-4	20.8	5.82	.280	.51292	3
	HO-5	20.7	5.49	.265	.51298	3
	C-121	19.5	5.39	.276	*.51295	6
	C-122	12.3	3.73	.303	.51291	2
	C-123	17.8	4.89	.275	.51292	2
	C-124	30.4	8.70	.286	.51294	3
	C-125	-	-	-	.51297	3
	C-126	25.0	6.55	.262	.51295	3
Kula series	H85-1	38.5	9.33	.242	.51300	2
	H85-2	42.5	9.91	.233	.51305	3
	H85-7	33.4	8.20	.246	.51302	2
	H85-8	33.3	7.98	.240	.51304	3
	H85-9	33.2	7.92	.239	.51303	2
	H85-10	35.2	7.98	.227	.51303	2
	H85-11	48.4	11.12	.230	.51301	3
	H85-12	43.6	9.99	.229	.51304	3
	H85-13	46.1	10.27	.223	.51309	1
	H85-14	37.8	8.07	.213	*.51305	5
	H85-15	32.5	7.25	.223	.51304	3
	H85-16	49.6	10.33	.208	.51307	3
	H85-21	30.6	6.92	.226	.51305	2
	H85-22	35.4	7.76	.219	.51308	1
	H85-23	35.3	7.71	.218	*.51299	4
	H85-24	63.1	11.98	.190	.51302	1
	H85-25	63.9	12.00	.188	.51301	3
	H85-31	69.2	12.62	.182	.51306	3
	H85-33	45.7	9.19	.201	.51304	2
	H62-2	39.2	9.17	.234	.51303	3
	H62-14	33.7	7.66	.227	.51302	2
	H83-1	-	-	-	.51304	2
	H83-7	-	-	-	.51300	2
	H65-4	30.7	6.85	.223	*.51302	1
Hana series	H65-8	26.8	6.35	.237	.51307	3
	H65-9	26.3	6.44	.245	.51311	2
	H65-10	26.8	6.43	.240	.51306	3
	H65-11	26.1	6.01	.230	.51310	2
	H65-13	27.1	6.59	.243	.51308	2
	H65-14	27.8	6.61	.238	.51310	3
	H62-47	29.4	6.73	.229	.51313	3
	H62-48	26.3	6.39	.243	.51310	3
	H62-49	23.1	5.48	.237	.51309	1

+ Average of 3 analyses
* Average of duplicate analyses

Figure 2-1: $^{87}Sr/^{86}Sr$ versus Rb/Sr diagram for the Haleakala samples.

□ = tholeiites from Honomanu volcanic series

Δ = alkalic basalts from the Kula volcanic series

○ = hawaiites and mugearites from Kula volcanic series

✱ = alkalic basalts and ankaramites from the Hana volcanic series

● = hawaiite from Hana volcanic series

Tholeiites with altered olivine rims and altered glass are circled.

Except for hawaiites and mugearites, the Haleakala samples show a general trend with negative slope between $^{87}Sr/^{86}Sr$ ratios and Rb/Sr ratios.

Figure 2-2: $^{143}Nd/^{144}Nd$ versus Sm/Nd for the Haleakala samples.

Symbols as in Figure 2-1. Additional symbol: (▣) transitional and alkalic basalts from the Honomanu series.

Figure 2-3: $^{143}Nd/^{144}Nd$ and $^{87}Sr/^{86}Sr$ correlation diagram.

• = data from Staudigel et al., 1981 samples from Loihi seamount

+ = data from O'Nions et al. 1977, samples from various Hawaiian islands

The two samples (HA5, and T-10) from Mauna Loa are indicated.

The rest of the symbols are as in Figure 2-2.

The two solid lines are the range of "mantle array".

Figure 2-4: Correlation of $^{87}Sr/^{86}Sr$ ratios with stratigraphic sequences. The depth for tholeiites is set at a depth greater than 300 meters and only the average $^{87}Sr/^{86}Sr$ ratio is shown. The depth for individual alkalic basalts is adjusted to the proper depth as they would be in drilled core H85 according to core

correlations and core logs (Chapter 1). The symbols are as in Figure 2-1.

Figure 2-5: Correlation of $^{143}Nd/^{144}Nd$ ratios and stratigraphic sequences. The symbols are as in Figure 2-1.

Figure 2-6: $^{87}Sr/^{86}Sr$ ratios plotted as a function of distance from Kilauea volcano measured along the trend of Hawaiian islands:

□ = tholeiite and transitional basalts

Δ = alkalic sample from shield building stage and alkalic stage

* = sample from post-erosional series

= range of $^{87}Sr/^{86}Sr$ ratios in shield building series including tholeiites, transitional basalts and alkalic samples erupted at the beginning of the shield building stage),

= range of $^{87}Sr/^{86}Sr$ ratios in alkalic series (including alkalic basalts erupted at the end of shield building stage and all alkalic samples erupted at alkalic stage),

= range of $^{87}Sr/^{86}Sr$ ratios in post-erosional series

Dashed lines indicate the measured range. Solid lines are defined by the maximum measured $^{87}Sr/^{86}Sr$ -2σ and the minimum measured $^{87}Sr/^{86}Sr$ $+ 2\sigma$ of samples from each volcanic series so that the lines represent minimum range in $^{87}Sr/^{86}Sr$ ratio at the 95% confidence level. Number of samples included is indicated on the right side of the lines which show the range of $^{87}Sr/^{86}Sr$ for each series. References are indicated by the numbers in parentheses: (1) Lanphere 1982; (2) Hart, 1973; (3) O'Nions et al., 1977; (4) Hofmann et al., 1978; (5) Lanphere et al., 1980;

(6) Feigenson *et al.*, 1982; (7) this study; (8) Clague, unpublished data; (9) DePaolo and Wasserberg, 1976; (10) Lanphere and Dalrymple, 1980; (11) Roden *et al.*, unpublished data.

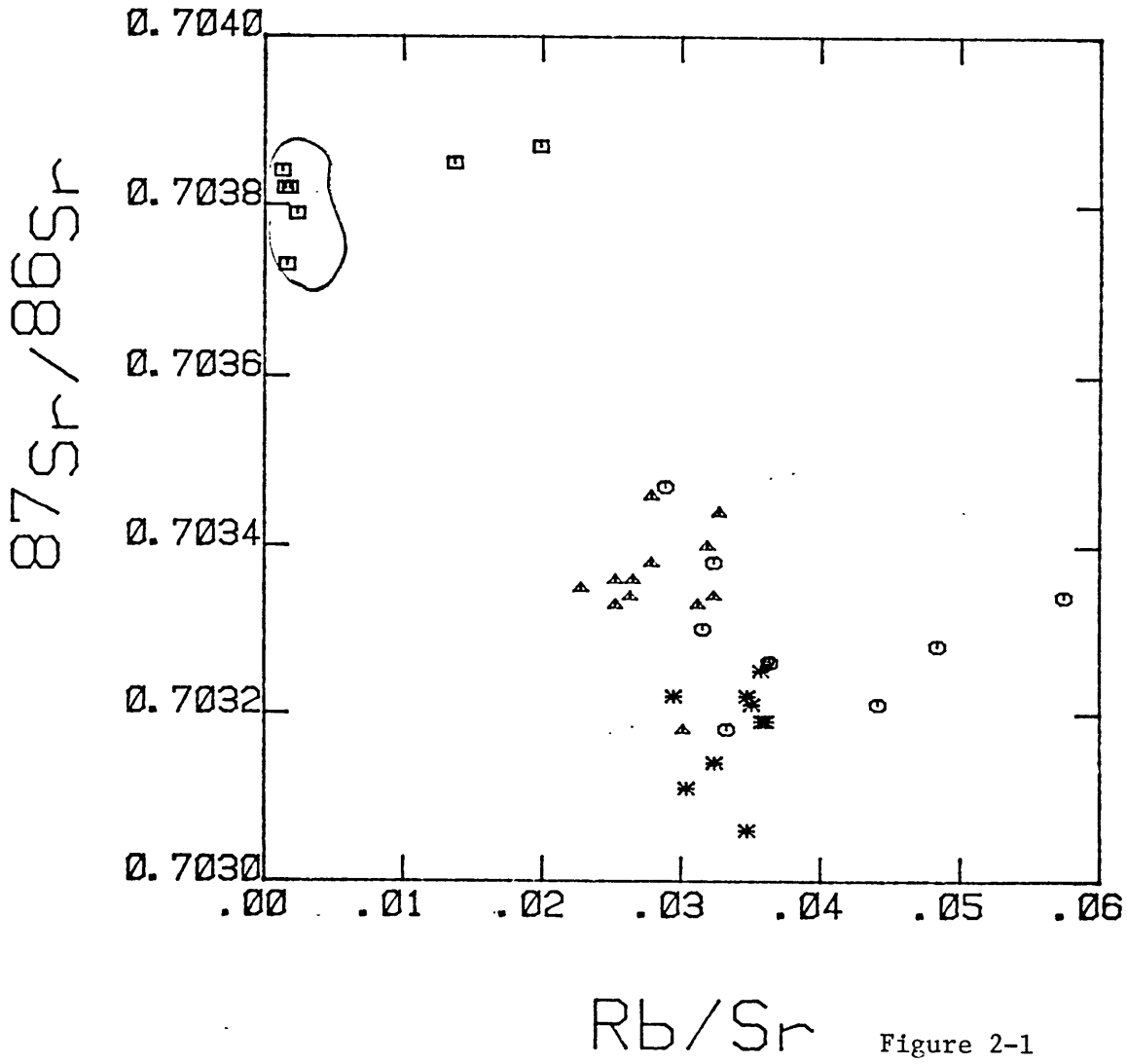

0.7040
0.7038
0.7036
0.7034
0.7032
0.7030
87Sr/86Sr
.00
.01
.02
.03
.04
.05
.06
Rb/Sr

Figure 2-1

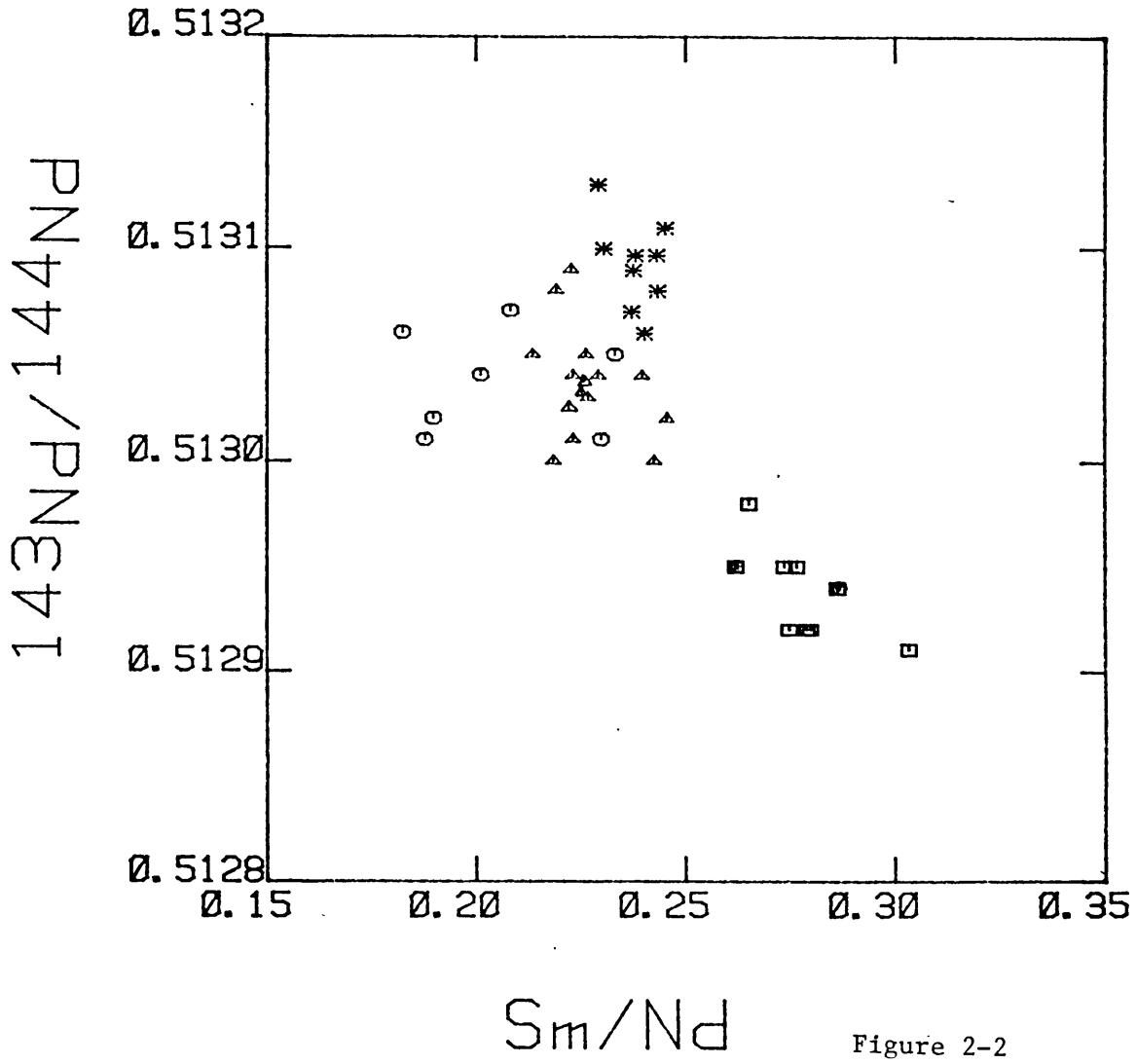

0.5132
0.5131
0.5130
0.5129
0.5128
143Nd/144Nd
0.15
0.20
0.25
0.30
0.35
Sm/Nd

Figure 2-2

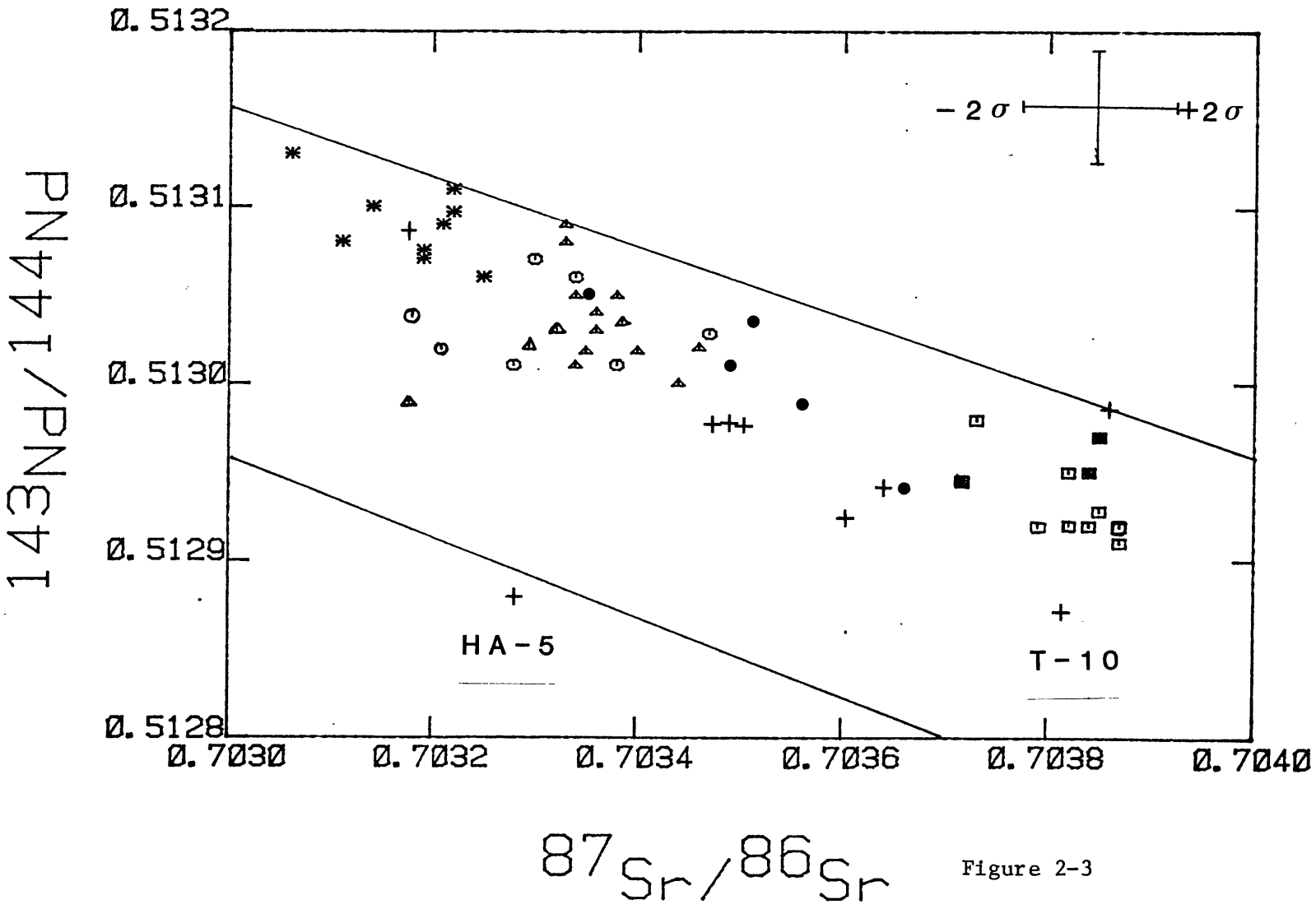

Ø.5132
Ø.5131
Ø.5130
Ø.5129
Ø.5128
143Nd/144Nd
Ø.7030
Ø.7032
Ø.7034
Ø.7036
Ø.7038
Ø.7040
87Sr/86Sr
−2σ
+2σ
HA-5
T-10

Figure 2-3

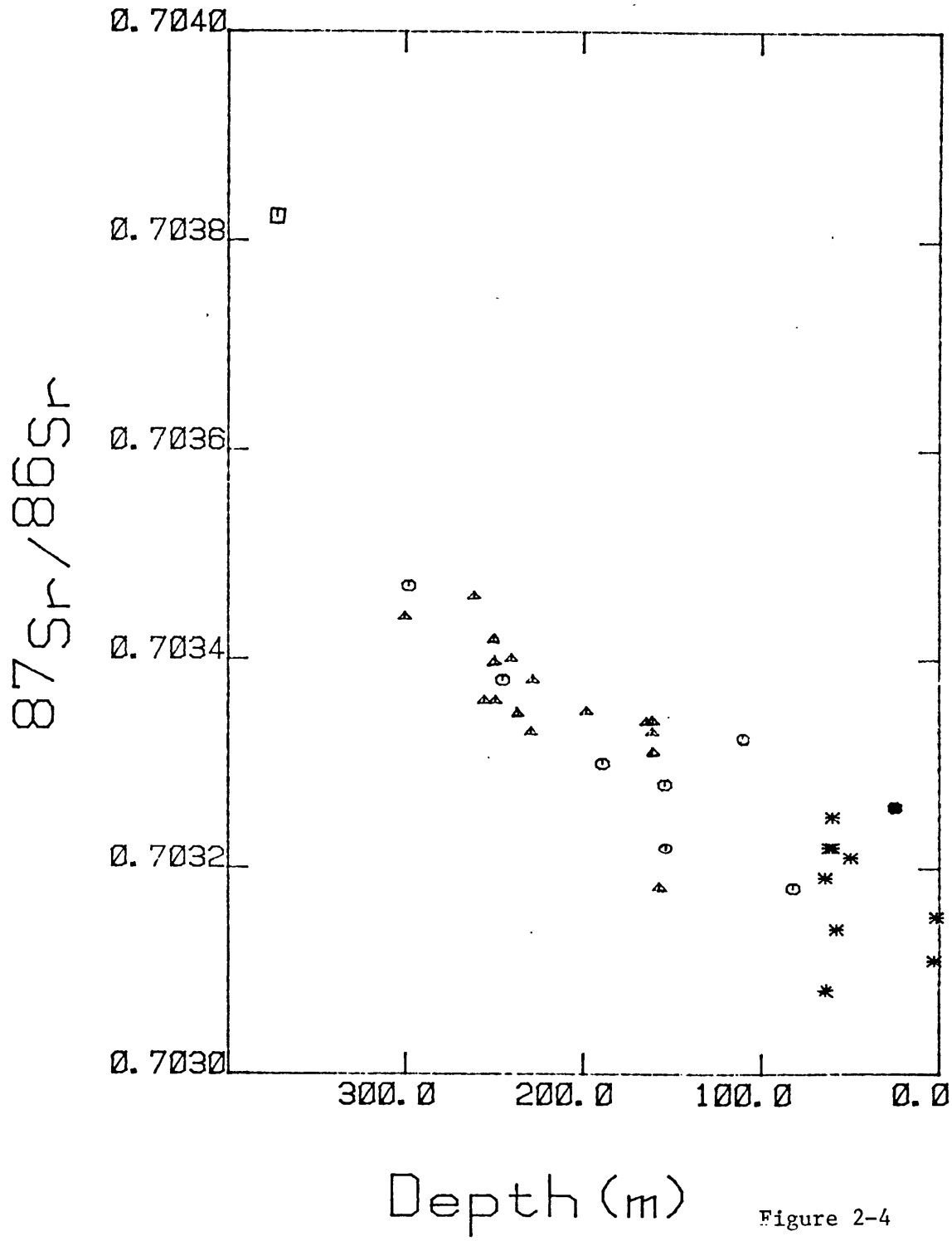

0.7040
0.7038
0.7036
0.7034
0.7032
0.7030
87Sr/86Sr
300.0
200.0
100.0
0.0
Depth (m)

Figure 2-4

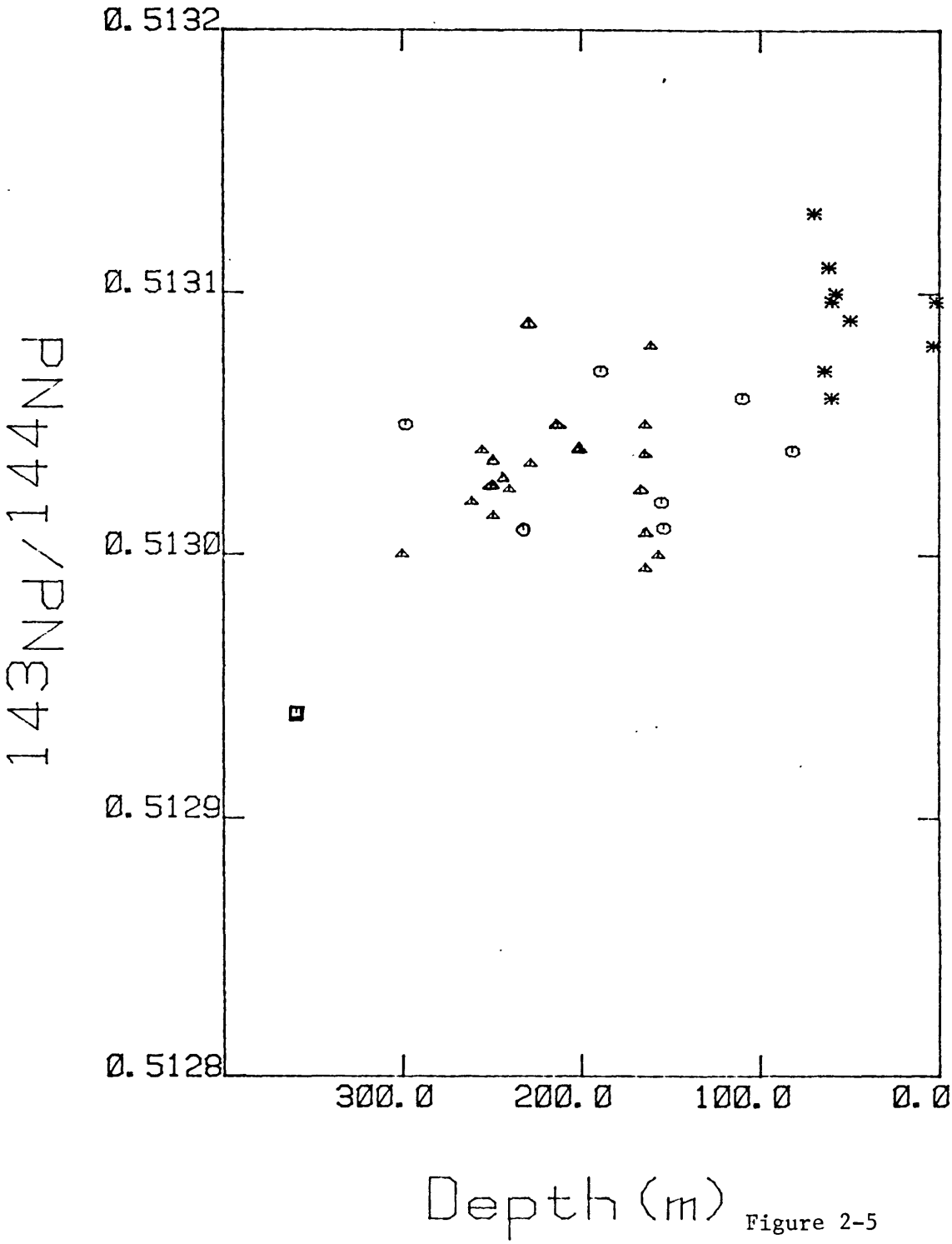

0.5132
0.5131
0.5130
0.5129
0.5128
143Nd/144Nd
300.0
200.0
100.0
0.0
Depth (m)

Figure 2-5

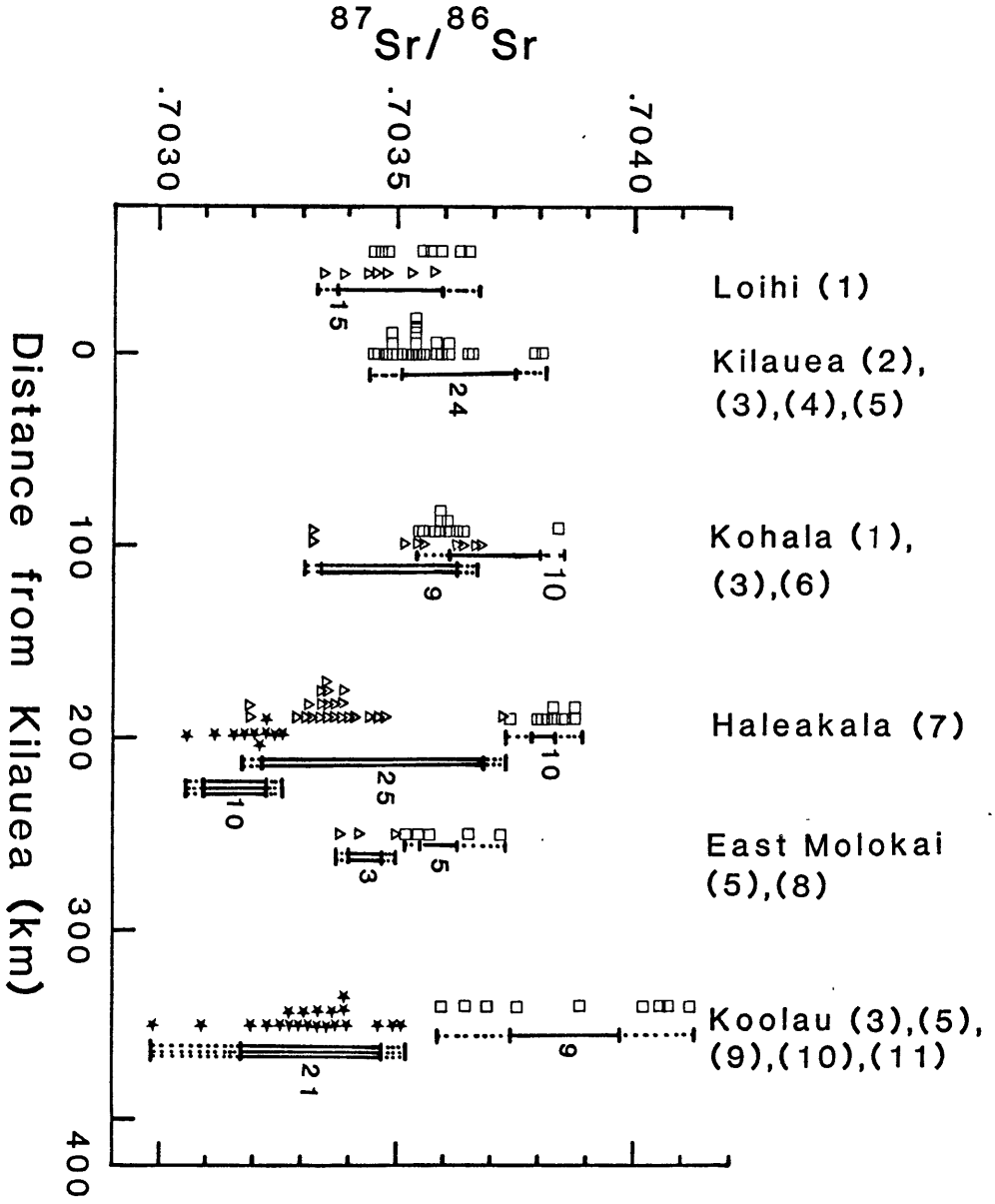

87Sr/86Sr
.7030
.7035
.7040
Distance from Kilauea (km)
0
100
200
300
400
15
24
9
10
10
25
10
3
5
21
9
Loihi (1)
Kilauea (2), (3),(4),(5)
Kohala (1), (3),(6)
Haleakala (7)
East Molokai (5),(8)
Koolau (3),(5), (9),(10),(11)

Figure 2-6

CHAPTER 3

TRACE ELEMENT GEOCHEMISTRY OF THE HALEAKALA VOLCANIC SERIES

1. Introduction

Following the pioneering papers of Schilling and Winchester (1967), Gast (1968) and Shaw (1970a), trace element abundances and abundance ratios have been used extensively to develop models for partial melting and fractionation processes in basalt petrogenesis and to infer source compositions (e.g., Kay and Gast, 1973; Sun and Hanson, 1975; Minster et al., 1977; Frey et al., 1978; Minster and Allegre, 1978; Clague and Frey, 1982). Such models are based on an understanding of trace element partitioning in solid/liquid systems. "Compatible" and "incompatible" are adjectives used to describe trace element behaviors in the solid-liquid systems; compatible elements have solid/liquid partition coefficients greater than 1 and are preferentially incorporated into the bulk solid during solid/liquid partitioning, whereas incompatible elements have solid/liquid partition coefficients less than 1 and are preferentially incorporated into the liquid. In this chapter highly incompatible trace elements are those with solid/liquid partition coefficients close to zero ($\leq$0.01, e.g. Ba, Rb, Th, Ta, Nb, La, Ce in ol + opx $\pm$ cpx $\pm$ sp $\pm$ gt assemblages, Sun et al., 1979, Wood et al., 1979c), and moderately incompatible trace elements are those with bulk solid/liquid partition coefficients less than 1 but substantially greater than zero (e.g. Sm, Eu, Zr, Hf in ol + opx + cpx $\pm$ sp $\pm$ gt assemblage). The incompatibility of an element is strongly dependent on the mineralogy of the solid, for example, Ba is a highly incompatible element in ol $\pm$ opx $\pm$ cpx $\pm$ gt $\pm$ spl assemblage but it is a moderately incompatible element in plagioclase dominated assemblage (e.g. Arth, 1976). Abundance ratios of highly incompatible elements are not very sensitive to variations in degree of partial melting and fractionation (Gast, 1968), thus such ratios in basalts can be used to evaluate source

compositions and source heterogeneity (e.g. Sun and Nesbit, 1977, Wood et al., 1979a,b,c, Clague and Frey, 1982). In contrast, abundance ratios involving highly incompatible elements and moderately incompatible elements or compatible elements are affected by partial melting and/or fractionation processes, thus such ratios are useful in evaluation of partial melting and/or fractionation processes (e.g., Allegre et al., 1977; Minster and Allegre, 1978; Clague and Frey, 1982). Since the incompatibility of trace elements between solids and liquids is dependent on mineral assemblages in the solid, relative behavior of trace elements (e.g. Ba vs. La) are useful in identifying the mineralogy of solids in equilibrium with liquids during melting and/or crystallization processes.

Trace element abundances (K, Rb, Sr, Ba, Th, Ta, Nb, REE, Hf and Zr) and their abundance ratios in the Haleakala volcanic series are presented in this chapter and are used to evaluate source heterogeneity, partial melting, fractionation and alteration processes. Also abundance ratios of these trace elements in the Haleakala volcanic series are compared to Mauna Loa tholeiites, Kilauea tholeiites, mid-ocean ridge basalts and chondrites.

2. Analytical Techniques

Seven tholeiites from the Honomanu volcanic series, 15 alkalic basalts, 4 hawaiites and 3 mugearites from the alkalic Kula volcanic series, 7 alkalic basalts, 2 ankaramites and 1 hawaiite from the post-erosional Hana volcanic series and two USGS standard rocks (BHVO-1, BCR-1) were analyzed for K, Rb, Sr, Ba, Zr, Nb, REE (La, Ce, Nd, Sm, Eu, Tb, Ho, Yb, La), Hf, Ta and Th abundances. The abundances of K, Rb, Sr, for most of the samples and Ba for 6 samples were determined by isotope dilution (I.D.) method (Hart and Brooks, 1977) at M.I.T. The abundances of

Ba, Zr and Nb for all the samples, Sr for most of the samples and Rb for 7 samples were determined by X-ray fluorescence (XRF) at the University of Massachusetts. BCR-1 was included in every set of these XRF analyses. The abundances of Rb, Sr, Ba in some of the samples were determined by both I.D. and XRF. Abundances of Rb determined by these two methods agree within 3% for samples with more than 1 ppm Rb and within 15% for samples with less than 1 ppm Rb (Table 2). The abundances of Sr and Ba determined by these two methods agree within 5% and 12%, respectively (Table 2). For those samples analyzed by both I.D. and XRF, values determined by I.D. method will be used.

The abundances of rare-earth elements (REE), Hf, Ta and Th for all the samples were determined by instrumental neutron activation analyses (INAA) at M.I.T. A sample (H85-8) was included in every set of analyses by INAA. Accuracy and precision of these trace element analyses can be evaluated by analyses of the standard rocks BHVO-1, BCR-1 and H85-8 (Table 1). Trace element abundances of BHVO-1 reported by Flanagan (1976) and Sun et al. (1979) and those of BCR-1 reported by Flanagan (1973) are listed in Table 1 for comparison.

3. Results

3-1 Trace element abundance variations

Trace element (K, Rb, Sr, Ba, REE, Hf, Ta and Th) abundances in the Haleakala samples are given in Table 2.

3-1(a) K, Rb, Sr, Ba, Th, Ta, Nb and La

This group of trace elements are commonly considered as highly incompatible trace elements in peridotite mineral assemblages (ol + opx + cpx ± gt ± sp) (e.g. Sun and Nesbitt, 1977; Wood et al., 1979a,b,c). In the Haleakala samples, abundances of these trace elements vary by factors

of 16 (K), 14 (Rb), 15 (Ba), 7 (Th), 9 (Ta), 11 (Nb), 9 (La) and 5 (Sr), respectively. A tholeiite (C122) and a mugearite (H85-31) define the range of these trace element abundances except for K, Rb and Sr. Mugearite H85-25 instead of H85-31 has the highest abundances of Sr. A slightly altered tholeiite (HO-4) has the lowest abundances of K and Rb among the Haleakala samples (Table 2). Abundances of these trace elements in Haleakala samples correlate positively with each other (e.g., Figs. 3-1a to g). Abundances of K, Rb, Ba, Th, Ta, Nb, Sr are plotted against a light-REE (La) because of its incompatibility in most common minerals (e.g. olivine, pyroxene, spinel, garnet, plagioclase, amphibole, phlogopite, magnetite) and high analytical precision (Table 1). On K vs. La and Rb vs. La diagrams (Figs. 3-1a and 3-1b) samples which show sign of alteration in thin section (Chapter 1) plot slightly below the trend established by fresh samples. For all other trace elements, fresh and altered samples fall on the same trends. When compared at constant La abundances, alkalic basalts from the post-erosional Hana volcanic series generally have higher K, Rb, Ba, Th, Ta, and Nb but lower Sr abundances than those from the alkalic Kula volcanic series (Fig. 3-1a to g).

3-1(b) Rare-earth elements (REE): La, Ce, Nd, Sm, Eu, Tb, Ho, Yb and Lu

Abundances of a light-REE (Ce) and a heavy-REE (Yb) are plotted against La on Figs. 3-1h and i. Like other highly incompatible elements Ce abundances in the Haleakala samples correlate strongly with La abundances (Fig. 3-1h). However, Yb abundances in Haleakala samples do not correlate with light-REE abundances (Fig. 3-1i). Alkalic basalts and hawaiites have higher La abundances than the tholeiites but have the same range of Yb abundances as tholeiites. Mugearites have higher La and Yb than alkalic basalts, hawaiites and tholeiites.

Ranges of chondrite-normalized REE abundances for Haleakala basalts from each Haleakala volcanic series are shown in Figure 3-2a (hawaiites and mugearites not included). The Haleakala basalts have higher LREE/HREE abundance ratios than chondrites (Fig. 3-2a), and light-REE abundances vary over a wide range (21 to 100 times that of chondrites). Alkalic basalts from the alkalic Kula volcanic series and post-erosional Hana volcanic series are more enriched in light-REE abundances than tholeiites from the Honomanu volcanic series (Fig. 3-2a). However, heavy-REE abundances in basalts from these three volcanic series are very similar and vary in a narrow range (6.5 to 11 times that of chondrites). Alkalic basalts from the post-erosional Hana volcanic series generally have lower REE abundances but have more fractionated distribution patterns (e.g. higher La/Ce and La/Yb ratios) than alkalic basalts from the Kula volcanic series (Fig. 3.2a). Chondrite-normalized REE abundances of individual samples are shown in Figures 3-2(b-g).

Honomanu volcanic series

Except for C122, tholeiites from the Honomanu volcanic series have parallel chondrite-normalized REE distributions. C122 has similar abundances of heavy-REE (Yb and Lu) as C123 but lower abundances of light-REE and intermediate-REE than C123 (Fig. 3-2b). Light-REE abundances in these tholeiites range from 22 (C122) to 41 (HO-1) times that of chondrites. Heavy-REE abundances range from 7 to 9 times that of chondrites. These Haleakala tholeiites have near chondritic REE distribution from La to Eu but are fractionated from Eu to Lu which is similar to the average tholeiites from Mauna Loa (Fig. 3-2b), Lanai and Kohala volcanoes (Leeman et al., 1980) and a prehistoric Kilauea tholeiite (EK80, Chen and Frey, unpublished data).

Kula volcanic series

Alkalic basalts from the Kula volcanic series have highly fractionated chondrite-normalized REE distributions (Figs. 3-2c to e). Light-REE abundances of these alkalic basalts range from 74 to 100 times chondrites, whereas heavy-REE abundances range from 8 to 11 times chondrites (Figs. 3-2c to e). Among these Kula alkalic basalts, three successive lavas (H85-8, H85-9 and H85-10) have similar major element and transition metal abundances (Chapter 2) and similar REE abundances (Table 2). H85-21 and H65-4 which are from similar depths have similar transitional and major element abundances except K, Rb, and H_2O. Thin iddingsite rims on olivine of H85-21 indicate that H85-21 is slightly altered, but H65-4 is very fresh in thin section. These two samples have the same REE abundances (Table 2); apparently, REE abundances were not affected by alteration.

Within the Kula volcanic series, younger alkalic basalts generally have more fractionated chondrite-normalized REE distribution than the older alkalic basalts (Fig. 3-9f to k). For example, H85-1 (depth = 300 meters, Table 2) has a similar Mg-value and similar abundances of intermediate-and heavy-REE (Eu, Tb, Ho, Yb, Lu) but lower light-REE (La, Ce, Nd, Sm) than H85-12 (depth = 240 meters) (Fig. 3-2c). Within the Kula and Kalic basalts there are several examples of cross-cutting chondrite-normalized REE patterns; e.g., H85-1 and H85-2 (Fig. 3-2C) and H85-14 and H85-15 (Fig. 3-2d). The oldest alkalic basalt from the Kula volcanic series (H85-1) has La/Ce (0.40) and La/Sm (2.97) ratios similar to that of the average recent tholeiites from Kilauea volcano (Table 6).

Chondrite-normalized REE abundances of hawaiites and mugearites from the Kula volcanic series are shown in Figure 3-2f. Light-REE abundances of these hawaiites and mugearites range from 90 to 188 times chondrites, whereas

heavy-REE range from 9 to 14 times chondrites. The mugearites have slightly higher heavy-REE abundances than the hawaiites and are more enriched in light-REE than hawaiites (Fig. 3-2f). Within the hawaiites LREE/HREE increases with decreasing age (Fig. 3-9f to k) and several hawaiites have crossing normalized REE patterns (e.g., Fig. 3-2f, H85-2 vs. H85-33).

Hana volcanic series

Chondrite normalized REE abundances of alkalic basalts from the post-erosional Hana volcanic series vary in a narrower range than alkalic basalts from the Kula volcanic series. Light-REE abundances of Hana alkalic basalts vary from 61 to 82 times chondrites and heavy-REE abundances vary from 6.5 to 8 times chondrites (Fig. 3-2g). Ankaramites (H65-13, H65-14) have similar REE abundances but have slightly more fractionated chondrite-normalized REE patterns than alkalic basalts from the same volcanic series (Fig. 3-2g). Compared to basalts from the Hana volcanic series hawaiite (H62-52) has similar heavy-REE (Yb, Lu) abundances but higher light- and intermediate-REE abundances.

3(c) Zr and Hf

Zr abundances in the Haleakala samples range from 103 ppm (C122) to 438 ppm (H85-24), and Hf abundance range from 2.6 ppm (C122) to 9.7 ppm (H85-25). Both Zr (Fig. 3-3a) and Hf (Fig. 3-3b) are positively correlated with La for samples within each Haleakala volcanic series. However at the same La abundance, samples from the post-erosional Hana volcanic series have lower Zr and Hf abundances than samples from the Kula volcanic series and Honomanu volcanic series. Abundances of Zr and Hf in all the Haleakala samples show a strong positive correlation and samples from all the three volcanic series fall on a single trend (Fig. 3-3c) with average Zr/Hf ratio of 40.

3-2 Ratios of trace element abundances

Ratios of trace element abundances such as K/Rb, K/Ba, Rb/Sr, Ba/La, Rb/La, Th/La, Nb/La, La/Ce, La/Nd, La/Sm, La/Eu, La/Yb, La/Lu and Nd/Sm are plotted vs. La abundances in Figures 3-4a to n. K/Rb ratios in the Haleakala samples vary from 2500 to 345 (Fig. 3-4a). However, the extremely high K/Rb ratios (>2000) are in altered tholeiites. The fresh tholeiites (HO-3 and C122) have K/Rb ratios of 567 and 525 respectively (Fig. 3-4a). Extremely high K/Rb ratios (up to 3500) have also been found in other altered Hawaiian tholeiites such as those from Kohala volcano (Feigenson et al., 1982). K/Rb ratios vary from 360 to 522 and 345 to 389, respectively, for alkalic samples from the Kula and Hana volcanic series. H85-13 which contains altered glass has the highest K/Rb ratio (522) among the alkalic samples (Fig. 3-3a). Samples with alteration features in thin section also have anomalous K/Ba (Fig. 3-4b), Rb/Sr (Fig. 3-4c), Rb/La (Fig. 3-4d) relative to the trends established by other samples.

Among fresh samples from the three Haleakala volcanic series, the alkalic basalts from the post-erosional Hana volcanic series have the lowest K/Ba ratios but highest Rb/Sr and Rb/La ratios and the tholeiites from the Honomanu volcanic series have the highest K/Ba ratios but lowest Rb/Sr and Rb/La ratios (Figs. 3-4b,c,d). Clague and Beeson (1980) reported lower K/Ba ratios in transitional basalts (K/Ba = 16±2) than in alkalic basalts (K/Ba = 26±3) from the East Molokai volcano. The oldest alkalic basalts in the Kula volcanic series (H85-1) has K/Ba ratio of 25 which is similar to that of the alkalic basalts from the East Molokai volcano. Fresh tholeiites from the Haleakala volcano have K/Ba ratios of 38 (C122) and 27 (HO-3) which are higher than alkalic basalts. However, the five Haleakala tholeiites which have alteration rims on olivine phenocrysts and

slightly altered glass have K/Ba ratio of 15±2 which is similar to that reported for transitional basalts on East Molokai volcano. However, in these Haleakala tholeiites, the lower K/Ba ratio are most likely due to alteration.

Samples from the three Haleakala volcanic series define distinct ranges of Rb/La, Ba/La, Nb/La and La/Ce ratios (Figs. 3-4d,e,g,h). Within each Haleakala volcanic series these ratios are independent of La abundances (Figs. 3-4d,e,g,h). Samples from the post-erosional Hana series have the highest Rb/La, Ba/La, Nb/La and La/Ce ratios and samples from the dominantly tholeiitic Honomanu series have the lowest Rb/La, Ba/La, Nb/La and La/Ce ratios. Th/La ratios for samples from the Kula volcanic series and Hana volcanic series behave as Rb/La, Ba/La, Nb/La and La/Ce ratios (Figs. 3-4d to h). However, the tholeiites are more scattered in Th/La ratios than alkalic samples (Figs. 3-4f). Since tholeiites have less than 1 ppm Th the INAA Th data have considerable uncertainty and the scatter of data points is likely due to analytical errors.

Unlike ratios of highly incompatible element abundances, La/Nd, La/Sm, La/Eu, La/Yb, La/Lu and Nd/Sm ratios in the Haleakala samples increase as La abundances increase (Fig. 3-4i to n). At similar La abundances, samples from the post-erosional Hana series have higher La/Nd, La/Sm, La/Eu, La/Yb and La/Lu ratios but similar or slightly lower Nd/Sm ratios than samples from the Kula volcanic series. The tholeiites have the lowest La/Nd, La/Sm, La/Eu, La/Yb, La/Lu and Nd/Sm among the samples from three Haleakala volcanic series.

4. Discussion

4-1 Effects of alteration on trace element abundances

All studied samples of the alkalic Kula volcanic series and the post-erosional alkalic, Hana volcanic series are from drill cores (Chapter 1). Most of these drill core samples are very fresh in thin section except samples H85-13, H85-15 and H85-21 from the Kula volcanic series and H65-9 and H65-13 from the Hana volcanic series. Alteration of these 5 alkalic samples is indicated by slightly altered glass (H85-13) or slightly to moderate iddingsitized rims on olivines (H85-15, H85-21, H65-9 and H65-13). The tholeiites were collected along Honomanu Bay and in thin section they appear less fresh than the drill core samples. Only C122 is very fresh in thin section. Olivine rims in HO-3 are slightly altered, and the other tholeiites have thin iddingsite rims on olivine and contain partially altered glass. Water content ranges from 0.44% to 1.13% for the altered alkalic and tholeiitic samples and ranges from 0.10% to 0.63% for those appearing fresh in thin section (Table 2). Clearly, altered samples tend to have higher water contents than the fresh samples.

Since trace element abundances in the samples reflect the integrated effects of source composition, the melting process, fractionation processes and alteration processes, the best samples for evaluating alteration effects are samples with varying degrees of alteration from the same lava flow or same batch of melts. H65-4 and H85-21; H65-8, H65-9 and H65-10; H65-13 and H65-14 are three groups of samples with these features. Judging from isotopic ratios (Chapter 2), major element compositions, transition metal abundances and stratigraphic positions (Chapter 1), each group of samples are probably from the same lava flow or same batch of melts. Samples H65-4, H65-8, H65-10, and H65-14 are fresh in thin section but

H85-21, H65-9 and H65-13 show signs of alteration (iddingsite rims on olivine). In each case, the altered samples have lower Rb, and K abundances and higher H_2O abundances than their fresh counterpart (Table 2). Since H85-21, H65-9 and H65-13 are only slightly altered, the difference between fresh and altered samples are only about 15% for Rb and about 10% for K (Table 2). However, other trace element abundances (e.g. Ba, Th, Nb, La, Ce, Sr, Nd, Zr, Hf, Sm, Yb, Lu) in the altered samples are within the experimental uncertainty of the abudances in fresh samples (Table 2).

For altered alkalic basalts H85-13 and H85-15 and the altered tholeiites, there are no counterparts of fresh samples from same flow to compare with. In thin section the altered tholeiites are the most altered samples studied, and they depart most strongly from K/Ba vs. La and Rb/La vs. La trends (Figs. 3-4b and d) established by fresh samples. H85-13 which contains altered glass also departs strongly from the Rb/La vs. La trend (Fig. 3-4d). Thus, alteration has removed alkali elements from these Haleakala samples and probably other Hawaiian samples (Feigenson et al., 1982). Moreover Rb is lost preferentially relative to K (e.g. K/Rb vs. La and K/Rb vs. depth, Figures 3-4a and 3-9a). However, among the tholeiites the extent of K and Rb loss does not correlate well with water content of the samples (Chapter 1 and Table 2). HO-4 has the lowest H_2O content among the tholeiites but it also has lowest content of K and Rb (Table 2). Nonetheless, the freshest tholeiite (C122) contains less H_2O than the rest of the tholeiites except for HO-4.

4-2 Source heterogeneity of the Haleakala basalts

In a peridotite source dominanted by olivine and orthopyroxene the partition coefficients between solid and liquid for K, Rb, Ba, La, Ce

Th, Ta and Nb (Table 3 and Sun and Nesbitt, 1977; Frey et al., 1978; Wood et al., 1979c) are very close to zero, thus these highly incompatible trace elements strongly partition into liquid during partial melting processes. Abundance ratios of these trace element abundances in derived melts deviate from source ratios only when degree of melting (F) is close to or smaller than bulk partition coefficient; therefore only very small degrees of partial melting (<<1 %) can change such ratios. Figure 3-5 shows examples of Ba/La, La/Ce and La variations in melts formed during an equilibrium partial melting process. For a mantle peridotite assemblage containing 60% olivine, 25% orthopyroxene, 10% clinopyroxene and 5% garnet (Clague and Frey, 1982), assuming non-modal equilibrium melting (Shaw, 1970a) and assuming the melt composed of 20% (olivine + orthopyroxene), 40% clinopyroxene and 40% garnet (Leeman et al., 1980), the Ba/La and La/Ce ratios in a 10% melt only increase by a factor of 1.01 while La abundance increases by a factor of 9.8 from the source values (Fig. 3-5). Even for 1% melting, the Ba/La and La/Ce ratios in the melt only increase by factors of 1.16 and 1.17 respectively, while La abundances in the melt increase by a factor of 81 from the peridotite source values (Fig. 3-5). Judging from the relative incompatibilities of Ba, Rb, Th, K, Ta, Nb and La in basaltic rocks (e.g. Sun and Nesbitt, 1977; White and Schilling, 1978; Wood et al., 1979c), variations of Th/La, K/La, Ta/La, Nb/La, Ba/K, K/Rb ratios during partial melting of peridotite assemblages should be similar to variations in Ba/La and La/Ce ratios. Thus for the degrees of melting (>3%), as generally estimated for basaltic magma (e.g. Gast, 1968; Sun and Hanson, 1975; Frey et al., 1978; Clague and Frey, 1982), varying degrees of partial melting of a peridotite source cannot effectively change ratios of highly incompatible trace element abundances such as Ba/La, Rb/La, Th/La and

La/Ce. Consequently, large variations (factor of 1.5) in these trace element abundance ratios in samples with a small range (< factor of 10) in incompatible element abundance requires heterogeneous mantle sources if the sources are assumed to contain ol > opx > cpx ± sp and ± gt.

In addition to an olivine-rich peridotite mantle source (e.g. Leeman et al., 1980; Clague and Frey, 1982), garnet pyroxenite has been proposed as a mantle source for Hawaiian basalts (e.g. Leeman et al., 1977; Hofmann and White, 1982). Since trace elements such as La and Ce are less incompatible in clinopyroxene than in olivine and orthopyroxene (Table 3), an increased proportion of clinopyroxene in the source decreases the incompatibility of La and Ce between solid and liquid. Increasing clinopyroxene in the source also decreases the incompatibility of Ba between solid and liquid but to a lesser extent than for La and Ce (Table 3). Consequently, a mantle source composed of abundant clinopyroxene is more effective in changing Ba/La and La/Ce ratios than an olivine-rich peridotite source. For example, Ba/La and La/Ce ratios can be changed by factors of 1.13 and 1.15 respectivley, by 5% melting, or by factors of 1.6 and 1.5, respectively, by 1% melting of a garnet pyroxenite mantle source composed of 40% orthopyroxene, 40% clinopyroxene and 20% garnet (Fig. 3-5).

Ba/La, Ba/K, Rb/La, Th/La, Rb/K, Nb/La, Ta/La, and La/Ce ratios in the fresh Haleakala basalts vary by factors of 2.9 (Ba/La), 2.5 (Ba/K), 2.3 (Rb/La), 1.7 (Th/La), 1.6 (K/Rb), 1.4 (Nb/La), and 1.3 (La/Ce), while La abundances in the Haleakala tholeiites and alkalic basalts vary only by a factor of 3.6 (Figs. 3-4a,b,d,e,f,g,h). Such variation can not be produced by equilibrium melting of a compositionally uniform olivine-rich peridotite source. Possibly, a clinopyroxene dominated mantle source could produce

the observed ranges of some trace element abundance ratios such as Ba/La and La/Ce if the post-erosional basalts were derived from very small degrees (<1%) of partial melting and the tholeiites were derived by large degrees of partial melting.

However, there is considerable evidence against a homogeneous source composition for Haleakala basalts. For example: (1). The most mafic tholeiites (Mg#73), alkalic basalt from the alkalic Kula series (Mg#56) and alkalic basalt from the post-erosional Hana series (Mg#59) all have Al_2O_3/CaO ratio (1.3) close to the chondritic value. The result is consistent with a residue dominated by olivine and orthopyroxene but would only be a fortuitous result if the residue contained significant clinopyroxene and/or garnet. (2) Alkalic basalts from the post-erosional Hana series have higher Ba/La, Ba/K, Rb/Ca, Th/La, Rb/K, Nb/La, La/Ce, La/Nd, La/Sm, La/Yb etc. ratios than alkalic basalts of the Kula series. If these alkalic basalts were derived from a homogeneous mantle source, the post-erosional alkalic basalts must be derived by smaller degrees of partial melting than Kula basalts and therefore they should have higher abundances of incompatible trace elements than Kula alkalic basalts. Although the post-erosional basalts contain higher abundances of K, Rb, Ba, Th, Ta, and Nb, they do not always contain higher La and Ce abundances than the Kula alkalic basalts with the same Mg-numbers (Table 2). Moreover, abundances of moderately incompatible trace elements (e.g. Nd, Sm, Eu, Zr, and Hf) in the post-erosional alkalic basalts are lower than those of the Kula alkalic basalts (Fig. 3-2a and Table 2). Higher trace element abundance ratios (e.g. Ba/La, Rb/La, La/Ce, La/Sm, La/Yb) but lower abundances of moderately incompatible trace elements in the post-erosional basalts relative to Kula alkalic basalts require that these series were

derived from different mantle sources (3) Although Ba/La, Rb/La, La/Ce, La/Nd, La/Sm, La/Yb etc. ratios increase in the sequence Honomanu series - Kula series - Hana series, Nd/Sm ratios do not increase in the same sequence (Fig. 3-4n). Some of the post-erosional alkalic basalts have lower Nd/Sm ratios than Kula alkalic basalts (Fig. 3-4n). Figure 3-6 shows that except for hawaiites and mugearites, fractionation is ineffective in changing Nd/Sm ratios in the Haleakala samples. Thus the inverse sequence of Nd/Sm ratios in the Kula and Hana alkalic basalts compared to other trace element abundance ratios cannot be attributed to different degrees of fractionation between Kula and Hana basalts. The increasing Nd/Sm ratios with increasing La abundances in the Haleakala basalts (Fig. 3-4n) indicate that Nd is more incompatible than Sm. Therefore lower or similar Nd/Sm ratios in the post-erosional Hana basalts indicate that the post-erosional Hana basalts and Kula basalts were not derived from a compositionally homogeneous source by different degrees of melting. (4) The strongest evidence against a homogeneous mantle source for Haleakala basalts is their heterogeneous isotopic ratios (Chapter 2), and the correlation of highly incompatible element abundance ratios such as Ba/La, Rb/La, Nb/La and La/Ce with $^{87}Sr/^{86}Sr$ ratios (Figs. 3-7a to d). Since isotopic ratios are unaffected by equilibrium partial melting events (Hofmann and Hart, 1978), correlation of these element abundance ratios with isotopic ratios requires that the Haleakala mantle sources have heterogeneous isotopic ratios as well as heterogeneous trace element abundances.

Non-linear correlations between La and Yb (Fig. 3-1i), Zr (Fig. 3-3a), Hf (Fig. 3-3b), Sm and Eu abundances in the Haleakala lavas indicate that trace element abundances of the Haleakala lavas have not resulted from simple two-component magma mixing (Langmuir et al., 1978). However,

correlations between highly incompatible trace element abundances (e.g. Figs. 3-1a to h), and between isotopic ratios and highly incompatible trace element abundance ratios (Figs. 3-7a to d) suggest that mixing of two mantle sources or mixing of at least 3 compositionally distinct melts derived from two mantle sources are plausible. Discussions of plausible processes which created heterogeneous Haleakala mantle sources and mixing processes which are consistent with the geochemical data will be presented in Chapter 4.

4-3 Evaluation of partial melting and fractionation processes

As just discussed, Haleakala lavas are derived from compositionally heterogeneous mantle sources. To avoid the complexity caused by source heterogeneity, only samples with similar isotopic ratios and similar highly incompatible trace element abundance ratios (e.g. Th/La, Nb/La, La/Ce) will be selected in evaluating partial melting and fractionation processes.

(a) Tholeiites

$^{87}Sr/^{86}Sr$ and $^{143}Nd/^{144}Nd$ ratios of the 7 tholeiites are within the analytical errors at the 99.7% confidence level (3σ) (Chapter 2), and Ba/La, Th/La, Nb/La and La/Ce ratios (Figs. 3-4e,f,g,h) of these 7 tholeiites are within the analytical errors at the 95% confidence level (2σ). These ratios are consistent with a homogeneous source for the tholeiites. Also, highly incompatible to intermediate incompatible trace element abundance ratios such as La/Sm, La/Eu, La/Yb and La/Lu of six tholeiites (HO-1, HO-3, HO-4, HO-5, C121, C123) are very similar (Figs. 3-4j to m) indicating that they may have been derived by the same degree of partial melting. The remaining tholeiite (C122) has lower La/Sm, La/Eu, La/Yb, La/Lu and Nd/Sm ratios (Fig. 3-4j to n) than other tholeiites, possibly, a larger degree of partial melting was required for C122. Bulk

rock and olivine major element compositions show that C122 may be close to a primary melt in equilibrium with mantle olivine composition of Fo_{90}.

Major element compositions of the six tholeiites (HO-1, HO-3, HO-4, HO-5, C121, C123) can be related to each other by addition or subtraction of mostly olivine and minor clinopyroxene (Chapter 1). Parallel chondrite-normalized REE abundances (Fig. 3-2b) for these six tholeiites are consistent with olivine dominated fractionation. Amounts of crystal fractionation were calculated for two (C121 and HO-1) tholeiites using major element compositions and assuming olivine in the mantle residue has composition of Fo_{90} (Chapter 1). C121 was calculated to represent residual melt after 20% olivine fractionatin and HO-1 was calculated to represent residual melt after 20% olivine and 11% clinopyroxene fractionation (Chapter 1). Transition metal abundances (Sc,V,Cr,Co,Ni) are consistent with these calculations based on major elements (Chapter 1). Using these mineral proportions and the degree of fractionation, the partition coefficients in Table 3 and assuming equilibrium fractionation, the abundances of trace elements (Ba, Nb, La, Ce, Sr, Nd, Sm, Eu, Yb, Lu) in the parental liquids were calculated (Table 4). Heavy REE (Yb and Lu) abundances in parental liquid of HO-1 were calculated using both the lowest and highest partition coefficients in the literatures (Table 3 and Frey et al., 1978 for review of partition coefficients) between clinopyroxene and liquids. The calculated parental liquid compositions using both C121 and HO-1 compositions agree very well (better than ±10%, Table 4). Abundances of highly incompatible trace elements such as Ba, Nb, La and Ce in the calculated parental liquid for C121 and HO-1 are about 1.3 times that of C122 (Table 4). A plausible interpretation is that the degree of melting required to derive C122 is about 1.3 times that of the other tholeiites;

for example, if C122 was derived by 13% melting, the other tholeiites were derived by about 10% melting.

Heavy REE (Yb and Lu) abundances of C122 and the parental liquid of the other tholeiites are very similar (Table 4). Apparently, HREE concentrations were independent of melting degrees which indicates that the bulk partition coefficients (P) between mineral phases entering the melts and the melts (Shaw, 1970a) was close to 1. Although clinopyroxene may have a Yb mineral/liquid partition coefficient close to 1 (Table 3), if the melt formed from olivine and orthopyroxene in addition to clinopyroxene, a P^{Yb} close to 1 is not possible because of the dilution effect of olivine and orthopyroxene entering into the melt (Table 3). The partition coefficient of Yb between garnet and liquid ranges from 1.3 (Harrison, 1981) to 11.8 (see Frey et al., 1978 for review of partition coefficients). Thus garnet is required in the mantle source of Haleakala tholeiites in order to explain their uniform HREE contents.

The conclusions regarding differences in melting degree and residual garnet are based on calculated parental liquid compositions with the assumption that all the tholeiitic samples formed in equilibrium with mantle olivine of Fo_{90}. This conclusion is not affected as long as all the tholeiitic samples formed in equilibrium with mantle olivine of similar composition. Different olivine compositions in their mantle source would only affect the estimated amounts of olivine fractionation and not the relative amounts of trace element abundances in the two types of tholeiites. The assumption that all these tholeiites were in equilibrium with olivine of similar compositions is plausible because trace element ratios such as Ba/La, Nb/La and La/Ce indicate that they can be derived from the same source and that the degrees of melting required to form these

tholeiites differed by only small amounts.

Trace element analyses for transitional basalt (C126) and alkalic basalt (C124) from the Honomanu volcanic series are not completed yet. However, isotopic ratios (Chapter 2) and La/Ce, La/Nd and La/Yb ratios of transitional basalt are very similar to the six tholeiites (Figs. 3-4h,i,l); thus, the transitional basalt can be related to these six tholeiites by fractionation. Major element compositions suggest that olivine and minor clinopyroxene are the fractionating phases (Chapter 1). The alkalic basalt (C124) from the Honomanu volcanic series has similar $^{87}Sr/^{86}Sr$, $^{143}Nd/^{144}Nd$ (within 3σ analytical error, Chapter 2) and the same La/Ce ratio as tholeiites but higher La/Yb ratio than tholeiites (Table 2) indicating that it may have been derived from similar mantle source but by a lower degree of melting.

(b) Alkalic samples - Kula series:

Three pairs of fresh alkalic samples (H65-4 vs. H85-22; H85-10 vs. H85-11 and H85-23 vs. H85-24) were selected for evaluation of fractionation and partial melting processes creating the alkalic samples. Each of the three pairs are successive lavas from the same drill core except H65-4 and H85-22. H65-4 is equivalent to H85-21 in stratigraphic position, isotopic ratios (Chapter 2), major element abundances (Chapter 1) and trace element abundances (Table 2) except for K, Rb and H_2O. H65-4 is very fresh in thin section but H85-21 is slightly altered, thus H65-4 was selected instead of H85-21 which is stratigraphically below H85-22. Samples H65-4, H85-22, H85-10 and H85-23 are alkalic basalts. H85-11 is a hawaiite and H85-24 is a mugearite. For each pair of samples, uniform isotopic ratios and La/Ce, Nb/La and Th/La ratios indicate that the two samples may have been derived from the same mantle source. Consequently, different major and trace

element abundances within each pair of samples may be due to differences in degree of fractionation and partial melting.

Major element compositions and transition metal abundances (Sc, V, Cr, Co, Ni) are consistent with a model whereby H85-22, H85-11 and H85-24 are differentiates from H65-4, H85-10 and H85-23, respectively. Trace element abundances in these samples can be used to test the validity of the fractionation models based on major element and transition metal abundances. Table 5 lists the calculated trace element abundances (Rb, Ba, Th, Sr, La, Ce, Nd, Sm, Eu, Yb and Lu) in the differentiated rocks assuming equilibrium fractionation of the mineral proportions inferred from the major element data and degrees of fractionation inferred from La abundances in the liquids by using partition coefficients in Table 3. Two sets of partition coefficients (Table 3), which are among the lowest and highest partition coefficients in the literature (e.g. Frey, et al., 1978, set 1 and set 2; Schnetzler and Philpotts 1970; Shih, 1972; Hart and Brooks, 1974; Zindler, 1980) are used in the calculations. The degrees of fractionation estimated from La abundances are similar to those inferred from major element modeling and from P_2O_5 abundances (Table 5 and Chapter 1). In general, the trace element abundances in the calculated residual liquids agree very well (±10%) with measured trace element abundances using both low and high partition coefficients except for Sm, Eu, Yb and Lu (Table 5). For Sm, Eu, Yb and Lu, the values calculated with high partition coefficients (set 2, Frey, et al., 1978) agree very well with the measured abundances, but the values calculated with low partition coefficients (set 1, Frey et al., 1978) are higher (up to 20%) than the measured abundances. The close agreement between calculated and measured incompatible (Table 5) and compatible (Chapter 1) trace elements coupled

with the similar degrees of fractionation estimated from major and trace element abundances and similar Sr and Nd isotopic ratios indicates that each pair of samples may be related by crystal fractionation.

These three parent-daughter pairs are identified in trace element abundance ratios vs. La abundances diagrams (Figs. 3-4b to n). In these figures the range of these three parent-daughter pairs span almost the entire range of the Kula samples (Figs. 3-4b to n). Consequently, variations in trace element abundance ratios in the Kula volcanic series are caused by crystal fractionation of compositionally distinct parental magmas (such as H85-10, H65-4 and H85-23) formed from compositionally distinct sources. Because source compositions are not known it is difficult to infer the range of partial melting required to generate these alkalic basalts. However, for samples derived from the same source (i.e. identical isotopic ratios and La/Ce and Th/La ratios), crystal fractionation of olivine, clinopyroxene, plagioclase and magnetite can produce the observed variations in trace element abundances (Figs. 3-4b to n) without requiring different degrees of melting.

Differences between alkalic basalts such as H65-4 and H85-22 require only small amounts of olivine, clinopyroxene, plagioclase and magnetite fractionation (Table 5); thus, the fractionation process was ineffective in changing trace element abundance ratios such as K/Ba, Rb/Sr, Rb/La, Ba/La, Th/La, Nb/La, La/Ce, La/Nd, La/Sm, La/Eu and Nd/Sm ratios (Figs. 3-4b to k, and Fig. 3-4n). However, major element modelling shows that derivation of hawaiites and mugearites from alkalic basalts requires abundant clinopyroxene and plagioclase fractionation (Table 5). Consequently, abundances of elements with significant mineral/melt partition coefficients for plagioclase and clinopyroxene are strongly affected by crystal

fractionation. For example, the partition coefficient between plagioclase and liquid for Ba is much larger than for La (Table 3); thus fractionation of abundant plagioclase decreases Ba/La ratio in the liquid. Similarly, La/Nd, La/Sm, Nd/Sm, La/Eu, La/Yb and La/Lu ratios increase in the residual melt if substantial clinopyroxene was fractionated and Rb/Sr ratio increases if substantial plagioclase was fractionated (Table 3). Variations in trace element abundance ratios from alkalic basalts to hawaiites and mugearites are shown in figures 3-4 (d to n), figure 3-6 and figures 3-8 (a to e). Th/La, Nb/La and La/Ce ratios (Figs. 3.4f,g,h, Fig. 3-8a) are quite constant, while Ba/La (Fig. 3-4e, 3-8b) decrease slightly and Rb/Sr (Fig. 3-4c), La/Nd, La/Sm, La/Eu, La/Yb, La/Lu and Nd/Sm (Figs. 3-4i to n, Fig. 3-6, Figs. 3-8c,d,e) increase. These trends are consistent with abundant plagioclase and clinopyroxene fractionation for deriving hawaiites and mugearites from alkalic basalts as predicted by major element modelling (Chapter 1).

(c) Alkalic samples - Hana series:

Alkalic basalts (H62-47, 48, 49, H65-8, 9, 10, 11) and ankaramites (H65-13, 14) from Hana volcanic series have a narrow range of trace element abundances (e.g. Fig. 3-2g). Except for H62-47, the alkalic basalts have similar isotopic ratios (Chapter 2) and highly incompatible trace element abundance ratios (e.g. Ba/La, Rb/La, Nb/La and La/Ce, Figs. 3-7a to d), thus these samples (except H62-47) may be derived from a similar mantle source. Among these alkalic basalts, trace element abundances correlate positively with Mg-numbers (Table 2). Five (H65-8, 9, 10, 11, H62-48) of the alkalic basalts have vary narrow ranges of trace element abundances (e.g., Ba, Sr and La vary by a factor of 1.1) (Table 2). Based on Sc concentrations in these samples (Chapter 1), minor amounts of clinopyroxene

fractionation can explain this narrow range of trace element variations.

Alkalic basalt, H62-47, has similar Ba/La, Rb/La, and Nb/La ratios as these five alkalic basalts but has the lowest La/Ce and $^{87}Sr/^{86}Sr$ ratio (Figs. 3-7a to d) and highest $^{143}Nd/^{144}Nd$ ratio (Chapter 2) among the alkalic basalts. Different isotopic ratios between H62-47 and the other alkalic basalts suggest that they were derived from distinct mantle sources or they represent mixtures of different mixing components and/or different mixing proportions. Possible processes which generate similar highly incompatible element ratios but different isotopic ratios between H62-47 and the other Hana alkalic basalts will be discussed in Chapter 4.

Another alkalic basalt (H62-49) contains abundant clinopyroxene and olivine crystals (cpx + ol ~20%), thus this sample is transitional between alkalic basalt and ankaramite. Most of the clinopyroxene crystals in this sample are large xenocrysts (Chapter 1). Lower abundances of incompatible trace elements such as Ba, Nb, La, Ce, Nd, Sm, Eu compared to the other five (H85-8, 9, 10, 11, H62-48) alkalic basalts (~ factors of 0.85 to 0.91) are likely due to dilution effect of xenocrystic clinopyroxene.

The other two ankaramites have slightly lower $^{87}Sr/^{86}Sr$ ratios and slightly higher Ba/La, Nb/La ratios (Table 2 and Figs. 3-7a to d) than the Hana alkalic basalts; thus they were probably derived from slightly different mantle sources than these Hana alkalic basalts. Major element compositions show that large olivine and clinopyroxene crystals in these ankaramites are probably accumulated crystals (Chapter 1).

4-4 Systematic variations in trace element abundance ratios as a function of stratigraphy

Alkalic samples of Kula and Hana volcanic series are from drill cores (Chapter 1); consequently, stratigraphic control for these alkalic samples

is very good. However, the drill cores do not contain tholeiites, but field relations conclusively show that the stratigraphic position of the tholeiites is beneath the Kula alkalic series. Trace element abundance ratios are plotted as a function of depth in Figures 3-9 (a to m) for samples from the Kula and Hana volcanic series. Average values of tholeiites from the Honomanu volcanic series are plotted at an arbitrary depth below the Kula alkalic series (Figs. 3-9a to m). The abundance ratios in Haleakala samples vary systematically with stratigraphic position (Figs. 3-9a to m). K/Rb and K/Ba decrease but Rb/La, Ba/La, Nb/La and La/Ce increase up the stratigraphic sections (Figs. 3-9a to f). Tholeiites, alkalic basalts, hawaiites, mugearites and ankaramites all fall in the same trends. In a mantle peridotite assemblage (ol + opx + cpx ± gt ± sp), the relative incompatibility of these trace elements is suggested to be Ba≈Rb≥Th≥K>Ta>Nb>La>Ce (e.g. Sun and Nesbitt, 1977; White and Schilling, 1978; Wood et al., 1979c). Thus the younger Haleakala lavas are more enriched in highly incompatible trace elements than the older lavas.

In the Nb/La vs. depth plot (Fig. 3-9e) alkalic basalt, H85-15, falls below the trend. This sample and H85-14 (Fig. 3-9e) contain magnetite phenocrysts (Chapter 1), therefore, the lower Nb/La ratio in H85-15 could be due to magnetite fractionation (e.g., Pearce and Norry, 1979). The abundance of FeO, TiO_2 and V in these two alkalic basalts are consistent with magnetite fractionation and with more magnetite fractionated from H85-15 than from H85-14 (Chapter 1).

In K/Rb, K/Ba and Rb/La, vs. depth plots, altered samples fall off the trends established by fresh samples (Figs. 3-9a to c). The most obvious example is the sample with altered glass (H85-13) which lies far below the Rb/La vs. depth trend but far above the K/Rb vs. depth trend when compared

to fresh samples from similar stratigraphic levels (Figs. 3-9a and c). Loss of K and Rb due to alteration with Rb loss exceeding that of K is suggested. The data points for tholeiites in plots involving K or Rb are the average values for fresh tholeiites (Figs. 3-9a to c).

La/Nd ratios in the Haleakala lavas also increase up the stratigraphic section (Fig. 3-9g). However, La/Sm, La/Eu, La/Yb, La/Lu and Nd/Sm ratios increase from tholeiites to the upper section of Kula alkalic basalts; thereafter, La/Sm, La/Eu, La/Yb and La/Lu ratios are quite constant but Nd/Sm ratios decrease up the stratigraphic section with relatively low ratios in the Hana alkalic basalts and ankaramites (Figs. 3-9h to l). La/Nd, La/Sm, La/Eu, La/Yb, La/Lu and Nd/Sm ratios of hawaiites and mugearites are higher than alkalic basalts from similar depths (Fig. 3-9h to k). As previously discussed, the crystal fractionation process which creates hawaiites and mugearites from alkalic basalts increases these trace element abundance ratios. Therefore, the high La/Nd, La/Sm, La/Yb, etc. ratios in the hawaiites and mugearites probably reflect fractionation processes and are not a direct reflection of the melting process or source composition.

In contrast, among the alkalic basalts and tholeiites, olivine is the dominate fractionating phase and clinopyroxene is a minor fractionating phase; such fractionation does not effectively change La/Nd, La/Sm, La/Eu, La/Yb, La/Lu, and Nd/Sm ratios (Fig. 3-6 and Figs. 3-8c to e). The systematic variations of La/Nd, La/Sm, La/Eu, La/Yb, La/Lu and Nd/Sm ratios in the stratigraphic sections must reflect variations in source composition and/or degree of melting. Thus, either the sources of the younger basalts are more enriched in light-REE relative to intermediate-REE and heavy-REE than the older basalts or the degree of melting decreases from the Honomanu

volcanic series to the late alkalic Kula volcanic series at a depth of about 160 meters. From late Kula volcanic series to recent post-erosional Hana series, La/Sm, La/Eu, La/Yb and La/Lu remain constant while Nd/Sm ratios decrease slightly (Fig. 3-9h to 1). These trends suggest that the degree of partial melting increased slightly during this period if the sources of the younger lavas had higher abundance ratios of highly incompatible elements relative to moderately incompatible elements.

Figure 3-9m show that Rb/Sr ratios in the Haleakala lavas correlate poorly with stratigraphic sequence. However, Rb/Sr ratios in the samples were affected by alteration and crystal fractionation. As discussed before, altered Haleakala samples tend to lose Rb, thereby decreasing their Rb/Sr ratios. Moreover, major element compositions shows that plagioclase is an important fractionating phase during late stage fractionation (Chapter 1). Since Sr is a compatible trace element in plagioclase (Table 3), fractionation of plagioclase increases Rb/Sr ratios in the residual liquid. Figure 3-9n shows that if only fresh samples with Mg-numbers greater than 43 are considered, Rb/Sr ratios in the Haleakala lavas increase up the stratigraphic section which is consistent with other trends indicating that the sources of younger lavas are more enriched in more incompatible trace element than the older lavas. In all these incompatible element vs. depth diagrams (Fig. 3-9a to n), ankaramites fall in the same trends as alkalic basalts.

4-5 Comparison of Haleakala basalts with modern Hawaiian basalts, mid-ocean ridge basalts and chondrites

Average trace element abundance ratios such as K/Rb, Ba/La, Nb/La, La/Ce, La/Sm, La/Yb, Zr/Hf for basalts from the three Haleakala volcanic series, Honomanu series, Kula series and Hana series, are compared with

average values for MORBs, chondrites and modern Hawaiian tholeiites such as those from Mauna Loa and Kilauea volcanoes in Table 6. As a group, the Hawaiian tholeiites have higher Ba/La, Nb/La, La/Ce, La/Sm and La/Yb ratios than the mid-ocean ridge tholeiites, i.e., they are relatively enriched in highly incompatible elements (Table 6, also Clague and Frey, 1980, Wright, 1981). The average Nb/La, La/Ce and La/Sm ratios in Haleakala tholeiites are very close to chondritic values but their average Ba/La ratio is lower and La/Yb ratios are higher than chondritic values (Table 6).

La/Ce, La/Sm and La/Yb ratios in average Mauna Loa tholeiites are slightly lower than the average Haleakala tholeiites (Table 6) but are identical to Haleakala tholeiite, C122 (Fig. 3-2b). The Kilauea tholeiites have Ba/La, Nb/La, La/Ce, La/Sm and La/Yb ratios intermediate between Haleakala tholeiites and alkalic basalts (Table 6). However, an early Kula alkalic basalt (H85-1) has Nb/La, La/Ce and La/Sm ratios similar to that of average Kilauea tholeiites. Average Ba/La and Nb/La ratios in alkalic basalts from the Kula and Hana volcanic series are close to chondritic values and higher than those in Haleakala, Mauna Loa, and Kilauea tholeiites (Table 6).

5. Summary of Conclusions

(1) Alteration of Haleakala samples decreases K and Rb abundances, and increases H_2O contents. All other trace elements studied were not obviously affected by alteration.

(2) Haleakala samples range widely in abundance ratios of highly incompatible elements such as K/Rb, K/Ba, Ba/La, Th/La, Nb/La and La/Ce although the total range in La content is less than a factor of 10. Heterogeneous mantle sources or mixing of at least two mantle sources are required to explain these trace element variations in Haleakala samples.

(3) The sources of the younger lavas had higher Ba/La, Rb/La, K/La, Th/La, Ta/La, Nb/La ratios than the sources of the older lavas. Light-REE (e.g. La) to intermediate-REE (e.g. Nd, Sm, Eu) and heavy-REE (Yb, Lu) abundance ratios indicate that sources of the younger lavas were also enriched in light-REE relative to intermediate-REE and heavy-REE or the degree of partial melting decreased from tholeiites to the late Kula alkalic basalts. Nd/Sm ratios in alkalic basalts from the Kula and Hana series suggest that the degree of partial melting may have increased slightly from the late Kula alkalic basalts to post-erosional Hana alkalic basalts.

(4) Tholeiites and alkalic basalts from the three Haleakala volcanic series have similar heavy-REE (Yb, Lu) abundances. When compared at the same Mg-number, the tholeiites have slightly higher Yb and Lu abundances than alkalic basalts (Table 2). Apparently, garnet was involved in the Haleakala basalt genesis.

(5) Among the seven Haleakala tholeiites, C122 was derived by larger degrees of partial melting than the other six tholeiites. However, Ba, Nb and LREE data indicate that the range in melting degree was only a factor of 1.3. Trace element abundance variations within the tholeiites (except C122) can be accounted for by subtraction or addition of olivine and minor clinopyroxene.

(6) Hawaiites and mugearites can be derived from their stratigraphically associated alkalic basalts by fractionation of abundant clinopyroxene and plagioclase and minor amounts of olivine and magnetite. Trace element abundance ratios such as Ba/La decrease while La/Sm, La/Eu, La/Yb, Nd/Sm and Rb/Sr increase in the residual melts during these fractionation processes.

(7) Although the two ankaramites have higher abundance ratios of incompatible elements such as Ba/La and Nb/La than alkalic basalts, on isotopic ratios vs. depth (Chapter 2) and all trace element abundance ratios vs. depth (Fig. 3-9a to n) diagrams ankaramites fall in the same variation trends as alkalic basalts. These trends imply that different isotopic ratios and highly incompatible element abundance ratios between ankaramites and alkalic basalts are likely due to differences in eruption ages rather than the difference in rock types. The xenocrystic clinopyroxene in H62-49 (transition between alkalic basalt and ankaramites) and xenocrystic olivine and clinopyroxene in ankaramites suggest that ankaramites are probably alkalic basalts which contain accumulated crystals.

(8) The Haleakala tholeiites have La/Ce, La/Nd and La/Sm ratios close to chondritic ratios while alkalic basalts have La/Ce, La/Nd and La/Sm ratios higher than chondritic ratios. If the Haleakala tholeiites and alkalic basalts were derived from peridotite sources by more than 1% partial melting, these REE abundance ratios suggest that the tholeiites can be derived from a source with a chondritic REE distribution and that the alkalic basalts were derived from sources with enriched LREE distribution patterns relative to chondrites.

(9) The Haleakala tholeiites have REE abundance ratios such as La/Ce, La/Sm, La/Yb very similar to average Mauna Loa tholeiites and some pre-historic Kilauea tholeiites (Chen and Frey, unpublished data). The oldest Kula alkalic basalt (H85-1) has La/Ce and La/Sm ratios very similar to modern Kilauea tholeiite. All these Hawaiian basalts are enriched in incompatible trace elements when compared to mid-ocean ridge basalts.

Table 1. Trace element abundances (ppm) of standard rocks (BHVO-1, BCR-1) and H85-8

	BHVO-1			BCR-1		H85-8
	a	b	c	a	d	a
K	4322	-	-	-	-	7717±17
Rb	9.1	10.1	8±2	(52)	47	18.3±0.1 (18.8)
Sr	397 (396)	(404)	326±62	332±10	330	690±2 (696)
Ba	133 (128)	(132)	133±2	680 (714±32)	675	297±2 (311)
Zr	178	170	145±16	192±4	190	244
Nb	18.7	20	19±4	12.3±1.0	13.5	30.3
La	15.4	14.4	17±2	24.1	26	24.7±0.4
Ce	37.6	36.7	33±5	53.6	53.9	58.7±1.6
Nd	23.6	23.4	23±6	28.0	29	33.3±1.6
Sm	6.11	5.79	5±1	6.30	6.6	7.98±0.16
Eu	2.02	2.00	1.7±0.2	1.90	1.94	2.74±0.14
Tb	1.02	-	0.8±0.2	1.1	1.0	1.07±0.06
HO	1.0	-	0.9±0.2	1.2	1.2	1.2±0.4
Yb	2.05	1.89	-	3.3	3.4	2.2±0.2
Lu	0.28	0.27	-	0.52	0.55	0.29±0.04
Hf	4.6	-	4±1	5.0	4.7	5.9±0.4
Ta	1.4	-	-	0.9	0.9	1.90±0.16
Th	1.0	-	0.8±0.2	5.4	6.0	1.8±0.2

a This study. The values of Rb, Sr and Ba listed inside the parentheses and Zr, Nb were determined by X-ray fluorescence (XRF) at University of Massachusetts. The values of K, and Rb, Sr, and Ba without parentheses were determined by isotope dilution (ID) method at M.I.T. The values of REE, Hf, Ta and Th were determined by instrumental neutron activation analyses (INAA) at M.I.T. Sr, Ba, Zr, Nb values for BCR-1 determined by XRF method are average of 10 replicates. K, Rb, Sr, Ba values for H85-8 by ID method are average of duplicates. REE, Hf, Ta and Th for H85-8 by INAA are average of 5 replicates. The errors listed in this table are 2σ errors.

b Sun *et al.* (1979).

c Flanagan (1976).

d Flanagan (1973).

Table 2: Trace element abundances (ppm) of Haleakala volcanic series

	Honomanu series								
	HO-1	HO-3	HO-4	HO-5	C-121	C-122	C-123	C-124	C-126
Rock type	Th	Th	Th	Th	Th	Th	Th	AB	Tran
depth+	(>300)	(>300)	(>300)	(>300)	(>300)	(>300)	(>300)	(>300)	(>300)
K (3)	2005	2490	1192	1266	1211	2158	1245	-	-
Rb (3)	0.82	4.39	0.44	0.51	0.50	4.11	0.55		
Rb (2)	-	-	0.50	-	0.55	4.61	-		
Sr (3)	353.	322.	343.	324.	336.	207.	308.		
Sr (2)	-	-	343.	-	332.	208.	-		
Ba (3)	-	-	94.	-	82.	-	-		
Ba (2)	105.	94.	92.	91.	77.	57.	90.		
Zr (2)	187.	158.	167.	163.	152.	103.	148.		
Nb (2)	13.7	12.8	14.6	14.5	12.4	7.2	11.9		
La (1)	13.6	10.8	12.5	12.1	11.6	7.1	10.3	19.7	16.0
Ce (1)	34.9	27.7	31.5	31.2	28.8	18.8	26.5	49.0	39.3
Nd (1)	21.8	18.5	20.8	20.7	19.5	12.3	17.8	30.4	25.0
Sm (1)	6.08	5.06	5.82	5.49	5.39	3.73	4.89	8.70	6.55
Eu (1)	2.35	1.95	2.02	2.10	1.94	1.39	1.86	2.88	2.45
Tb (1)	1.10	0.90	0.96	0.86	0.96	0.71	0.87	1.14	1.02
Ho (1)	1.3	1.1	1.0	1.2	1.0	0.8	0.96	1.31	1.37
Yb (1)	2.28	1.98	2.27	2.15	2.13	1.73	1.79	2.65	2.69
Lu (1)	0.31	0.27	0.31	0.30	0.27	0.24	0.24	0.39	0.38
Hf (1)	4.6	4.1	4.24	4.26	4.19	2.64	3.68	5.7	5.1
Ta (1)	1.1	0.8	1.0	1.0	0.63	0.51	0.77	1.30	0.96
Th (1)	0.9	0.8	0.9	0.9	0.8	0.8	1.0	1.4	1.2
Mg#**	57	62	61	61	60	73	(70)	46	57
H_2O	1.13	0.59	0.46	0.79	0.87	0.55	0.77	-	-

+ "depths" listed in this table are meters beneath the ground surface of drill hole 85. Depths in the parentheses are adjusted depths based on field relationship and core correlations (Chapter 1)

* the number in the parentheses indicates: (1) determined by INAA method (2) by XRF method (3) by I.D. method

** Mg# = Mg number = $(Mg/Mg + Fe^{2+})$ assuming $Fe^{3+}/(Fe^{2+} + Fe^{3+}) = 0.10$ (Chapter 1).

Table 2 (continued)

Kula series

	H85-1	H85-2	H85-7	H85-8	H85-9	H85-10	H85-11	H85-12	H62-2	H85-13
Rock type	AB	ha	AB	AB	AB	AB	ha	AB	AB	AB
depth	300	299	261	255	252	249	245	240	(~239)	229
K	8136	9525	7388	7717	7056	7056	12495	9547	10032	9658
Rb	19.0	21.7	18.1	18.3	17.2	17.4	30.1	22.9	23.6	18.5
Rb	18.7	-	-	18.8	-	-	30.2	-	-	-
Sr	580.	752.	649.	690.	769.	688.	930.	719.	725.	733.
Sr	582.	753.	-	696.	-	-	942.	-	-	-
Ba	-	-	-	297.	-	-	481.	-	-	-
Ba	328.	343.	320.	311.	321.	313.	482.	435.	419.	420.
Zr	291.	297.	241.	244.	238.	238.	370.	299.	285.	304.
Nb	32.5	33.5	30.1	30.3	29.1	29.6	47.1	37.3	37.2	39.6
La	27.7	29.8	25.5	24.7	24.5	24.9	39.7	32.9	30.5	32.6
Ce	68.7	72.0	59.8	58.7	58.2	59.0	92.7	76.0	70.8	79.1
Nd	38.5	42.5	33.4	33.3	33.2	35.2	48.4	43.6	39.2	46.1
Sm	9.33	9.91	8.20	7.98	7.92	7.98	11.12	9.99	9.17	10.27
Eu	3.28	3.56	2.97	2.74	2.92	2.68	3.67	3.34	3.21	3.29
Tb	1.25	1.37	1.31	1.07	1.26	1.27	1.47	1.27	1.25	1.35
Ho	1.5	1.4	1.1	1.2	1.1	1.1	1.5	1.4	1.3	1.5
Yb	2.69	2.58	2.12	2.21	2.16	2.05	2.84	2.64	2.62	2.70
Lu	0.38	0.35	0.29	0.29	0.27	0.30	0.38	0.37	0.34	0.36
Hf	6.96	7.71	6.11	5.94	6.07	6.00	8.56	7.38	6.82	7.48
Ta	2.4	2.1	2.0	1.9	1.8	1.8	3.5	2.5	2.4	2.4
Th	2.1	2.3	1.8	1.8	1.9	2.0	2.8	2.5	2.3	2.2
Mg#	42	41	46	47	47	48	42	43	45	40
H_2O	0.63	-	0.37	0.27	0.42	0.45	0.44	0.53	0.33	0.60

Table 2 (continued)

Kula series

	H85-14	H85-15	H85-16	H85-21	H65-4	H85-22	H62-14	H85-23	H85-24	H85-25
Rock type	AB	AB	ha	AB	AB	AB	AB	AB	Mu	Mu
depth	228	198	189	164	(164)	161	(160)	157	155	154
K	8600	7256	12702	6292	7222	8657	8061	8544	16142	17985
Rb	20.7	16.5	30.7	17.2	19.9	23.5	23.1	23.8	44.4	49.
Rb	-	-	-	-	-	-	-	-	-	-
Sr	743.	724.	974.	653.	616.	754.	689.	790.	1006.	1012.
Sr	-	-	963.	-	-	-	-	789.	1010.	999.
Ba	-	-	-	-	-	-	-	418.	-	-
Ba	359.	332.	585.	360.	350.	431.	411.	427.	766.	810.
Zr	251.	204.	337.	200.	200.	212.	228.	229.	438.	436.
Nb	34.5	27.9	57.1	33.1	33.3	37.3	37.2	40.	79.1	78.6
La	27.7	24.5	44.1	25.4	25.9	30.7	29.6	30.8	60.6	61.4
Ce	67.9	57.3	99.0	57.9	58.0	68.1	66.0	67.9	135.0	134.0
Nd	37.8	32.5	49.6	30.6	30.7	35.4	33.7	35.3	63.1	63.9
Sm	8.07	7.25	10.33	6.92	6.85	7.76	7.66	7.71	11.98	12.00
Eu	2.85	2.63	3.51	2.38	2.38	2.73	2.67	2.74	3.97	3.92
Tb	1.12	1.09	1.34	0.95	1.08	0.94	1.15	1.08	1.49	1.53
Ho	1.1	1.2	1.3	1.1	1.0	1.2	0.86	1.2	1.4	1.6
Yb	2.00	2.05	2.66	1.91	1.92	2.06	2.45	2.19	3.30	3.25
Lu	0.27	0.30	0.38	0.26	0.27	0.27	0.36	0.29	0.46	0.47
Hf	6.20	5.69	7.86	4.95	4.87	5.31	5.71	5.77	9.58	9.72
Ta	2.0	1.8	3.30	2.1	2.1	2.2	2.3	2.2	4.4	4.5
Th	2.0	1.8	4.1	2.1	2.1	2.5	2.6	2.7	5.5	5.5
Mg#	51	56	43	54	54	45	47	45	37	37
H_2O	0.48	0.58	-	0.89	0.21	0.26	0.52	0.54	-	-

Table 2 (continued)

	Kula series		Hana series						
	H85-31	H85-33	H62-47	H65-8	H65-9	H65-10	H62-48	H65-11	H62-49
Rock type	Mu	ha	AB	AB	AB	AB	AB	AB	AB
depth	110	82	70	64	62	60	(59)	58	(50)
K	18809	11681	8054	7717	7161	7696	7245	6800	6200
Rb	52.8	30.4	22.5	21.7	18.4	21.7	20.2	18.8	17.9
Rb	-	-	-	21.7	-	-	-	-	-
Sr	919.	913.	649.	603.	626.	608.	583.	582.	511.
Sr	902.	1104.	-	605.	-	-	-	-	-
Ba	-	-	430.	-	-	-	-	-	-
Ba	867.	541.	485.	433.	422.	406.	391.	391.	326.
Zr	426.	274.	194.	183.	180.	181.	173.	166.	151.
Nb	79.8	54.	35.9	33.6	32.9	33.5	31.	31.1	27.5
La	61.9	39.5	27.1	25.0	25.3	25.3	24.1	23.7	20.2
Ce	143.0	88.0	60.2	53.1	52.9	52.6	49.6	50.6	42.9
Nd	69.2	45.7	29.4	26.8	26.3	26.8	26.3	26.1	23.1
Sm	12.62	9.19	6.73	6.35	6.44	6.43	6.39	6.01	5.48
Eu	4.31	3.33	2.33	2.23	2.26	2.22	2.21	2.21	1.95
Tb	1.70	1.24	1.21	0.94	0.93	0.91	1.07	0.97	0.84
Ho	1.6	1.1	1.2	1.0	1.0	0.9	1.2	0.9	0.9
Yb	3.71	2.29	1.90	1.86	1.80	1.89	1.82	1.83	1.80
Lu	0.48	0.31	0.23	0.25	0.26	0.26	0.26	0.27	0.22
Hf	9.57	6.47	4.69	4.34	4.51	4.29	4.30	4.12	3.77
Ta	4.6	3.5	2.4	2.1	2.0	1.9	1.8	2.1	1.7
Th	5.4	3.5	2.6	2.4	2.9	2.5	2.3	2.6	2.0
Mg#	35	43	52	54	54	54	54	56	58
H_2O	-	-	0.25	0.10	0.44	0.17	0.18	0.33	0.24

Table 2 (continued)

	Hana series		
	H62-52	H65-13	H65-14
Rock type depth	ha (25)	ank 3	ank 2
K	11369	6228	7053
Rb	33.	17.	20.2
Rb	-	-	-
Sr	-	561.	565.
Sr	908.	-	-
Ba	-	-	-
Ba	650.	507.	468.
Zr	244.	174.	174.
Nb	49.9	35.	35.4
La	37.	25.2	25.3
Ce	79.6	52.6	53.4
Nd	38.7	27.1	27.8
Sm	8.50	6.59	6.61
Eu	3.02	2.36	2.28
Tb	1.20	0.94	0.91
Ho	1.2	1.1	0.9
Yb	1.93	1.76	1.73
Lu	0.28	0.26	0.23
Hf	5.91	4.20	4.32
Ta	2.8	2.1	2.0
Th	3.5	2.7	2.7
Mg#	46	59	59
H_2O	-	0.63	0.34

Table 3. Trace element partition coefficients*

	olivine		orthopyroxene		clinopyroxene		garnet		plagioclase	
	low	high	low	high	low	high	low	high	low	high
Rb	0.0005		0.0005		0.0037		0.002		0.019	0.36
Ba	0.0003		0.0005		0.0016		0.003		0.15	0.40
K	0.0004		0.0005		0.0013		0.003		0.18	-
Sr	0.0002	0.019	0.0003	0.024	0.072	0.095	0.007	0.01	1.2	-
La	0.0005	0.0021	0.0002	0.0021	0.02	0.084	0.001	0.004	(0.023)	(0.113)
Ce	0.0008	0.0033	0.0005	0.004	0.04	0.166	0.0033	0.02	0.023	0.113
Nd	0.0013	0.0055	0.0019	0.0083	0.09	0.382	0.0184	0.087	0.023	0.069
Sm	0.0019	0.0098	0.0028	0.0147	0.14	0.736	0.0823	0.32	0.024	0.040
Eu	0.0019	0.0088	0.0036	0.0171	0.16	0.753	0.1333	0.38	0.14	0.39
Yb	0.0040	0.0202	0.0286	0.1443	0.20	1.01	4.0	11.48	0.006	0.030
Lu	0.0048	0.0238	0.038	0.19	0.19	0.95	7.0	13	0.006	0.037

* Rb, Ba, K, Sr partition coefficients from Philpotts and Schnetzler (1970), Philpotts et al., (1972); Hart and Brooks, (1974); Shimizu and Kushiro, (1975); Arth, (1976); Zindler, (1980). Partition coefficients for rare-earth elements between olivine/liquid, orthopyroxene/liquid clinopyroxene/liquid and garnet/liquid are set 1 and set 2 partition coefficients from Frey et al. (1978). These two sets of partition coefficients are among the lowest and highest partition coefficients in the literature. Rare earth partition coefficients between plagioclase and liquid are compiled from Schnetzler and Philpotts (1970) and Shih (1972) for basaltic compositions. Bulk partition coefficients for Th, Ta and Nb are assumed to be intermediate between Ba and La in a peridotite (ol + opx + cpx ± gt ± sp) mineralogy (Sun and Nesbitt, 1977; Wood et al., 1979c).

Table 4. Trace element abundances (ppm) in C122 and calculated parental liquid of C121 and HO-1

	C122	L^P_{C121}	L^P_{HO-1}	L^P/C122
Ba	57	66	72	1.21
Nb	7.2	9.9	9.5	1.35
La	7.1	9.3	9.4	1.32
Ce	18.8	23.0	24.2	1.26
Sr	207	269	246	1.24
Nd	12.3	15.6	15.3	1.25
Sm	3.73	4.31	4.29	1.15
Eu	1.39	1.55	1.66	1.15
Yb	1.73	1.70	1.63(1.84)+	0.96(1.02)
Lu	0.24	0.22	0.22(0.25)+	0.92(0.98)

L^P_{C121} and L^P_{HO-1} are the calculated parental liquid compositions for C121 and HO-1, respectively, assuming the parental liquid was in equilibrium with mantle olivine of Fo90. Proportion and amount of mineral fractionation based on major element modeling (Chapter 1). Set 1 partition coefficients from Frey et al. (1978) are used. (Table 3, lower values).

+ Using set 2 partition coefficients from Frey et al. (1978) which is among the highest partition coefficients in the literature.

L^P/C122: average compositions of L^P_{C121} and LHO-1 compared to the composition of C122.

Table 5. Comparisons of calculated and measured trace element abundances in H85-22, H85-11 and H85-24

	H85-22 alkalic basalt			H85-11 hawaiite			H85-24 mugearite		
	cal(l)+	cal(h)+	meas.	cal(l)+	cal(h)+	meas.	cal(l)+	cal(h)+	meas.
Rb	23.8	23.5	23.5	28.8	26.7	30.1	47.4	43.0	44.4
Ba	410	412	431	503	475	481	809	745	766
Th	2.5	2.5	2.5	3.3	3.3	2.8	5.6	5.6	5.5
Sr	695	694	754	872	873	930	1053	1060	1006
La	30.7	30.7	30.7	39.7	39.7	39.7	60.6	60.6	60.6
Ce	68.6	68.2	68.1	93.3	91.5	92.7	133	129	135
Nd	36.2	34.6	35.4	54.8	51.5	48.4	67.7	63.2	63.1
Sm	8.0	7.7	7.8	11.4	10.5	11.1	14.6	12.3	12.0
Eu	2.8	2.6	2.7	4.0	3.3	3.3	4.9	3.9	4.0
Yb	2.2	2.1	2.1	3.1	2.5	2.8	4.1	3.2	3.3
Lu	0.32	0.29	0.27	0.46	0.38	0.38	0.54	0.44	0.46
*F(M.E)	78.1	78.1		58.2	58.2		42.5	42.5	
*F(P_2O_5)	83.0	83.0		61.1	61.1		47.9	47.9	
*F(La)	84.1	83.3		62.3	59.3		49.9	47.0	
parent	H65-4	H65-4		H85-10	H85-10		H85-23	H85-23	

+ Calculated trace element abundances using the proportions of mineral fractionation from major element modelling (Chapter 1), degree of fractionation from La abundances and partition coefficients in Table 3. Cal (l) represent values calculated from low partition coefficients and cal (h) represent values calculated from high partition coefficients from Table 3. Partition coefficients between magnetite and liquid are assumed to be zero. Bulk partition coefficient for Th is assumed to be zero. Equilibrium fractionation equation from Shaw (1970) is used.

* F(M.E), F(P_2O_5), F(La) represent amount of residual liquid based on major element modelling, P_2O_5 concentration in the lavas (Chapter 1) and La concentration in the lavas, respectively.

From major element least-square regression calculations (Chapter 1):
(H85-22) = (H65-4) - 5.5% ol - 10.2% cpx - 4.6% plag - 1.6% Mt
(H85-11) = (H85-10) - 0.8% ol - 21.6% cpx - 15.1% plag - 4.2% Mt
(H85-24) = (H85-23) - 3.9% ol - 21.1% cpx - 22.8% plag - 9.6% Mt

Table 6. Comparison of average trace element abundance ratios in Haleakala volcanic series, Mauna Loa tholeiites, Kilauea tholeiites, mid-ocean ridge basalts and chondrites

	Honomanu	Kula[a]	Hana[a]	ML[b]	KL[b]	MORB[c]	chondrites[d]
Ba/La	8±1	13±1	17±1	9	9	4	11-13
Nb/La	1.11±0.07	1.2±0.2	1.33±0.04	1.0	1.2	1.0	1.2-1.6
La/Ce	0.39±0.01	0.43±0.02	0.47±0.01	0.38	0.40	0.33	0.38
La/Sm	2.1±0.1	3.4±0.3	3.9±0.1	1.8	2.5	0.9	1.8
La/Yb	5.4±0.6	12±3	13.5±0.9	4.3	7.3	0.7	1.7

a Hawaiites and mugearites are not included in the average.

b Data from Basaltic Volcanism Study Project (1981). ML: Mauna Loa tholeiites. KL: Kilauea tholeiites.

c Data from Hart (1976); Sun et al. (1979); Wood et al. (1979c).

d From Clague and Frey (1982).

Figure 3-1: Variations of trace element abundances (ppm) in Haleakala volcanic series

(a) K vs. La, (b) Rb vs. La, (c) Ba vs. La, (d) Th vs. La, (e) Ta vs. La, (f) Nb vs. La, (g) Sr vs. La, (h) Ce vs. La, (i) Yb vs. La.

□: Tholeiites from Honomanu volcanic series

■: Transitional basalt and alkalic basalt from Honomanu volcanic series

△: Alkalic basalts from Kula volcanic series

○: Hawaiites and mugearites from Kula volcanic series

✶: Alkalic basalts and ankaramites from Hana volcanic series

●: Hawaiite from Hana volcanic series

Altered samples are circled in (a) and (b)

Figure 3-2: Chondrite-normalized rare-earth element (REE) abundances in Haleakala volcanic series

(a) Ranges of REE in each of the three Haleakala volcanic series (hawaiites and mugearites not included).

(b) Chondrite-normalized REE abundances in tholeiites from Haleakala, Mauna Loa and Kilauea volcanoes, solid lines are the two Haleakala samples with highest and lowest light-REE abundances. Average Mauna Loa tholeiites (ML) average historical Kilauea tholeiites (KL) are from Basaltic Volcanism Study Project (1981).

☼: a prehistory tholeiite from Kilauea volcano (EK80, Chen and Frey, unpublished data). (c) (d) and (e) chondrite-normalized REE abundances in alkalic basalts from Kula volcanic series.

(f) Chondrite-normalized REE abundances in hawaiites and

mugearites from Kula volcanic series, (g) chondrite-normalized REE abundances in alkalic basalts, hawaiite and ankaramites from Hana volcanic series. Solid lines in (c), (d), (e), (f), and (g) are for samples with the highest and lowest light-REE in each diagram. The sample numbers listed in (c), (d), (e) and (g) are arranged in stratigraphic sequence.

Figure 3-3: Variations of trace element abundances (ppm) in Haleakala volcanic series. (a) Zr vs. La, (b) Hf vs. La, (c) Zr vs. Hf. Symbols as in Figure 3-1.

Figure 3-4: Variations of trace element abundance ratios with La abundances in Haleakala volcanic series. (a) K/Rb vs. La, (b) K/Ba vs. La, (c) Rb/Sr vs. La, (d) Rb/La vs. La, (e) Ba/La vs. La, (f) Th/La vs. La, (g) Nb/La vs. La, (h) La/Ce vs. La, (i) La/Nd vs. La, (j) La/Sm vs. La, (k) La/Eu vs. La, (l) La/Yb vs. La, (m) La/Lu vs. La, (n) Nd/Sm vs. La. Symbols as in Figure 3-1. Altered samples are circled in (a), (b), (c), (d), (e) and (f). Three pairs of samples (H65-4 vs. H85-22, H85-10 vs. H85-11, H85-23 vs. H85-24) believed to be related by crystal fractionation (discussed in section 4-3) are connected by solid lines in (b) to (n). Error bars in (f) and (g) are $\pm 2\sigma$.

Figure 3-5: Enriched factors of trace element abundance ratios (La/Ce and Ba/La) and trace element abundance (La) by partial melting process. Enriched factors are defined as trace element abundances or abundance ratios relative to source values. Solid lines are for non-modal equilibrium partial melting of a peridotite source. Dashed lines are for non-modal equilibrium

partial melting of a pyroxenite source. See text for detail. Degree of melting (1%, 5% and 10%) are marked by solid dots on solid and dashed lines.

Figure 3-6: Variation of Nd/Sm ratios with Mg-numbers in the Haleakala volcanic series. Symbols as in Figure 3-1. Three pairs of samples related by crystal fractionation as discussed in section 4-3 are marked and connected by solid lines.

Figure 3-7: Correlations of trace element abundance ratios with $^{87}Sr/^{86}Sr$ ratios in Haleakala volcanic series. (a) Ba/La vs. $^{87}Sr/^{86}Sr$, (b) Rb/La vs. $^{87}Sr/^{86}Sr$, (c) Nb/La vs. $^{87}Sr/^{86}Sr$, (d) La/Ce vs. $^{87}Sr/^{86}Sr$. Symbols as in Figure 3-1 except for ankaramites. Ankaramites are indicated by ▩. Altered samples are circled in (b). Samples H62-47 and H62-49 which discussed in Section 4-3(c) are marked by "47" and "49".

Figure 3-8: Variations of trace element abundance ratios with Mg-numbers in the Haleakala volcanic series. (a) La/Ce vs. Mg-numbers, (b) Ba/La vs. Mg-number, (c) La/Sm vs. Mg-number, (d) La/Eu vs. Mg-number, (e) La/Yb vs. Mg-number. Symbols as in Figure 3-1. Three pairs of samples related by crystal fractionation and discussed in section 4-3 are marked and connected by solid lines.

Figure 3-9: Correlations of trace element abundance ratios in Haleakala volcanic series with stratigraphic sequences. (a) K/Rb vs. depth, (b) K/Ba vs. depth, (c) Rb/La vs. depth, (d) Ba/La vs. depth, (e) Nb/La vs. depth, (f) La/Ce vs. depth, (g) La/Nd vs. depth, (h) La/Sm vs. depth, (i) La/Eu vs. depth, (j) La/Yb vs. depth, (k) La/Lu vs. depth, (l) Nd/Sm vs. depth, (m) Rb/Sr vs.

depth. Symbols as in Figure 3-1. Ankaramites are the two samples plotted at depths of 2 meters and 3 meters. Depths in these plots are meters beneath ground surface of Holes 85 and 65. Samples from drill holes other than Holes 85 and 65 were adjusted depths (Chapter 1). Sea level is at a depth of around 300 meters. Average trace element abundance ratios in tholeiites are plotted at an arbitrary depth greater than the bottom of Kula volcanic series based on field observations. Altered samples are circled in (a), (b), (c) and (m). Only fresh tholeiites are included in the averages of K/Rb, K/Ba, Rb/La and Rb/Sr ratios for tholeiites. (n) Rb/Sr vs. depth for fresh samples with Mg-number greater than 43.

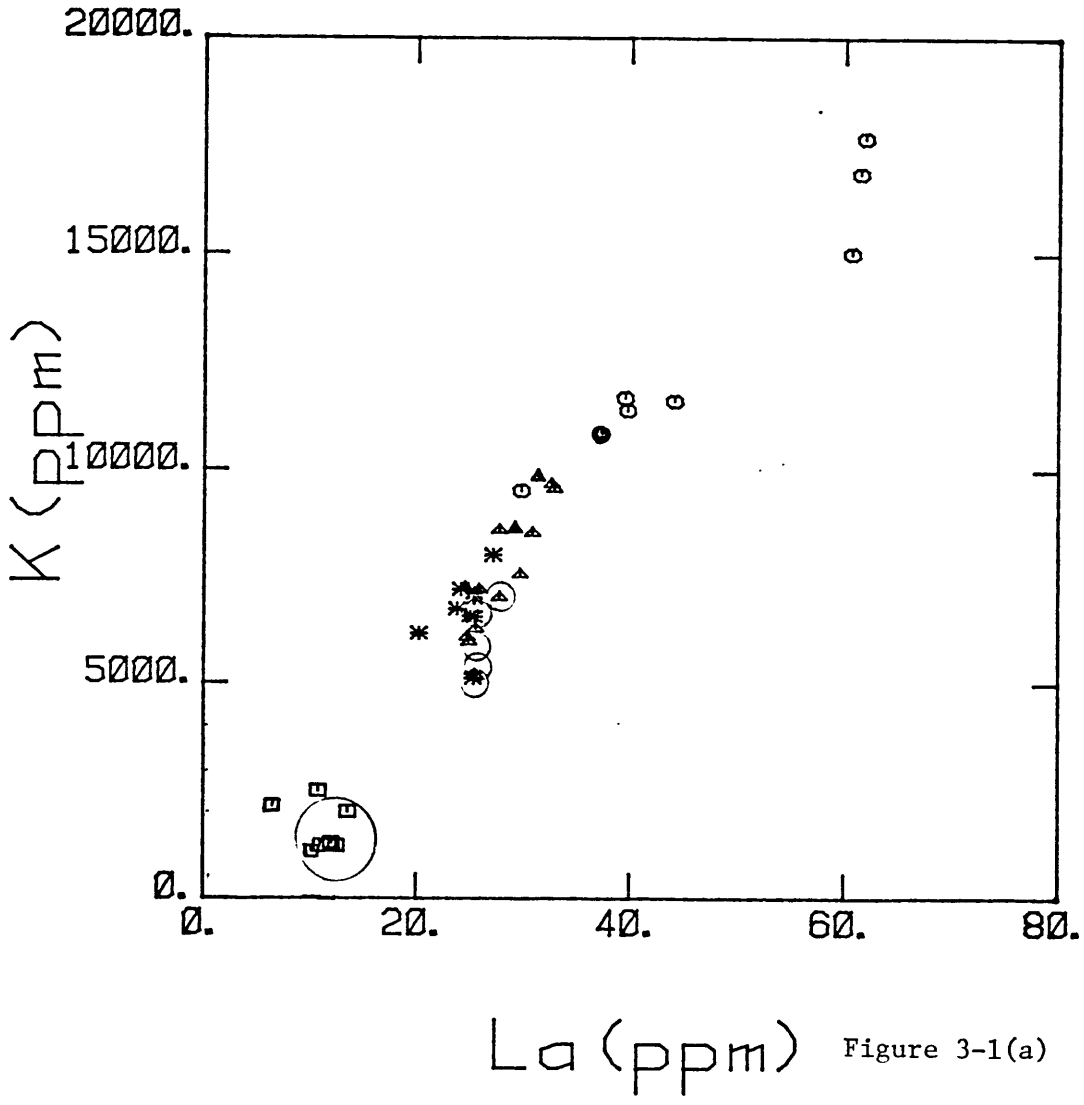


Figure 3-1(a)

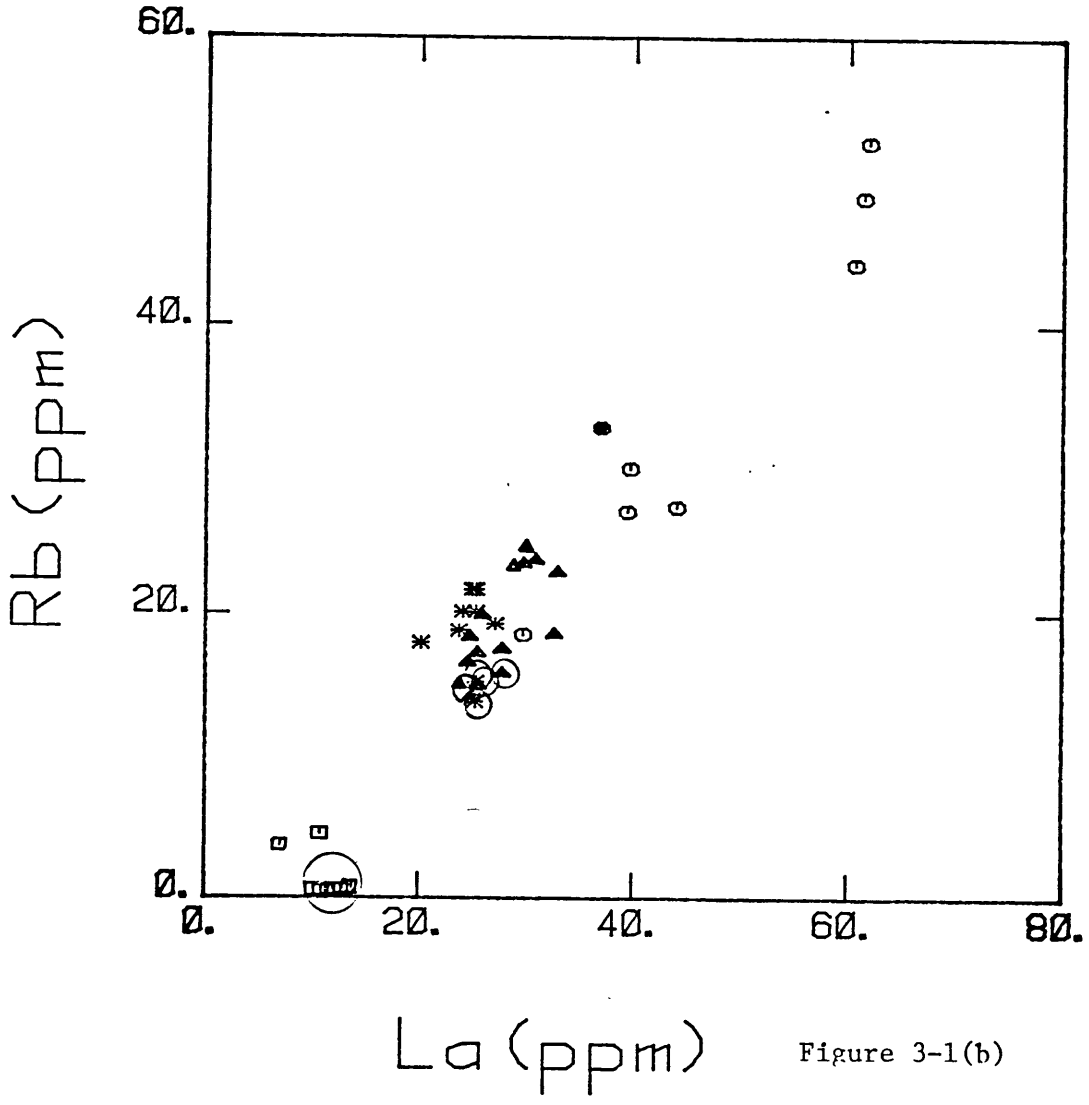


Figure 3-1(b)

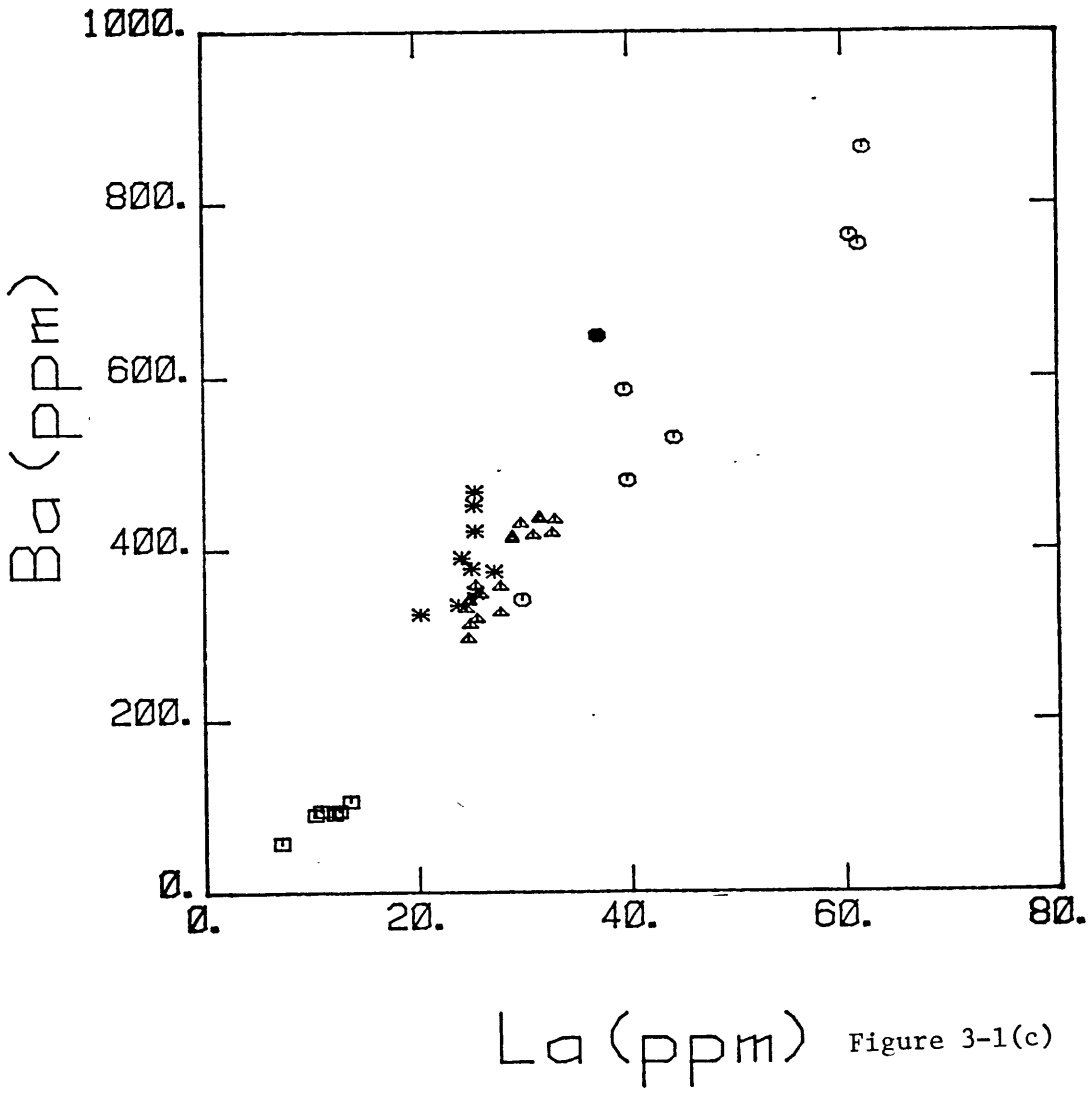


Figure 3-1(c)

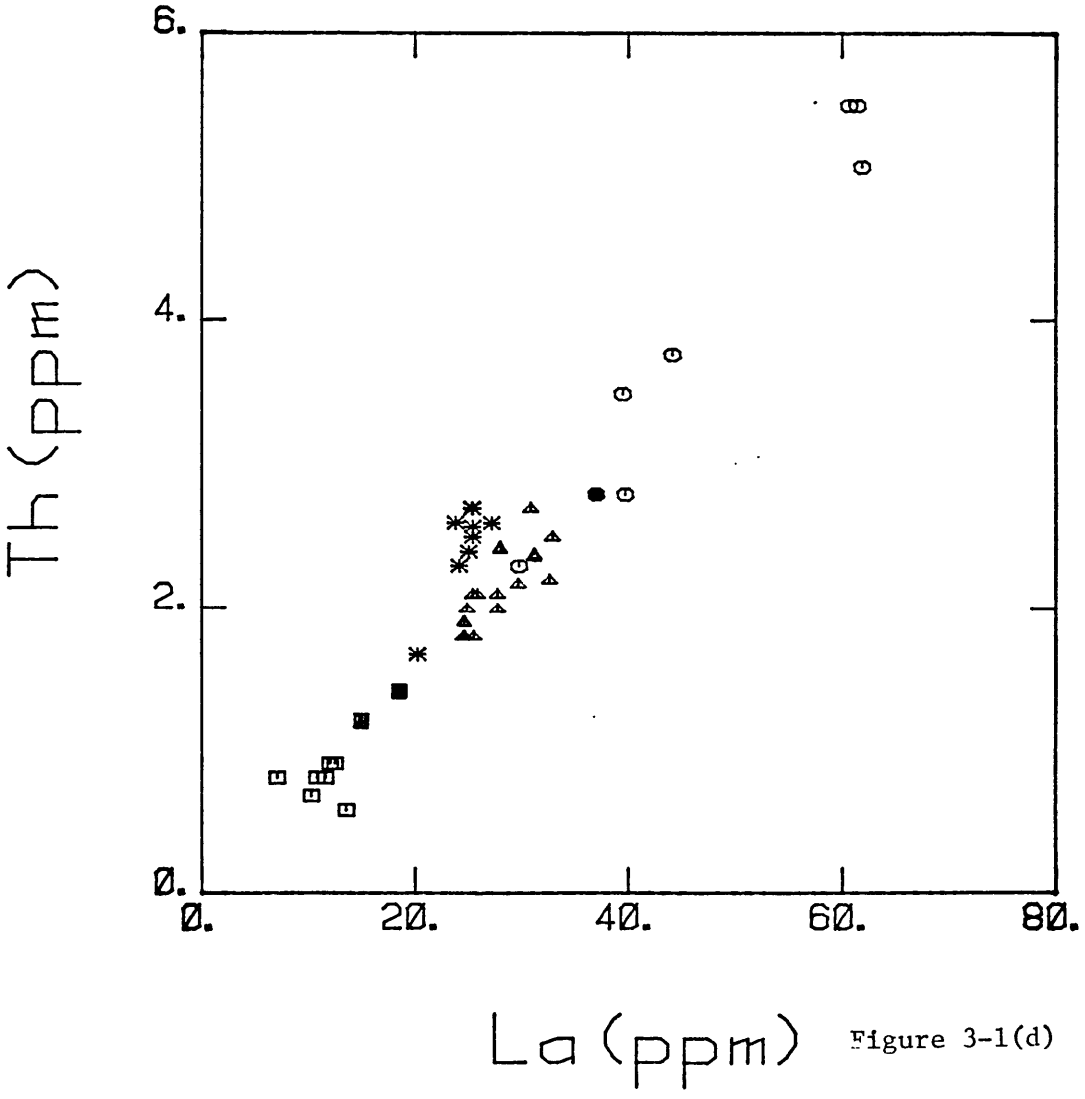


Figure 3-1(d)

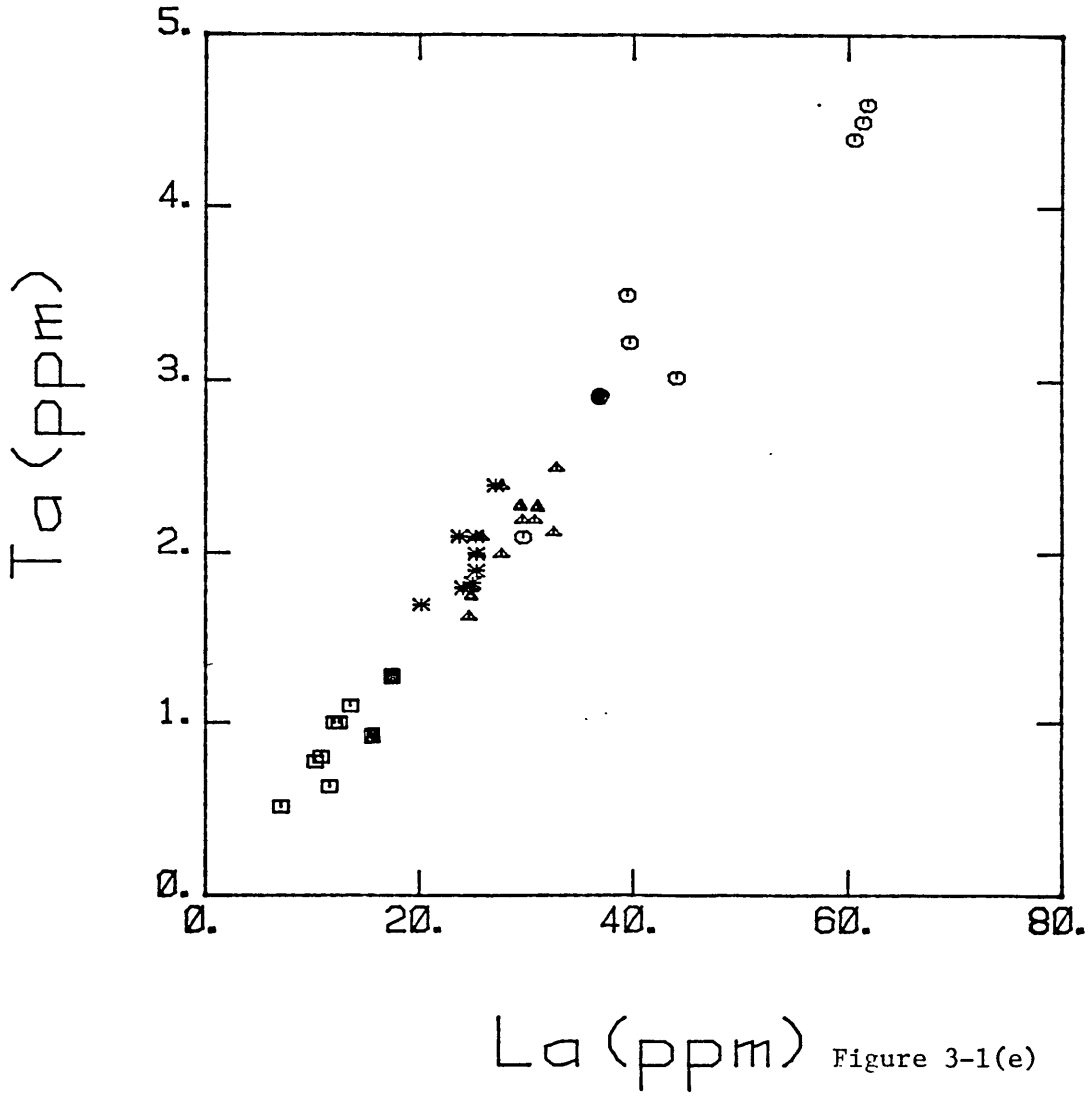


Figure 3-1(e)

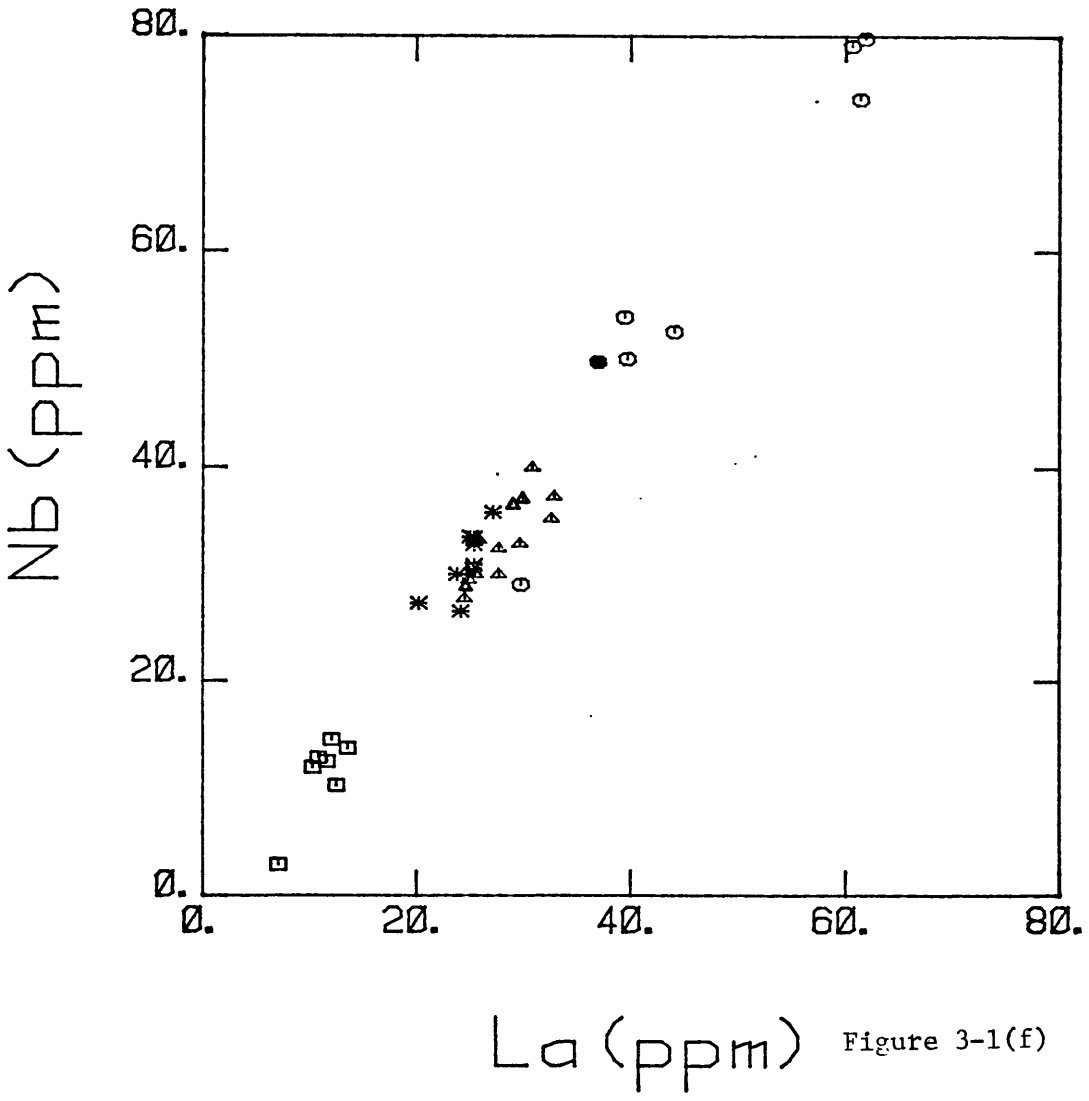


Figure 3-1(f)

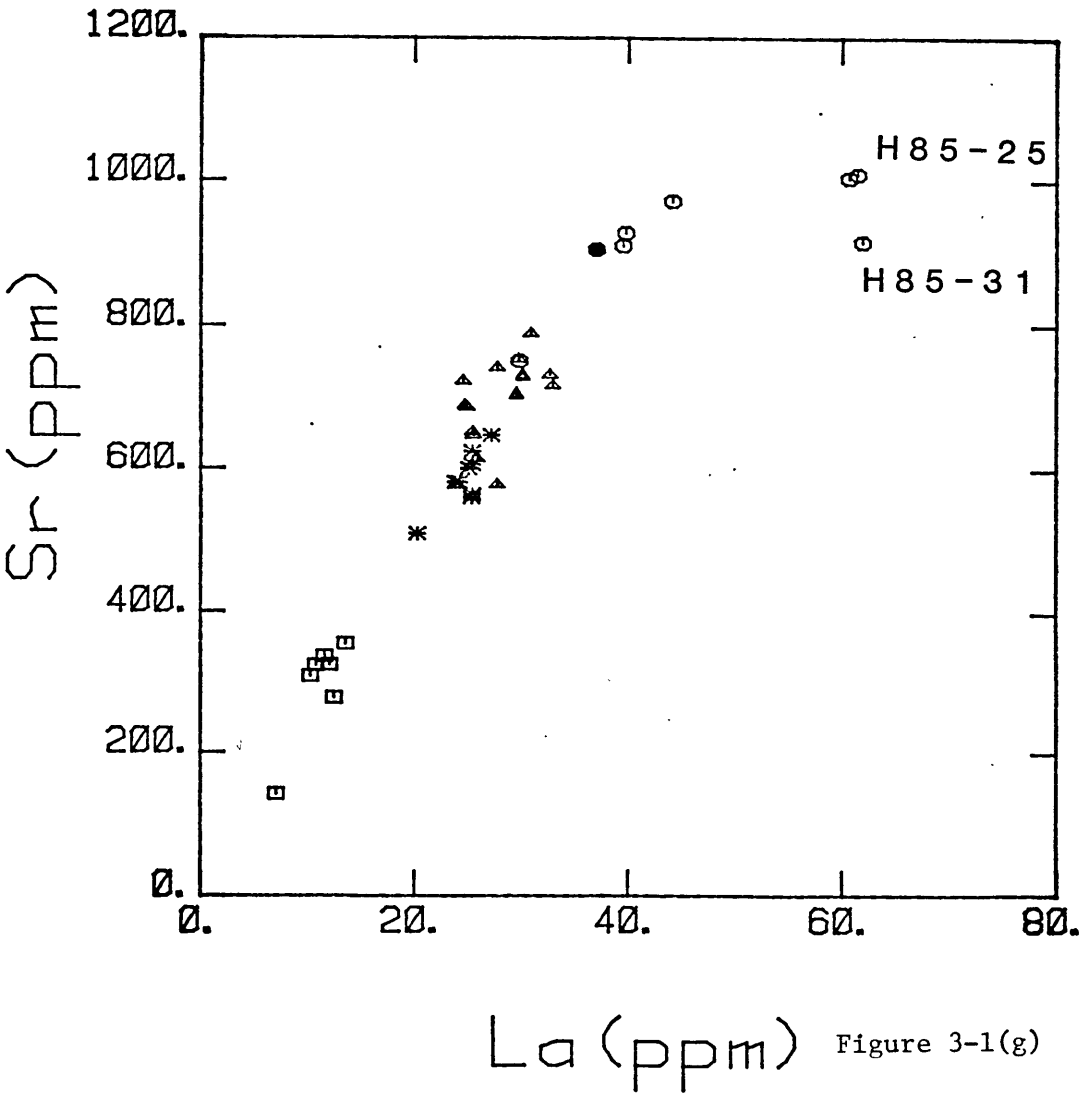

1200.
1000.
800.
600.
400.
200.
0.
Sr (ppm)
H85-25
H85-31
0.
20.
40.
60.
80.
La (ppm)

Figure 3-1(g)

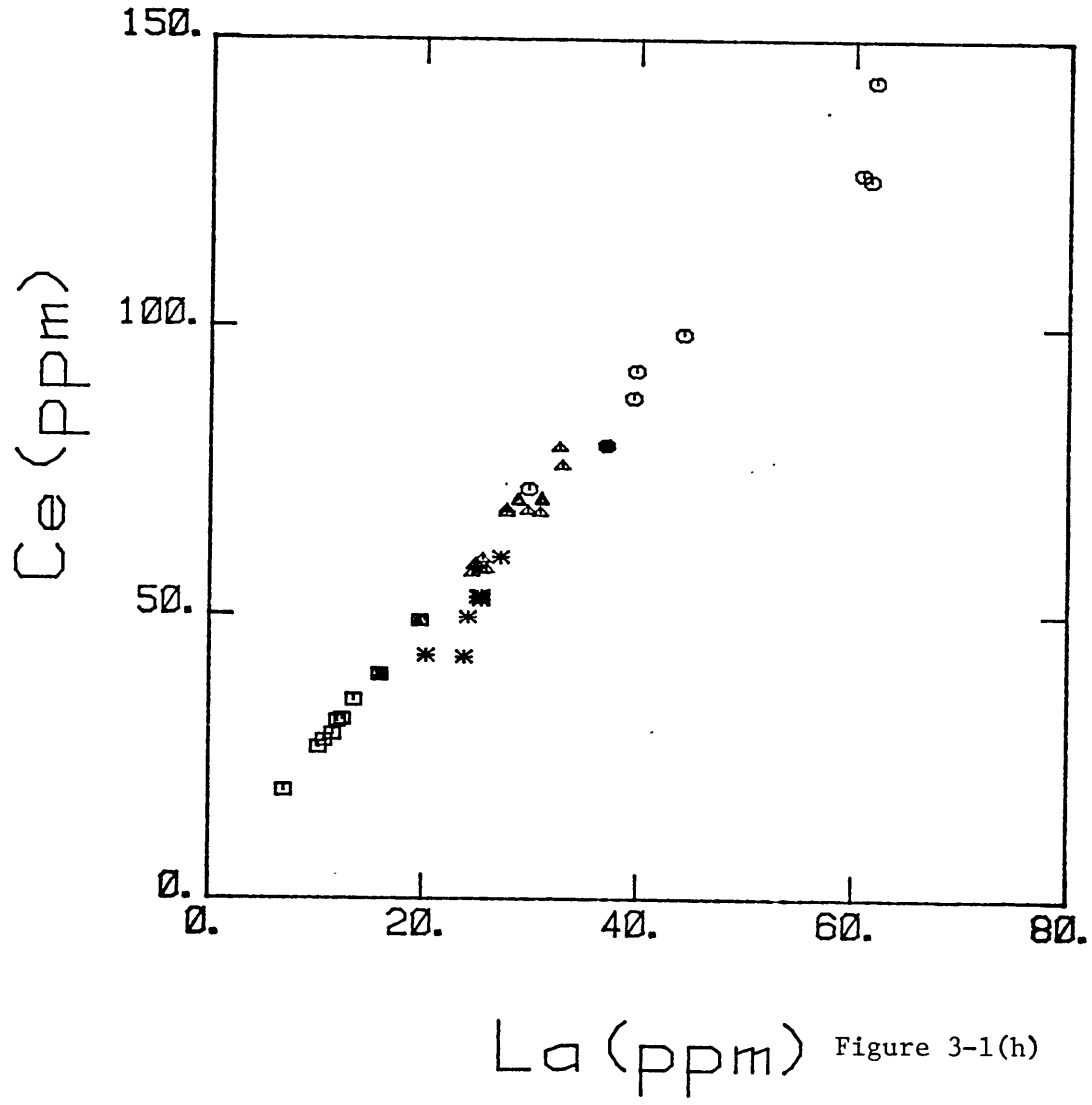


Figure 3-1(h)

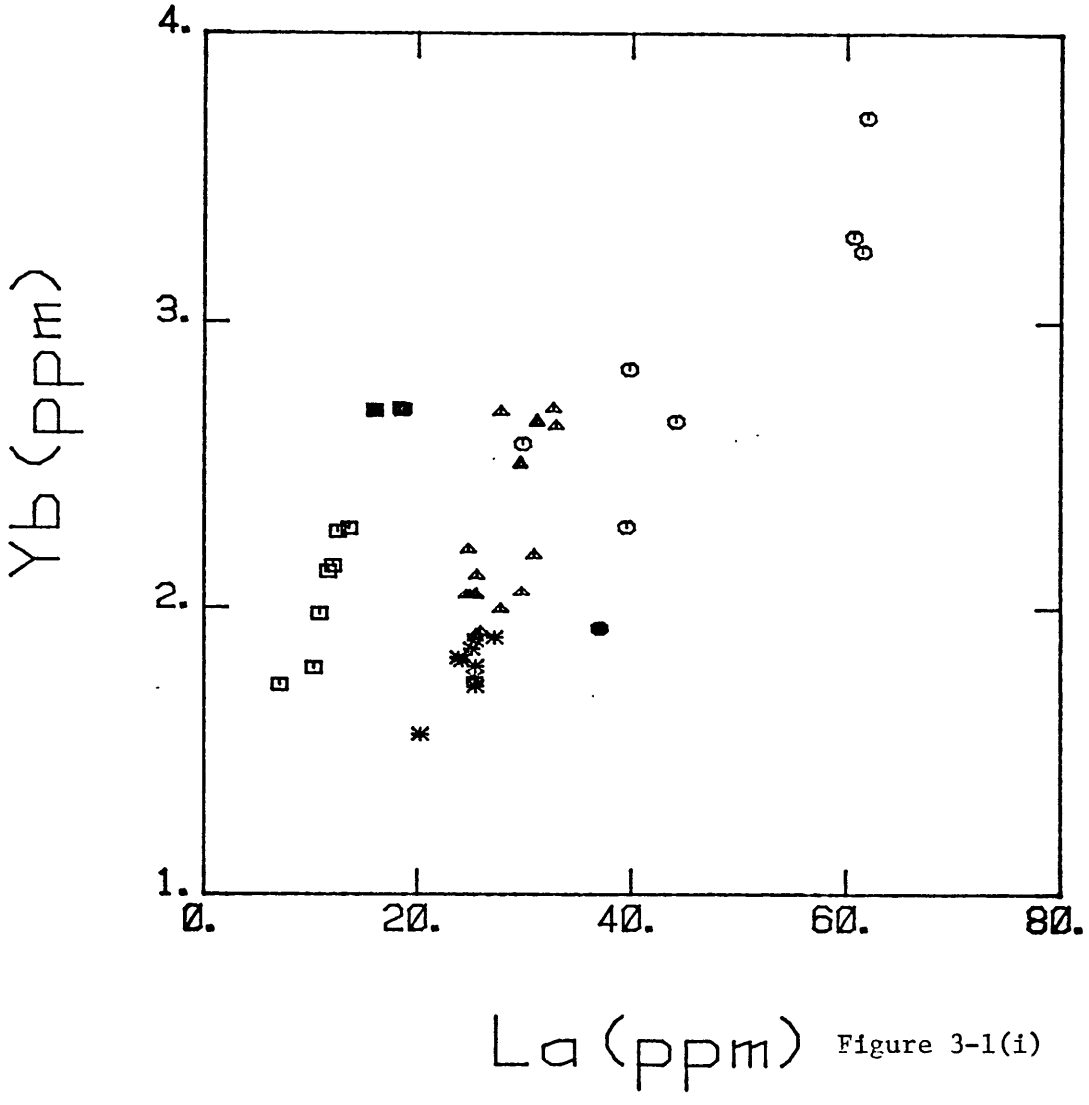


Figure 3-1(i)

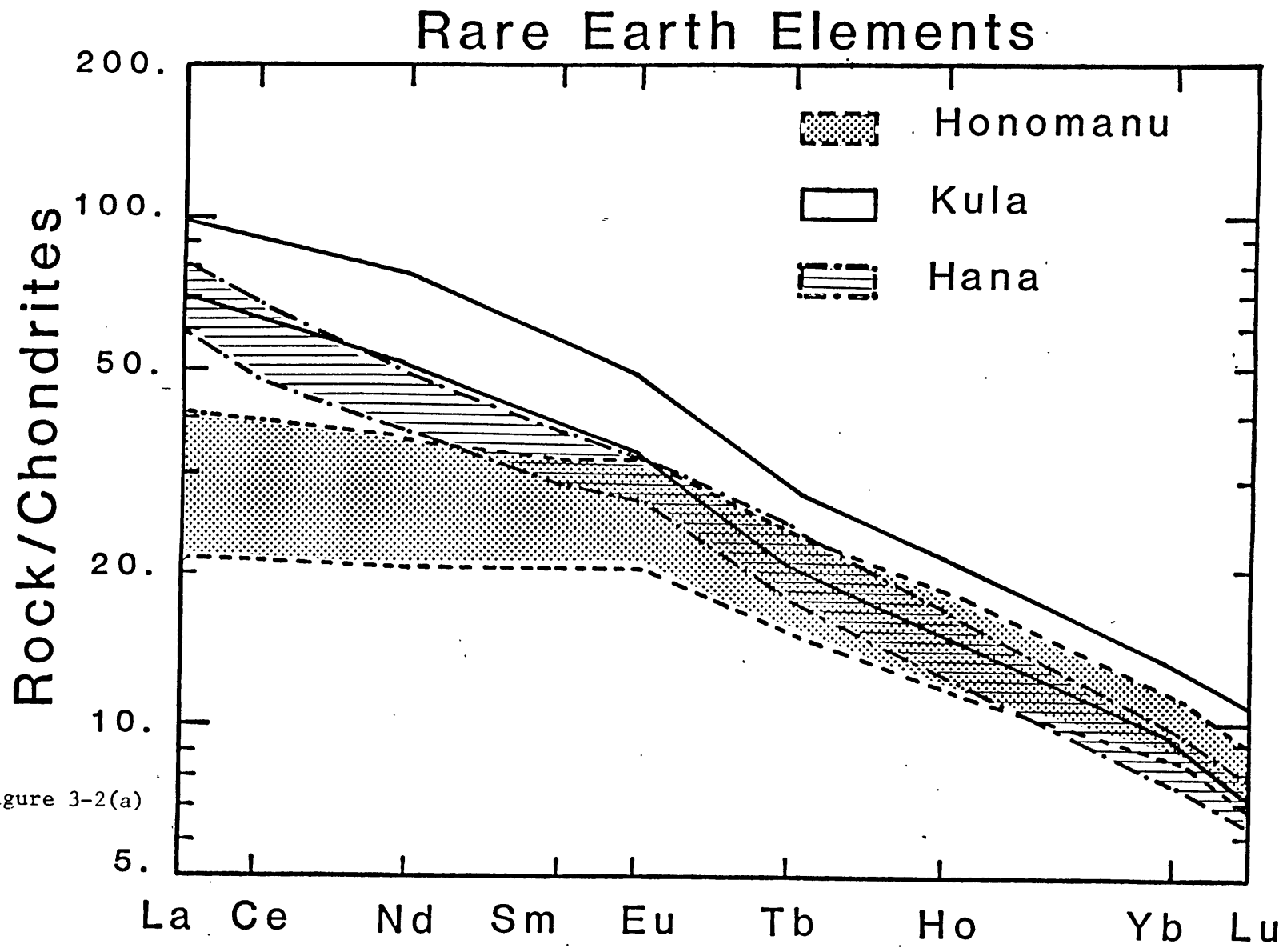

Rare Earth Elements
200.
100.
50.
20.
10.
5.
Rock/Chondrites
Honomanu
Kula
Hana
La
Ce
Nd
Sm
Eu
Tb
Ho
Yb
Lu

Figure 3-2(a)

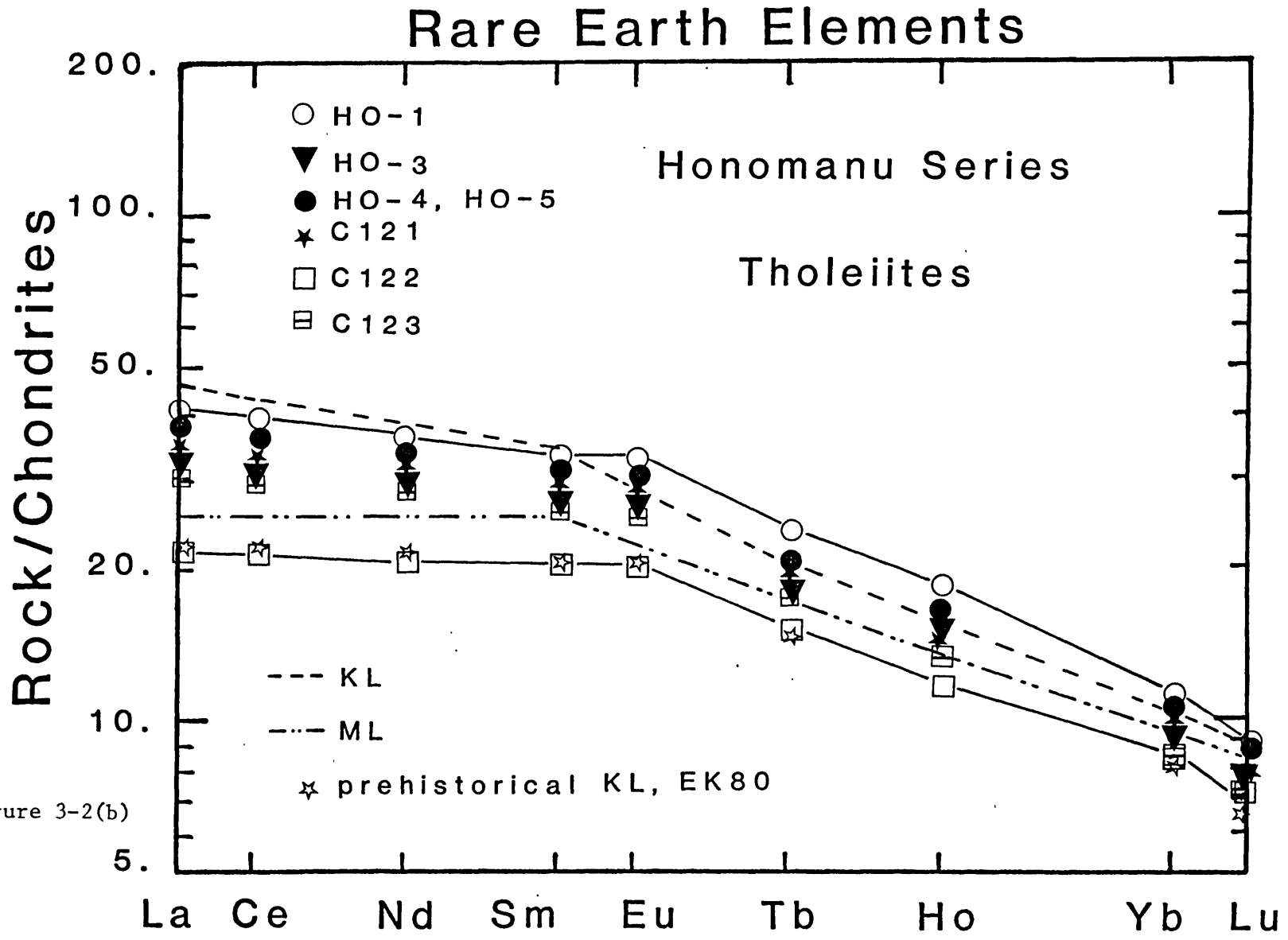

Rare Earth Elements
200.
100.
50.
20.
10.
5.
Rock/Chondrites
HO-1
HO-3
HO-4, HO-5
C121
C122
C123
Honomanu Series
Tholeiites
KL
ML
prehistorical KL, EK80
La
Ce
Nd
Sm
Eu
Tb
Ho
Yb
Lu

Figure 3-2(b)

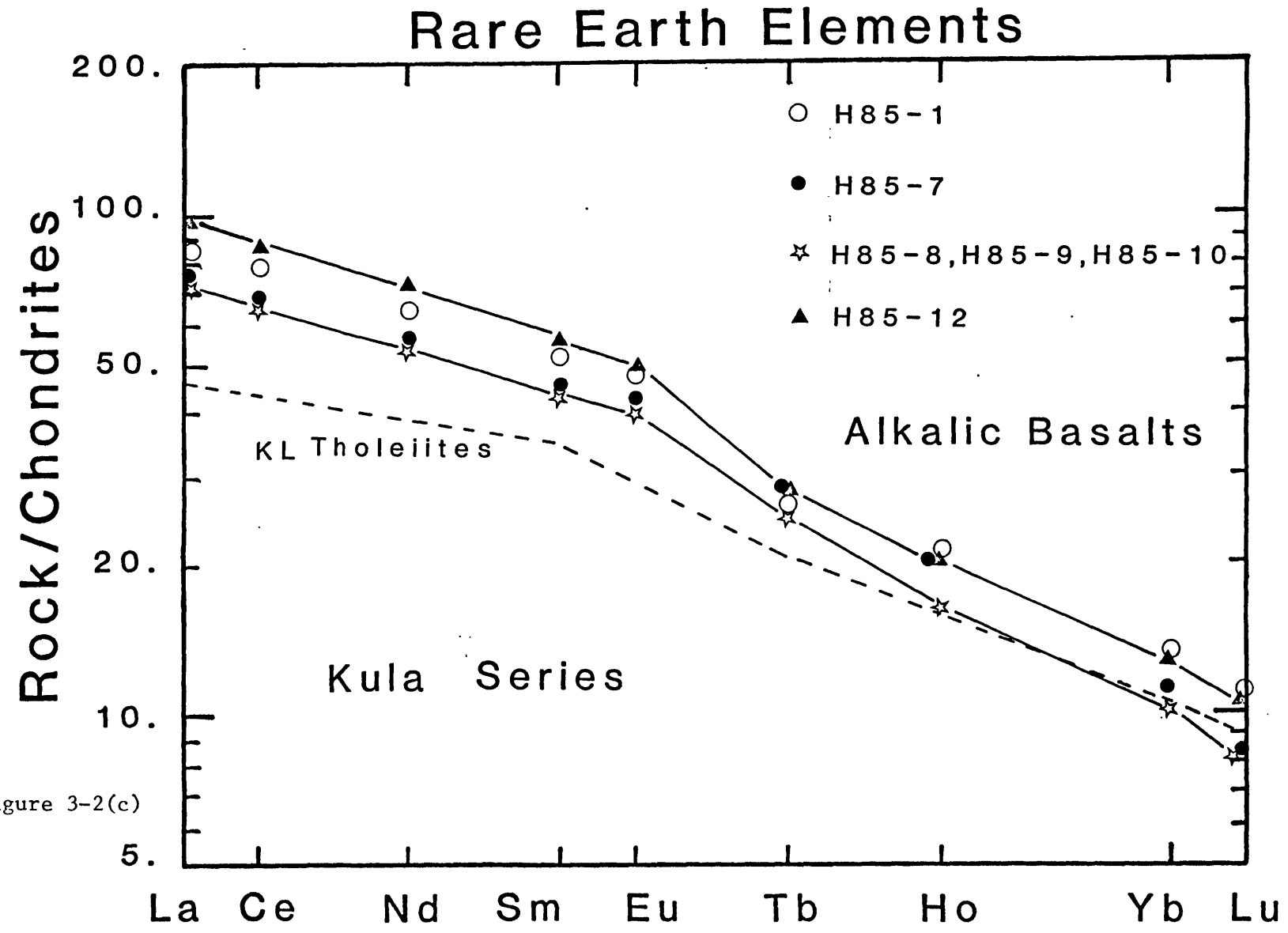

Rare Earth Elements
200.
100.
50.
20.
10.
5.
Rock/Chondrites
H85-1
H85-7
H85-8,H85-9,H85-10
H85-12
KL Tholeiites
Alkalic Basalts
Kula Series
La
Ce
Nd
Sm
Eu
Tb
Ho
Yb
Lu

Figure 3-2(c)

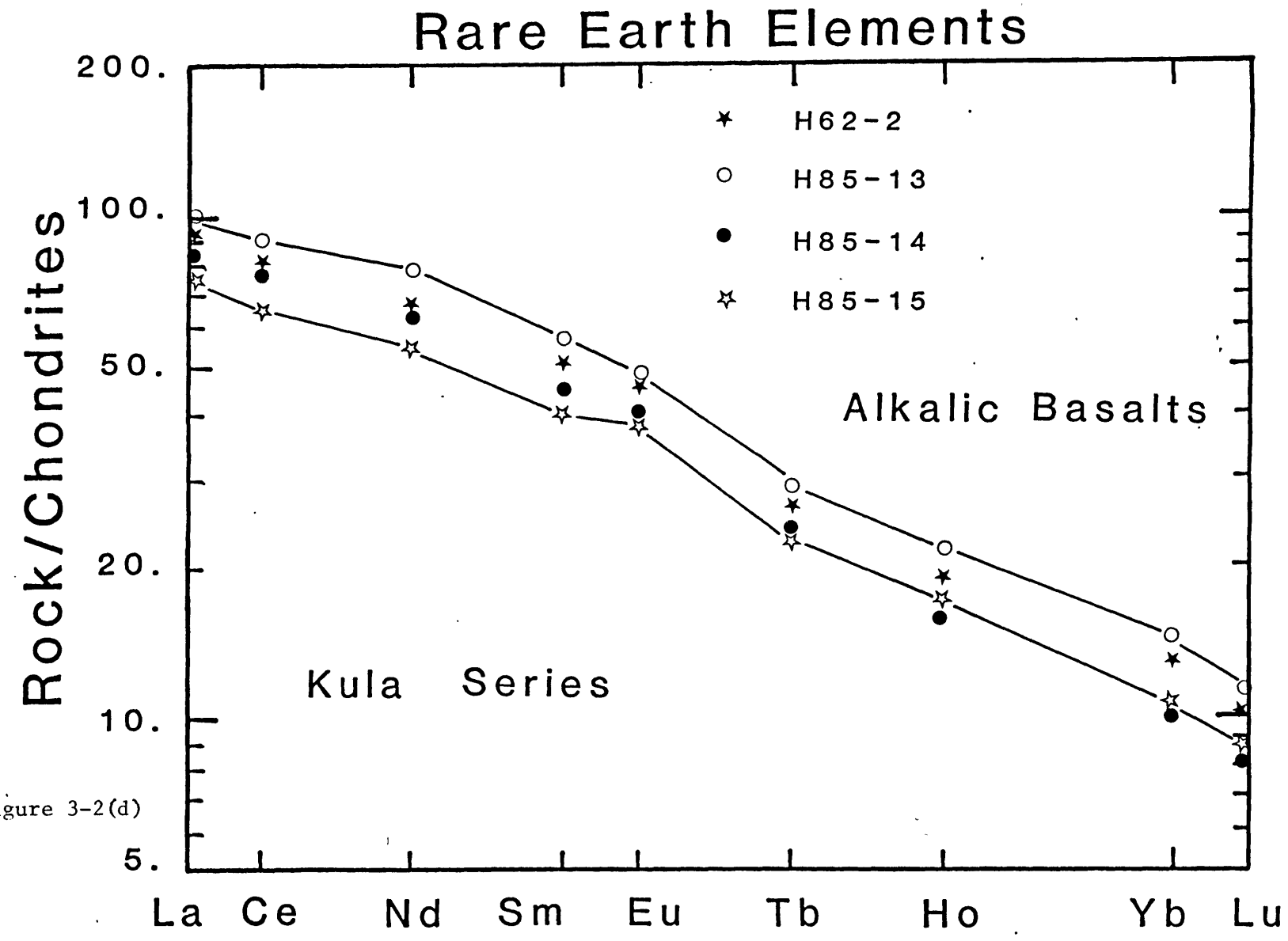

Rare Earth Elements
200.
100.
50.
20.
10.
5.
Rock/Chondrites
H62-2
H85-13
H85-14
H85-15
Alkalic Basalts
Kula Series
La
Ce
Nd
Sm
Eu
Tb
Ho
Yb
Lu

Figure 3-2(d)

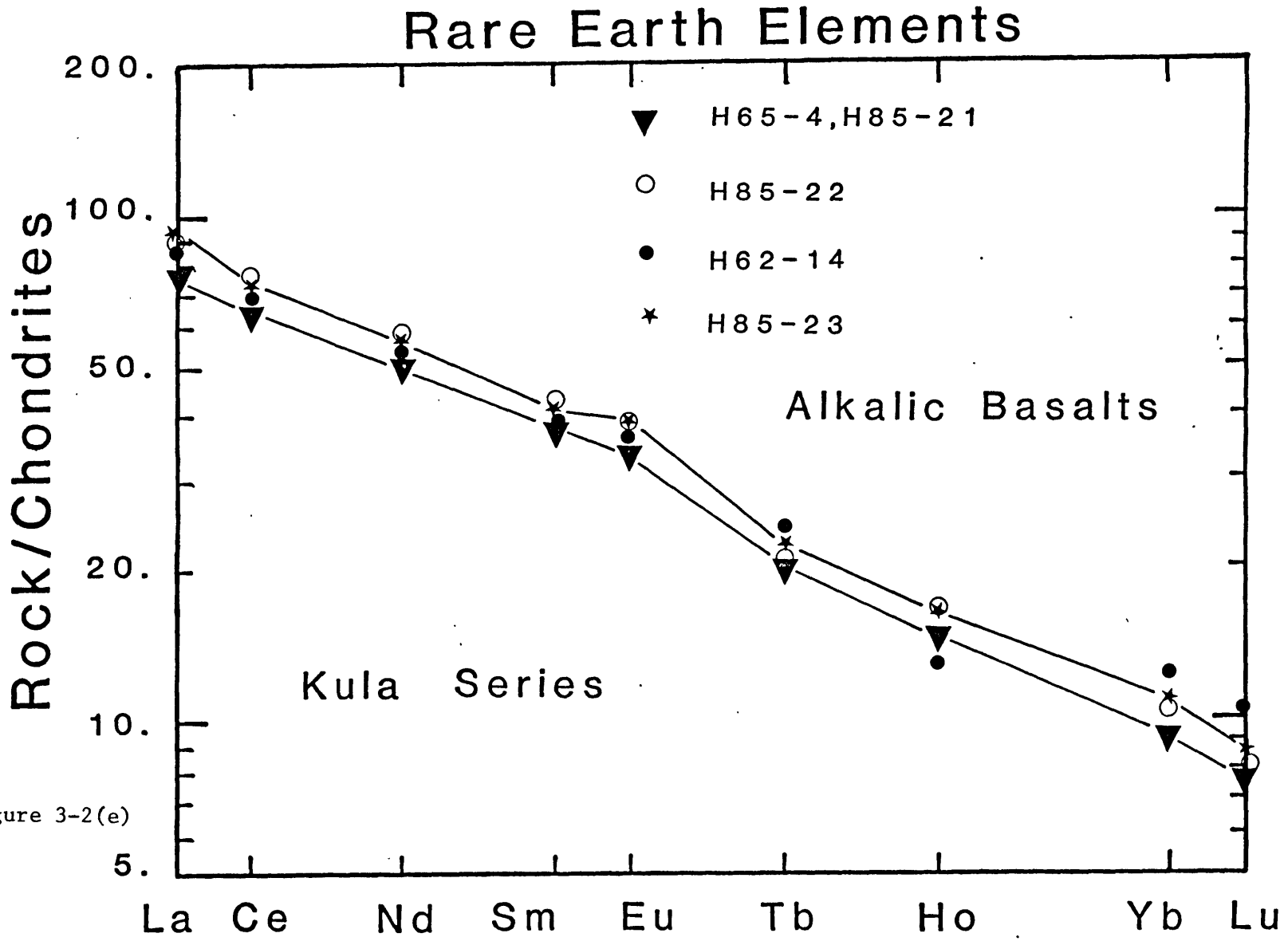

Rare Earth Elements
200.
100.
50.
20.
10.
5.
Rock/Chondrites
H65-4,H85-21
H85-22
H62-14
H85-23
Alkalic Basalts
Kula Series
La
Ce
Nd
Sm
Eu
Tb
Ho
Yb
Lu

Figure 3-2(e)

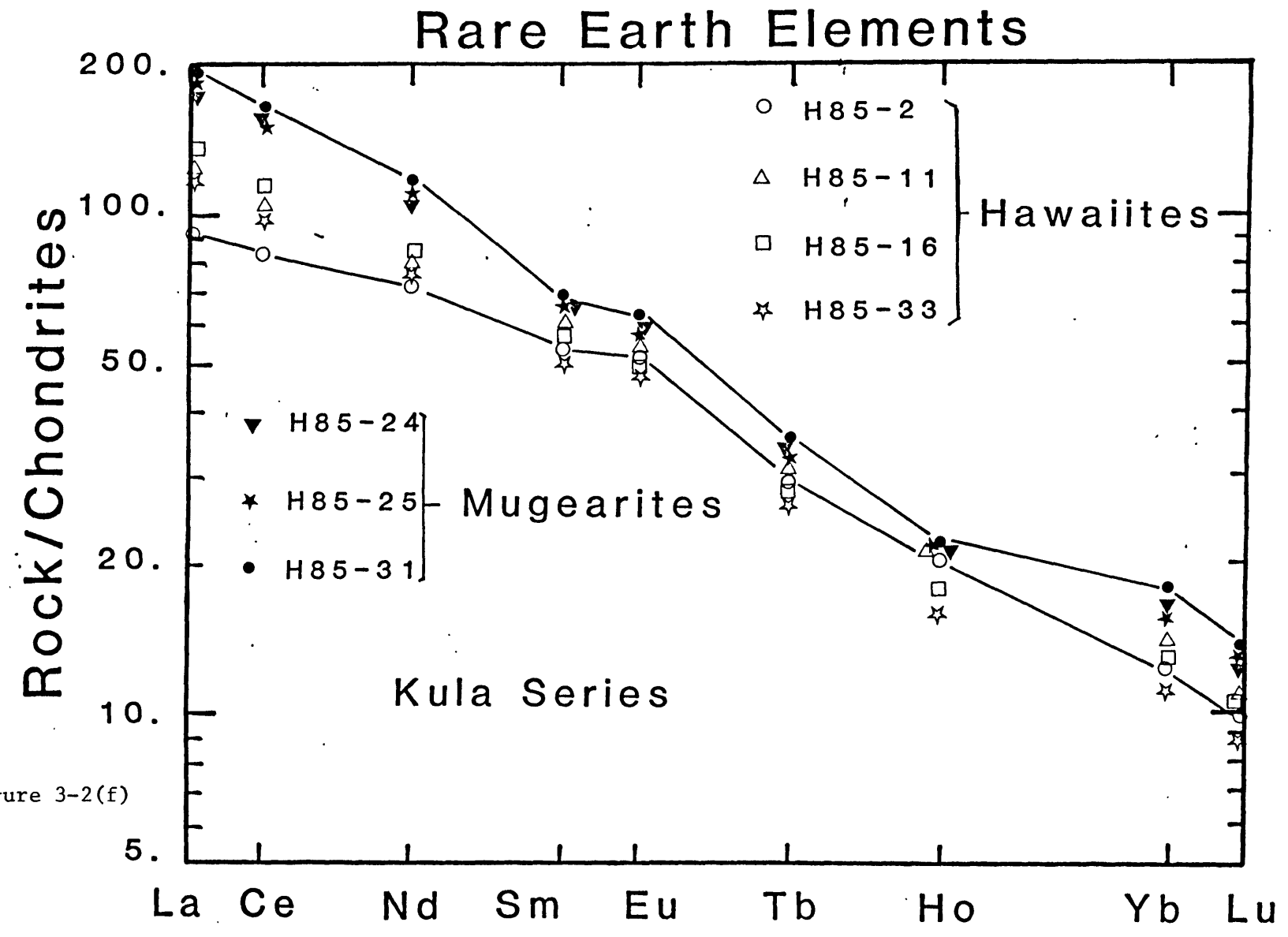

Rare Earth Elements
200.
100.
50.
20.
10.
5.
Rock/Chondrites
H85-2
H85-11
H85-16
H85-33
Hawaiites
H85-24
H85-25
H85-31
Mugearites
Kula Series
La
Ce
Nd
Sm
Eu
Tb
Ho
Yb
Lu

Figure 3-2(f)

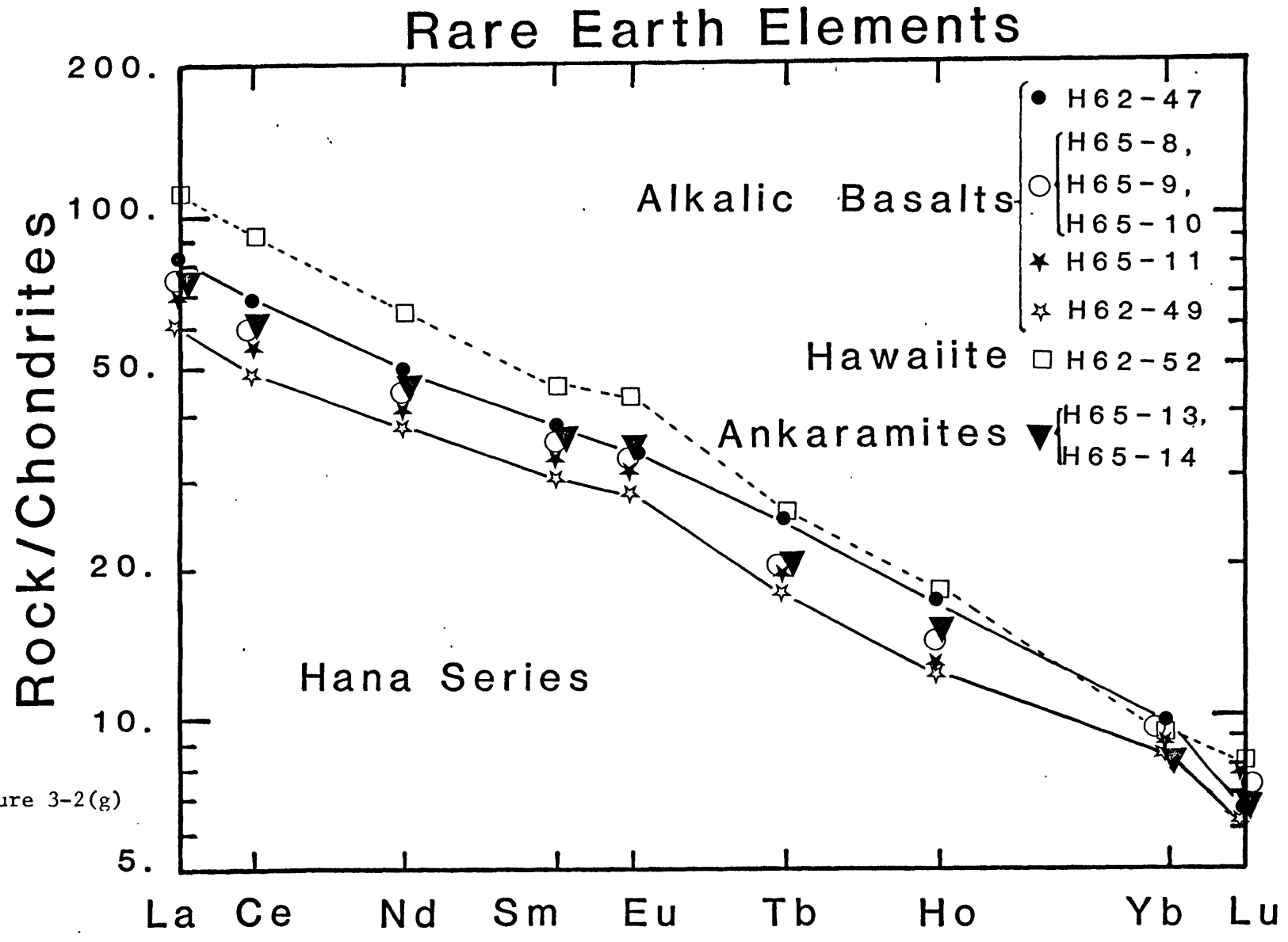

Rare Earth Elements
200.
100.
50.
20.
10.
5.
Rock/Chondrites
Alkalic Basalts
H62-47
H65-8,
H65-9,
H65-10
H65-11
H62-49
Hawaiite
H62-52
Ankaramites
H65-13,
H65-14
Hana Series
La
Ce
Nd
Sm
Eu
Tb
Ho
Yb
Lu

Figure 3-2(g)

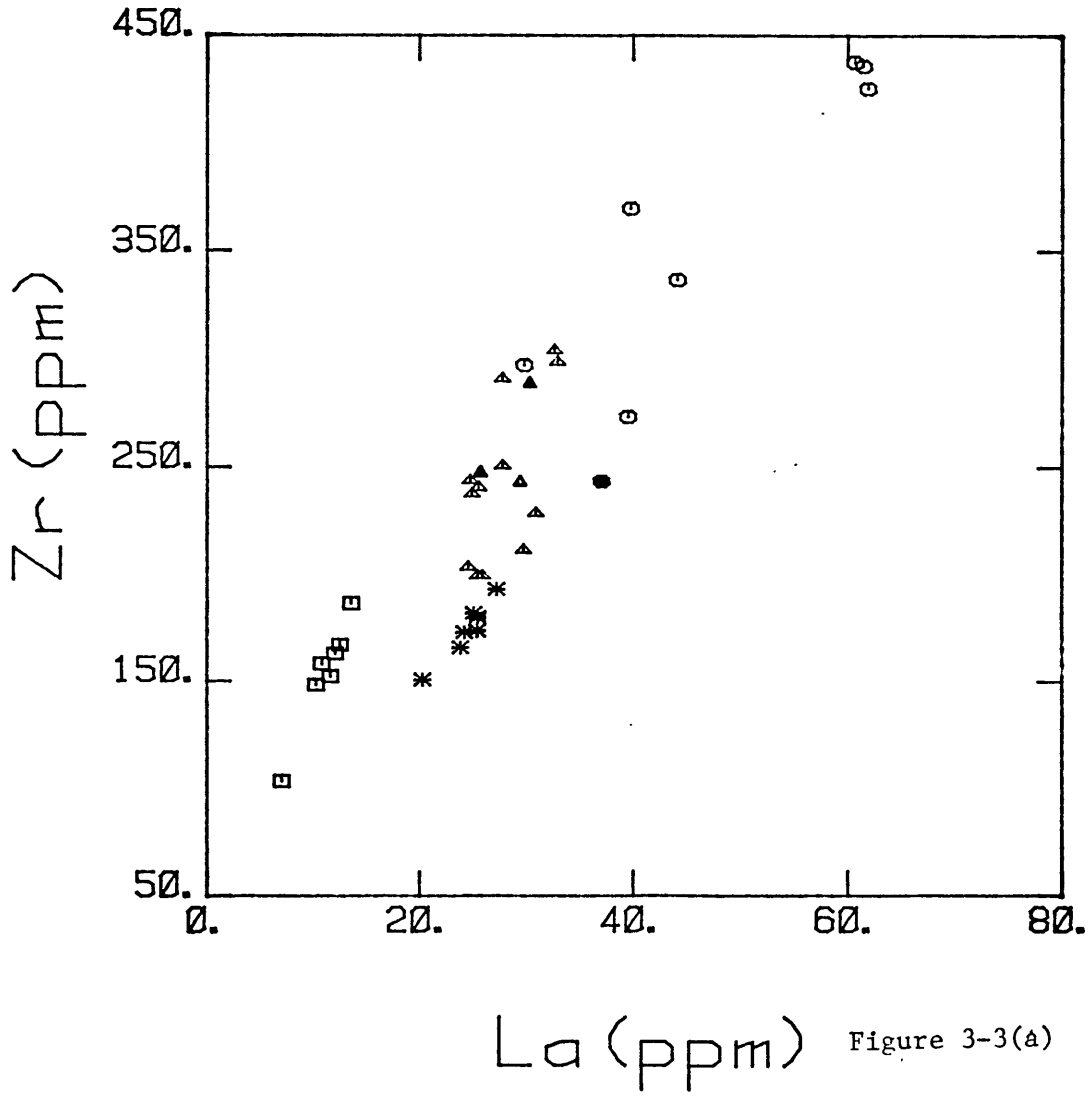


Figure 3-3(a)

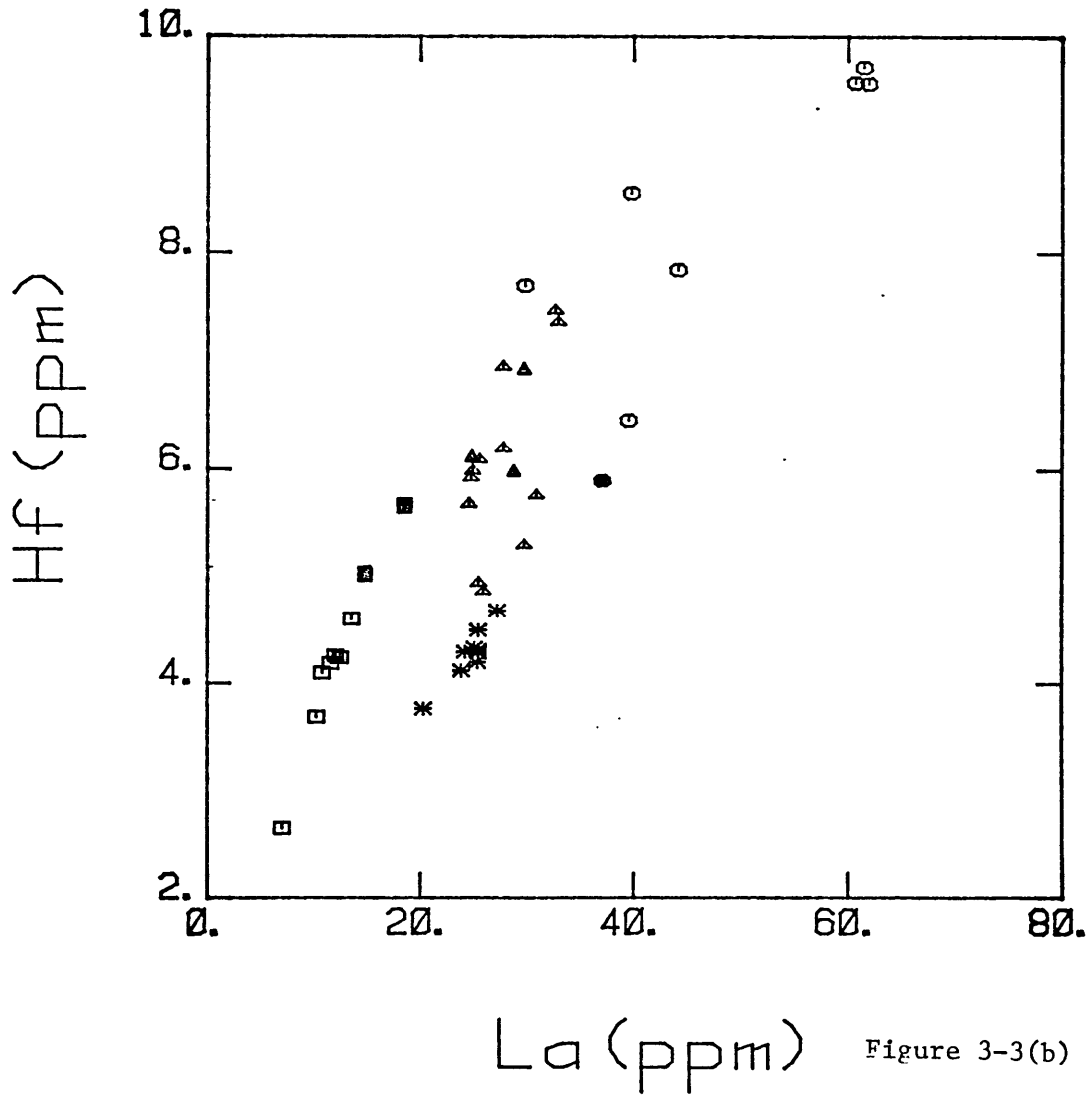


Figure 3-3(b)

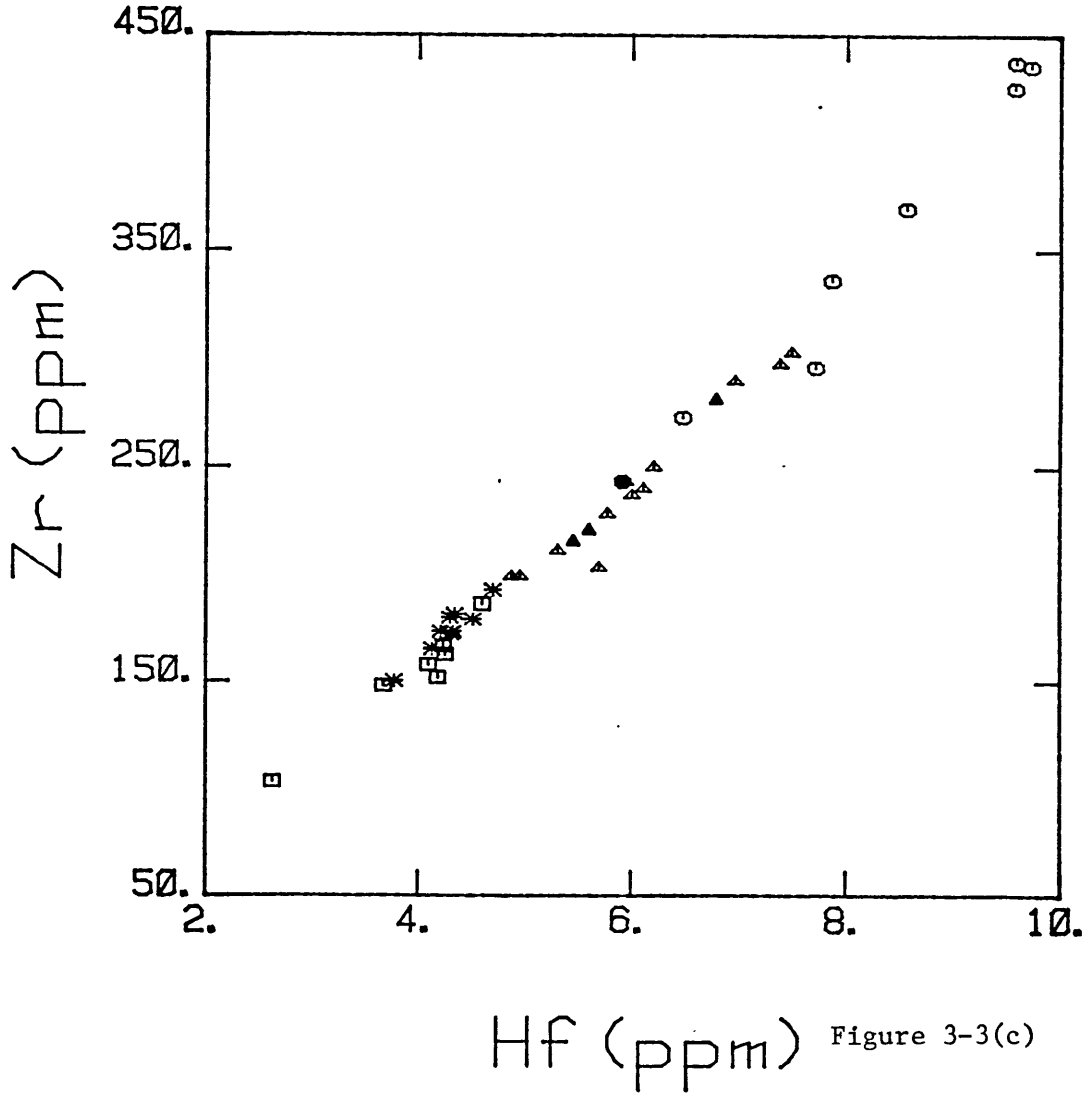


Figure 3-3(c)

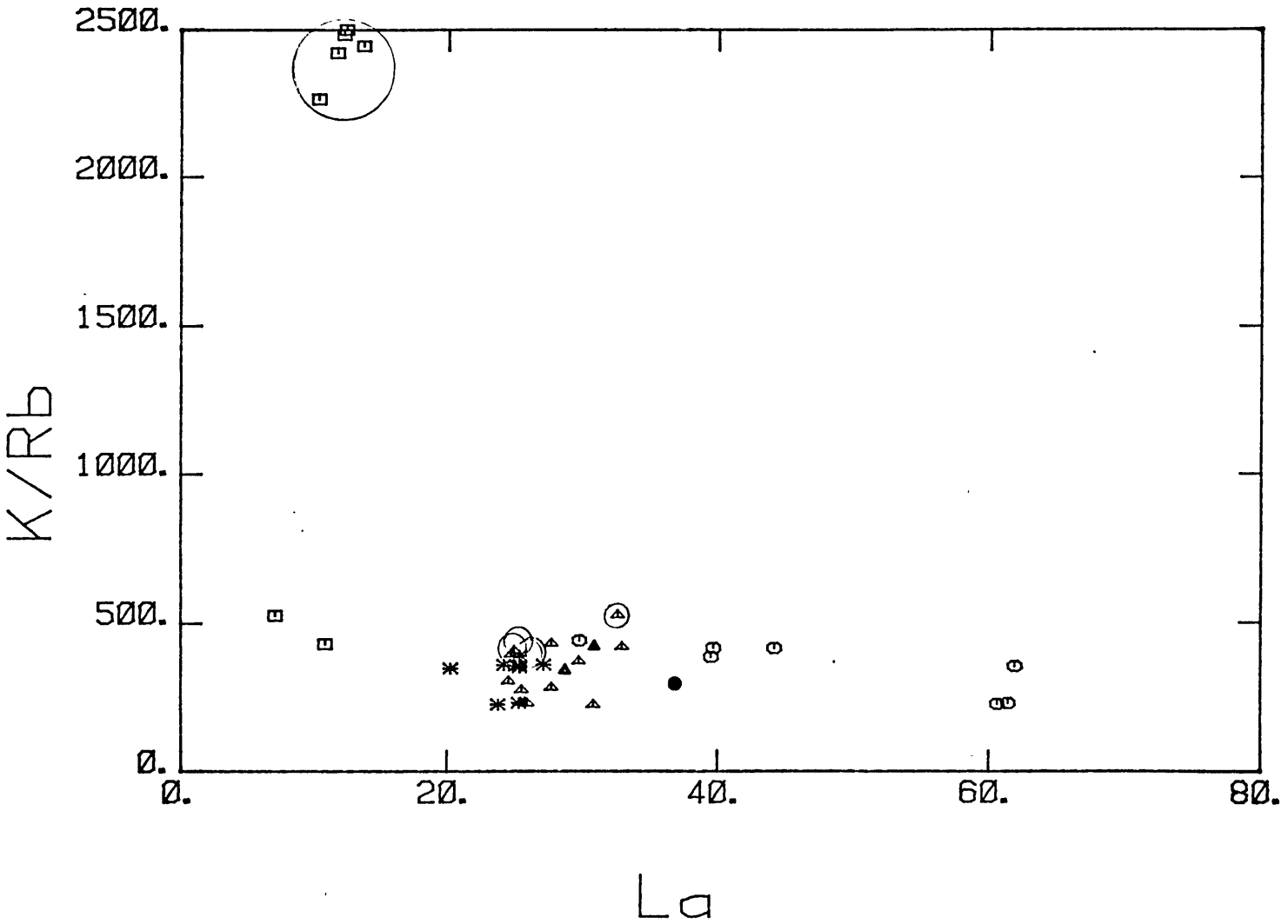


Figure 3-4(a)

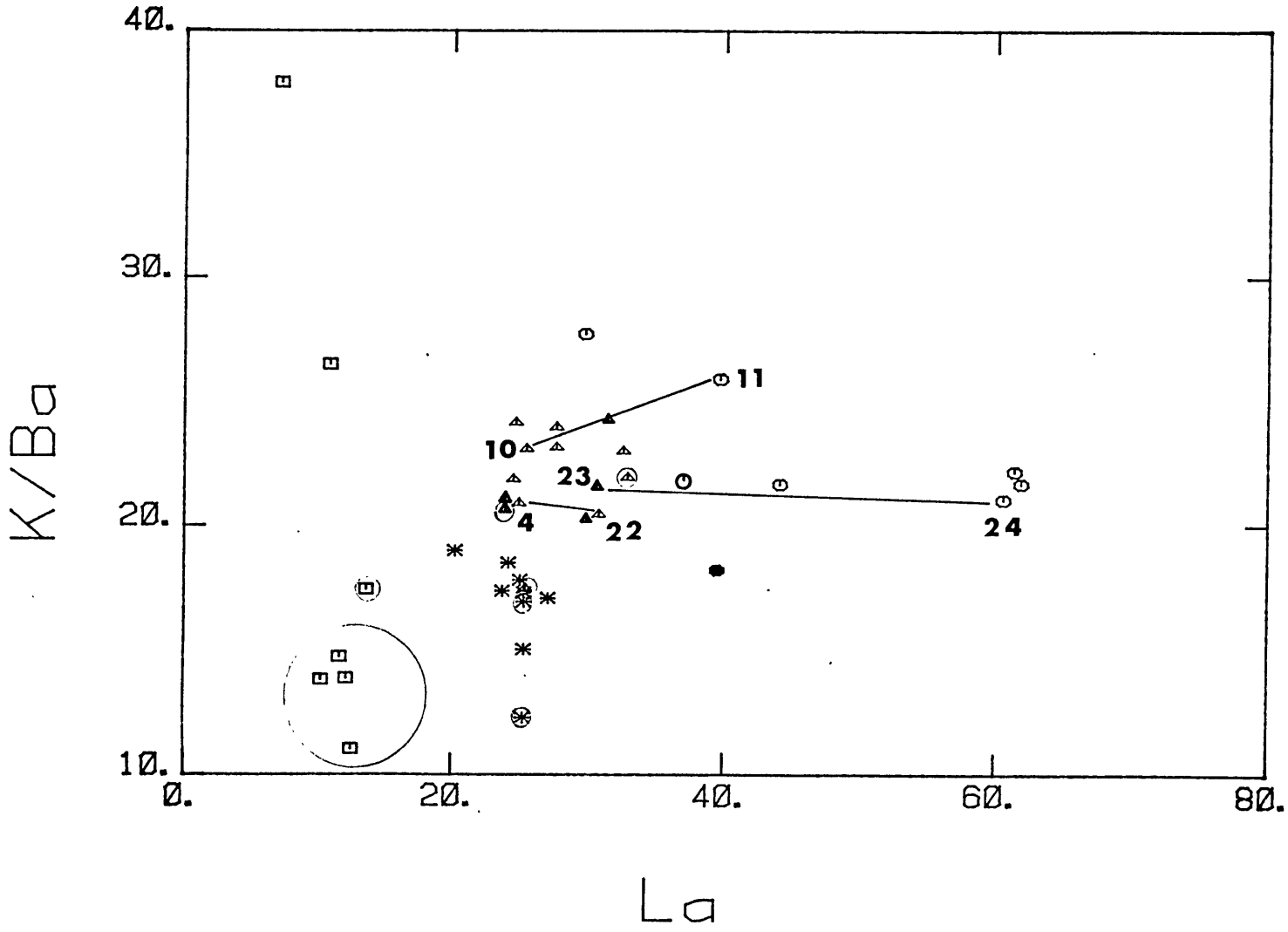


Figure 3-4(b)

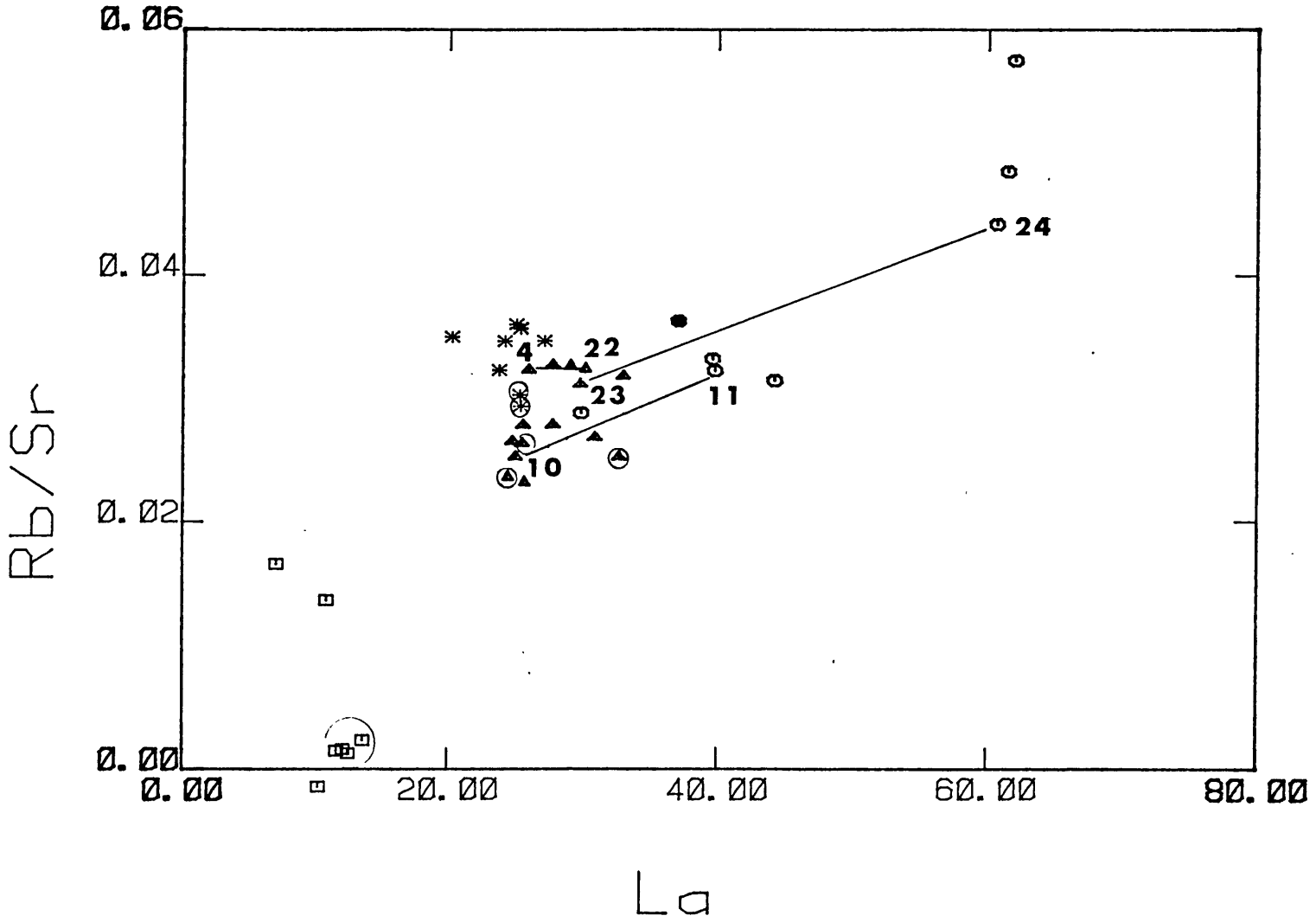


Figure 3-4(c)

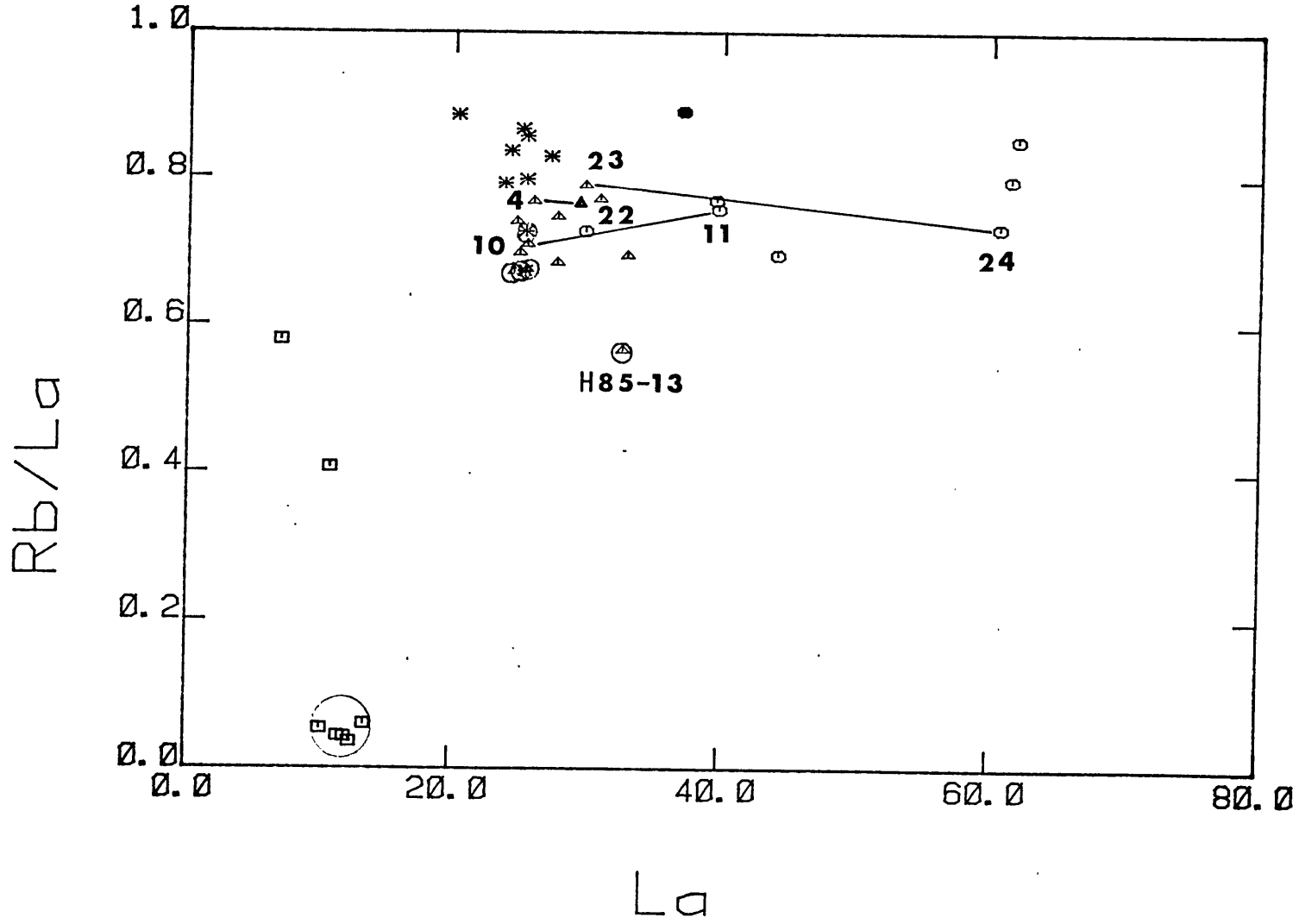


Figure 3-4(d)

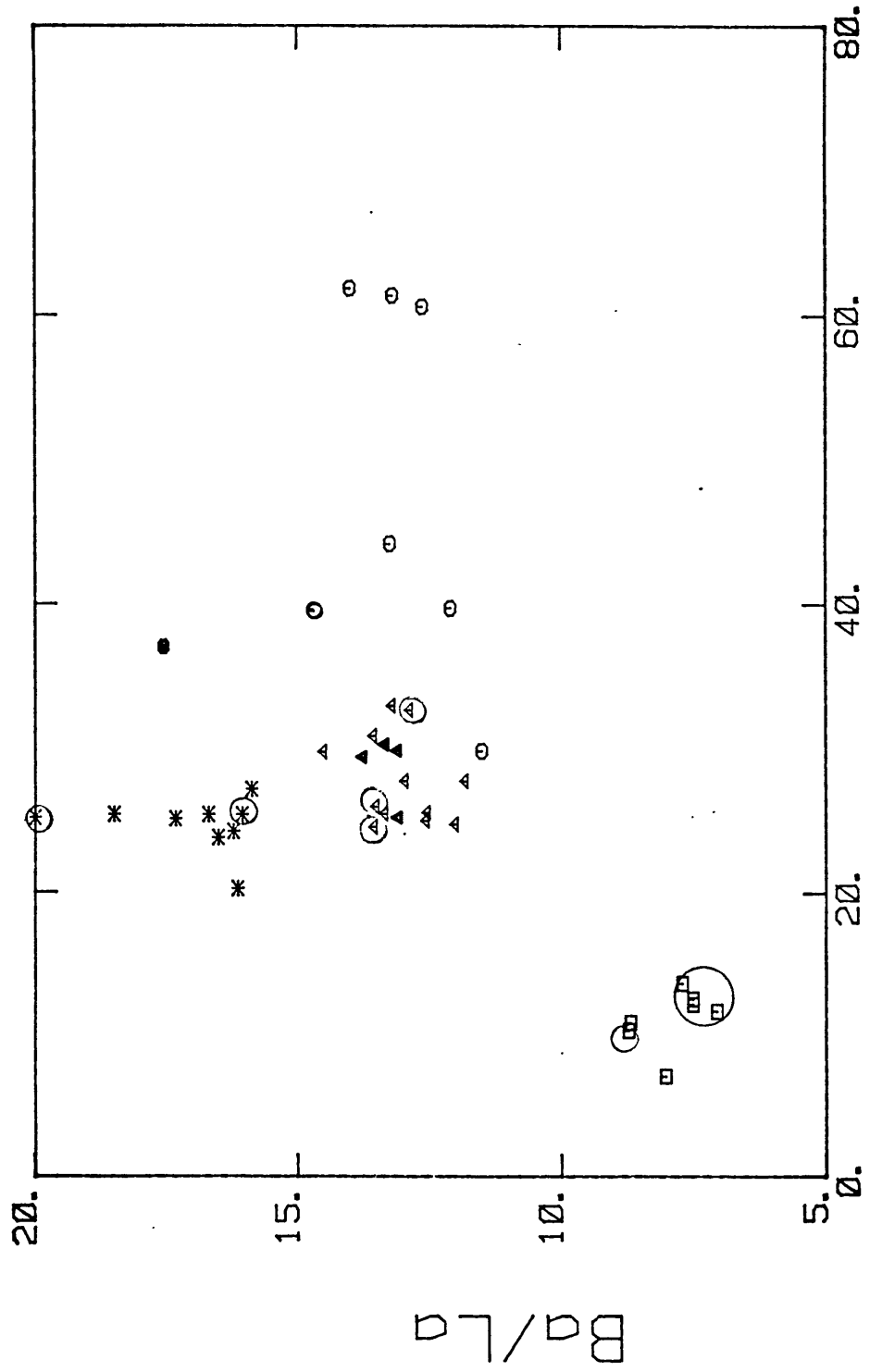


Figure 3-4(d)

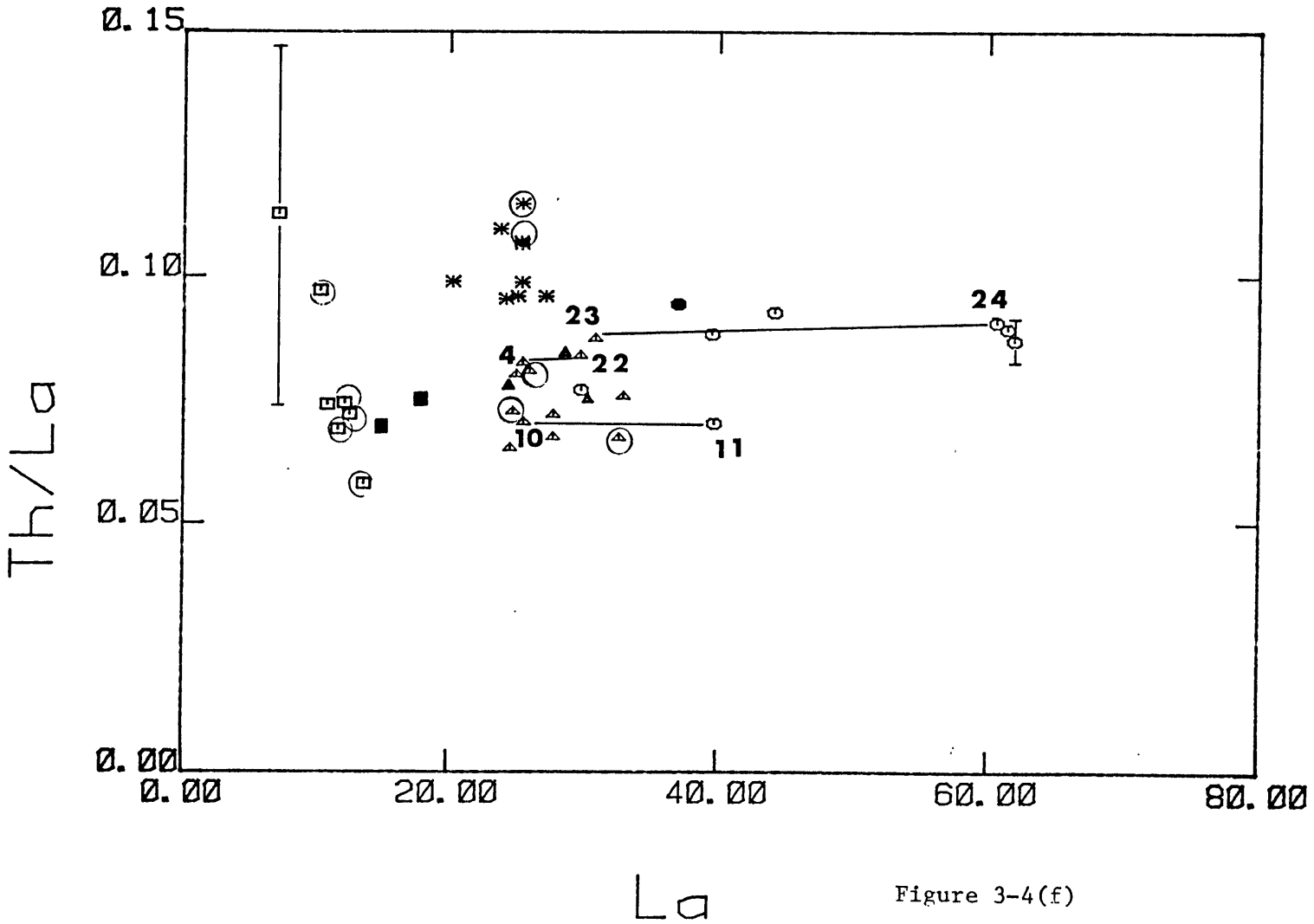


Figure 3-4(f)

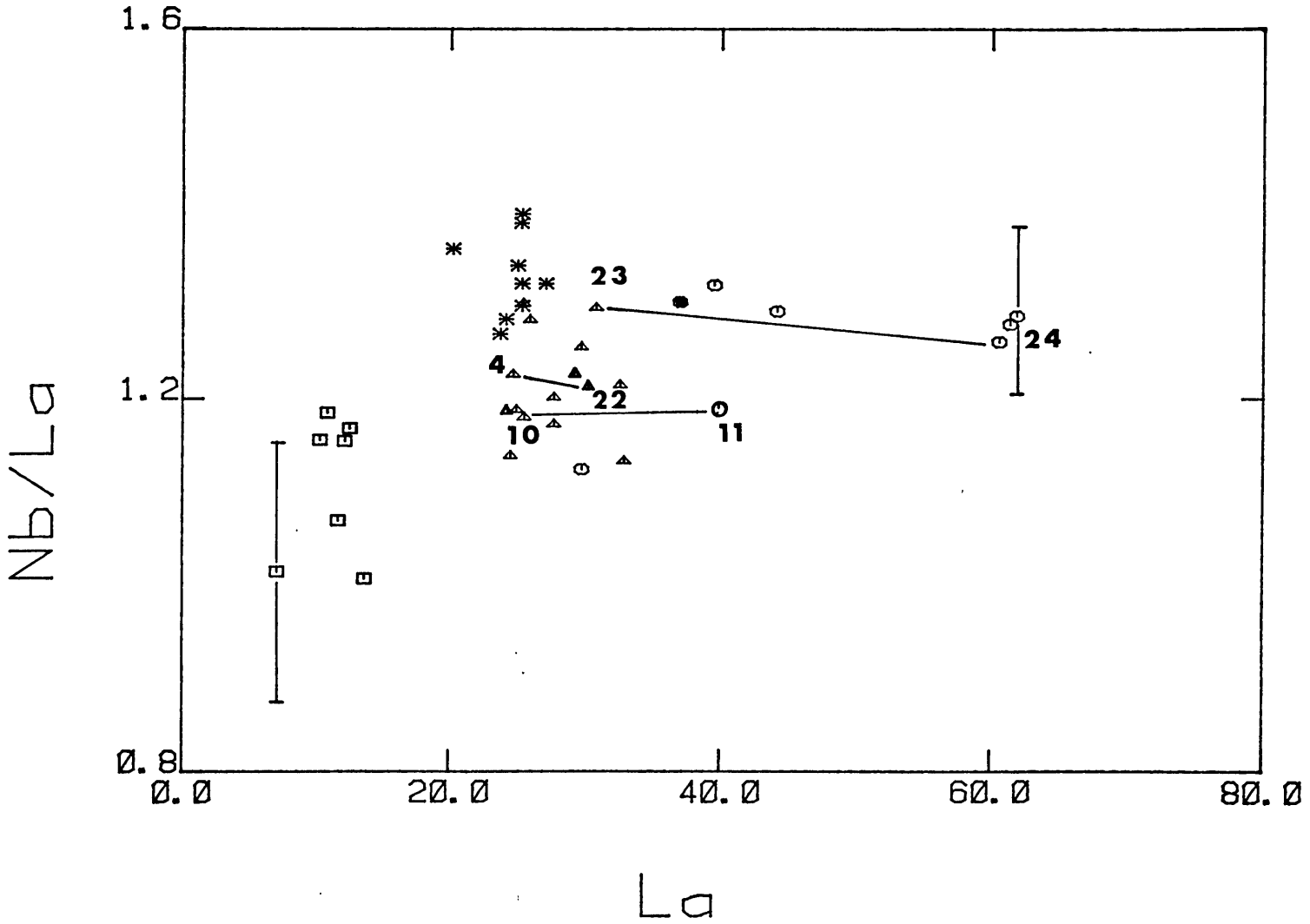


Figure 3-4(g)

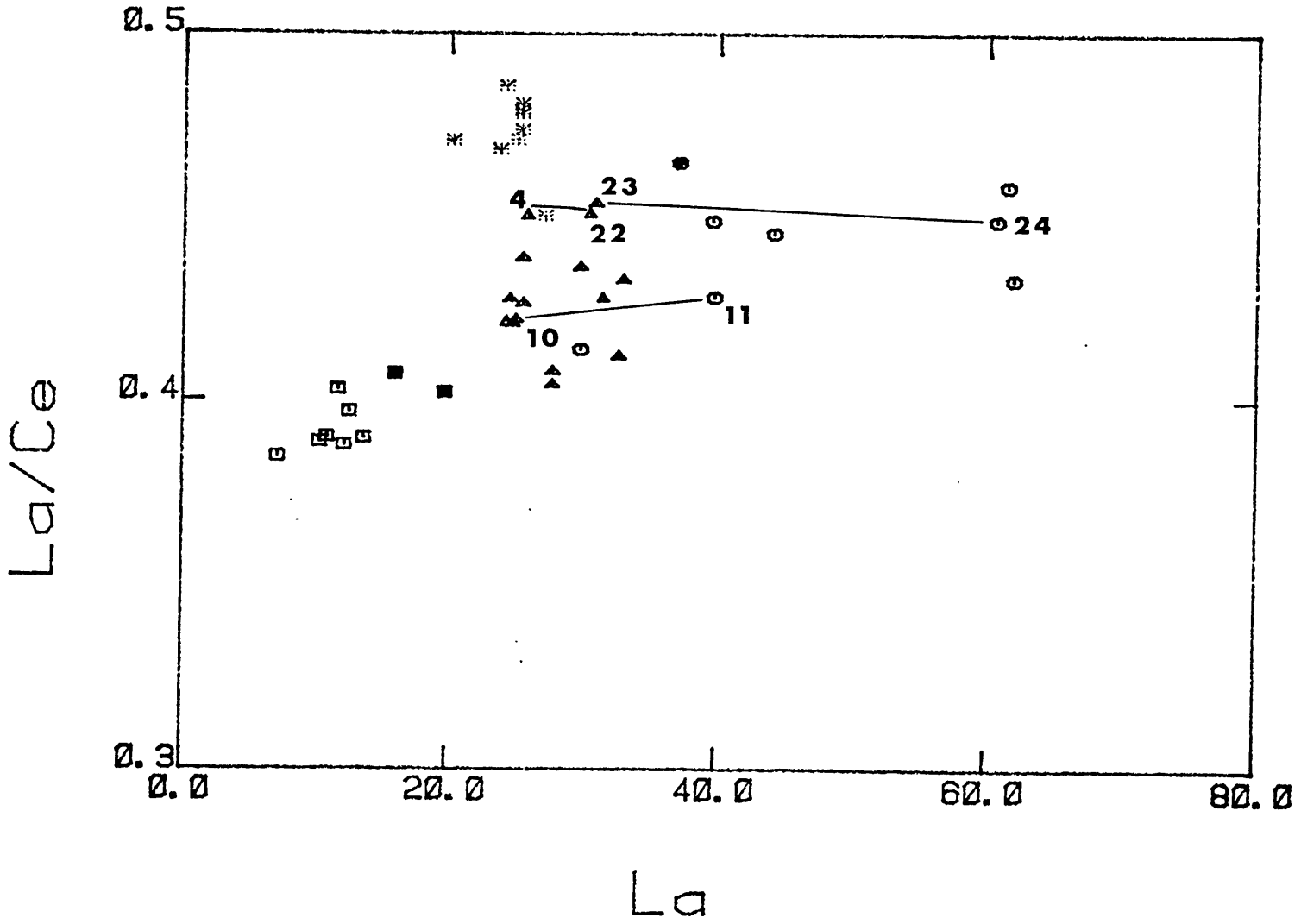


Figure 3-4(h)

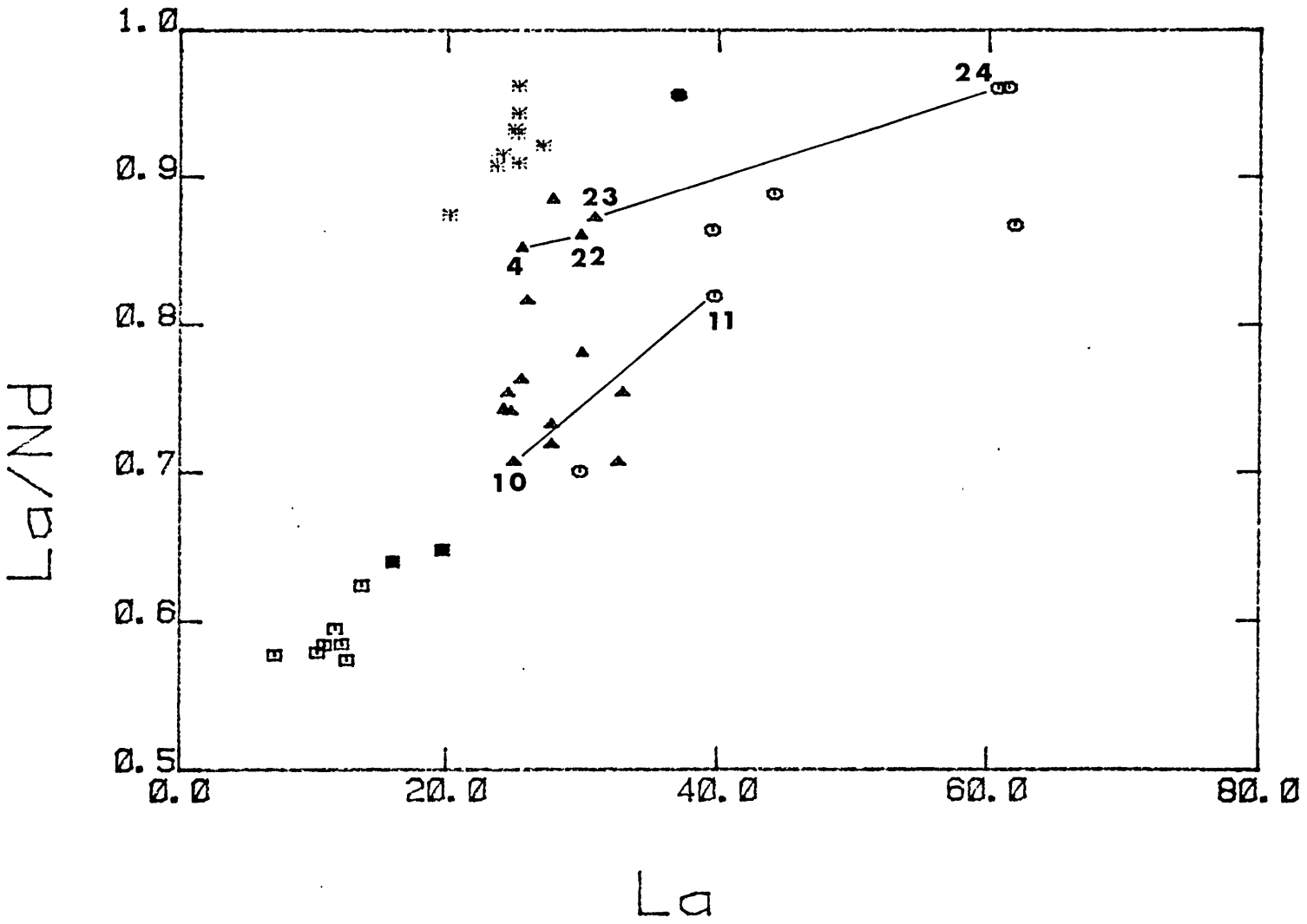


Figure 3-4(i)

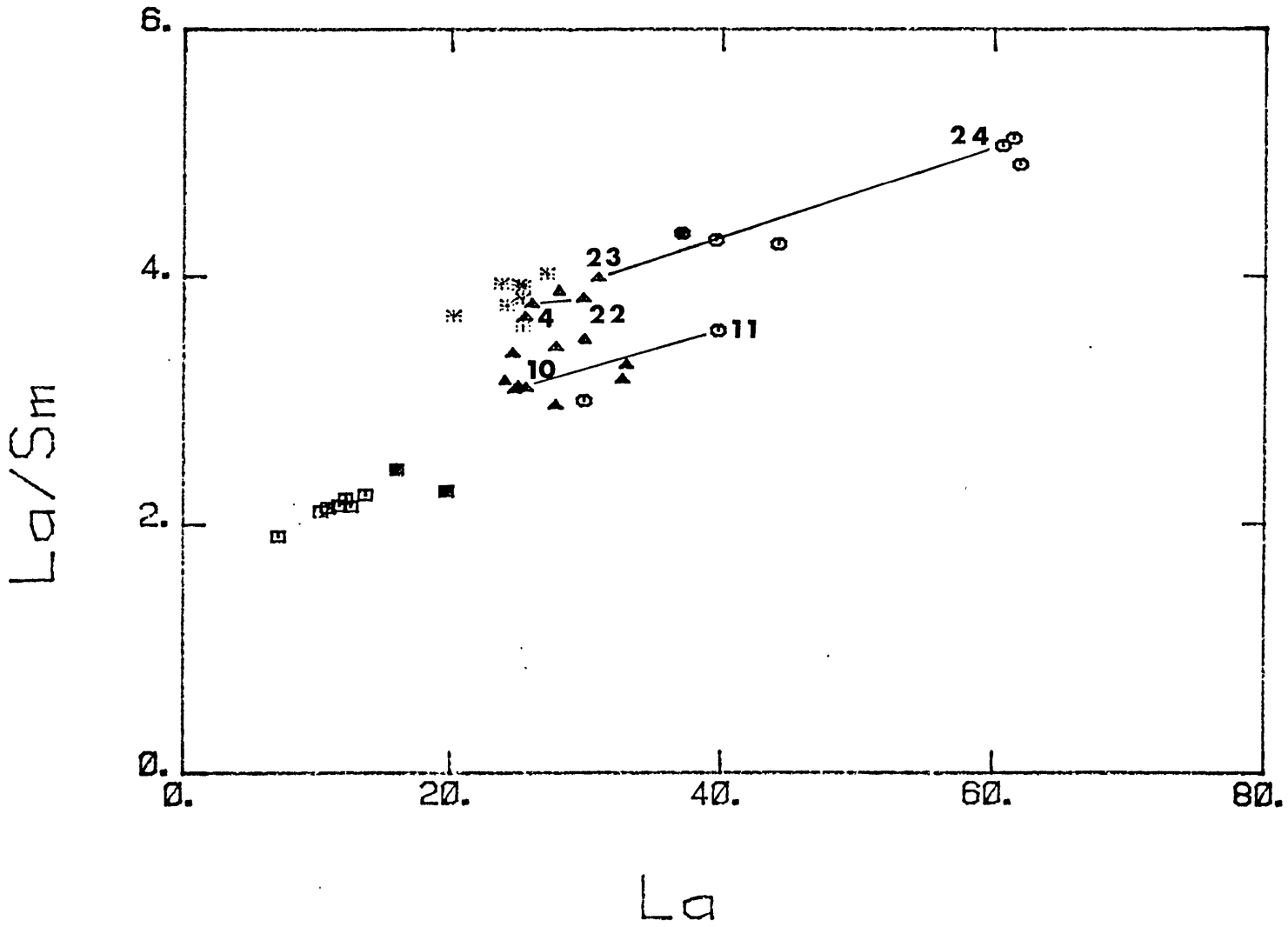


Figure 3-4(j)

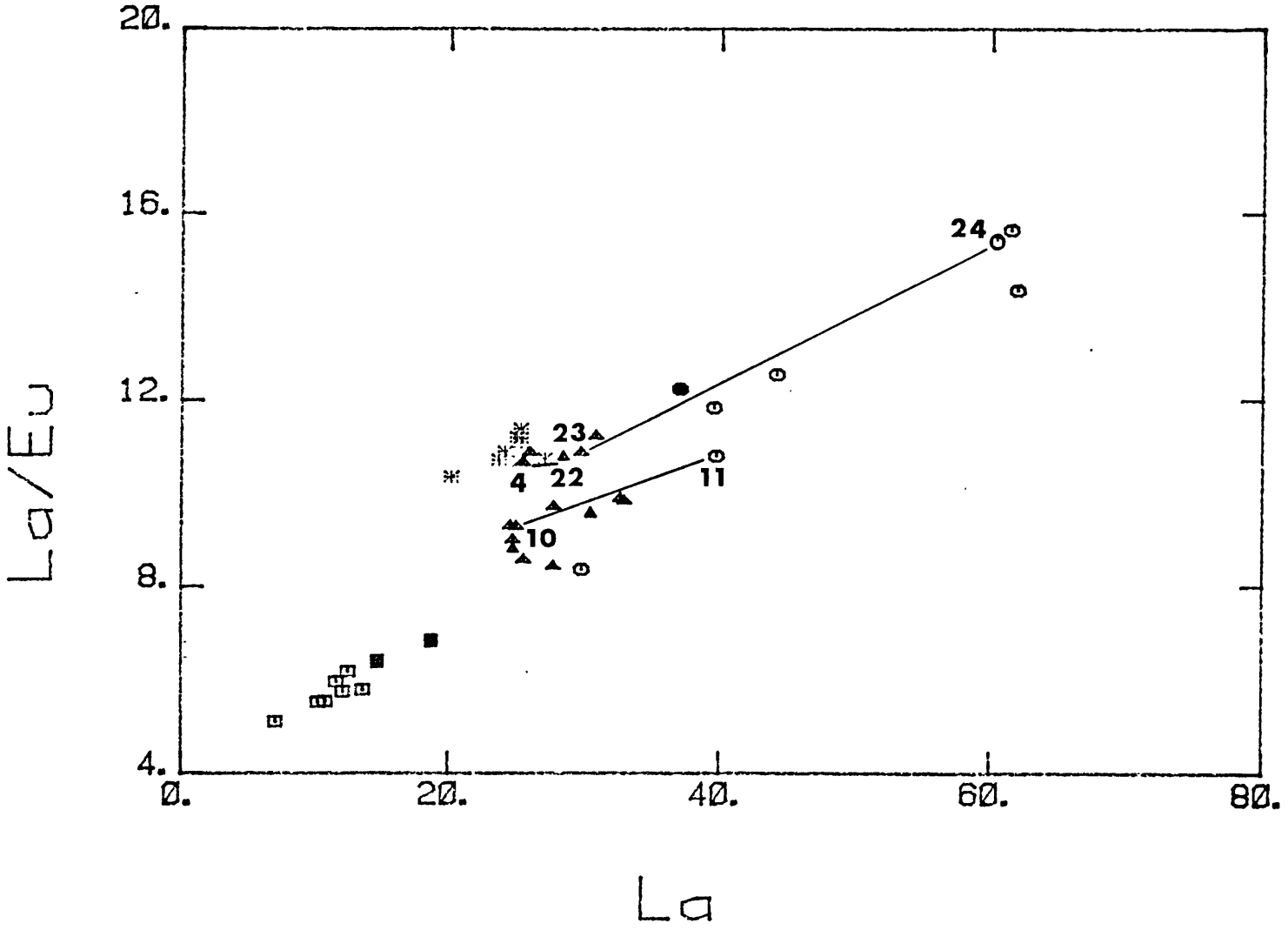


Figure 3-4(k)

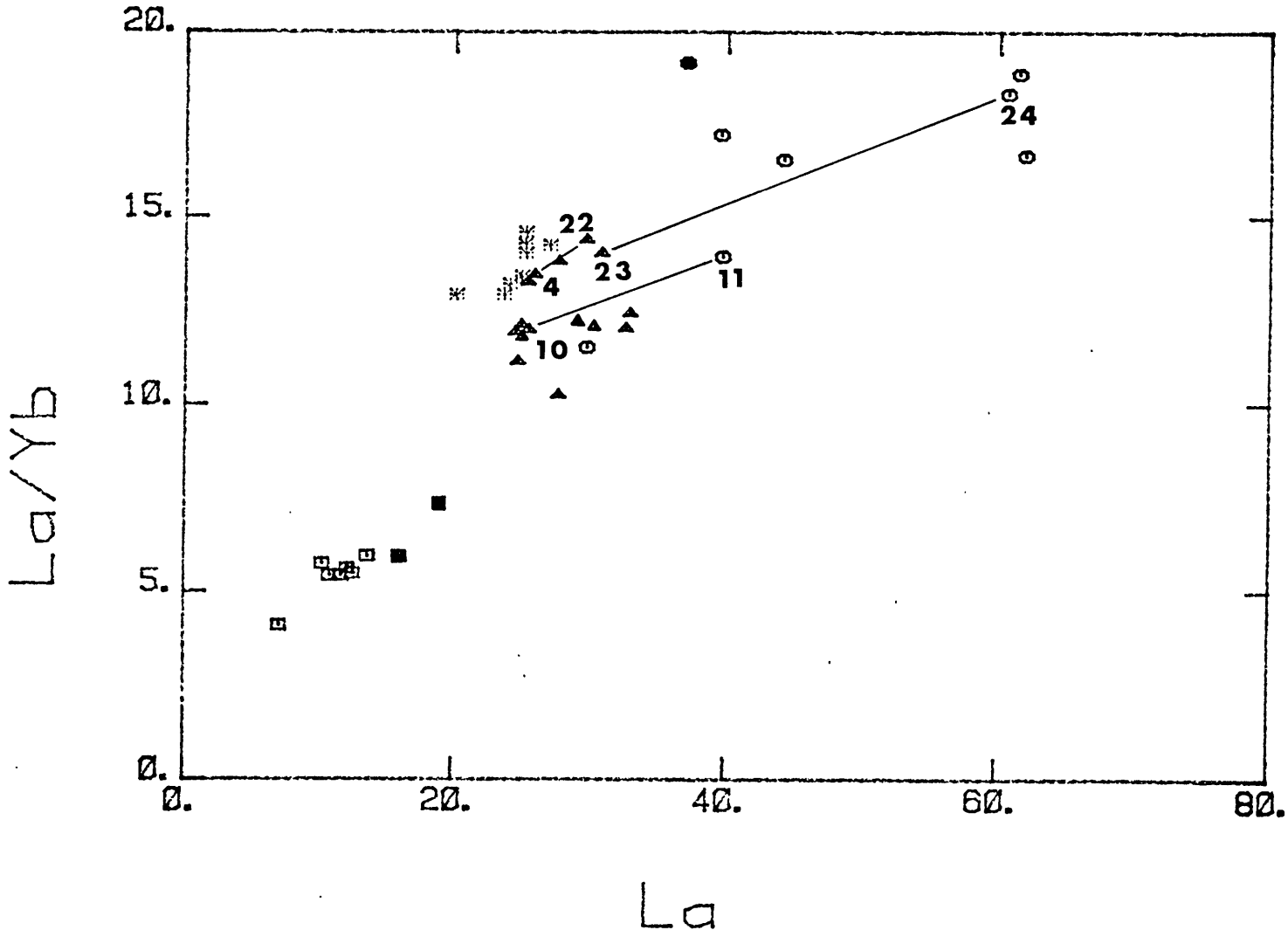


Figure 3-4(1)

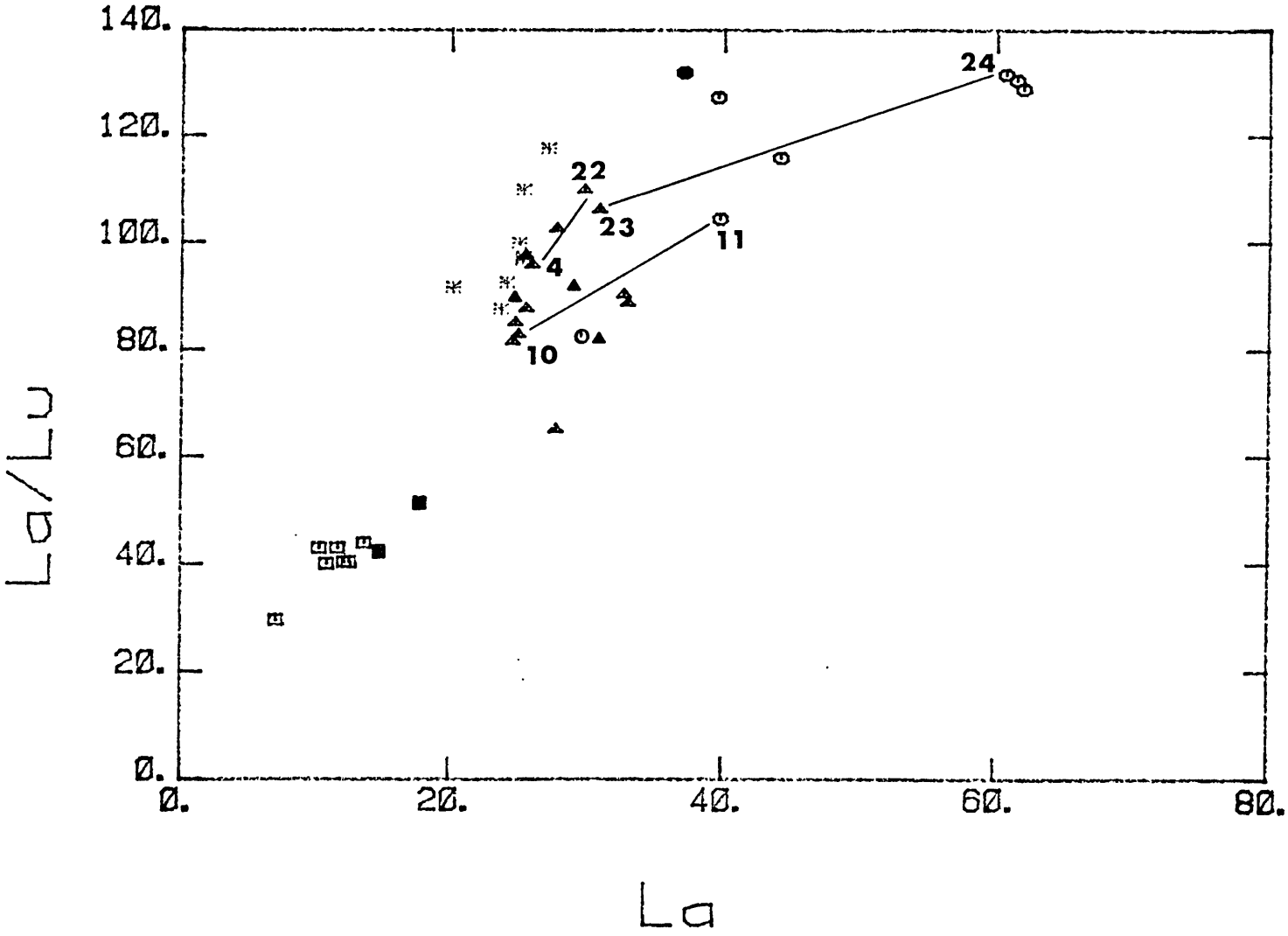


Figure 3-4(m)

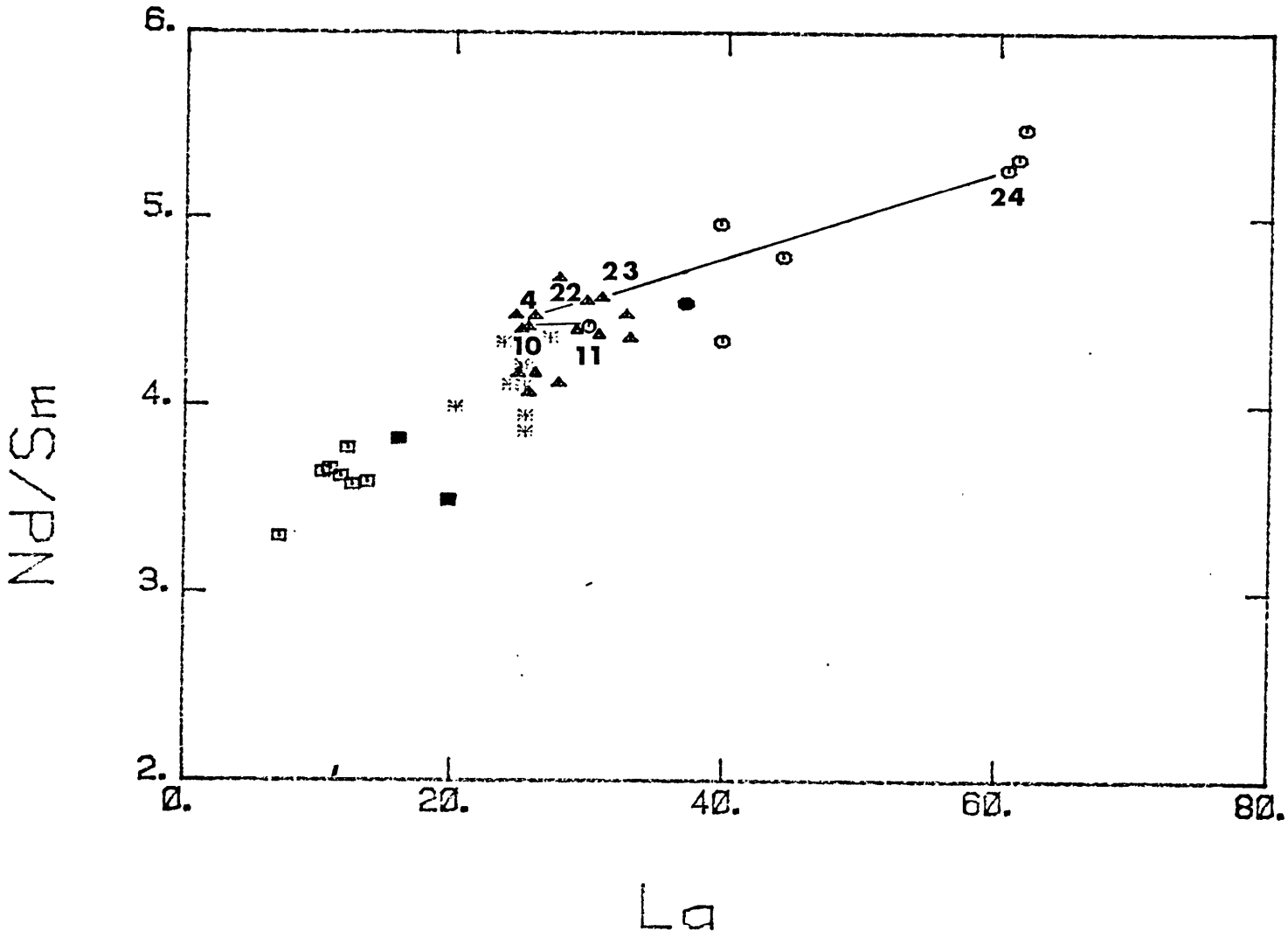


Figure 3-4(n)

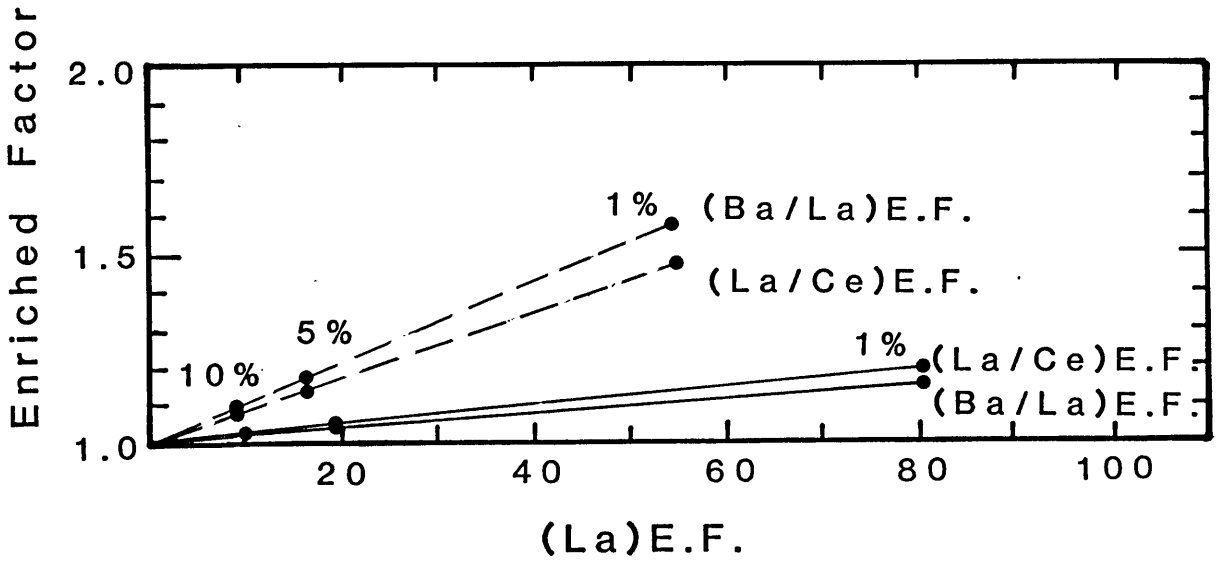

Enriched Factor
2.0
1.5
1.0
20
40
60
80
100
(La)E.F.
1%
(Ba/La)E.F.
(La/Ce)E.F.
5%
10%
1%
(La/Ce)E.F.
(Ba/La)E.F.

Figure 3-5

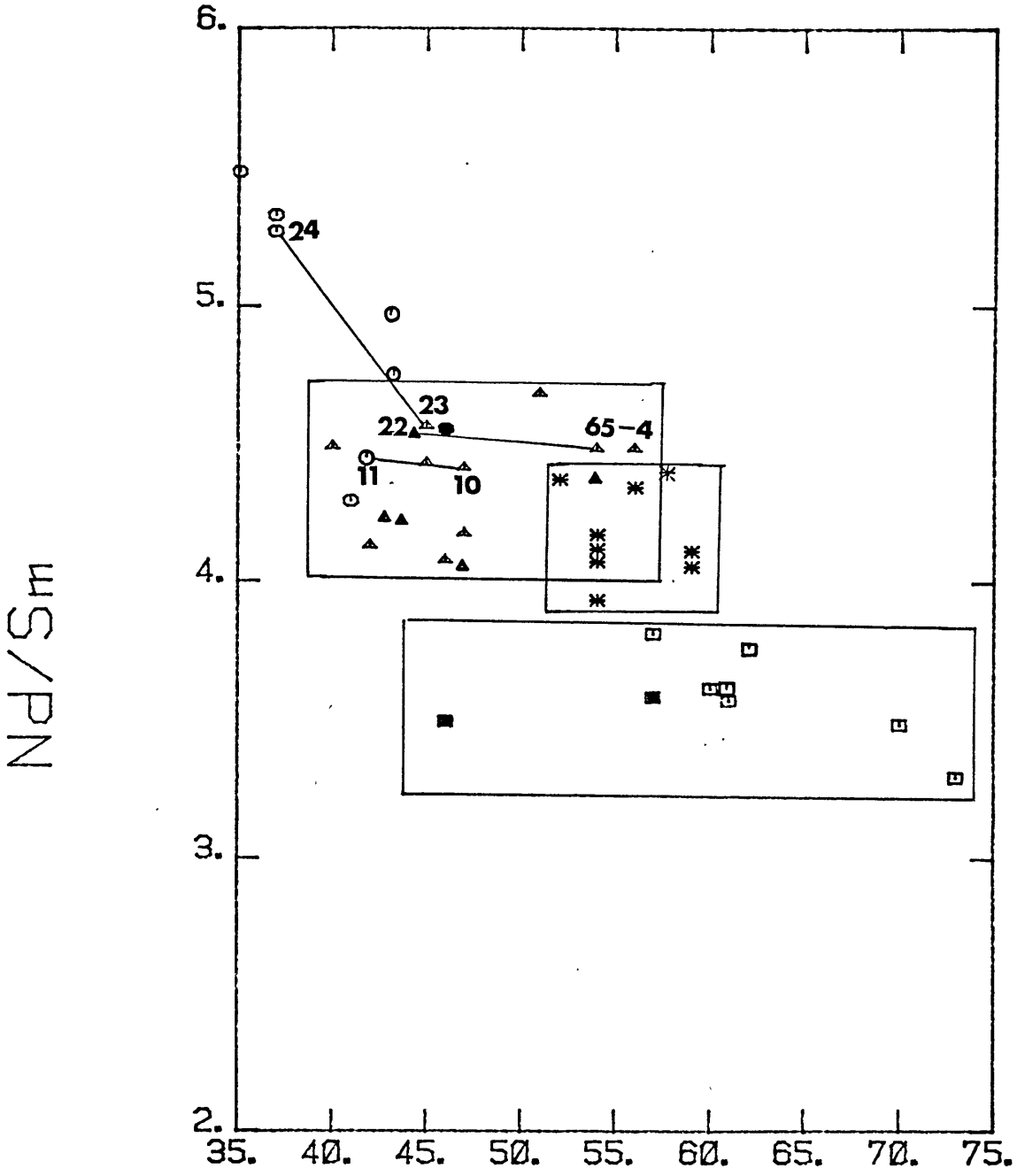


Figure 3-6

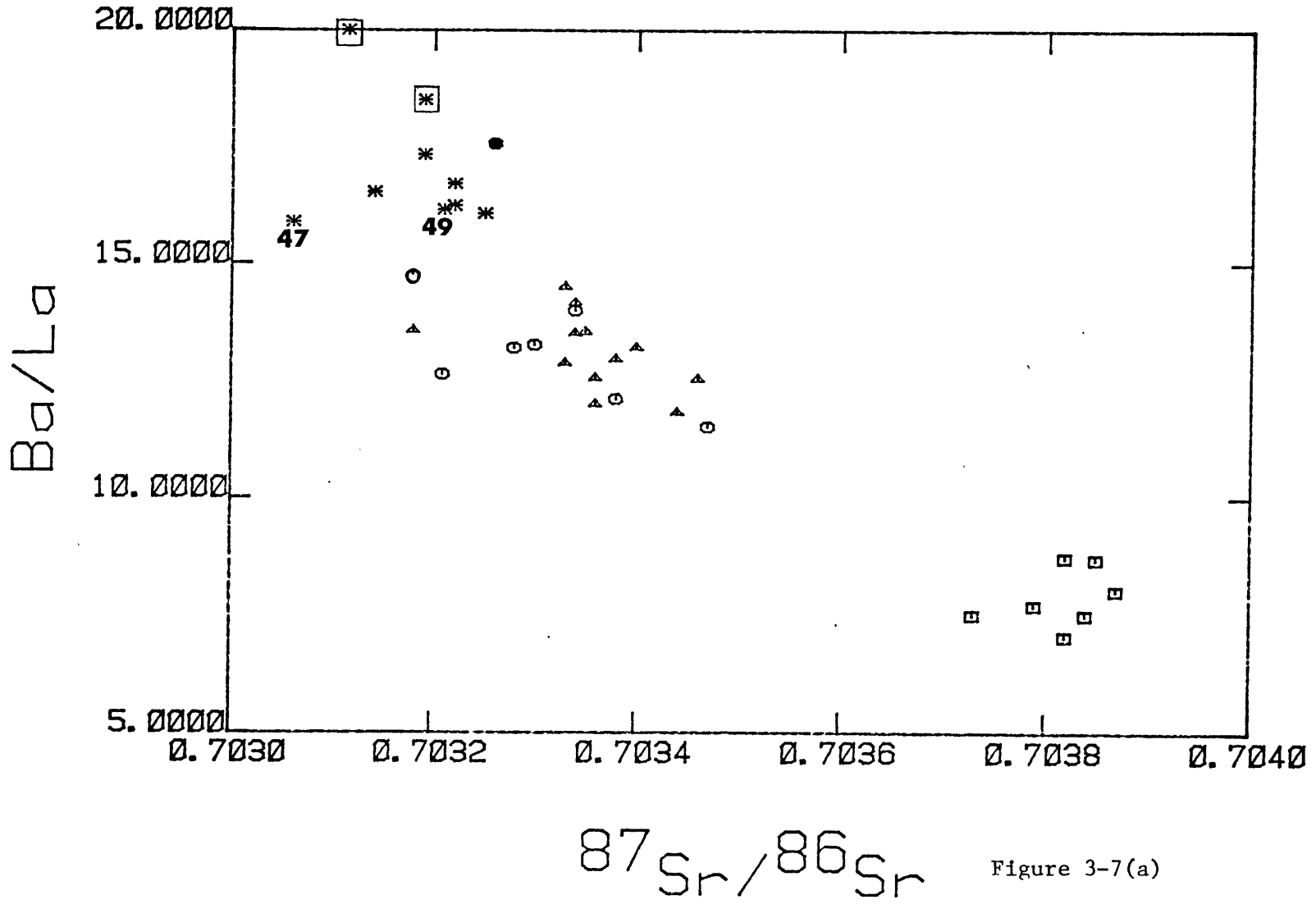

20. 0000
15. 0000
10. 0000
5. 0000
Ba/La
47
49
0. 7030
0. 7032
0. 7034
0. 7036
0. 7038
0. 7040
87Sr/86Sr

Figure 3-7(a)

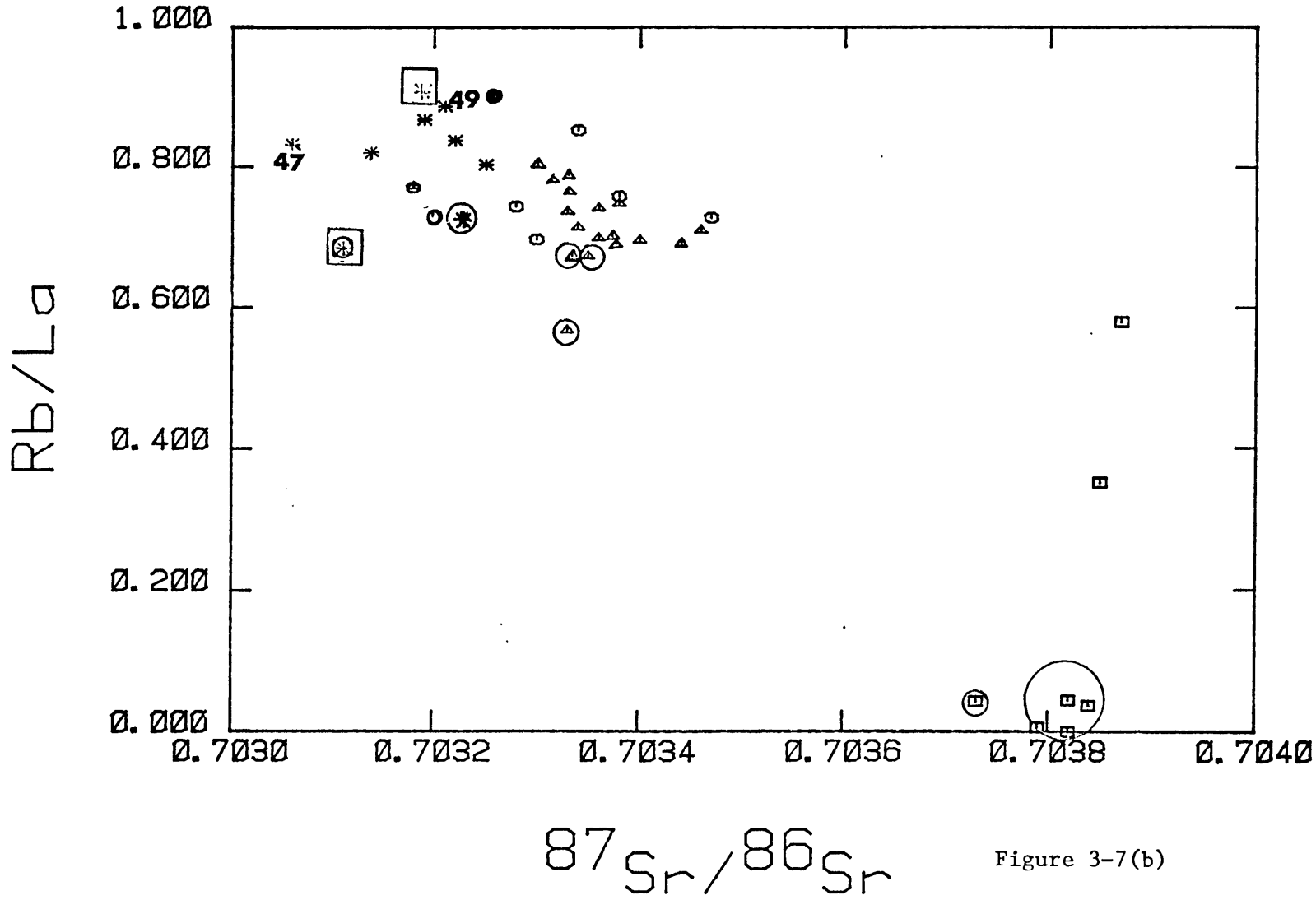

1.000
0.800
0.600
0.400
0.200
0.000
Rb/La
47
49
0.7030
0.7032
0.7034
0.7036
0.7038
0.7040
87Sr/86Sr

Figure 3-7(b)

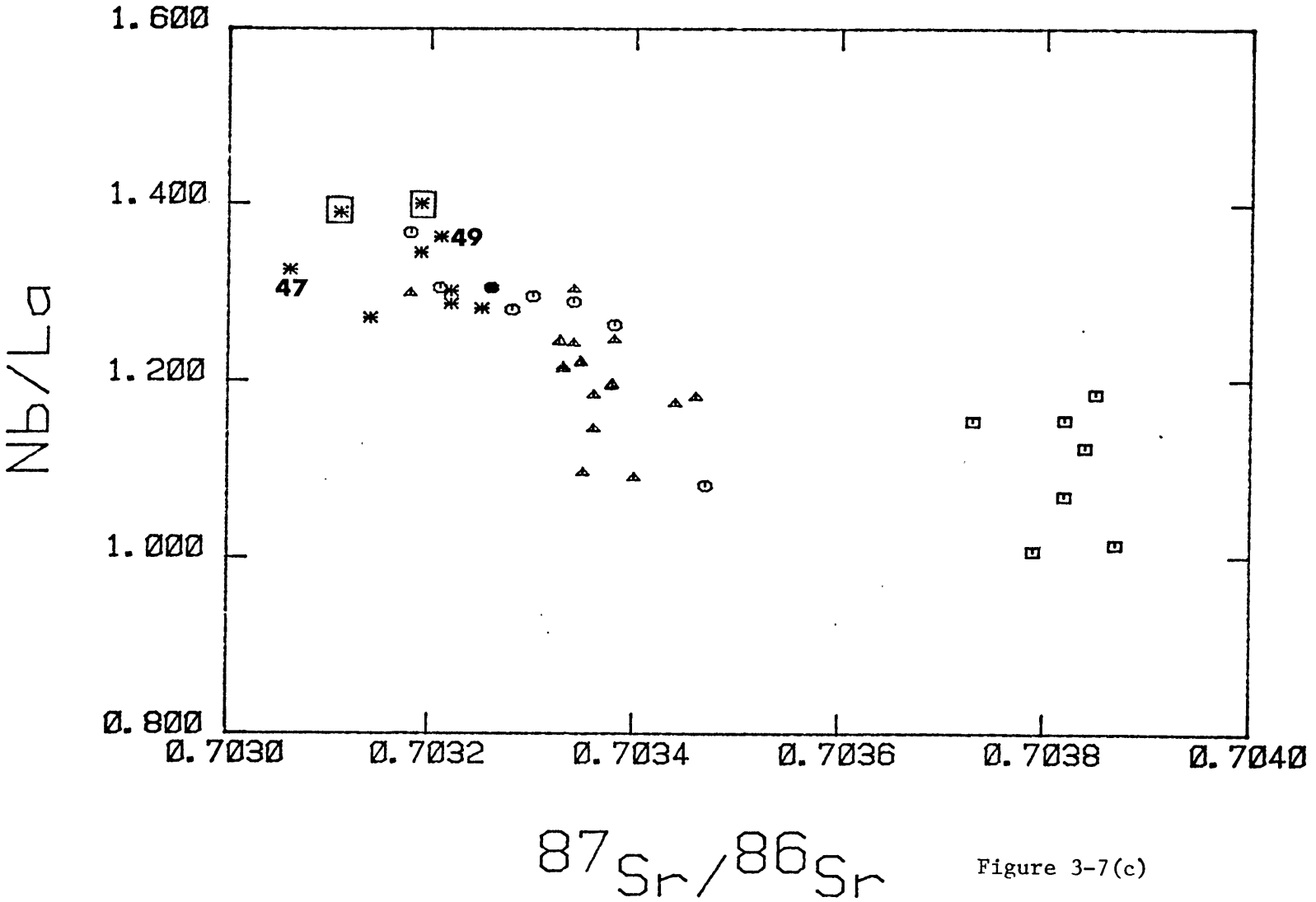

1.600
1.400
1.200
1.000
0.800
Nb/La
0.7030
0.7032
0.7034
0.7036
0.7038
0.7040
87Sr/86Sr
47
49

Figure 3-7(c)

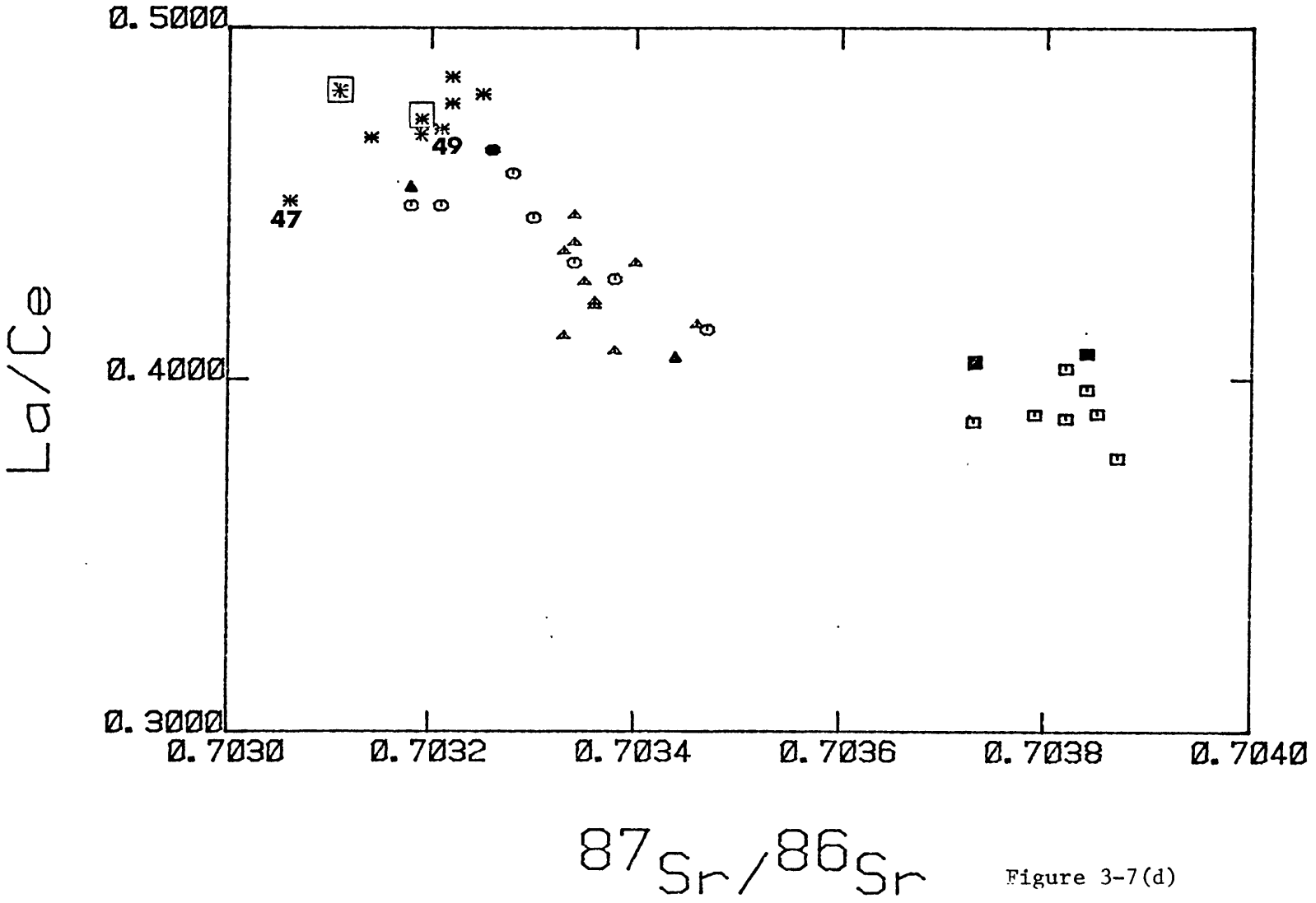

0.5000
0.4000
0.3000
La/Ce
0.7030
0.7032
0.7034
0.7036
0.7038
0.7040
87Sr/86Sr
47
49

Figure 3-7(d)

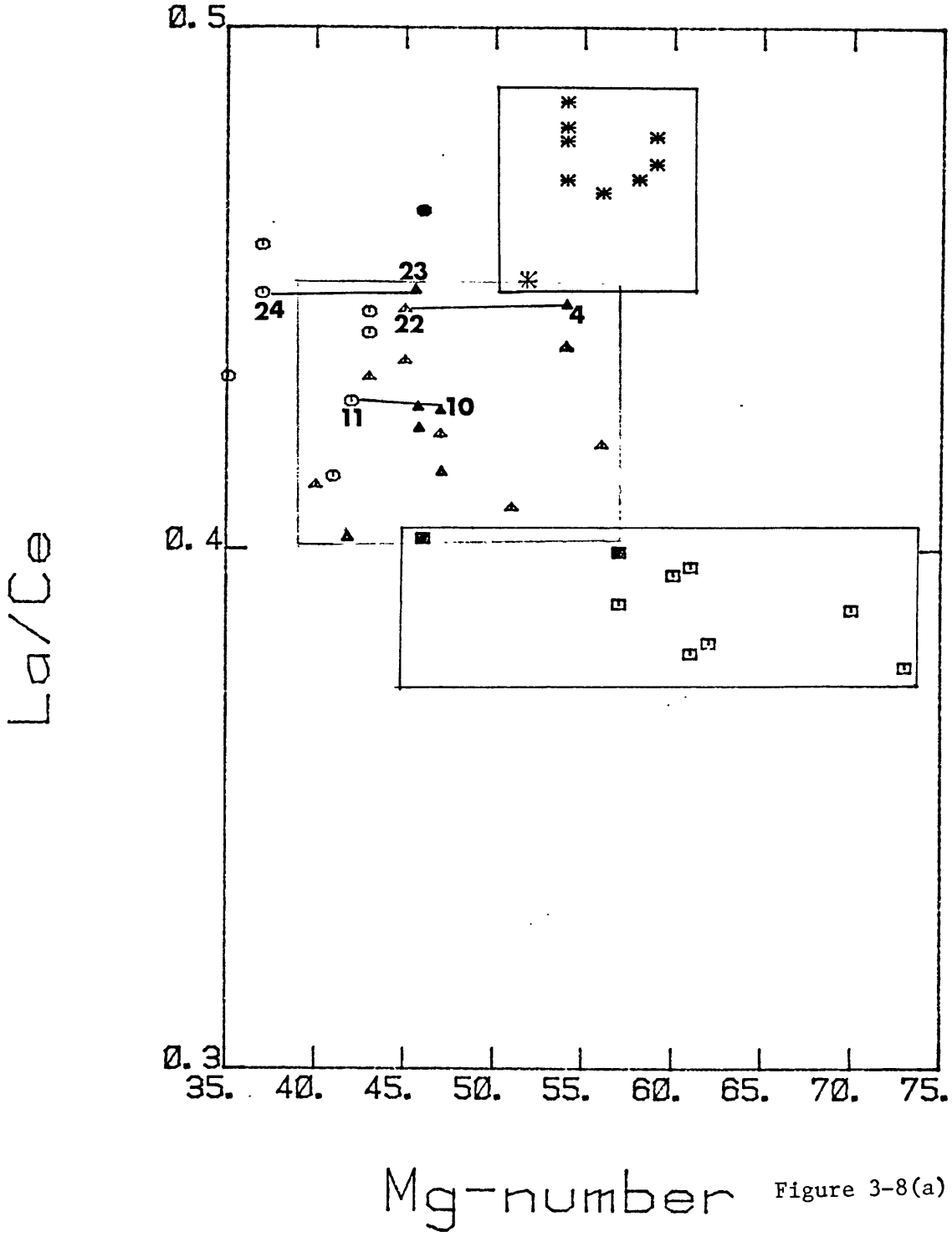


Figure 3-8(a)

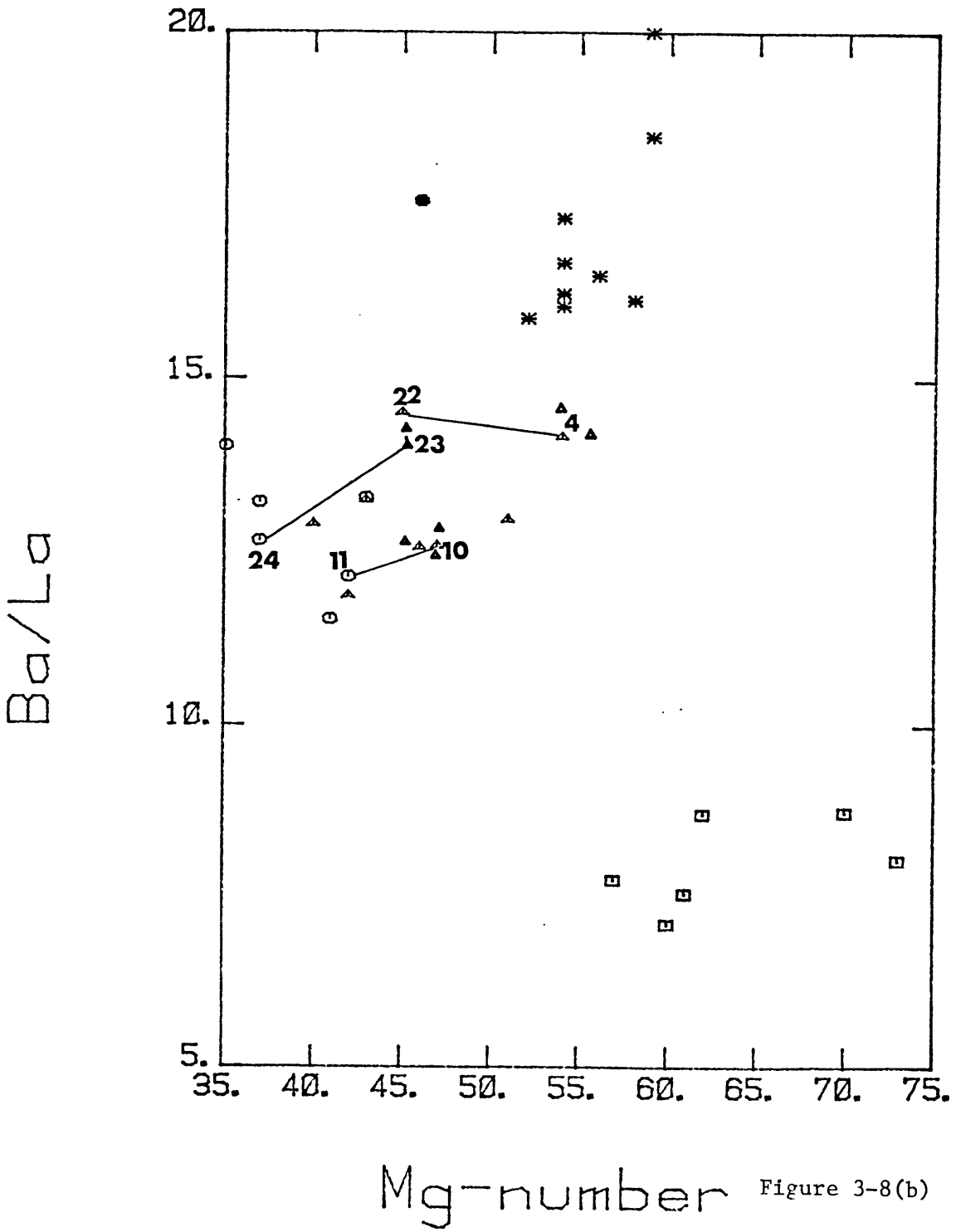


Figure 3-8(b)

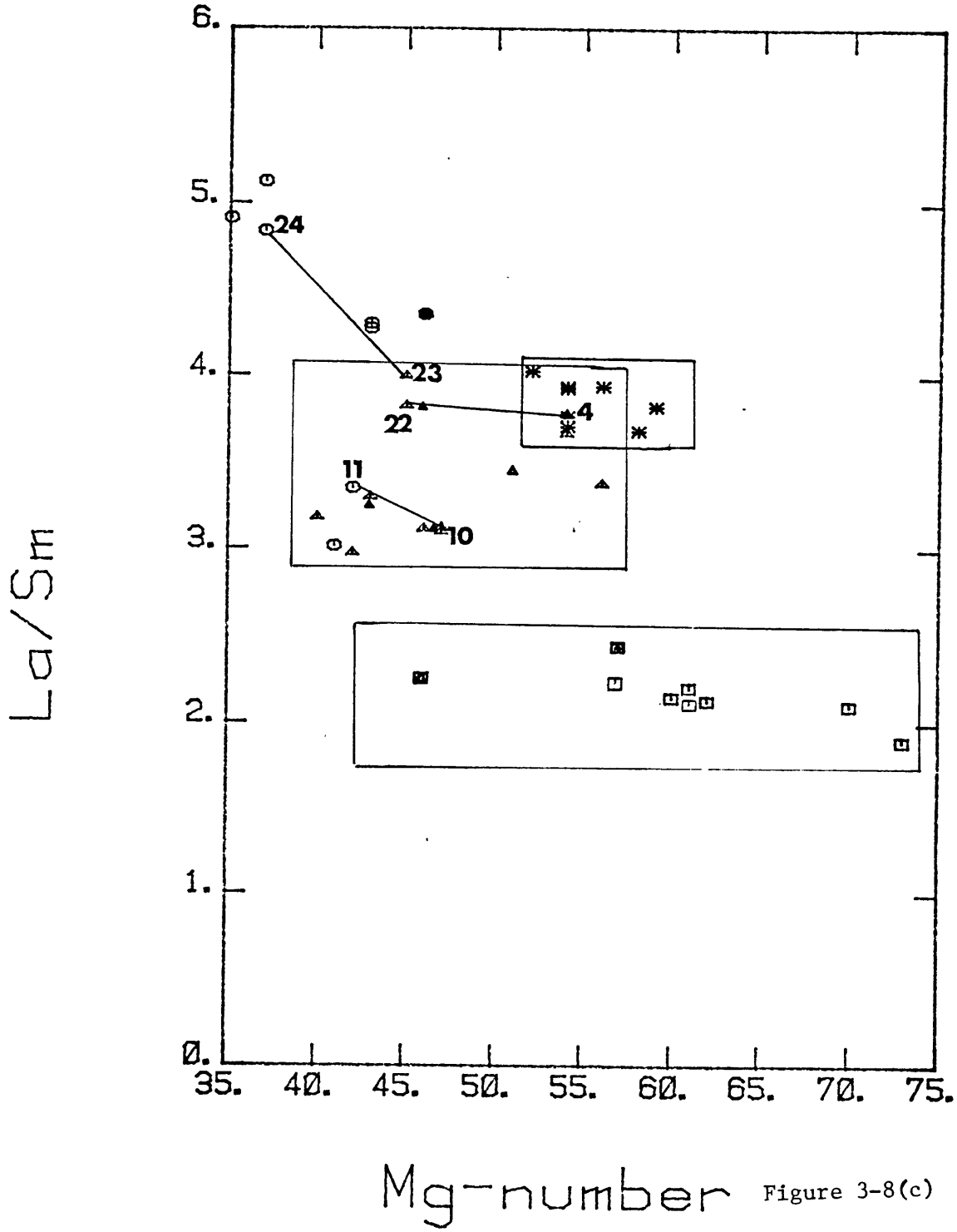


Figure 3-8(c)

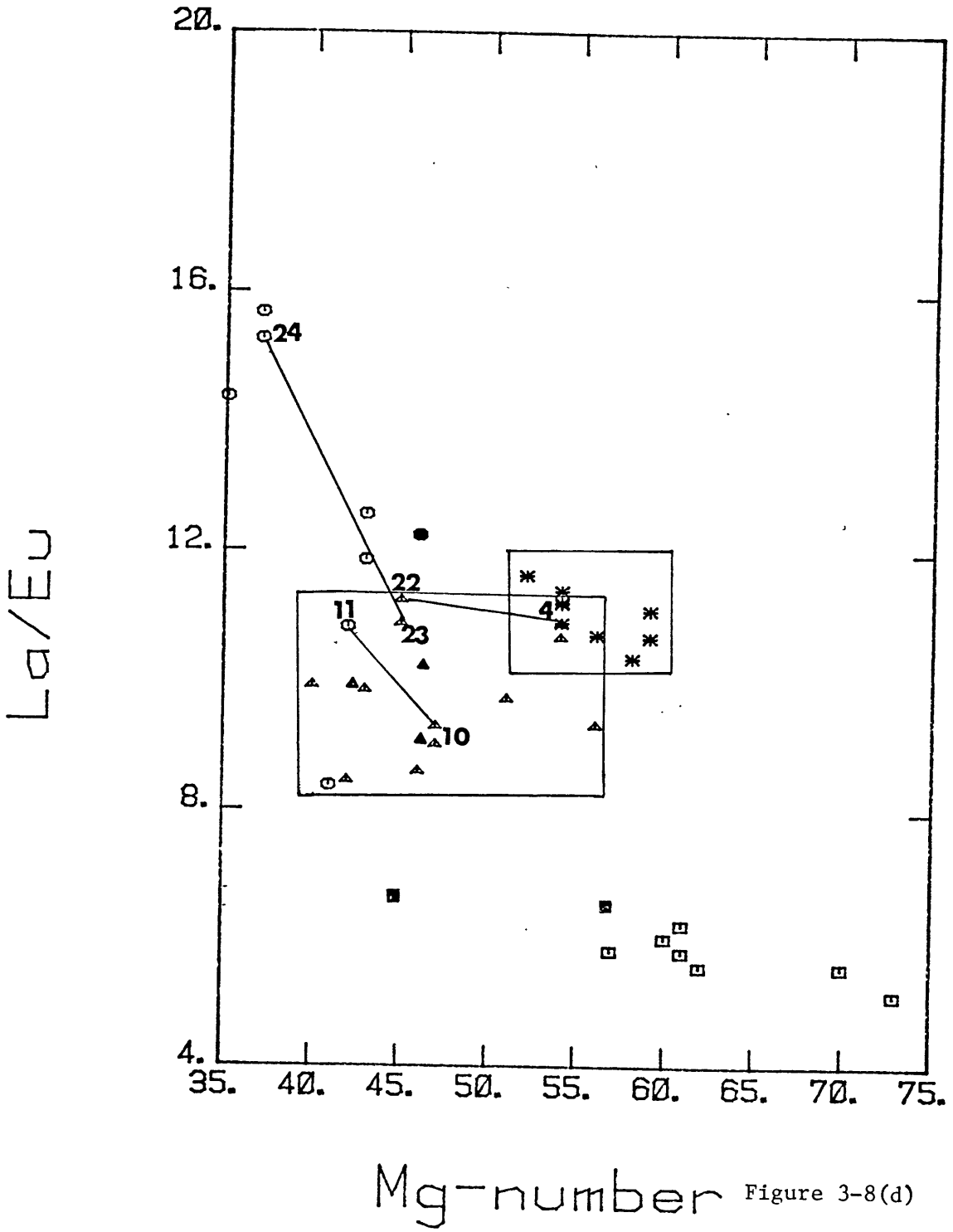


Figure 3-8(d)

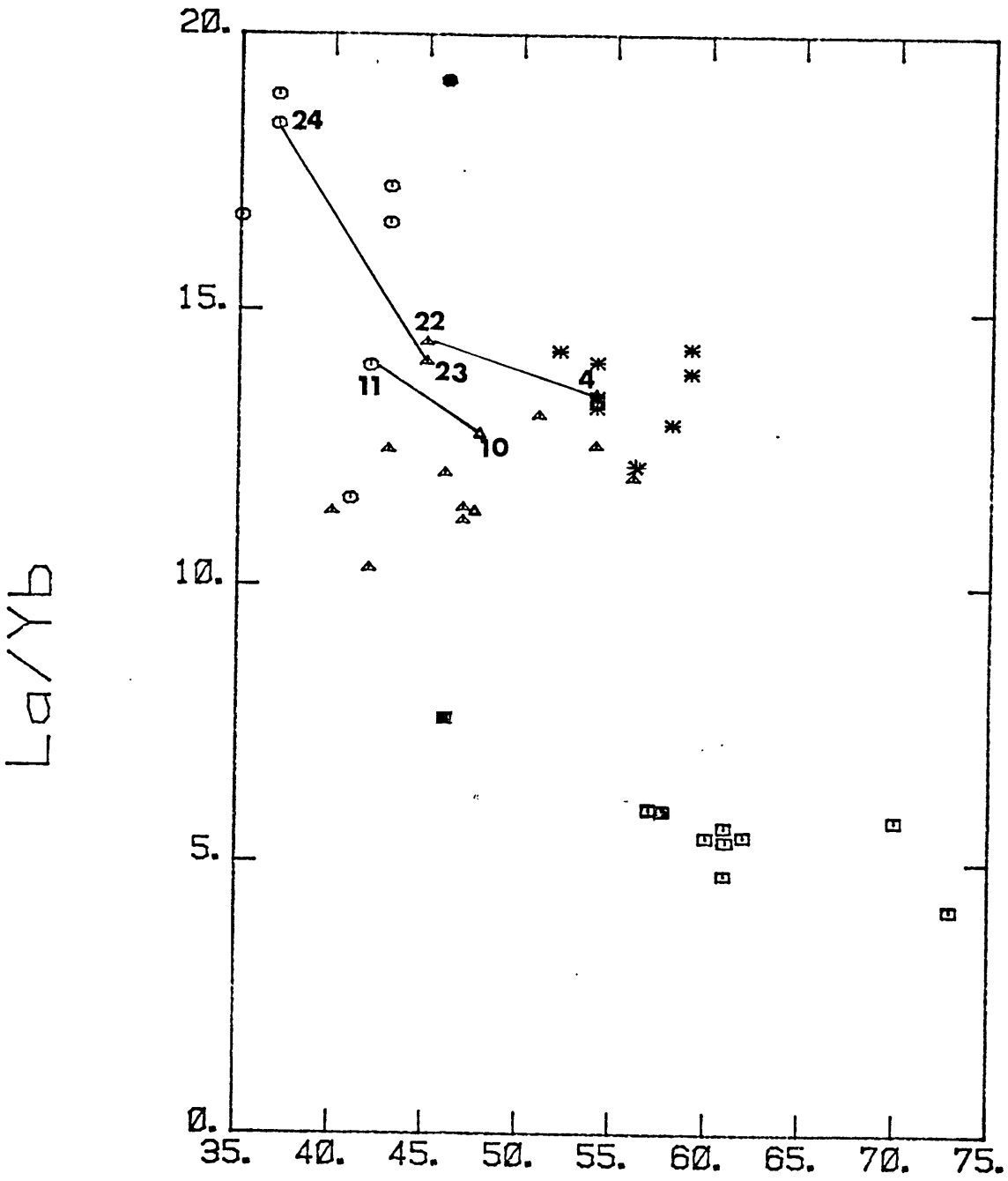


Figure 3-8(e)

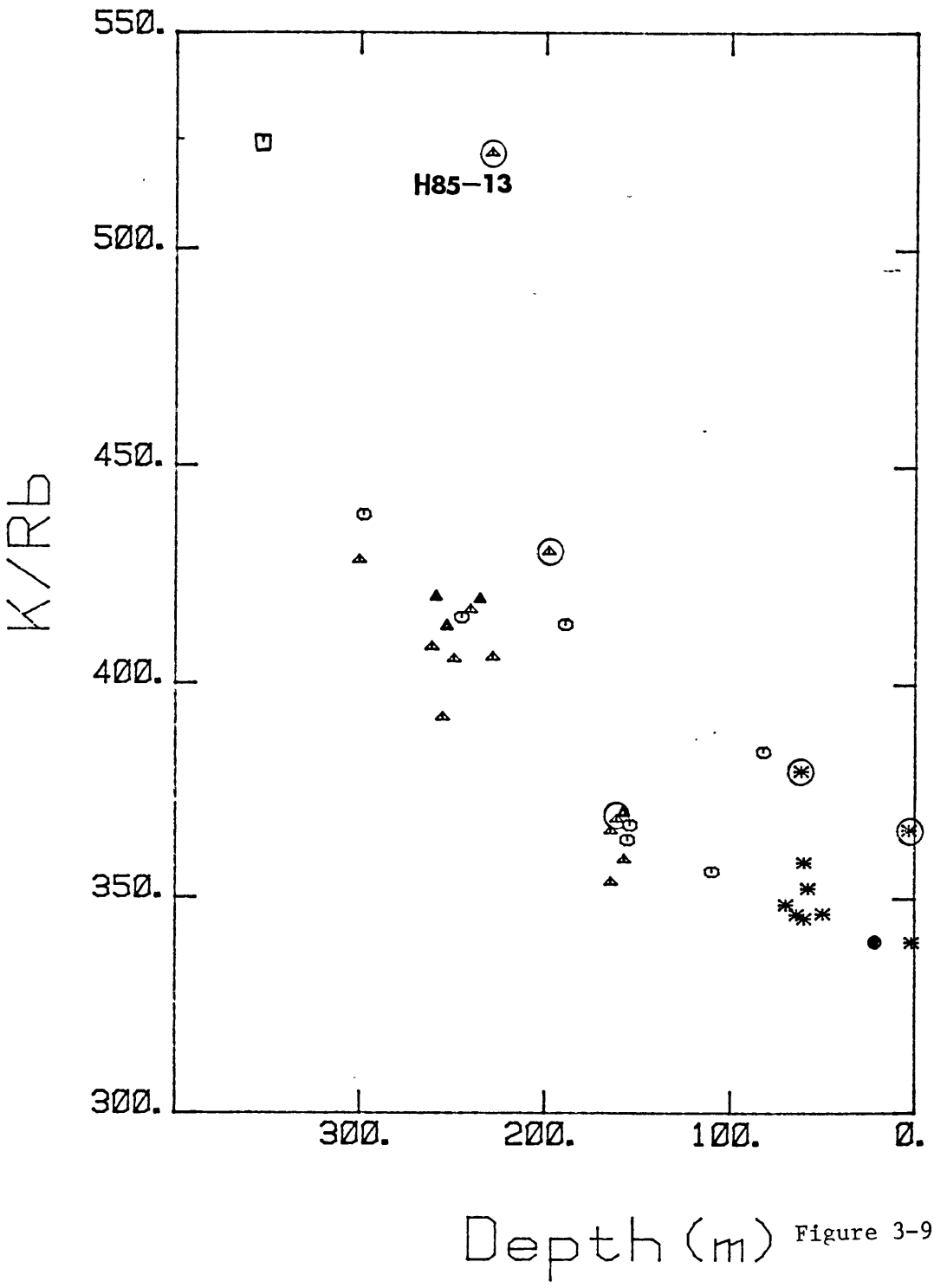


Figure 3-9(a)

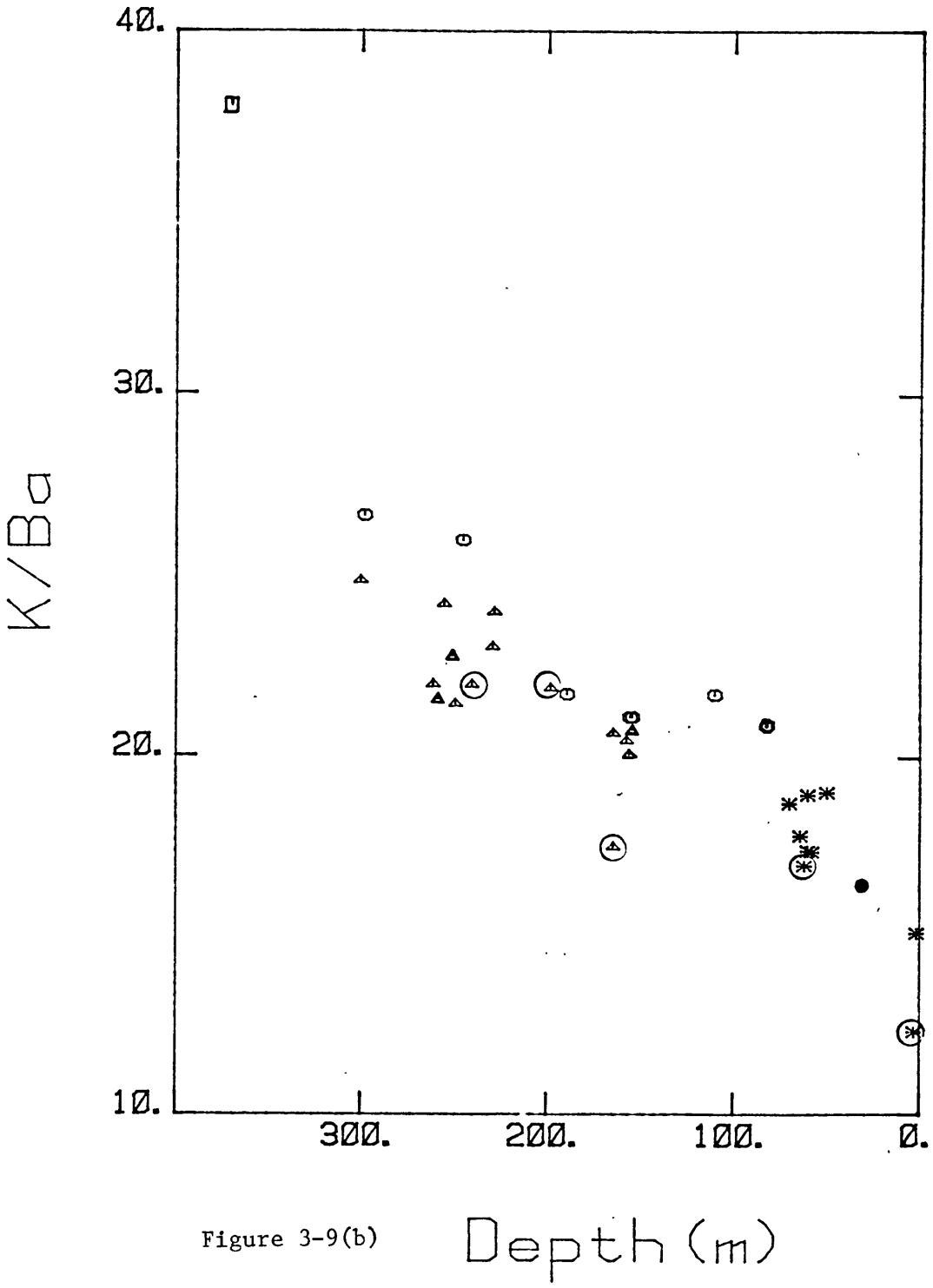


Figure 3-9(b)

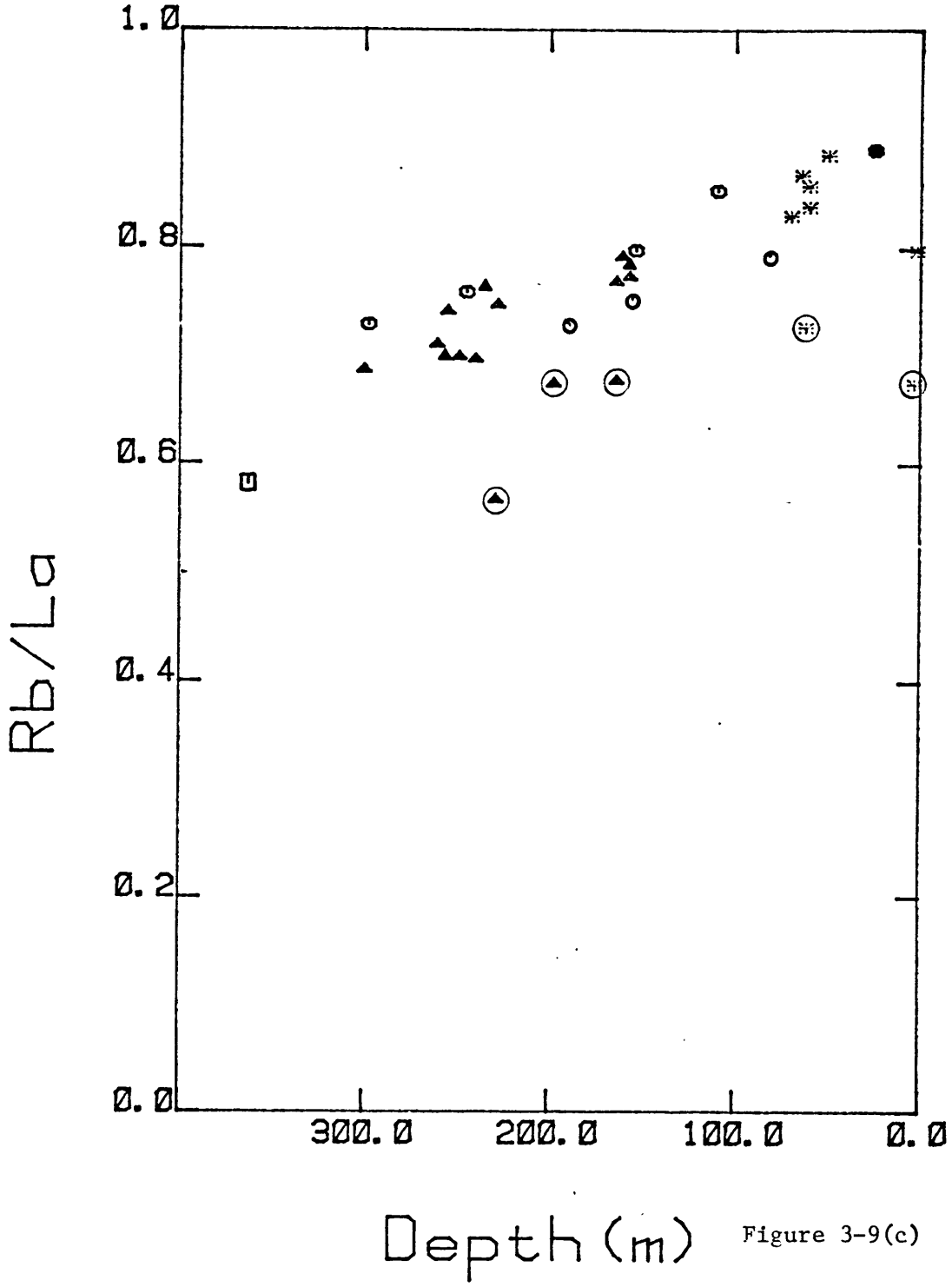


Figure 3-9(c)

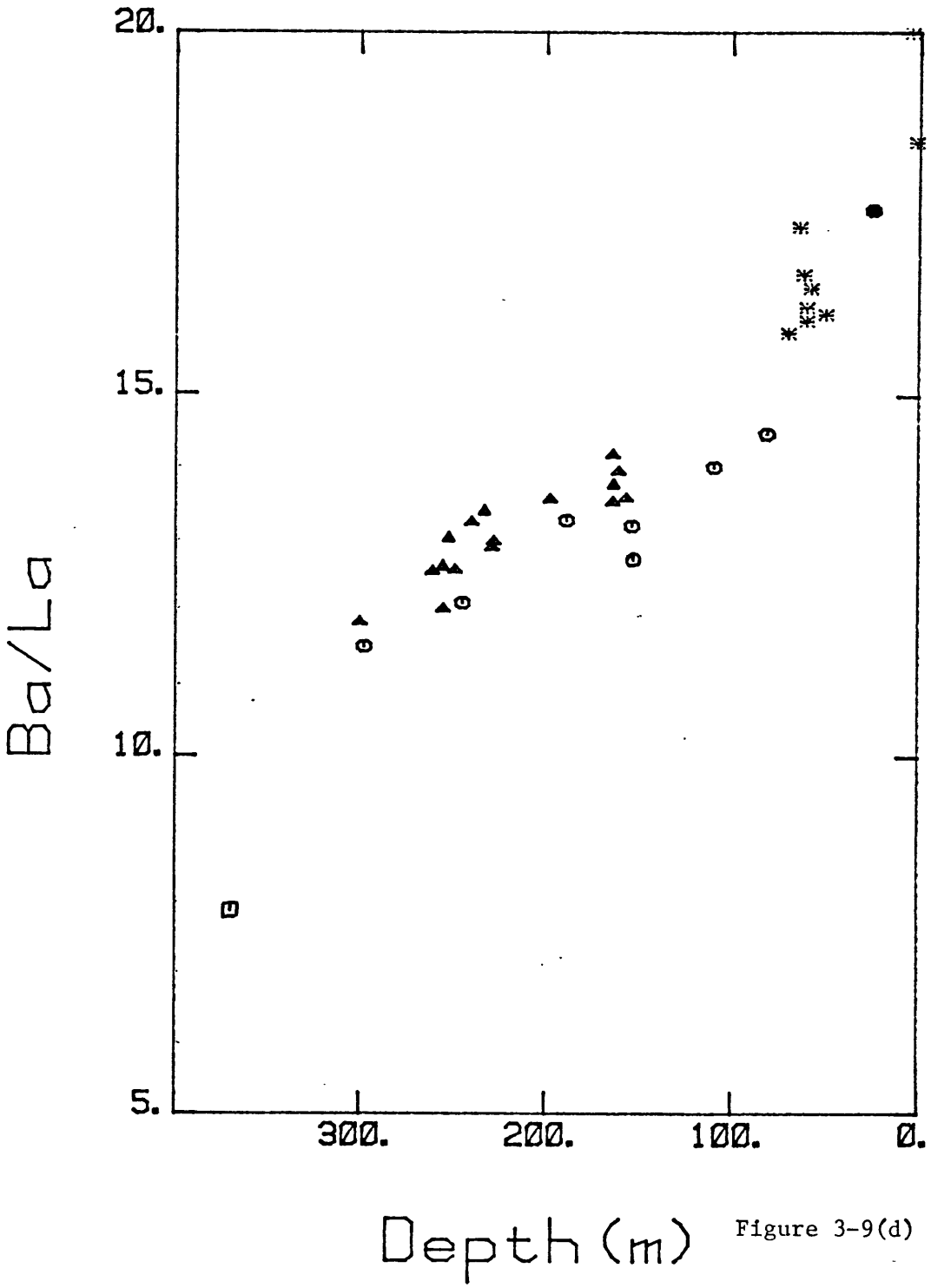


Figure 3-9(d)

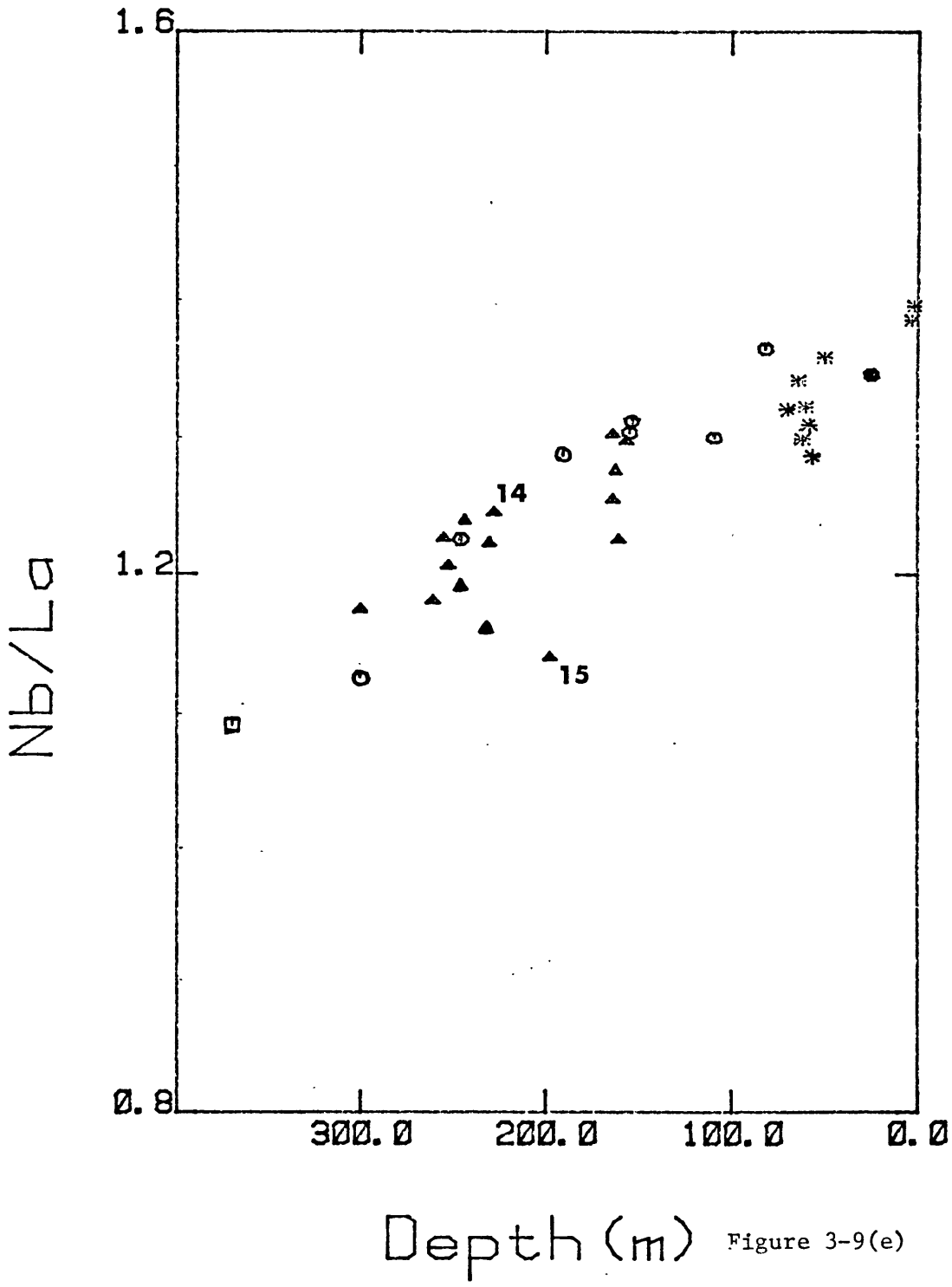


Figure 3-9(e)

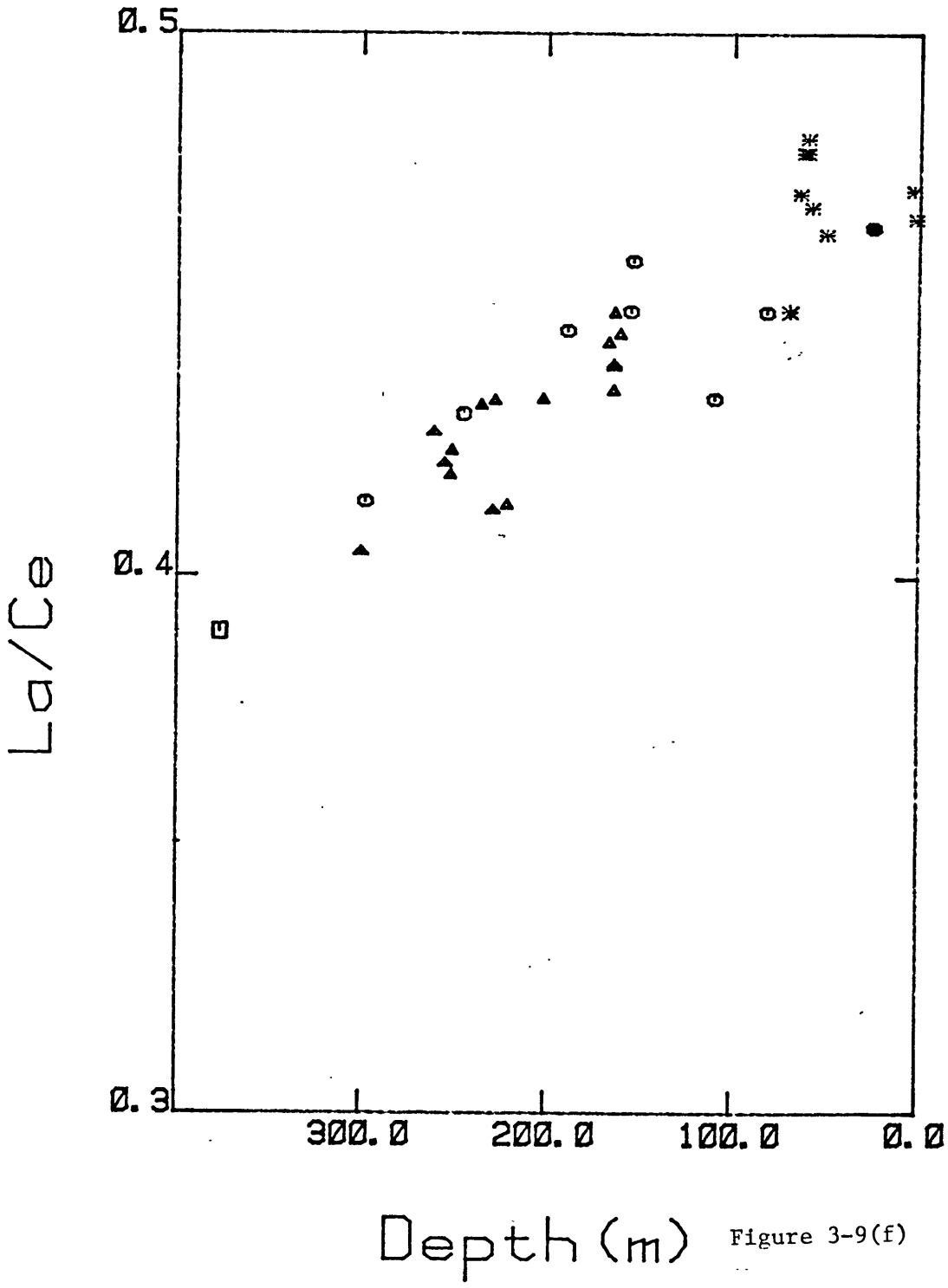


Figure 3-9(f)

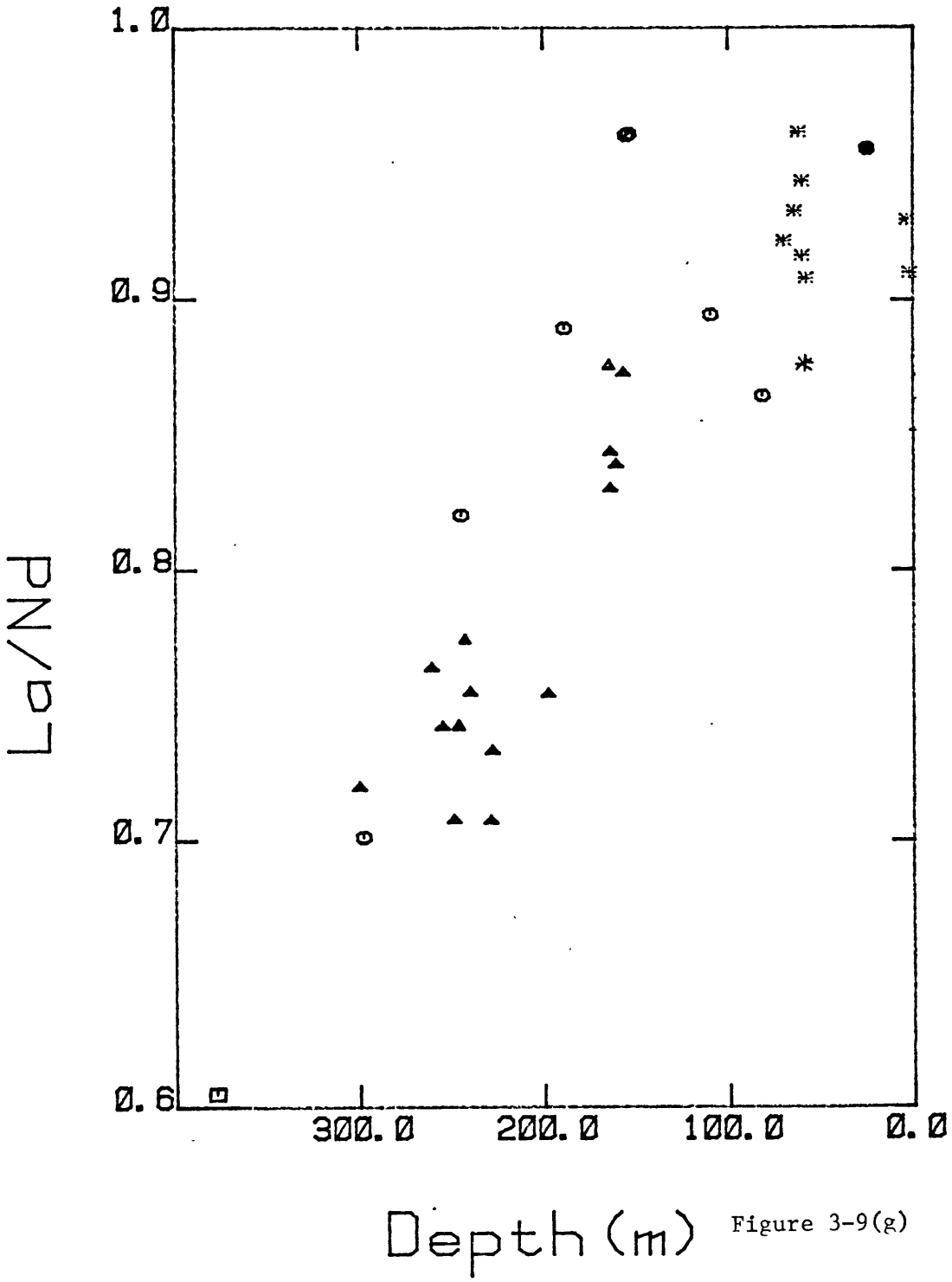


Figure 3-9(g)

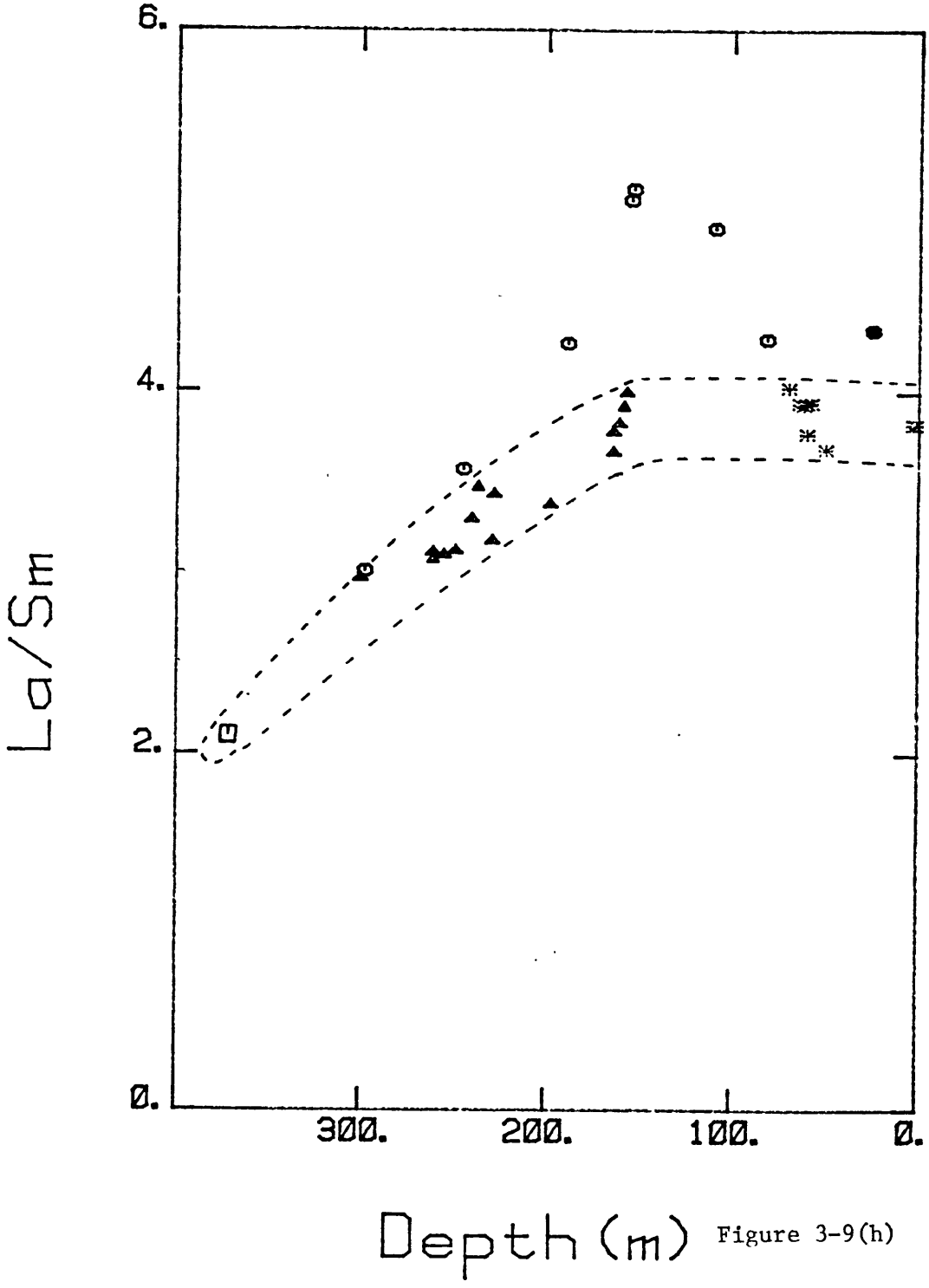


Figure 3-9(h)

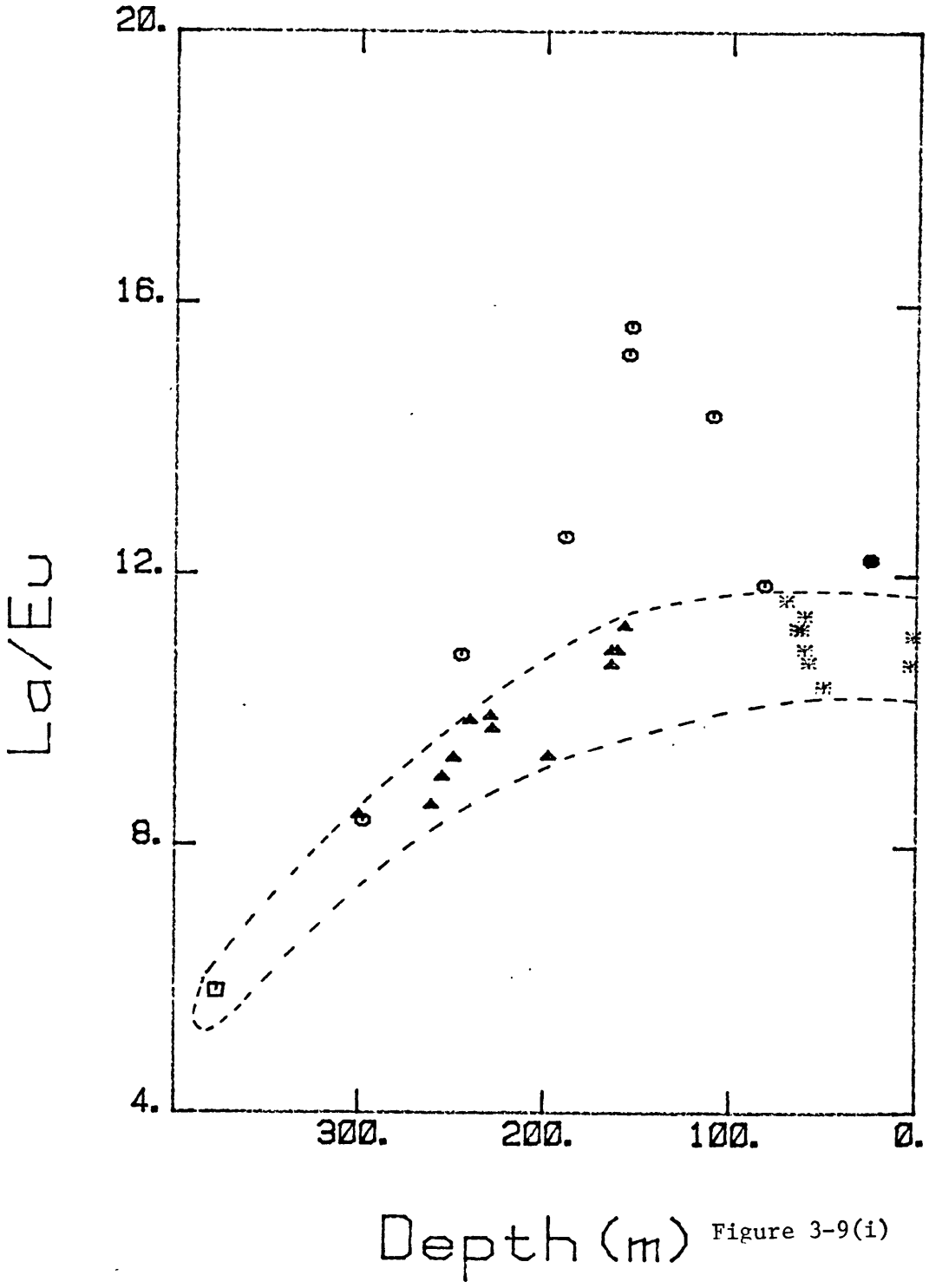


Figure 3-9(i)

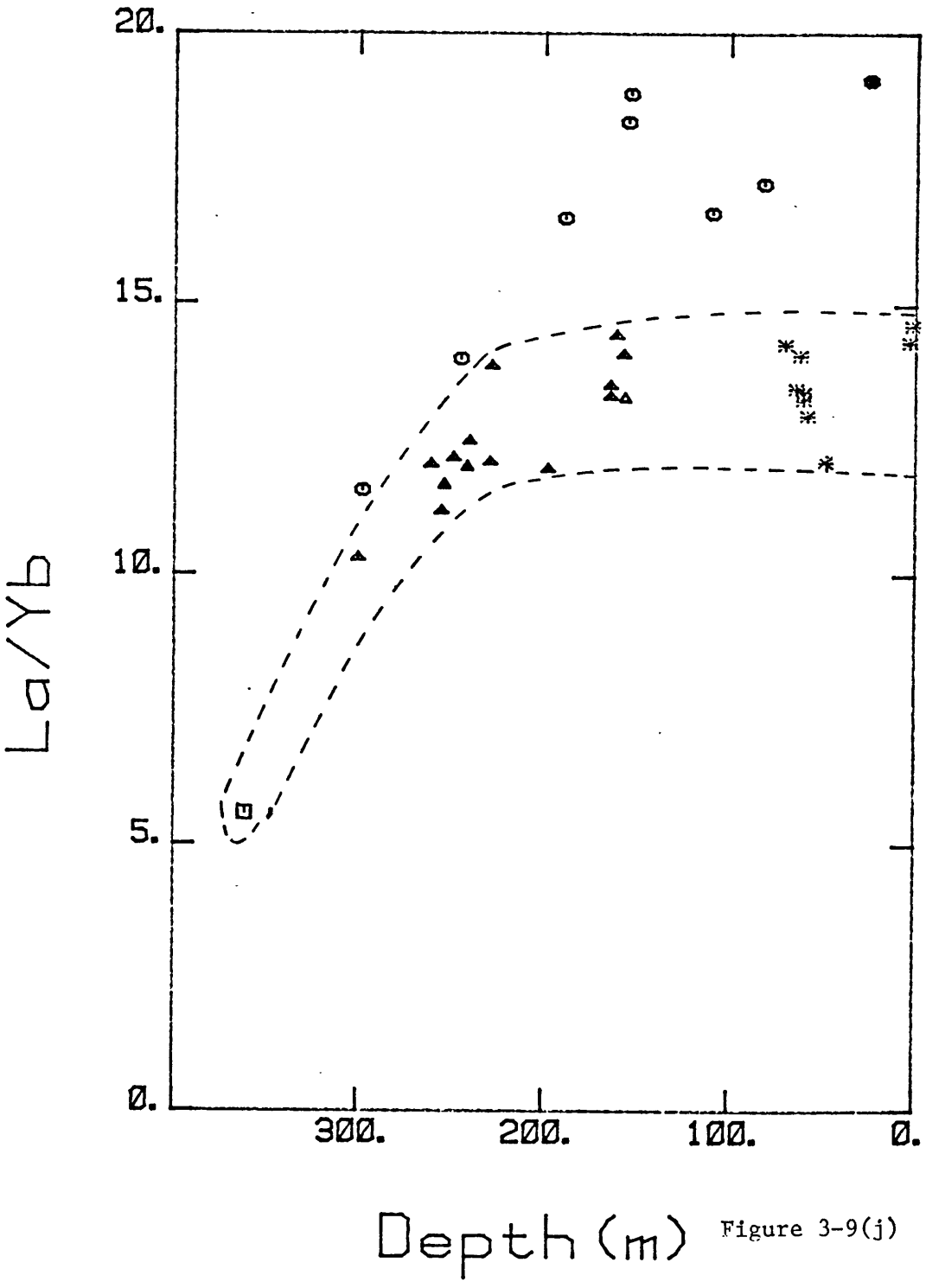


Figure 3-9(j)

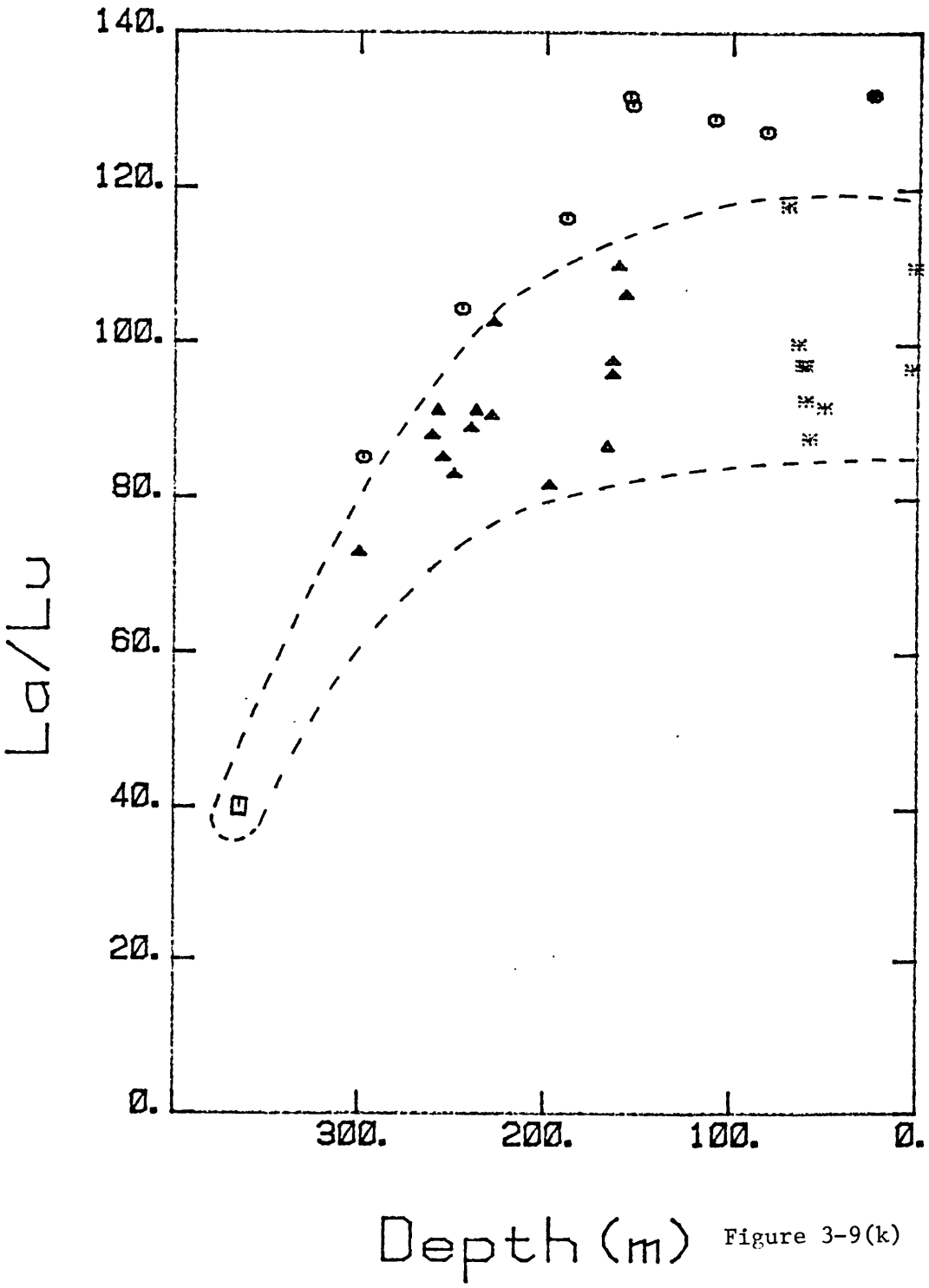


Figure 3-9(k)

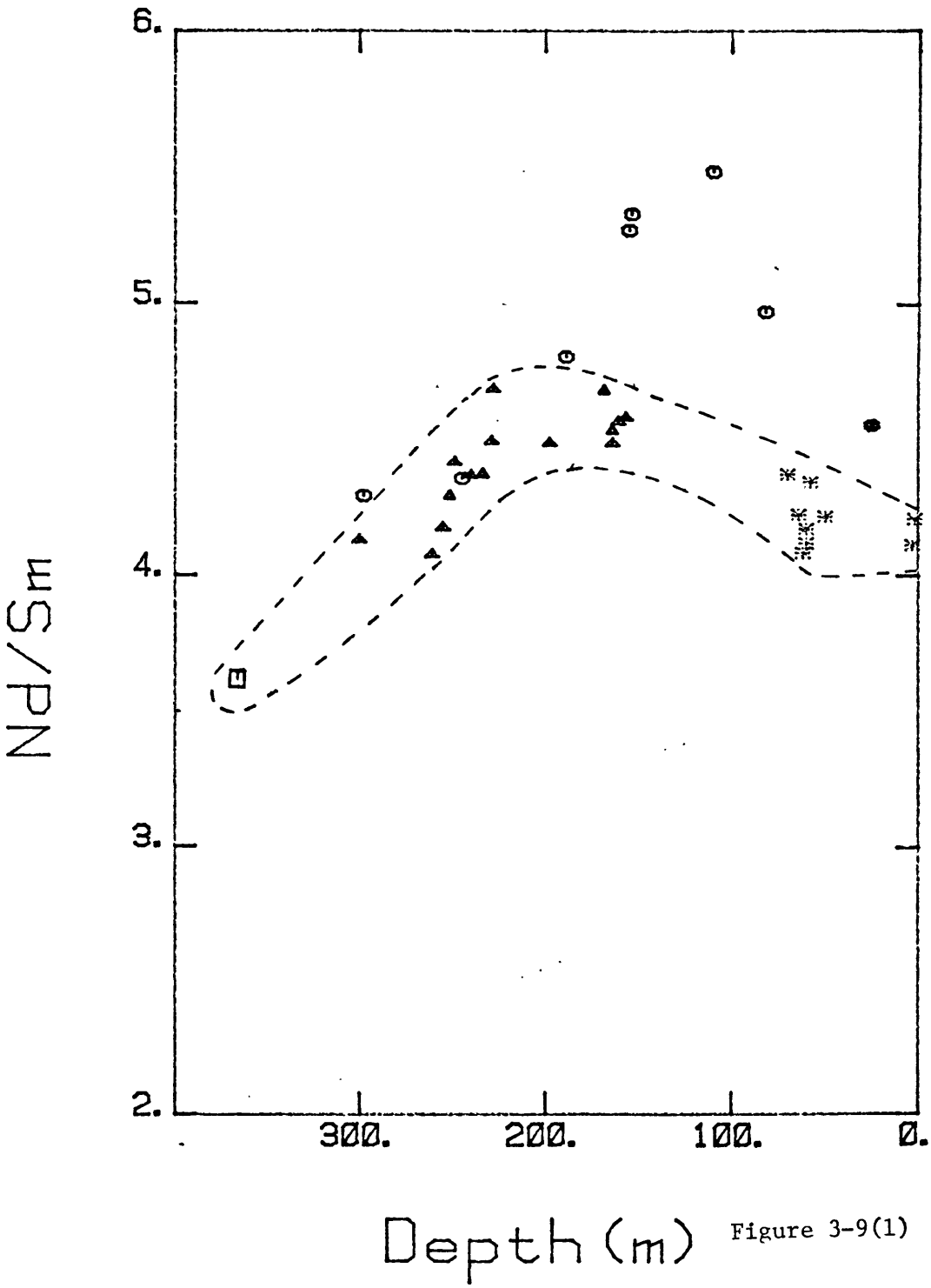


Figure 3-9(1)

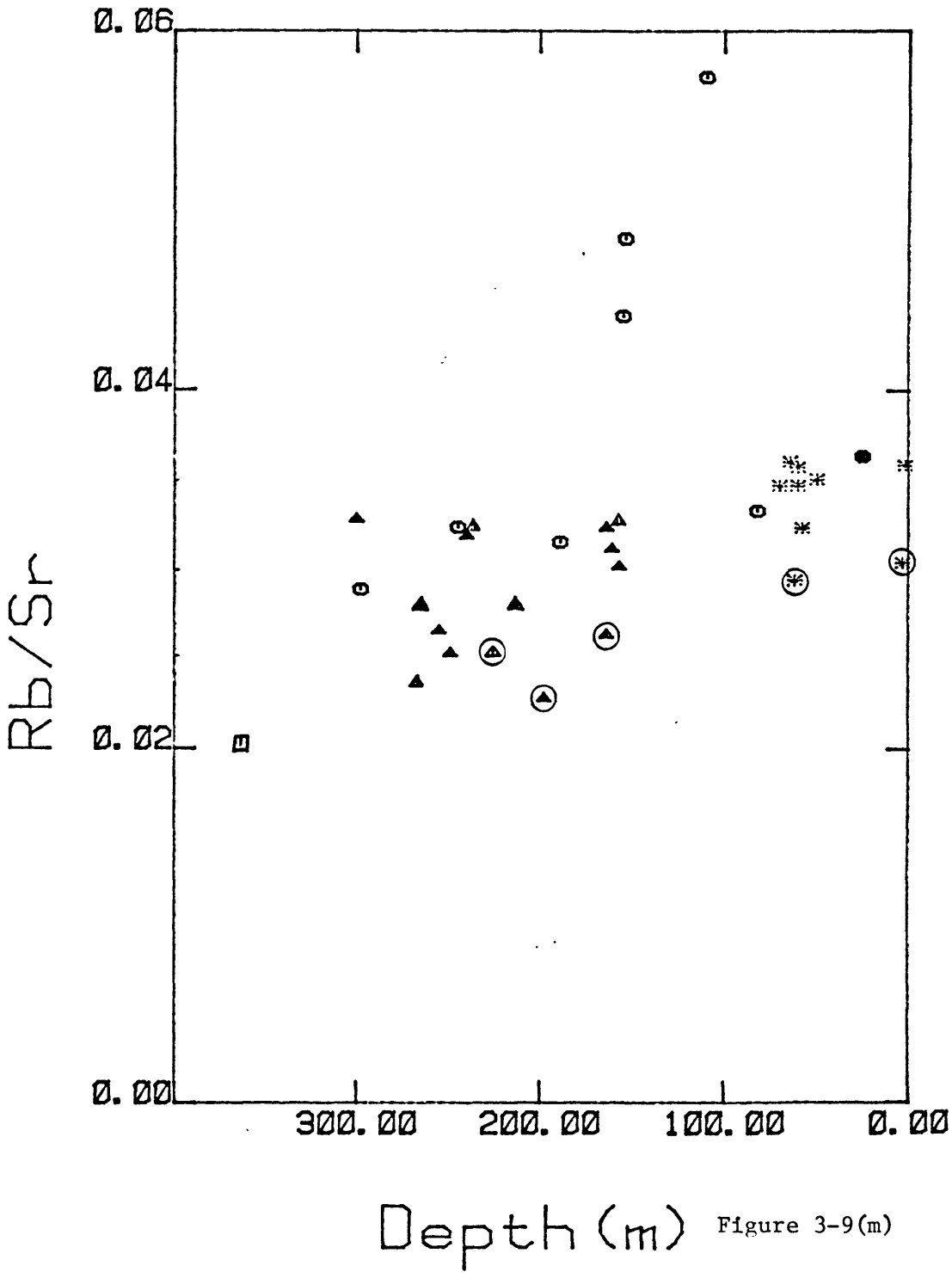


Figure 3-9(m)

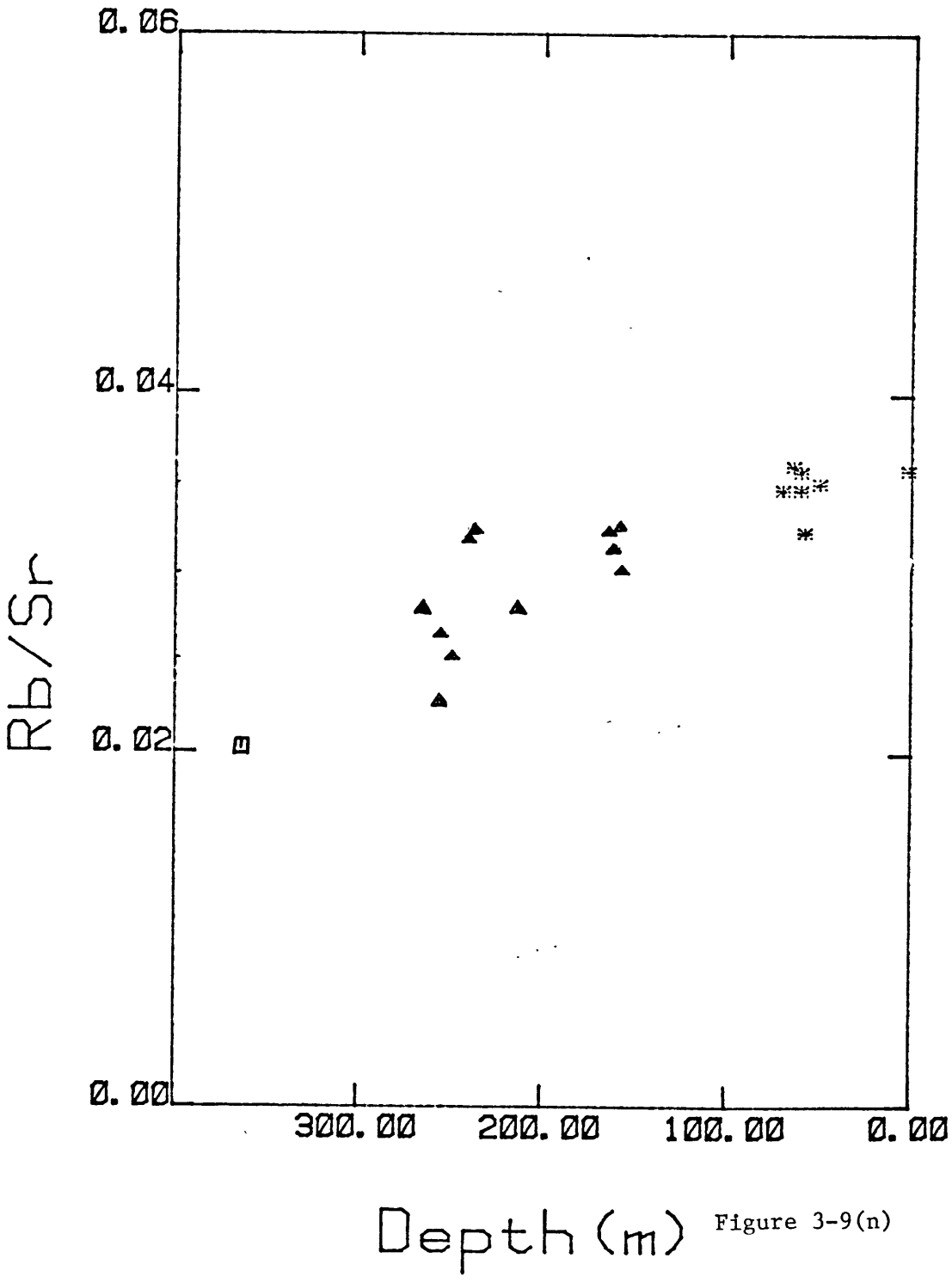


Figure 3-9(n)

CHAPTER 4

ORIGIN OF HAWAIIAN THOLEIITES AND ALKALIC BASALTS - GEOCHEMICAL EVIDENCE FOR CONTAMINATED MANTLE PLUMES

1. Introduction

The volcanic shields of Hawaii appear to be composed dominantly of tholeiitic basalt; however, alkalic basalt dominates the last stages of volcanism, and may precede tholeiites during early shield construction (e.g. Loihi Seamount, Moore et al., 1982). An understanding of the relationship between tholeiitic and alkalic Hawaiian basalts would provide constraints on the mantle sources and mantle processes related to hot-spot activity.

Previous studies on the origin of Hawaiian tholeiites and alkalic basalts have led to contrasting conclusions. Derivation of alkalic basalts from a tholeiitic parent by crystal fractionation was proposed based on major element compositions (Kennedy, 1933; Powers, 1935; Tilley, 1950; Powers, 1955; Macdonald and Katsura, 1964) and lead isotopic compositions (Tatsumoto, 1978). However, high pressure experimental studies (e.g. Yoder and Tilley, 1962; Kushiro, 1965; MacGregor, 1965; Green and Ringwood, 1967; Kushiro, 1968; Ito and Kennedy, 1968; MacGregor, 1968; O'Hara, 1968; Kushiro, 1973) suggested that these two types of magma are generated by partial melting of mantle peridotite at varying depth.

Gast (1968) showed that the trace element abundances and incompatible element ratios in alkalic basalts cannot be consistently explained by fractional crystallization from a tholeiitic parent. He suggested that alkalic basalts were generated by small degrees (3-7%) of partial melting of garnet bearing peridotites with rare earth abundances of 2 to 5 times chondrites whereas tholeiites were derived by larger degree of partial melting (20-30%). Using a similar approach, it has been shown that alkalic basalts can be derived by larger degrees of melting of mantle peridotites if this source was enriched in incompatible elements (e.g., Ba, Sr, Th, U,

LREE) relative to chondrites (Sun and Hanson, 1975; 1976; Frey et al., 1978).

Many studies on the origin of tholeiites and alkalic basalts have focussed on the isotopic and trace element abundance differences between ocean ridge tholeiites and ocean island basalts. These studies showed that the mid-ocean ridge tholeiites generally have lower $^{87}Sr/^{86}Sr$ ratios, higher $^{143}Nd/^{144}Nd$ ratios and are more depleted in incompatible trace elements (e.g. K, Rb, Cs, Th, La, Ce, Zr, Nb) than ocean island basalts (e.g. Tatsumoto et al., 1965; Hart et al., 1973; Schilling, 1973; Sun, 1973; Sun and Hanson, 1975; Sun and Jahn, 1975; Brooks et al., 1976; DePaolo and Wasserburg, 1976a,b; Duncan and Compston, 1976; Kay et al., 1970; Richard et al., 1976; O'Nions et al., 1977; Hedge, 1978; Hofmann and Hart, 1978; White and Schilling, 1978; Tatsumoto, 1978; Kurz et al., 1982a and b). The upwelling "mantle plume" model initially proposed by Morgan (1971, 1972) has been widely accepted and utilized to explain these trace element and isotopic differences between ocean ridge tholeiites and ocean island basalts (e.g. Schilling, 1973, 1975; Hart et al., 1973; Sun and Hanson, 1975; Hofmann and Hart, 1978; White and Schilling, 1978). In these plume type models, the mid-ocean ridge basalts are derived from a depleted source in the asthenosphere or in the upper mantle while the ocean island basalts are derived from a rising compositionally primitive (i.e. higher $^{87}Sr/^{86}Sr$, lower $^{143}Nd/^{144}Nd$ and with higher abundances of incompatible elements than the MORB source) mantle plume. Recently, Hofmann and White (1982) proposed that ancient, subducted oceanic crust instead of primitive mantle material is the source of the plume.

Instead of a mantle plume, Hanson (1977) proposed an upper mantle source composed of peridotite with small (about 4 cm thick), closely spaced

(within tens of centimeters) pyroxenite veins as the source for ocean island basalts. Evidence for this model are the pyroxenite veins that commonly exist in ultramafic nodules (e.g. Wilshire and Shervais, 1975) and alpine peridotite (Wilshire and Pike, 1975). Hanson (1977) suggested that the greater enrichment of incompatible elements in alkalic basalts relative to tholeiites results from preferential melting of the pyroxenite veins so that melts formed by low degrees of melting are dominantly formed from the pyroxenites. Because this model involves compositionally distinct sources for alkalic and tholeiitic basalts, it also accounts for varying trace element abundance ratios as a function of melting degree.

In all the previously proposed models, compositionally different mantle sources for ocean ridge tholeiites and ocean island basalts are generally accepted. However, a homogeneous source is commonly proposed for the tholeiitic and alkalic basalts from a single ocean island volcano. For example, recent studies of two Hawaiian volcanoes, Kohala volcano, Hawaii (Feigenson and Hofmann, 1980) and East Molokai volcano (Clague and Beeson, 1980), suggest that the trace element abundance differences between tholeiites and alkalic basalts within each volcano are a result of different degrees of partial melting.

In contrast, detailed studies of other Hawaiian volcanoes such as Loihi (Clague and Frey, 1982; Kurz et al., 1982a; Staudigel et al., 1981), Haleakala volcano (Chen et al., 1981), East Molokai volcano (Clague, personal communication, 1982), Koolau volcano (Roden, et al., 1981; Clague and Frey, 1982) show that the tholeiites generally have higher $^{87}Sr/^{86}Sr$, $^{3}He/^{4}He$, and lower $^{143}Nd/^{144}Nd$ ratios despite their lower abundances of incompatible elements than alkalic basalts from the same volcano. Moreover, negative correlations between isotopic ratios (e.g. $^{87}Sr/^{86}Sr$)

and trace element ratios (e.g. Rb/Sr, La/Ce, Th/La, Ba/La, La/Yb) occur in samples from Loihi seamount and Haleakala volcano (Chapters 2,3). Negative correlations between isotopic ratios and ratios of highly incompatible trace elements to slightly less incompatible trace elements are not a predicted feature of previous models. In this chapter, I propose alternative models which can explain the observed isotopic and trace element abundance variations in Hawaiian tholeiites and alkalic basalts.

2. Alternative Mantle Models For the Origin of Hawaiian Tholeiites and Alkalic Basalts

2.1 Metasomatic Model

The $^{87}Sr/^{86}Sr$ and $^{143}Nd/^{144}Nd$ ratios for the three Haleakala volcanic series require that their sources had lower Rb/Sr and higher Sm/Nd than proposed bulk earth ratios. This conclusion contrasts with high Rb/Sr and low Sm/Nd in Haleakala basalts (Chapters 2 and 3), and Chen et al. (1981) proposed that the mantle source of Haleakala basalts had experienced incompatible element enrichment as a result of metasomatism.

Wright (1981) suggested that Hawaiian tholeiites ts could be produced by melting of a mid-ocean ridge basalt (MORB)-type source at the base of the thinned lithosphere beneath Hawaii if the lithosphere had undergone metasomatism. He proposed that the metasomatic constituents may originate as low-melting fractions in the low-velocity zone and were composed of a nepheline-normative fluid and iron sulfide or iron oxide (Wright, 1981). However, the isotopic differences between Hawaiian basalts and mid-ocean ridge basalts are not consistent with this model. Contamination of Hawaiian basalts by altered oceanic crust was proposed to explain the isotopic difference between Hawaiian tholeiites and mid-ocean ridge basalts (Wright, 1981), but this explanation is inconsistent with the negative

correlation between isotopic ratios and trace element abundances in Haleakala basalts (Chapters 2 and 3).

Chen et al. (1981) noted that if the depth of melting increases from the tholeiitic to alkalic stage (e.g., Macdonald and Powers, 1968; Jackson and Wright, 1970) the vertical variations in isotopic ratios and trace element abundances in the Hawaiian mantle can be inferred. For example, relative to the tholeiites the incompatible trace element ratios (e.g. La/Ce, Nb/La, Ta/La, Th/La, Ba/La, Rb/Sr) and $^{143}Nd/^{144}Nd$ are higher and $^{87}Sr/^{86}Sr$ is lower than in Haleakala alkalic basalt (Chapters 2 and 3). Consequently, with increasing depth in the Hawaiian mantle these abundance ratios of incompatible trace elements and $^{143}Nd/^{144}Nd$ increase and $^{87}Sr/^{86}Sr$ decreases. Chen et al. (1981) also proposed that the isotopic differences ($^{87}Sr/^{86}Sr$ and $^{143}Nd/^{144}Nd$) between the Hawaiian basalts and the mid-ocean ridge basalts were due to growth of radiogenic isotopes with time. In other words, the proposed metasomatic events for Haleakala basalts were "ancient". The isotopic compositions of the Haleakala basalts provide constraints on the ages of possible enrichment and depletion events, but in order to calculate an age several estimates must be made. Firstly, what are the isotopic ratios in the metasomatic fluid? The negative correlations between isotopic ratios and trace element abundances (e.g. Figure 4-1, Figure 4-2, also Chapter 3) suggest that the metasomatic fluid which must be highly enriched in incompatible trace elements cannot have higher $^{87}Sr/^{86}Sr$ and lower $^{143}Nd/^{144}Nd$ than the unmetasomatized mantle. If the metasomatic fluid had higher $^{87}Sr/^{86}Sr$ and lower $^{143}Nd/^{144}Nd$ ratios a positive correlation rather than negative correlation between isotopic ratios and parent/daughter abundance ratios is expected for ancient and recent metasomatic events. Since lower $^{87}Sr/^{86}Sr$ and

higher $^{143}Nd/^{144}Nd$ ratios than the mid-ocean ridge basalts are never observed in terrestrial samples, it is reasonable to assume that the metasomatic fluid had the same isotopic ratios ($^{87}Sr/^{86}Sr$ and $^{143}Nd/^{144}Nd$) as the MORB-type source. The assumption that the MORB-type depleted source extends beneath the lithosphere is supported by results of mass balance calculations which show that more than one-third of the earth's mantle must have been depleted to form the continents (Allegre et al., 1979, Jacobsen and Wasserburg, 1979; DePaolo, 1980; O'Nions et al., 1980; Allegre et al., 1982).

Secondly, the parent/daughter ratios (Rb/Sr, Sm/Nd) for the metasomatized sources must be estimated. Since partial melting and fractionation processes tend to increase Rb/Sr and Nd/Sm ratios, the Rb/Sr ratio and Nd/Sm ratio in the basalt represent the upper limits of Rb/Sr, Nd/Sm ratios for the mantle source if surface alteration did not occur (note that surficial Rb loss has been inferred for some Haleakala samples, Chapter 3). The freshest, least-fractionated samples from the tholeiitic series, the alkalic series and the post-erosional series, respectively, of Haleakala volcano were selected for the following calculations. In Table 1, I summarize the data used in the depletion-enrichment age calculations. Table 2 summarizes the ages of depletion or enrichment events calculated from Rb-Sr and Nd-Sm systems assuming a two-stage evolution for the MORB source and a three-stage evolution for the Hawaiian basalt sources. In case 1, the Rb/Sr and Nd/Sm ratios in the basalts is taken to be upper limits of the Rb/Sr and Nd/Sm ratios in their sources, and the ages calculated from these Rb/Sr and Nd/Sm ratios would represent the oldest depletion ages and the oldest/youngest enrichment ages for their sources, depending on if the Rb-Sr system or the

Nd-Sm system is used. In this case (Table 2) the oldest depletion age for the MORB source is calculated to be 2.96 b.y. from the Rb-Sr data of a most-depleted mid-ocean ridge basalt (AD-3, O'Nions et al., 1977). Metasomatism of this MORB-type source at different ages could have produced the mantle sources for Haleakala basalts. The calculated metasomatic age is 4.2 b.y., 1.2 b.y. and 0.88 b.y. for the source of the tholeiitic series, alkalic series and post-erosional series, respectively. From the Nd-Sm system, the maximum age of depletion is calculated to be 4.2 b.y. and the enrichment age is calculated to be 2.2 b.y., 0.56 b.y. and 0.46 b.y. for the source of the tholeiitic series, alkalic series and post-erosional series, respectively. It is significant that the depletion-enrichment ages calculated from the Rb-Sr and Nd-Sm do not agree. Also, the calculated enrichment age for the source of tholeiites is older than the depletion age (Table 2) in Rb-Sr system which is inconsistent with the assumption that the sources for the Hawaiian basalts were enriched from a MORB-type source.

In case 2, I consider the effect of partial melting on the Rb/Sr and Nd/Sm ratios and the effect on the calculated ages of depletion-enrichment events. Source mineralogy, proportions of constituent minerals in the melt, degree of partial melting and partition coefficients have to be estimated. The source mineralogy is assumed to be 60% olivine, 25% orthopyroxene, 10% clinopyroxene and 5% garnet (Frey and Green, 1974; Clague and Frey, 1982). The proportion of constituent minerals into the melt is taken as 20% (olivine + orthopyroxene), 40% clinopyroxene and 40% garnet (Davis and Schairer, 1965; Kushiro, 1968, 1969; Leeman et al., 1980). The partition coefficients used are listed in Table 3 (taken from Hart and Brooks, 1974; Shimizu, 1974; Frey et al., 1978). The minimum

degree of partial melting is assumed to be 10% for the tholeiites and 5% for the alkalic basalts (e.g. Gast, 1968; Frey et al., 1978; Leeman et al., 1980; Wright, 1981). The Rb/Sr and Sm/Nd ratios of the MORB, Haleakala tholeiites and Haleakala alkalic basalts are then corrected to their source values according to the estimated parameters (e.g. source mineralogy, degree of melting, etc.). In this case, the depletion age calculated from the Rb-Sr system (2.8 b.y.) and the Nd-Sm system (2.7 b.y.) agree very well. If the sources for Hawaiian tholeiites and alkalic basalts are enriched from this MORB-type source, the "metasomatic age" is calculated to be 2.1 b.y., 520 m.y. and 420 m.y. for the source of tholeiitic series, alkalic series and the post-erosional series, respectively, from the Nd-Sm system (Fig. 4-3). In this case, the source of the tholeiitic series was enriched in incompatible elements earlier, but to a lesser extent, than the source of the alkalic series and post-erosional series. However, the "metasomatic ages" calculated from Rb-Sr system do not agree with the ages calculated from Nd-Sm system (Table 2).

The present-day isotopic ratios and parent/daughter ratios for the Haleakala tholeiites and alkalic basalts can be due to differences in the "depletion age" rather than the "metasomatic age" as assumed in Case 1 and 2. In Case 3, I assumed that the metasomatic event for the sources of tholeiitic series, alkalic series and post-erosional series occurred at the same time and the isotopic differences among the mid-ocean ridge basalts, the Haleakala tholeiites and alkalic basalts were due to differences in depletion time. In this case, Rb/Sr and Nd/Sm ratios in the basalts are corrected for partial melting events as in case 2. From the Nd-Sm system, the "metasomatic age" is calculated to be 420 m.y. if the "depletion age" for the source of the post-erosional series is the same as the average

"depletion age" (2.7 b.y.) of the MORB source (Fig. 4-4a). The depletion event for the tholeiitic series and alkalic series is then calculated to be 1.3 b.y. and 2.3 b.y. respectively (Table 2). The source for the tholeiitic series was depleted later (1.3 b.y.) than the source of the alkalic series (2.3 b.y.) and the post-erosional series (2.7 b.y.) (Fig. 4-4a).

These calculations show that the isotopic and parent/daughter ratios of the Hawaiian tholeiites and alkalic basalts can be derived by varying the enrichment and/or depletion time of their mantle sources. However, a serious weakness of this model is seen from these calculations. For example, the "depletion age" calculated from the Nd-Sm and Rb-Sr systems agree well, but the "metasomatic age" calculated from these two systems do not agree (e.g. in case 3, 1.1 b.y. from the Rb-Sr system, 420 m.y. from the Nd-Sm system, (Fig. 4-4a, 4-4b)). Plausible explanations are: (1) the observed isotopic and trace element trends are not due to ancient metasomatic events as proposed in this model, but rather reflect recent mixing events. This interpretation will be discussed later. (2) the evolutionary history of the Hawaiian mantle is more complicated than the assumed three-stage history; that is, the events of enrichment and depletion could be continuous or multi-stage and the extent of Nd/Sm, Rb/Sr enrichment or depletion for each enrichment and depletion events could be variable. In this case the estimated Rb/Sr and Sm/Nd ratios in the Hawaiian mantle sources represent only the final state attained as a result of variable amounts and stages of enrichment-depletion events. Consequently, the "metasomatic ages" calculated for a three-stage evolution model may not represent the real metasomatic ages and the "metasomatic ages" calculated from Rb-Sr system and Nd-Sm system may be different.

In addition to the problem of different "metasomatic ages" between the Rb-Sr and Nd-Sm system, several other difficulties arise with this model. For example,

(1) This model requires a Hawaiian mantle with negative trends between the isotopic ratios and parent/daughter abundance ratios. That is, the sources for the post-erosional volcanic series are more enriched in incompatible trace elements (e.g. Ba, Rb, La, Ta, Nb, Th, LREE) but have lower $^{87}Sr/^{86}Sr$ ratios and higher $^{143}Nd/^{144}Nd$ ratios than the sources for the alkalic volcanic series and the tholeiitic series. Inverse correlations between trace element and isotopic compositions in the upper mantle are uncommon. Ultramafic nodules in alkalic basalts such as the Honolulu volcanics (Jackson and Wright, 1970) provide insight about the trace-element and isotopic compositions of the Hawaiian upper mantle. Although nodules with La/Ce, Nd/Sm and LREE/HREE ratios higher than chondrites have been found in the Hawaiian volcanoes (e.g. Schilling, 1966; Reid and Frey, 1971; Shimizu, 1975; Leeman et al., 1977; Frey, 1980), they commonly have $^{87}Sr/^{86}Sr$ and $^{143}Nd/^{144}Nd$ ratios similar to alkalic basalts (Powell and DeLong, 1966; O'Neil et al., 1970; Shimizu, 1975; O'Nions et al., 1977; Lanphere and Dalrymple, 1980). There are no negative correlations between incompatible trace element enrichment and isotopic compositions ($^{87}Sr/^{86}Sr$ ratios and $^{143}Nd/^{144}Nd$ ratios) for these ultramafic nodules. However, some of these Hawaiian nodules may represent solid segregations from alkalic basalts rather than source material for the Hawaiian basalts (Frey, 1980). Thus, the lack of negative correlations between parent/daughter abundance ratios and isotopic compositions in these ultramafic nodules does not eliminate the possibility of such a correlation existing in the Hawaiian upper mantle.

However, alpine peridotites and ultramafic nodules from world-wide localities show no correlation or roughly positive correlation between parent-daughter abundance ratios and isotopic compositions (e.g. Burwell, 1975; Shimizu, 1975; Jacobsen and Wasserburg, 1979; Chen and Frey, 1980; Menzies and Murthy, 1980a,b; Roden et al., 1980; Stosch et al., 1980; Zindler and Jagoutz, 1980). Negative correlations between trace-element enrichment and isotopic ratios have never been found in the upper mantle samples. Consequently, it seems unlikely that the Hawaiian mantle is characterized by inverse correlations between the parent/daughter abundance ratios and isotopic compositions.

(2) Mechanisms such as propagating fractures along zones of weakness have been proposed to explain linear chains of mid-plate volcanism (e.g. Jackson and Wright, 1970; McDougall, 1971, Shaw, 1973; Shaw and Jackson, 1973). However, mid-plate swells (Dietz and Menard, 1953; Sclater et al., 1975; Watts, 1976; Crough, 1978; Detrick and Crough, 1978) can not be explained by fracture mechanisms. The heat flux measurements (Sclater et al., 1976), the gravity and geoid anomalies (Watts, 1976; Haxby and Turcotte, 1978) over the Hawaiian Swell can best be explained by a basal heating model (Crough and Thompson, 1976; Detrick and Crough, 1978; Crough, 1978).

Although the fixity of hot-spots is still under debate, the "hot-spot" hypothesis has been widely accepted as the explanation for mid-plate swell and mid-plate volcanism (Willson, 1963a, 1963b; Morgan, 1971, 1972; Clague and Jarrard, 1973; Molnar and Atwater, 1973; Minster et al., 1974; Chase, 1978; Crough, 1978; Detrick and Crough, 1978; Minster and Jordan, 1978; Crough et al., 1980; Lanphere et al., 1980). The linear Hawaiian-Emperor seamount chain is the most well-known example of mid-plate hot-spot

volcanism. According to these hot-spot hypotheses, the thermal energy for the volcanism and the swell is from "hot-spots" located in the deep mantle beneath the lithosphere. If the source of the Hawaiian basalts is in the lithosphere, a basal heating model should first induce partial melting near the base of the lithosphere with subsequent melting proceeding upward to shallower depths. However, field observations show that alkalic basalts, and nephelinitic rocks generally erupt after shield-building tholeiites in the Hawaiian volcanoes (e.g. Powers, 1935, 1955; Tilley and Scoon, 1961; Macdonald and Katsura, 1964; Jackson and Wright, 1970; Beeson, 1976; Clague and Beeson, 1980; Lanphere and Dalrymple, 1980) and experimental studies show that below 30 Kb the nephelinitic rocks and alkalic basalts are generated at greater depth than the tholeiites (e.g. Yoder and Tilley, 1962; O'Hara, 1965; Green and Ringwood, 1967; Kushiro, 1968, 1973). Thus a combination of field observations and high pressure experimental studies suggest that partial melting proceeds to greater depth (Macdonald and Powers, 1968; Jackson and Wright, 1970; Clague and Beeson, 1980) as Hawaiian volcanoes evolve. This downward melting sequence is in conflict with the hot-spot basal heating hypothesis.

This conflict does not preclude a model based on mantle metasomatism, but it does argue against a vertically zoned mantle which with increasing depth has lower $^{87}Sr/^{86}Sr$, higher $^{143}Nd/^{144}Nd$ and is richer in incompatible trace elements.

The shear melting and thermal feedback model proposed by Shaw (Shaw, 1969, 1970b, 1973; Shaw and Jackson, 1973; Jackson and Shaw, 1975; Shaw, 1980) is another alternative explanation for hot-spot volcanism. They showed that under certain shear stress, strain rate and mantle viscosity, the Hawaiian volcanic periodicity can be explained by a shear melting

thermomechanical system. Feigenson and Spera (1980, 1981) further applied the shear melting model and suggested that the observed eruption sequence in Hawaiian volcanoes - i.e. tholeiites, alkalic basalts and melilite-nepheline basalts - can be explained by decreases in the externally imposed shear stress to the source area. In their model, the higher trace-element abundances in the alkalic basalts relative to the tholeiites was attributed to a smaller degree of melting for alkalic basalts, and a homogeneous source composition was assumed. However, for Hawaiian volcanoes which have been studied in detail (e.g. Loihi seamount, Kohala volcano, Haleakala volcano, East Molokai, Koolau volcano), isotopic differences between tholeiites and alkalic basalts are apparent where abundant high-precision isotopic data are available (Chapter 2). This observation also applies to Kohala samples which Feigenson and Spera (1981) used to establish their model since the alkalic basalts they analyzed generally showed lower $^{87}Sr/^{86}Sr$ than the tholeiites (Feigenson and Hofmann, 1980). Because the variations in highly-incompatible trace element abundance ratios (e.g. Th/La, Ta/La, Nb/La, La/Ce) and isotopic ratios in the tholeiites and alkalic basalts cannot be attributed to various degrees of partial melting of a homogenous mantle source (Chapters 2 and 3), a heterogeneous mantle source is required for the Hawaiian basalts. Therefore a shear melting model requires a close correlation between relative time of melting, degree of melting and source composition.

(3) If the different geochemical characteristics of Haleakala basalts result from a metasomatized mantle, this metasomatism may be confined to the lithosphere since most of the evidence for mantle metasomatism comes from studies of upper mantle xenoliths in basalts and kimberlites (e.g., Frey and Green, 1974; Shimizu, 1975; Frey and Prinz, 1978; Chen and Frey,

1980; Menzies and Murthy, 1980a,b; Ottonello, 1980; Stosch and Seck, 1980). Possible processes creating metasomatized lithosphere are uprising melts or fluids from the asthenosphere (e.g., Frey and Green, 1974; Stosch and Seck, 1980; Wright, 1981; Bailey, 1982) and CO_2-rich fluids exsolved from crystallizing melts within the upper mantle (e.g. Bailey, 1982; Roden, 1982).

Melting of lithosphere to generate Hawaiian basalts has previously been proposed (e.g. Detrick and Crough, 1978; Lanphere et al., 1980; Feigenson and Hofmann, 1980; Wright, 1981). However, Bargar and Jackson (1974) estimated that the average volumes for large Hawaiian tholeiitic shields are 20,000 to 30,000 km^3. Based on seismic refraction studies (Shor and Pollard, 1964; Furumoto et al., 1968), Jackson and Wright (1970) estimated an even larger volume (45,000 km^3) for the Koolau shield on the island of Oahu. If Hawaiian tholeiites were generated by 20 per cent partial melting of the mantle source (Ringwood, 1975), 20,000 km^3 to 45,000 km^3 of the tholeiite require partial melting of a 50-km-diameter cylinder 50 km to 100 km in depth underlying the Hawaiian volcanoes. Consequently, most of the underlying lithosphere is required to generate a major Hawaiian tholeiitic shield. If Hawaiian tholeiites were generated by less than 20 per cent partial melting (e.g. Leeman et al., 1977; Feigenson and Spera, 1980, 1981), melting of only lithosphere to generate the Hawaiian tholeiites and alkalic basalts is impossible.

Because of these difficulties a model for Hawaiian basalts based only on partial melting of metasomatized lithosphere seems unsatisfactory. Mixing of at least two components is a simple explanation for inverse trends between the isotopic ratios and parent/daughter ratios (Fig. 4-1, Fig. 4-2) and this model is evaluated below.

2-2 Mixing Model

Plausible mixing processes which may explain the geochemical data for Haleakala basalts are: (1) contamination of Hawaiian basalts by seawater or sediments such as deep-sea carbonates or oceanic crust, (2) mixing of magmas at shallow depth, (3) mixing of magmas or mixing of sources in the mantle. The first hypothesis has already been rejected as a mixing process capable of explaining the isotopic and parent/daughter abundance variations in Haleakala basalts (Chapter 2).

There is little evidence for shallow magma mixing in the Haleakala basalts. Only the ankaramites which contain reversely zoned clinopyroxene and olivine have positive evidences for low pressure mixing (Chapter 1). Moreover, variations of isotopic ratios and highly incompatible element abundance ratios (e.g. La/Ce, Th/La, Nb/La) are correlated with time of eruption rather than extent of differentiation (Chapters 2 and 3). Highly differentiated hawaiites and mugearites have the same range of isotopic ratios (Chapter 2) and highly incompatible element abundance ratios (e.g. La/Ce, Th/La, Nb/La) as less differentiated basalts. Thus, the Haleakala lavas do not have the characteristics expected of magma mixing in an evolving crustal magma chamber (e.g., O'Hara and Mathews, 1981). Finally, as discussed below the geochemical trends of the Haleakala basalts are not consistent with mixing of only two components.

Consequently, the mixing process must occur in the mantle, either by mixing of sources and/or mixing of magmas. Langmuir et al. (1978) discussed equations and diagrams useful for identifying a mixing process and the mixing end-members in a two-component system. On a ratio-ratio plot, data consistent with mixing will lie along a hyperbolic curve for both isotopic and elemental ratios if the denominators for the ratios on the abscissa and

ordinate are not the same. If the denominators are the same, the mixing curves will be linear. However, partial melting may change some trace element abundance ratios; therefore mixing of solids or mixing of melts derived from various degrees of melting of two solids may only be reflected on plots involving ratios of incompatible trace elements and isotopes (Langmuir et al., 1978). Such plots have been made for Haleakala samples (Fig. 4-5a to c). For ratios of highly incompatible elements such as Ba/La, Th/La, Nb/La and Ce/La (Figs. 4-5a to c), the data show negative correlations and suggest possible mixing. Mixing trends are also observed on element abundance ratio vs. isotopic ratio plots (e.g. La/Ce vs. $^{87}Sr/^{86}Sr$, Fig. 4-6 and Chapter 3) and isotopic ratio vs. isotopic ratio ($^{143}Nd/^{144}Nd$ vs. $^{87}Sr/^{86}Sr$, Fig. 4-7) plot. On all these plots, the tholeiites and alkalic basalts from the post-erosional series form the two ends of the mixing trends.

Langmuir et al. (1978) defined a coefficient r which describes the curvature of a mixing line.

$$r = a_1b_2/a_2b_1$$

where a_1 and a_2 are the denominators of the ratios along the ordinate and b_1 and b_2 are the denominators of the ratios along the abscissa (Fig. 4-8). For two-component mixing systems, if a negative slope is observed, the mixing curve will be convex upwards when $r>1$ and convex downward when $r<1$ (Fig. 4-8). For example, on La/Ce vs. $^{87}Sr/^{86}Sr$ plot (Fig. 4-6), the coefficient r = (Ce/Sr) in the post erosional basalt/(Ce/Sr) in the tholeiite. Since the alkalic basalts are more enriched in incompatible trace elements than the tholeiites (Chapter 3), we have r greater than 1 for these Haleakala basalts. However, the observed curvature for Haleakala basalts is not consistent with the predicted curvature (c.f. Figs. 4-6 and

4-8). This suggests that the mixing process is more complicated than simple two-component mixing.

In the following discussion the end-members are inferred for a complex mixing process, then the proposed mixing model is quantitatively evaluated.

(A) Identification of end-members

As mentioned previously, the tholeiites and the youngest post-erosional basalts always define the opposite ends of the mixing trend. Therefore, constraints on the end-member compositions can be obtained from the tholeiites and post-erosional basalts. On $^{143}Nd/^{144}Nd$ vs. $^{87}Sr/^{86}Sr$ plot (Figs. 4-7), the Haleakala basalts plot between the bulk earth and the mid-ocean ridge basalts (MORB). This suggests that the primitive mantle and the MORB source could be the end-members. (In this discussion, mantle with bulk earth Sr and Nd isotopic ratios will be defined as primitive mantle). The average La/Ce ratio for the tholeiites is 0.38 which is very close to the value for chondrites and the primitive mantle (Haskin et al., 1968; Wood et al., 1979c; Sun et al., 1979) and consistent with the hypothesis that primitive mantle could be one end-member. Based on the observations that Hawaiian basalts have higher $^{143}Nd/^{144}Nd$ and lower $^{87}Sr/^{86}Sr$ ratios than the primodial mantle, Hofmann and White (1982) suggested that Hawaiian basalts were not generated from primordial mantle plumes. They proposed a model whereby ancient subducted oceanic crusts is a source instead of the primitive mantle. However, their arguments may not be valid if mixing was an important process in creating Hawaiian basalts. Moreover, the unusually high $^{3}He/^{4}He$ values in Hawaiian basalts (Kaneoka and Takaoka, 1980; Kurz, 1982a) is not consistent with ancient oceanic crust as an important component in Hawaiian basalts. In contrast, a primitive mantle component

as one end-member is consistent with the high $^{3}He/^{4}He$ ratios in Hawaiian basalts.

The isotopic ratios and trace element compositions of the post-erosional basalts suggest that the second end-member had $^{87}Sr/^{86}Sr$ and $^{143}Nd/^{144}Nd$ ratios close to mid-ocean ridge basalts but with higher La/Ce, La/Sm and Nb/La ratios and higher abundances of incompatible trace elements than the primitive mantle (Chapter 3). Incipient melts (<1% melting) from a MORB-type source are the most likely candidates for these isotopic and trace-element characteristics. Based on helium and strontium isotopic ratios, Kurz et al. (1982a) suggested that the MORB source and primitive mantle were mixing end-members for generating Hawaiian basalts. On a $^{3}He/^{4}He$ vs. $^{87}Sr/^{86}Sr$ plot, they estimated that the curvature coefficient (r) is greater than 1 where r = (He/Sr) in the MORB end-member/(He/Sr) in the primitive mantle. A high (He/Sr) abundance ratio in the MORB end-member also requires that this end member be a melt derived from very small degree partial melting of MORB source rather than the MORB source itself and is consistent with our hypothesis. We propose that the sources of Haleakala basalts are mixtures of a primitive mantle composition with varying amounts of incipient melt derived by partial melting of a MORB-type source. This model can be tested quantitatively.

(B) Quantitative Evaluation of the Proposed Mixing Model

The primitive mantle composition and normal MORB source composition used in our model calculations are listed in Table 4. The primitive mantle composition is assumed to be about twice the abundances in chondrites except for Rb. The REE abundances for chondrites are taken from Haskin et al. (1968) for a chondrite composite and other chondritic values are from average values of L-chondrites from Mason (1979). The Rb abundance for

primitive mantle is estimated from average bulk earth $^{87}Rb/^{86}Sr$ ratio (Table 1) and Sr abundance. The estimated primitive mantle composition is very similar to that estimated by Wood et al. (1979c) except for Nb (Table 4). Their Nb abundance in primitive mantle was calculated for Archaean mantle (Sun and Nesbitt, 1977). The difference between these estimated Nb values is about 30 per cent. The $^{87}Sr/^{86}Sr$ value (0.7047) and $^{143}/Nd/^{144}Nd$ (0.51265) for the primitive mantle is the average value of present-day bulk Earth estimates (DePaolo and Wasserburg, 1976a,b; O'Nions et al., 1977; Allegre et al., 1979; Jacobsen and Wasserburg, 1979).

The range of "normal" MORB compositions were compiled from the literature (Frey et al., 1974; Hart, 1976; White and Schilling, 1978; Bougault et al., 1979; Sun et al., 1979) and the average values are used to estimate the source composition assuming that MgO-rich MORBS ($Mg/Mg+Fe^{2+}$ > 0.66, White and Schilling (1978)) were derived by 15% melting (Fig. 4-9). The estimated MORB source compositions fall between the "limits" of MORB source estimated by White and Schilling (1978). These limits of MORB source were estimated from most-primitive (Mg# >0.66) MORB with degrees of melting between 10% and 30% and mantle mineral assemblages of olivine 45-75%, orthopyroxene 15-40%, clinopyroxene 0-25%, garnet 0-15% and plagioclase 0-10%. The MORB source composition used in the model only affects the calculated proportions of the end-members and not the trace-element abundances calculated for the sources of Hawaiian basalts. The $^{87}Sr/^{86}Sr$ and $^{143}Nd/^{144}Nd$ ratios for the MORB source are assumed to be the same as the most depleted MORB (AD-3) reported by O'Nions et al. (1977).

Mixing relations between incipient melts from the MORBS and the primitive mantle are constructed on a La/Ce vs. $^{87}Sr/^{86}Sr$ plot (Fig. 4-10).

The diagram shows that the alkalic basalts and tholeiites from the Haleakala volcano can be derived from sources which are mixtures of 96% to 99% primitive mantle and 1% to 4% of melts formed by 0.1% to 1% partial melting of a MORB source.

Three samples (C122, H65-4, and H65-11) from Haleakala were selected to further evaluate this model. The stratigraphic positions of these samples are indicated in Figures 4-11 and Figure 4-12. These three samples fall within the isotopic and trace element abundance variation trends (e.g. Figs. 4-11 and 4-12) and are representative samples from Haleakala. Sample C122 is from the tholeiitic series, with a Mg number of 73 and MgO content of 16.6% (Chapter 1). If this sample represents melt it was in equilibrium with olivine composition of Fo_{88} to Fo_{90} for K_d between 0.36 and 0.29 (Roeder and Emslie, 1970; Longhi et al., 1978; O'Hara et al., 1975; Arndt, 1977; Irvine, 1977). Samples H65-4 and H65-11 are from alkalic series and post-erosional series, respectively. These two samples with Mg-number of 54 and 59, respectively are among the least-fractionated alkalic basalts in the Haleakala volcanic series (Chapter 1). Olivine in equilibrium with such melts would have the compositions of Fo_{78} to Fo_{84}. Based on the olivine inclusions in Hawaiian basalts the olivine composition in the mantle is commonly estimated to be around Fo_{85} to Fo_{92} (e.g., Ross et al., 1954; White, 1966; Kuno, 1969); therefore the tholeiitic sample could be close to primitive melt, and no correction was made for fractionation. However, trace element abundances for the two alkalic basalts, H65-4 and H65-11, were corrected for 25% and 21% olivine fractionation. These corrections are first order approximations and assume only olivine as a fractionating phase from a parental melt with 16.6% MgO (Chapter 1).

The model has been tested to see if it can account for the variations in isotopic ratios ($^{87}Sr/^{86}Sr$ and $^{143}Nd/^{144}Nd$) and abundances of the incompatible trace elements Rb, Ba, Th, Ta, Nb, La, Ce, Sr, Nd and Sm. Abundances of less incompatible trace elements such as Yb and Lu were not calculated because these elements are very sensitive to the mantle mineralogy assumed and the partition coefficients chosen. Partition coefficients for Rb, Ba, Th, Ta, Nb, La, Ce, Sr, Nd and Sm used in the calculations are listed in Table 3. I have assumed a mantle composed of 60% olivine, 25% orthopyroxene, 10% clinopyroxene and 5% garnet (Clague and Frey, 1982) and used the non-modal equilibrium partial melting equation derived by Shaw (1970a). The melting proportions of the constituent minerals were assumed to be (olivine:orthopyroxene:clinopyroxene:garnet) = (10%:10%:40%:40%) (Davis and Schairer, 1965; Kushiro, 1968, 1969; Leeman et al., 1977; Frey et al., 1978).

It is likely that the source may also contain accessory phases such as phlogopite, amphibole and apatite, but these phases are assumed to be eliminated by the melting process. Linear correlation of P_2O_5, K and Rb with highly incompatible trace elements such as La and Ce in the fresh Haleakala samples support the conclusion that apatite, phlogopite or amphibole were not in the mantle residue (Chapters 1 and 3). Detailed predictions of the model are dependent on the chosen partition coefficients, initial mode and melt mode but the general applicability of the model is not dependent upon these parameters.

The degree of melting of the MORB source and the proportions of the two end-members (partial melts from a MORB source and a primitive mantle source) for the sources of Haleakala basalts can be estimated from the La/Ce ratios and $^{87}Sr/^{86}Sr$ ratios of the basalts (Fig. 4-10). The source

of the tholeiite (C122) was estimated to be a mixture of 1.7% of melt derived by 1% partial melting of a MORB source and 98.3% primitive mantle source. The source of an alkalic basalt (H65-4) from the alkalic series was estimated to be a mixture of 2.5% melt formed by 0.25% partial melting of a MORB source and 97.5% primitive mantle source. The source for a post-erosional alkalic basalt (H65-11) was estimated to be a mixture of 3.3% melt derived by 0.2% partial melting of a MORB source and 96.7% primitive mantle source (Fig. 4-10).

The trace element abundances (Ba, Rb, Th, Ta, Nb, La, Ce, Sr, Nd, Sm) of melts derived by 1%, 0.25% and 0.2% melting of the MORB source (Table 3) were calculated and the source compositions for the tholeiite and alkalic basalts were then estimated using the end-member compositions and proportions of the end-members derived from Figure 4-10. The calculated trace element abundances (Ba, Rb, Th, Ta, Nb, La, Ce, Sr, Nd, Sm) and isotopic compositions ($^{87}Sr/^{86}Sr$ and $^{143}Nd/^{144}Nd$) of these mixed sources are listed in Table 5 and shown in Figure 4-13. The calculated source for the Hawaiian tholeiite has a flat trace element distribution pattern when the trace element abundances in the source are normalized to the abundances in the primitive mantle whereas the calculated sources for the alkalic basalts have strongly convex upwards trace-element distribution patterns except for Ba (Fig. 4-13). These sources are enriched in Ba and light-REE relative to the primitive mantle or chondrites but are relatively depleted in Rb, Th and Ta (Fig. 4-13).

The La and Ce concentrations in the selected samples and their calculated sources can be used to determine the degrees of partial melting (F) required to generate the basalts by non-modal equilibrium partial melting (Shaw, 1970a). The assumed source mineralogy and proportions of

mineral phases in the melts were as discussed previously. These calculations show that the tholeiite (C-122) can be derived by 16% partial melting and the alkalic basalts by 12% (H65-4) and 16% (H65-11) partial melting from their respective calculated sources.

Trace element abundances (Ba, Rb, Th, Ta, Nb, La, Ce, Sr, Nd, Sm) in these derived melts were determined by using these F values and the source compositions (Table 5). The measured and calculated trace element abundances and isotopic ratios are listed in Table 6 and the comparison serves as a quantitative test for the adequacy of the mixing model. The calculated and measured $^{87}Sr/^{86}Sr$ ratios and $^{143}Nd/^{144}Nd$ ratios are within the experimental uncertainties. The difference between the calculated and measured trace element abundances are less than 25 per cent for all the elements and generally better than 10% (Fig. 4-14). Two-pairs of Nd and Sm concentrations are listed in Table 6. They are calculated based on partition coefficient set 1 of Frey et al. (1978) and partition coefficients reported by Harrison (1981) (Table 3). These pairs of partition coefficients are among the lowest and highest partition coefficients reported for Nd and Sm in garnet. Nd abundances calculated using the lower partition coefficients (Frey et al. 1978) are in very good agreement with the measured abundances (better than 5%, Table 6 and Fig. 4-14). However, Nd abundances calculated using higher partition coefficients (Harrison, 1981) are within 16% of the measured values. The measured Sm abundances are intermediate between the values calculated using the two pairs of partition coefficients and values calculated using both pairs of partition coefficients are within 16% of the measured values (Table 6 and Fig. 4-14).

The normalized distribution patterns of the tholeiites and the alkalic basalts mimic the normalized distribution pattern of their source (compare Fig. 4-13 with Fig. 4-15). Except for Ba, the tholeiite has flat or slightly convex upwards distribution patterns whereas the alkalic basalts have strongly convex upwards distribution patterns (Fig. 4-15). The alkalic basalts (e.g. H65-11) from the post-erosional volcanic series has lower Ce, Sr, Nd, Sm abundances, similar La, Nb, Ta, Rb abundances but higher Ba abundance than the alkalic basalts (e.g. H65-4) from the alkalic volcanic series. This kind of crossing normalized trace-element distribution pattern (crossing at light-REE) cannot be derived from various degrees of partial melting from a homogeneous mantle source because Ba, Rb, Th, Ta, Nb, La Ce, and Sr are all highly incompatible trace elements. The proposed mixing model reproduces the crossing trace element distribution patterns for the two alkalic basalts (Fig. 4-15). In conclusion, this quantitative evaluation of the mixing model reproduces very well the trace-element (Ba, Rb, Th, Ta, Nb, La, Ce, Sr, Nd, Sm) abundances and the isotopic ratios ($^{87}Sr/^{86}Sr$ and $^{143}Nd/^{144}Nd$) of the Haleakala tholeiites and alkalic basalts. In Chapter 3, we noticed a post-erosional alkalic basalt (H62-47) which has a lower $^{87}Sr/^{86}Sr$ ratio but similar highly incompatible element abundance ratios (e.g. Ba/La, Nb/La, La/Ce) when compared to other post-erosional alkalic basalts. Figure 4-10 shows that a slightly higher proportion of incipient melt in the lavas or source can produce slightly lower $^{87}Sr/^{86}Sr$ ratio but similar La/Ce ratio in the basalt.

3. Discussion

The proposed mixing model for the origin of Haleakala tholeiites and alkalic basalts is unique among the petrogenetic models previously proposed for ocean island tholeiites and alkalic basalts. In addition to primitive

mantle as one end-member, melts formed by low melting degrees of a MORB source are identified as the end-member which has the high incompatible trace element abundances. In order to explain the high trace element abundances of ocean island tholeiites and alkalic basalts relative to mid-ocean ridge basalts, previous models have proposed sediments, ancient oceanic crust (Hofmann and White, 1982), altered oceanic crust (e.g. Wright, 1981), metasomatized upper mantle (e.g. Anderson, 1982), enriched wall-rocks (Allegre and Bottinga, 1974), or pyroxenite veins (Hanson, 1977) as the source material or end-member which has high trace element abundances. Basalts derived from these previously proposed sources or end-members would have concordant variations of trace element abundances and isotopic ratios, i.e. the samples with higher trace element enrichments such as Rb/Sr, Nd/Sm and La/Ce would have the same $^{87}Sr/^{86}Sr$ or higher $^{87}Sr/^{86}Sr$ ratios and the same $^{143}Nd/^{144}Nd$ or lower $^{143}Nd/^{144}Nd$ ratios than the samples with lower trace element enrichments. However, Haleakala tholeiites and alkalic basalts have inverse trends between parent/daughter abundance ratios and isotopic ratios (Chapter 2, and Figs. 4-1, 4-2, 4-6).

Such negative correlations between parent/daughter abundance ratios and isotopic ratios is common among the Hawaiian basalts. For example, basalts from Loihi seamount (Staudigel et al., 1981, Frey and Clague, 1982; Lanphere, 1982), Koolau volcano on the island of Oahu (Lanphere and Dalrymple, 1980; Roden et al., 1981; Clague and Frey, 1982) and the East Molokai volcano (Clague and Beeson, 1980; Clague, personal communication) also show an inverse relation between isotopic ratios and parent/daughter abundance ratios and between $^{87}Sr/^{86}Sr$ and La/Ce ratios (e.g. Fig. 4-16). The two end-members of proposed mixing model, i.e. the incipient melts from a MORB source and the primitive mantle, have the compositional

characteristics which can generate the observed inverse relationship between the isotopic variations and trace element enrichments (e.g. $^{87}Sr/^{86}Sr$ vs. Rb/Sr, $^{143}Nd/^{144}Nd$ vs. Sm/Nd, $^{87}Sr/^{86}Sr$ vs. La/Ce) for the Hawaiian tholeiites and alkalic basalts.

The MORB source compositions in our model were calculated assuming that primitive MORB were derived by about 15% partial melting (White and Schilling, 1978; Wood et al., 1979c). If the primitive MORB were derived by greater than 15% partial melting, the estimated trace element abundances of MORB source is increased and the estimated proportions of IM (incipient melt from the MORB source) to PM (primitive mantle) are decreased accordingly. For example, if MORB were derived by about 25% partial melting of MORB source, the estimated proportions of IM:PM would be 1:99, 1.5:98.5 and 2:98, instead of 1.7:98.3, 2.5:97.5 and 3.3:96.7 (Table 5) for the source of tholeiite (C122), alkalic basalt from the alkalic series (H65-4) and alkalic basalt from the post-erosional series (H65-11), respectively.

In our calculation we have assumed that the partial melts from a MORB source mixed and equilibrated with the four-phase (olivine + orthopyroxene + clinopyroxene + garnet) primitive mantle to form the sources of the Hawaiian basalts. This may seem to imply that the primitive mantle remains solid until the mixing process is completed. However, this is not a pre-requisite of the model. Our calculated results will be valid if the partial melt from a MORB source mixed with a partially molten primitive mantle as long as the bulk system was in equilibrium. Hofmann and Hart (1978) have shown that melt is a very efficient short circuit for local equilibration, therefore equilibrium melting is a plausible melting process in the mantle.

These mixing calculations also apply for magma mixing. For example, in our calculations, sample C122 (tholeiite) can be generated by 16% partial melting of a source which was a mixture of 1.7% IM and 98.3% primitive mantle (Table 5 and 6). Since the IM enters completely into the final melt (C-122), the partial melt from the MORB source would contribute about 10% to the final melt and the melt from the primitive mantle (MPM) would contribute about 90% to the final melt. Therefore, by mixing two magmas IM and MPM, where IM is the melt derived by 1% melting of the MORB source and MPM is the melt derived by about 14% partial melting of a primitive mantle, in the proportion of 10 IM to 90 MPM produces a melt with the trace element compositions and isotopic ratios equal to our calculated compositions for C122. The proportions of IM to MPM to generate the alkalic basalts in the same manner are about 22 to 78 and 21 to 79 (Table 7). Thus, both mixing mechanisms can generate the variations in trace element abundances and isotopic ratios observed in Hawaiian basalts.

Common features of these two mixing mechanisms are

(1) both processes require a MORB source and a primitive mantle source.

(2) the proportion of MORB source and primitive mantle source required in both processes is the same. If the primitive MORB were generated by 25% partial melting and if the primitive mantle contains about 2 times chondrites in trace element abundances, the proportion of MORB source to primitive mantle source is about 1:1, 6:1 and 10:1 to generate the end-members for tholeiites, alkalic basalts from alkalic series and alkalic basalts from post-erosional series, respectively.

(3) both mechanisms require the MORB source to have undergone small degrees (0.1% to 1%) of partial melting and the primitive mantle source to have undergone large degrees (12%-16%) of partial melting.

(4) the partial melts from the MORB source contribute about 10% in the tholeiitic melts and about 20% in the alkalic melts for both mixing mechanisms.

(5) the proportions of primitive mantle material to partial melts from MORB source decreased as the volcano evolved from tholeiitic stage to the post-erosional stage.

(6) the ratios of primitive mantle material to IM are higher for the alkalic basalts erupted in the initial stage of the volcano (Loihi) than the alkalic basalts erupted after the shield building stage (Fig. 4-16).

(7) Incipient melts of ocean crust have the same isotopic ratios and highly incompatible trace element abundance ratios (e.g. La/Ce, Nb/La, Ba/La, Rb/Sr, Nd/Sm) as incipient melts from a MORB source. However, the volume of oceanic crust, required by the mixing models exceeds the volume of oceanic crust available. Moreover, melting of oceanic crust is not consistent with seismic velocity, heat flow measurements and gravity anomalies over the Hawaiian islands (Ellsworth, 1977; Crough, 1978; Detrick and Crough, 1978). Thus the ocean crust is ruled out as an end-member of the mixing model.

Numerical calculations (Allegre et al., 1979; Jacobsen and Wasserburg, 1979; DePaolo, 1980; Allegre et al., 1982) showed that the lower mantle is relatively primitive and more than one-third of the Earth's mantle may be depleted like a MORB-type source. Thus, the two end-members required in the mixing model are abundant and such mixing may be a common occurrence.

In this case we might expect other examples where tholeiitic basalt has higher $^{87}Sr/^{86}Sr$ and lower $^{143}Nd/^{144}Nd$ than associated alkalic basalt which has higher Rb/Sr and lower Sm/Nd. For Nd isotopes there are too few data for geographically associated samples to evaluate this prediction, but there are several areas where basalts have an inverse correlation between Rb/Sr and $^{87}Sr/^{86}Sr$; for example, Nunivak Island in the Bering Sea is another oceanic sample (Menzies and Murthy, 1980b; Roden, 1982) and continental basalt examples include the Rio Grande Rift (Lipman and Mehnert, 1975; Crowley and Giletti, 1982) the Afar volcanics, Ethiopia (Barbari et al., 1980), and eastern China (Zhou and Armstrong, 1982). Consequently, the model proposed here may have general applicability for some oceanic and continental basalt suites. We further note that a positive correlation between Rb/Sr and $^{87}Sr/^{86}Sr$ results from the model when the degree of melting of the MORB source exceeds 1-2% (Fig. 4-16).

In the following, we adopt a two-layer mantle hypothesis and propose a mantle model to explain Hawaiian volcanism. The steps we envision are:

(1) Primitive mantle plumes rise from the lower mantle and the upwelling primitive mantle plumes become partially molten due to decompression.

(2) Heat from the upwelling mantle plumes is transferred to the MORB source which are wall-rocks and induces the partial melting (0.1% to 1%) of these wall-rocks. These melts from the wall-rocks mix with the upwelling plumes. The estimated volume of Hawaiian tholeiitic shields (Bargar and Jackson, 1974), our calculated ratios of MORB source to primitive mantle and degrees of partial melting required to derive the tholeiites suggest that the lower lithosphere and asthenosphere underneath the Hawaiian Emperor chain must undergo partial melting. Crough (1978) and Detrick and Crough (1978) have suggested that the

heat flow measurements and gravity anomalies over the Hawaiian swells can best be explained if the lower lithosphere has experienced partial melting. Three dimensional inversion of P-wave travel times show that a localized low velocity zone continues from the asthenosphere into the lithosphere below the island of Hawaii (Ellsworth, 1977). Our calculations are consistent with these geophysical observations.

(3) In the early stages of Hawaiian volcanism (e.g. Loihi seamount) only a a small degree of partial melting (<1%) occurred in the wall-rocks and the basalts are composed of large proportions of primitive mantle material (Fig. 4-16). During the shield building stage of volcanism, the volcano may be directly over the hot-spot, and the degrees of partial melting in both the primitive mantle plumes (~16%) and the wall-rocks (~1%) are the largest among all the evolutional stages of the volcano. The basalts generated at this stage are tholeiitic, composed of 10% incipient melts from the MORB source wall-rocks and 90% partial melt from the mantle plumes. Because these tholeiites contain the highest proportion of primitive material (Table 7) they have higher $^{3}He/^{4}He$ ratios (Kurz, 1982a), higher $^{87}Sr/^{86}Sr$ ratios, lower $^{143}Nd/^{144}Nd$ and lower incompatible element abundances than the alkalic basalts.

After the shield building stage, the volcano moves gradually away from the hot-spot and the supply of primitive plume material and heat decreases. At this stage the eruption frequency decreases, the degrees of partial melting in the plume and the wall-rocks decreases and the relative contribution of the plume type material to the basalts is decreased. Basalts erupted at this stage are alkalic basalts. Finally, during the terminal stages of the volcanism, the plume supply

decreases rapidly. The contributions of plume material to the melts become even less than in the alkalic stage and the melts became nephelinitic.

Tholeiites from Suiko Seamount, central Emperor Ridge, have the lowest $^{87}Sr/^{86}Sr$ observed in Hawaiian tholeiites (Lanphere et al., 1980); consequently they contain the largest amount of melt derived from a MORB source (Fig. 4-16). Lanphere et al. (1980) noted that Suiko Seamount formed on younger oceanic crust than currently active Hawaiian volcanoes. Possibly, the thermal regime beneath younger crust enables a larger proportion of MORB source melt to mix with the upwelling primitive mantle.

(4) The magmas possibly segregated from their sources at a depth of about 40 km to 60 km which might be marked by the focal depth of the deepest earthquakes beneath Hawaii (Eaton, 1962; Koyanagi and Endo, 1971; Unger and Ward, 1979; Butler, 1982). Magmas are transported to a shallower reservoir (2-6 km) below the volcano (Eaton, 1962; Koyanagi et al., 1976). Crystal fractionation occurs during magma transport and in the shallow reservoir (e.g. Wright, 1971) prior to eruption of magmas.

This mantle model can explain the trace element (e.g. Ba, Rb, Th, Ta, Nb, La, Ce, Sr, Nd, Sm) abundances and isotopic ($^{87}Sr/^{86}Sr$, $^{143}Nd/^{144}Nd$ and $^{3}He/^{4}He$) variations of the Hawaiian tholeiites and alkalic basalts and is consistent with the field observations (e.g. Macdonald, 1968), and geophysical and tectonic studies (e.g. Eaton, 1962; Wilson, 1963a,b; Morgan, 1971, 1972; Koyanagi et al., 1976; Ellsworth, 1977; Detrick and Crough, 1978; Crough, 1978; Shaw, 1980) of Hawaiian volcanism.

4. Conclusions

Trace element abundances (Ba, Rb, Th, Ta, Nb, La, Ce, Sr, Nd, Sm) and isotopic variations (e.g. $^{87}Sr/^{86}Sr$, $^{143}Nd/^{144}Nd$, $^{3}He/^{4}He$) of the Hawaiian tholeiites and alkalic basalts can be best explained by a mixing model. The mixing end-members are identified to be (IM) partial melts derived from various degrees of partial melting of a MORB source wall-rock and primitive mantle plumes rising from lower mantle. The mixing process can be mixing of IM with partially molten primitive mantle plumes to form the sources of Hawaiian basalts, or, mixing of IM with melts derived by large degrees (12%-16%) of partial melting of the primitive mantle plumes. The contribution of the primitive mantle material to the basalts decreases as volcanoes evolve, and the magmas become more alkalic and more enriched in incompatible trace elements. Our mixing model is also consistent with field observations and geophysical studies of Hawaiian volcanism. An important implication of the model is that the large size, 20-30,000 km^3, of many Hawaiian volcanoes (Bargar and Jackson, 1974) and the degrees of melting that we infer for the mixing components requires that the entire lower lithosphere and much of the asthenosphere beneath a Hawaiian volcano must be involved in its creation. The proposed mixing model may have general applicability for some oceanic and continental basalts which show inverse trends of parent/daughter abundance ratios and isotopic ratios.

Table 1. Rb-Sr and Nd-Sm Parameters Used in the Depletion-Enrichment Age Estimates

	Bulk Earth	MORB (AD-3)	C122[8]	H65-4[8]	H65-14[8]
$(^{87}Sr/^{86}Sr)^{o}$	0.69877[1]	-	-	-	-
$(^{87}Sr/^{86}Sr)$present day	0.7047[2]	0.7023	0.70387	0.70338	0.70319
$^{87}Rb/^{86}Sr$	0.0888[3]	0.0326	0.0575	0.0933	0.1032
$(^{143}Nd/^{144}Nd)^{o}$	0.50679[4]	-	-	-	-
$(^{143}Nd/^{144}Nd)$present day	0.51265[5]	0.51329	0.51291	0.51301	0.51309
$(^{147}Sm/^{144}Nd)$	0.1930[6]	0.217	0.191	0.141	0.150

[1]Minster et al., 1979.

[2]Average value of present-day Bulk Earth estimates (DePaolo and Wasserburg, 1976a,b; O'Nions et al., 1977; Allegre et al., 1979).

[3]Calculated from single stage evolution of $(^{87}Sr/^{86}Sr)_{o}$ at 4.55 b.y. to present-day $(^{87}Sr/^{86}Sr)$.

[4]Average of initial $(^{143}Nd/^{144}Nd)$ values for Juvinas and Angrados Reis at 4.55 b.y. (Lugmair et al., 1975; Lugmair and Marti, 1977).

[5]Average value of present-day Bulk Earth estimates (DePaolo and Wasserburg, 1976a,b, O'Nions et al., 1977; Allegre et al., 1979; Jacobsen and Wasserburg, 1979).

[6]Calculated from single stage evolution of $(143Nd/144Nd)_{o}$ at 4.55 b.y. to the present-day $(^{143}Nd/^{144}Nd)$.

[7]The most depleted mid-ocean ridge basalt (O'Nions et al., 1977)

[8]This study.

Table 2. Ages of Enrichment-depletion Events Calculated From Rb-Sr and Nd-Sm Isotopic Systems

		MORB (AD-3)	Tholeiitic Series (C122)	Alkalic Series (H65-4)	Post-erosional Series (H65-14)
Case 1:	$*t_d^{Rb-Sr}$	2.96 b.y.	2.96 b.y.	2.96 b.y.	2.96 b.y.
	$*t_e^{Rb-Sr}$	-	4.3 b.y.	1.2 b.y.	0.88 b.y.
	$**t_d^{Nd-Sm}$	4.2 b.y.	4.2 b.y.	4.2 b.y.	4.2 b.y.
	$**t_e^{Nd-Sm}$	-	2.2 b.y.	0.56 b.y.	0.46 b.y.
Case 2:	t_d^{Rb-Sr}	2.8 b.y.	2.8 b.y.	2.8 b.y.	2.8 b.y.
	t_e^{Rb}	-	4.7 b.y.	1.5 b.y.	1.1 b.y.
	t_d^{Nd-Sm}	2.7 b.y.	2.7 b.y.	2.7 b.y.	2.7 b.y.
	t_e^{Nd-Sm}	-	2.1 b.y.	0.52 b.y.	0.42 b.y.
Case 3:	t_d^{Rb-Sr}	2.8 b.y.	1.4 b.y.	2.5 b.y.	2.8 b.y.
	t_e^{Rb-Sr}	-	1.1 b.y.	1.1 b.y.	1.1 b.y.
	t_d^{Nd-Sm}	2.7 b.y.	1.3 b.y.	2.3 b.y.	2.7 b.y.
	t_e^{Nd-Sm}	-	0.42 b.y.	0.42 b.y.	0.42 b.y.

$*t_{d \text{ or } e}^{Rb-Sr}$: calculated age of depletion or enrichment event based on Rb-Sr system.

$**t_{d \text{ or } e}^{Nd-Sm}$: calculated age of depletion or enrichment event based on Nd-Sm system

Table 3. Partition Coefficients

	Cpx	Opx	Ol	Gart	Data Sources
La	0.02	0.0005	0.0005	0.001	(3)
Ce	0.04	0.0009	0.0008	0.0033	(3)
Sr	0.072	0.0002	0.0005	0.007	(1,2,4)
Nd	0.09	0.0019	0.0013	0.0184	(3)
				0.10	(5)
Sm	0.14	0.0028	0.0019	0.08	(3)
				0.32	(5)

Ba and Rb bulk solid/liquid P.C. assumed to be zero (4). Th, Ta, Nb bulk solid/liquid P.C. assumed to be 0.001.

[1]Philpotts et al., 1972

[2]Hart and Brooks, 1974

[3]Frey et al., 1978

[4]Zindler, 1980

[5]Harrison, 1981

Cpx: clinopyroxene
Opx: orthopyroxene
Ol: olivine
Gart: garnet

Table 4. Estimated Trace Element Abundances (ppm) and Isotopic Ratios in the Normal-MORB Source and Primordial Mantle

	Normal[1] MORB Source	Primitive[2] Mantle	Primitive[3] Mantle
Ba	2.0	8.0	7.56
Rb	0.1	0.73	0.86
Th	0.02	0.086	0.096
Ta	0.016	0.049	0.043
Nb	0.31	0.86	0.62
La	0.31	0.71	0.71
Ce	0.95	1.90	1.90
Sr	13.2	23.7	23
Nd	0.86	1.2	1.29
Sm	0.32	0.39	0.385
*$^{87}Sr/^{86}Sr$	0.7023	0.7047	
*$^{143}Nd/^{144}Nd$	0.5133	0.51265	

*from Table 1

[1]Averge compositions of normal mid-ocean ridge basalts were compiled from data given by Frey et al. (1974), Hart (1976), Sun and Nesbitt (1977) White and Schilling (1978), Bougault et al. (1979), Sun et al. (1979), Wood et al. (1979c). Primitive MORB can be generated from this MORB source by about 15% partial melting.

[2]The primitive mantle compositions are estimated to be approximately 2.15 times the abundances in chondrites except for Rb which is estimated from average bulk earth $^{87}Rb/^{86}Sr$ ratio (in Table 1) and Sr abundance. The chondritic values are from Mason (1979), Haskin et al. (1968), compiled by Clague and Frey (1982).

[3]Primitive mantle compositions estimated by Wood et al. (1979c).

Table 5. Estimates of Source Compositions (ppm) for Haleakala Volcanic Series

	Tholeiitic series	Alkali series	Post-erosional series
Ba	11.26	27.8	40.74
Rb	0.89	1.72	2.38
Th	0.12	0.23	0.31
Ta	0.073	0.16	0.23
Nb	1.32	3.06	4.40
La	1.12	2.26	3.01
Ce	2.96	5.11	6.50
Sr	35.98	55.32	67.96
Nd	1.88^{+},$1.78^{\#}$	2.77^{+},$2.39^{\#}$	3.37^{+},$2.85^{\#}$
Sm	0.57^{+} $0.52^{\#}$	0.75^{+},$0.62^{\#}$	0.87^{+},$0.70^{\#}$
$^{87}Sr/^{86}Sr$	0.70387	0.70331	0.70312
$^{143}Nd/^{144}Nd$	0.51289	0.51301	0.51307
$^{*}f(MORB)$	1%	0.25%	0.2%
$^{**}IM:PM$	1.7:98.3	2.5:97.5	3.3:96.7
$^{***}IM:PM$	1:99	1.5:98.5	2:98

*degree of partial melting of MORB-type source.

**IM = incipient melt from MORB source. The MORB source compositions are listed in Table 4 and MORB reflect ~15% melting of this source. PM = primitive mantle.

***The MORB source compositions were estimated by assuming that MORB derived by 25% partial melting of MORB source.

+Partition coefficent for garnet from set 1, Frey et al., (1978).

#Partition coefficient for garnet from Harrison (1981).

Table 6. Measured and Calculated Trace-element Abundances for Tholeiites and Alkalic Basalts From Haleakala Volcanic Series

	Tholeiitic Series (C122)		Alkalic Series (H65-4)*		Post-erosional series (H65-11)*	
	Measured	Calculated	Measured	Calculated	measured	Calculate
Ba	57	72	262	241	309	254
Rb	4.61	5.7	14.9	14.9	14.9	14.9
Th	0.8	0.73	1.6	1.96	2.1	1.91
Ta	0.51	0.46	1.56	1.40	1.6	1.4
Nb	7.2	8.3	25.0	26.3	24.5	27.3
La	7.1	7.1	19.4	19.4	18.7	18.7
Ce	18.8	18.6	43.5	43.3	40.0	40.1
Sr	207	225	462	463	459	417
Nd	12.3	$11.7^{+}, 11.1^{\#}$	23.0	$22.8^{+}, 19.6^{\#}$	20.9	$20.5^{+}, 17.5^{\#}$
Sm	3.7	$3.5^{+}, 3.3^{\#}$	5.13	$5.97^{+}, 4.93^{\#}$	4.75	$5.28^{+}, 4.32^{\#}$
$^{87}Sr/^{86}Sr$	0.70387	0.70387	0.70334	0.70331	0.70314	0.70312
$^{143}Nd/^{144}Nd$	0.51291	0.51289	0.51301	0.51302	0.51310	0.51307
F	16%		12%		16%	

*Trace-element abundances have been corrected for fractionation
+Partition coefficient for garnet from set 1 (Frey et al., 1978)
#Partition coefficient for garnet from Harrison, (1981).

Table 7. Comparison of Sources Mixing and Magmas Mixing

	C122	H65-4	H65-11
	(I) Mixing of Sources		
IM:PM	1.7:98.3	2.5:97.5	3.3:96.7
f	1%	0.25%	0.2%
F	16%	12%	16%
	(II) Mixing of Magmas		
IM:MPM	10:90	22:78	21:79
f	1%	0.25%	0.2%
F'	14%	9%	13%

IM = incipient melt derived by f degree of partial melting of MORB source

F = degree of partial melting the mixed source

F' = degree of partial melting the primitive mantle source

PM = primitive mantle

MPM = melt from the primitive mantle by F' degree of partial melting

The MORB source compositions were calculated assuming that the primitive MORB were derived by 15% partial melting of the MORB source.

Figure 4-1: Correlation of $^{87}Sr/^{86}Sr$ ratios with Rb/Sr ratios for Haleakala basalts (hawaiites and mugearites not included)

□ = tholeiites from Honomanu volcanic series

Δ = alkalic basalts from Kula volcanic series

* = alkalic basalts from post-erosional, Hana volcani series

Tholeiites circled in left diagram contain olivine with altered rims and slightly altered glass, and we interpret the extremely low Rb/Sr ratios as a result of alteration.

Figure 4-2: Correlation of $^{143}Nd/^{144}Nd$ ratios with Sm/Nd ratios for Haleakala basalts. Symbols as in figure 4-1.

Figure 4-3: $^{143}Nd/^{144}Nd$ evolution diagram for the sources of basalts from the thoeliitic series, alkalic series and post-erosional series, Haleakala volcano on east Maui, showing three-stage evolution models. t_d is the age when the Haleakala mantle source became depleted (higher Sm/Nd) relative to bulk Earth composition. t_e^{th}, t_e^{alk} and t_e^{post} are the metasomatic ages when the mantle sources for basalts of the tholeiitic series, alkalic series and post-erosional series, respectively, experienced metasomatism. See text for discussion. Data shown for case 2 of Table 2.

Figure 4-4: (a) $^{143}Nd/^{144}Nd$ evolution diagram for the sources of Haleakala basalts.

(b) $^{87}Sr/^{86}Sr$ evolution diagram for the sources of Haleakala basalts

t_d^{th}, t_d^{alk}, t_d^{post} are the calculated ages when the mantle sources of basalts from the tholeiitic series, alkalic series and post-erosional series, respectively, became depleted

relative to bulk Earth's compositions. t_e is the age when metasomatism occurred for the mantle sources of the three Haleakala volcanic series. See text for discussion.

Figure 4-5: (a) Ba/ La versus Ce/La, (b) Th/La versus Ce/La and (c) Nb/La versus Ce/La for samples from Haleakala. Error bars indicate $\pm 2\sigma$.

⊡: tholeiites from Honomanu volcanic series

△: alkalic basalts from the alkalic Kula volcanic series

⊙: hawaiites and mugearites from Kula volcanic series

✳: alkalic basalts and ankaramites from the post-erosional Hana volcanic series

●: hawaiite from Hana volcanic series

Figure 4-6: La/Ce versus $^{87}Sr/^{86}Sr$ for samples from Haleakala. Symbols as in Figure 4-5. Additional symbol: (transitional basalt and alkalic basalt from Honomanu series).

Figure 4-7: $^{143}Nd/^{144}Nd$ versus $^{87}Sr/^{86}Sr$ showing field for mantle array defined by basalts. Shaded field indicates region for mid-ocean ridge basalt (MORB) which define the high $^{143}Nd/^{144}Nd$ and low $^{87}Sr/^{86}Sr$ end of the mantle array. Haleakala basalts lie between the MORB field and estimates for bulk earth values. Symbol in upper right indicates ±2 sigma uncertainty.

□: samples from Honomanu volcanic series;

Δ: samples from alkalic Kula series;

✳: samples from post-erosional Hana series.

Figure 4-8: Mixing curves for various curvature coefficient r. Where $r = a_1 b_2/a_2 b_1$ (after Langmuir et al. (1978)).

Figure 4-9: Trace element variation diagram for mid-ocean ridge basalts and estimated source for mid-ocean ridge basalts normalized to primitive mantle compositions. The range of MORB compositions (upper) is compiled from Frey et al. (1974); Hart (1976); White and Schilling (1978); Bougault et al., (1979); Sun et al., (1979); The range of estimated MORB source is from White and Schilling (1978). Th, Ta, and Nb values were not given in their estimates thus range of these elements are shown as dash lines.

Δ and ● show the average values of trace element compositions for MORB and its source used in this model. These MORB source abundances (●) were chosen so that MgO-rich MORBs (Mg# >66, White and Schilling (1978)) can be derived by 15% melting.

Figure 4-10: Plot of La/Ce versus $^{87}Sr/^{86}Sr$ ratios for samples from Haleakala. Symbols as in Figure 4-7. The three samples used to quantitatively test the model are circled. The vertical axis from the MORBs source point indicates La/Ce abundance ratio as function of melting degree for 0.1 to 2% melting of a MORB source containing 0.31 ppm La, 0.95 ppm Ce and 13.2 ppm Sr. (These MORB source abundances were chosen so that MgO-rich MORBs can be derived by 15% melting). The vertical axis from the primitive mantle (P.M.) indicates La/Ce abundance ratio for 5% melting of a primitive mantle source. The solid lines with negative slope are mixing lines for mixtures of primitive mantle (La = 0.71 ppm, Ce = 1.90 ppm, Sr = 23.7 ppm) with melts formed by low degrees of melting of a

MORB source. The dashed, near vertical lines connect points with the equal ratios of end-member components; i.e. 5:95 indicates 5% of the melt from a MORB source and 95% primitive mantle. Error bars on the upper right are ±2σ.

Figure 4-11: Variation of $^{87}Sr/^{86}Sr$ ratios with the depth. Symbols as in Figure 4-5. The samples used in our model calculations are circled (C122, H65-4 and H65-11).

Figure 4-12: Variation of La/Ce ratios with depth. Symbols as in Figure 4-11.

Figure 4-13: Trace element variation diagram for the calculated Haleakala sources normalized to primitive mantle compositions.
The solid lines show the values calculated from lower partition coefficients (Frey et al., 1978, set 1) and the dashed lines show the values calculated from higher partition coefficients (Harrison, 1981) listed in Table 3.
□ tholeiitic series
Δ alkalic series
* post-erosional series

Figure 4-14: Quantitative evaluation of the mixing end-members and their proportions deduced from Figure 4-10 for the three representative samples (C122, H65-4 and H65-11).
Predicted Nd isotopic ratios are in excellent agreement with observed ratios.
The vertical axis indicates the ratio of calculated to observed abundances for highly and moderately incompatible trace elements. Most of the calculated data are within ±10% of the observed abundances and all data points fit to better

than ±25%. Nd and Sm values calculated using high partition coefficients and shown in dashed symbols.

Figure 4-15: Comparison of the calculated and measured trace element distribution pattern for tholeiite and alkalic basalts from the Haleakala volcanic series.

□ are measured values for the tholeiite C122

Δ are the measured values for H65-4 from the alkalic volcanic series

☆ are the measured values for H65-11 from the post-erosional series

The calculated values are shown as lines. Nd values are calculated from the lower partition coefficients in Table 3. Sm values are average values calculated from the two pairs of partition coefficients in Table 3.

Figure 4-16: La/Ce abundance ratio versus $^{87}Sr/^{86}Sr$ for Hawaiian basalts. Honolulu volcanics are a post-erosional suite ranging from alkalic olivine basalt to nepheline melilite (Clague and Frey, 1982). Their wide range in La/Ce at a uniform $^{87}Sr/^{86}Sr$ requires constant mixing proportions, but a wide range (0.05 to 0.25%) in melting degree of a MORB source. Field encloses data for 15 basalts (Lanphere and Dalrymple, 1980; Clague and Frey, 1982; Roden and Frey, unpublished data).

Koolau shield tholeiites underlie the Honolulu Volcanics and have distinctly higher and variable $^{87}Sr/^{86}Sr$. Compared to the alkalic Honolulu Volcanics, the Koolau tholeiites require higher degrees of melting of a MORB source, but smaller amounts of this melt mixed in variable proportions. Field

encloses data for seven tholeiites (Lanphere and Dalrymple, 1980; Leeman et al., 1980; Roden and Frey, unpublished data). Loihi Seamount consists of tholeiitic and alkalic basalts; the latter have higher La/Ce but have lower $^{87}Sr/^{86}Sr$ than the tholeiites. Field encloses data for 12 basalts (Frey and Clague, 1982; Lanphere, 1982).

Suiko Seamount in the Central Emperor Ridge consists of alkalic basalts which overlie tholeiites. Field encloses data for 6 samples (Bence et al., 1980; Clague and Frey, 1980; Lanphere et al., 1980). Note that these samples have the lowest $^{87}Sr/^{86}Sr$ ratios and require the largest amount of a component derived from a MORB source.

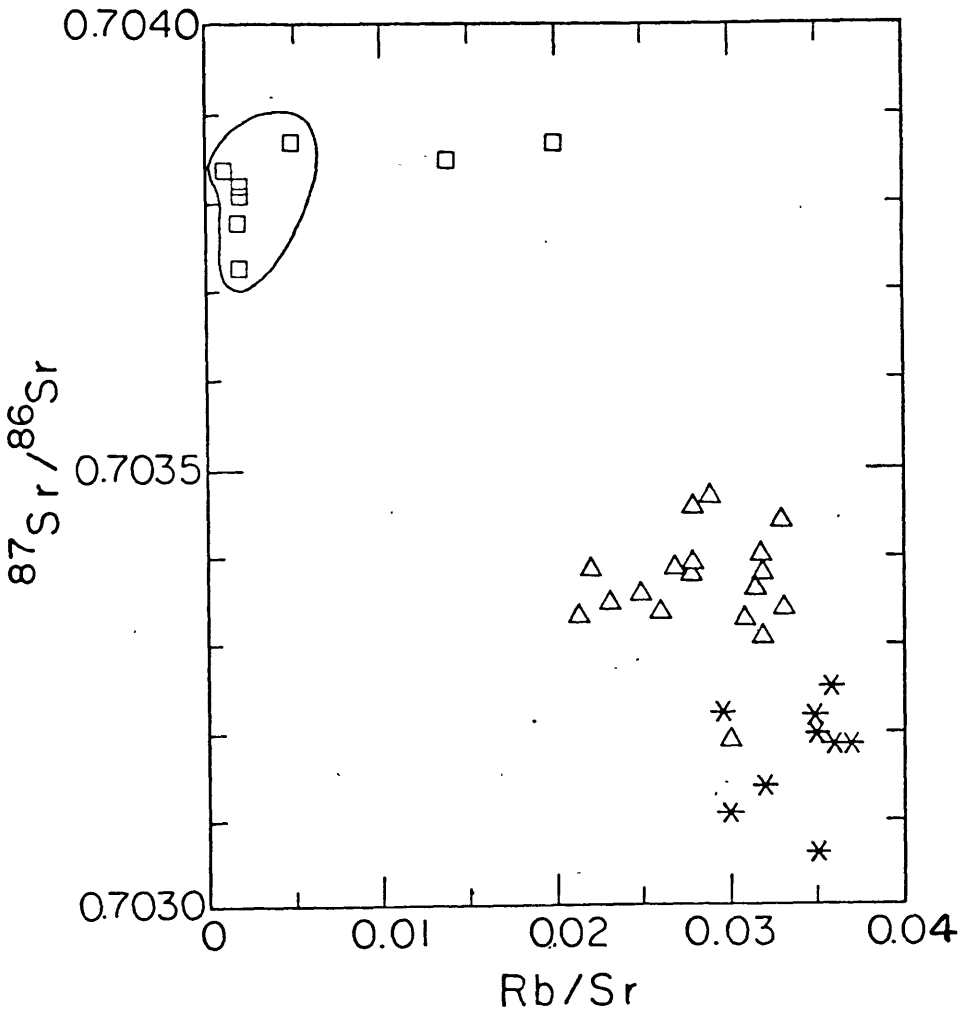


Figure 4-1

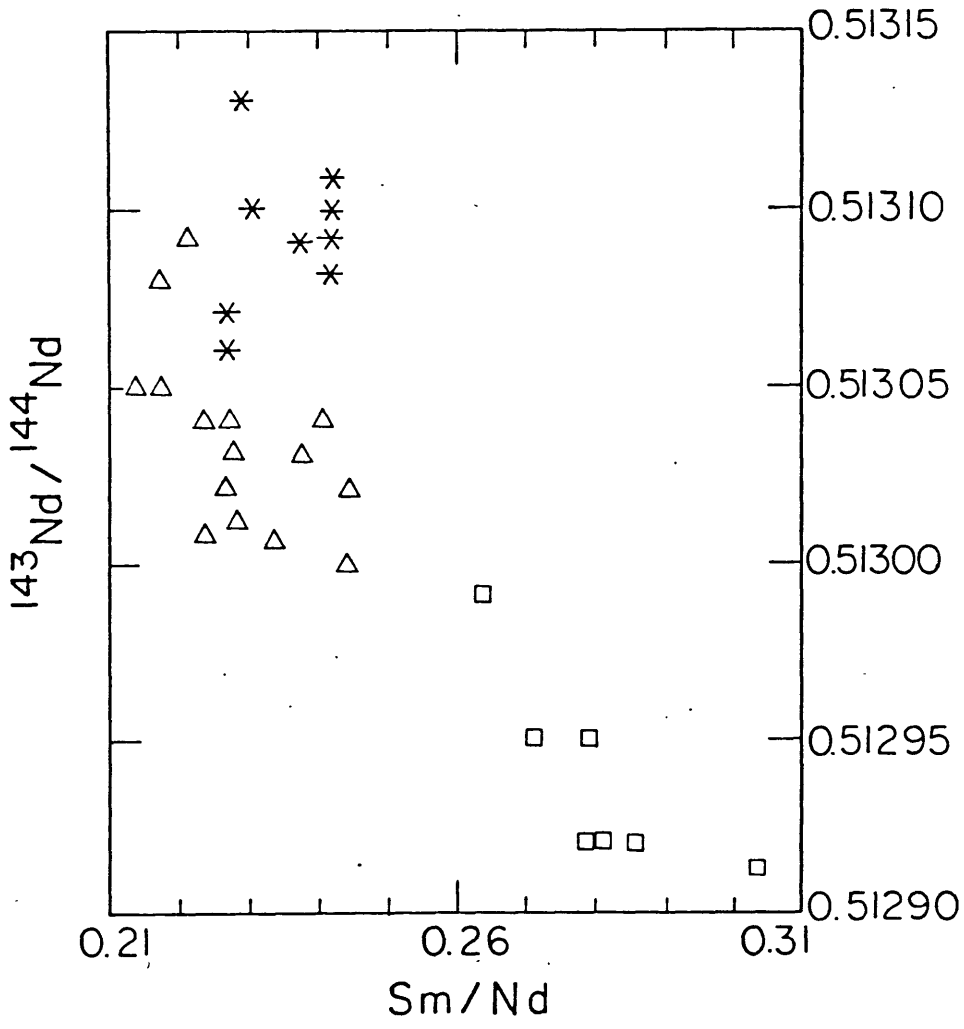

0.51315
0.51310
0.51305
0.51300
0.51295
0.51290
0.21
0.26
0.31
Sm/Nd
143Nd/144Nd

Figure 4-2

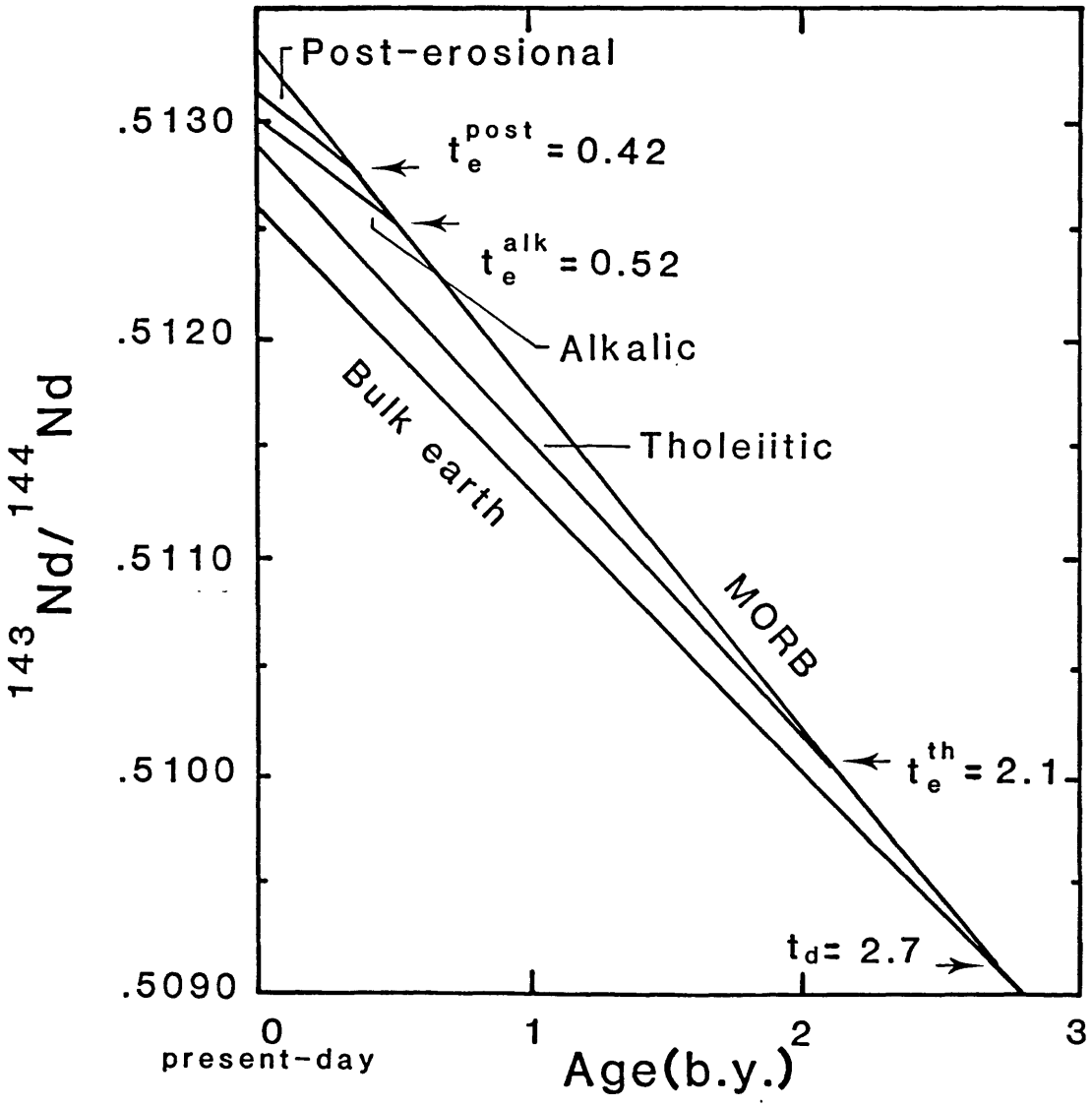

Post-erosional
$t_e^{post} = 0.42$
$t_e^{alk} = 0.52$
Alkalic
Tholeiitic
Bulk earth
MORB
$t_e^{th} = 2.1$
$t_d = 2.7$
.5130
.5120
.5110
.5100
.5090
$^{143}Nd/^{144}Nd$
0
present-day
1
2
3
Age(b.y.)

Figure 4-3

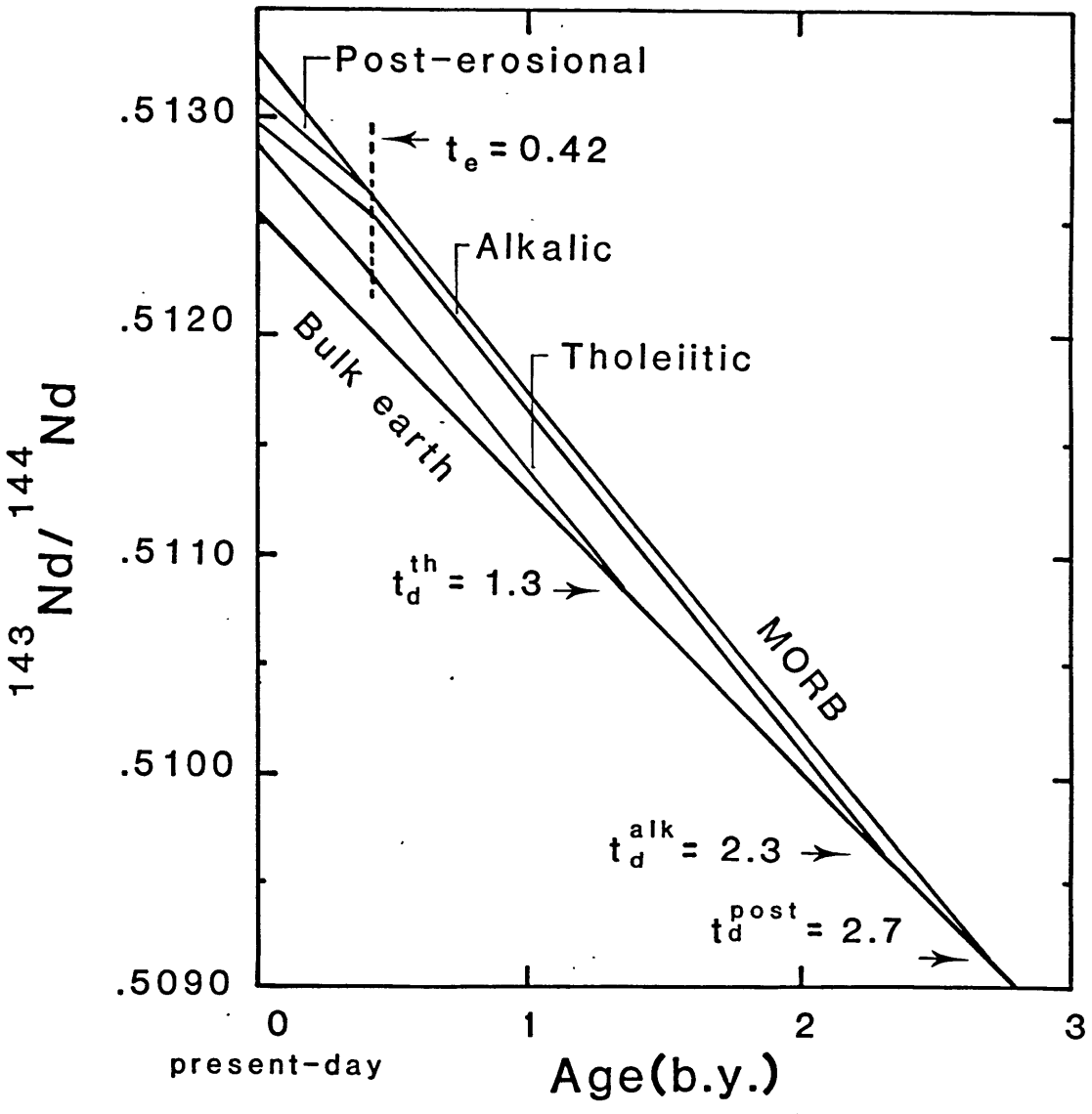

Post-erosional
$t_e = 0.42$
Alkalic
Tholeiitic
Bulk earth
$t_d^{th} = 1.3$
MORB
$t_d^{alk} = 2.3$
$t_d^{post} = 2.7$
.5130
.5120
.5110
.5100
.5090
$^{143}Nd/^{144}Nd$
0
present-day
1
2
3
Age(b.y.)

Figure 4-4(a)

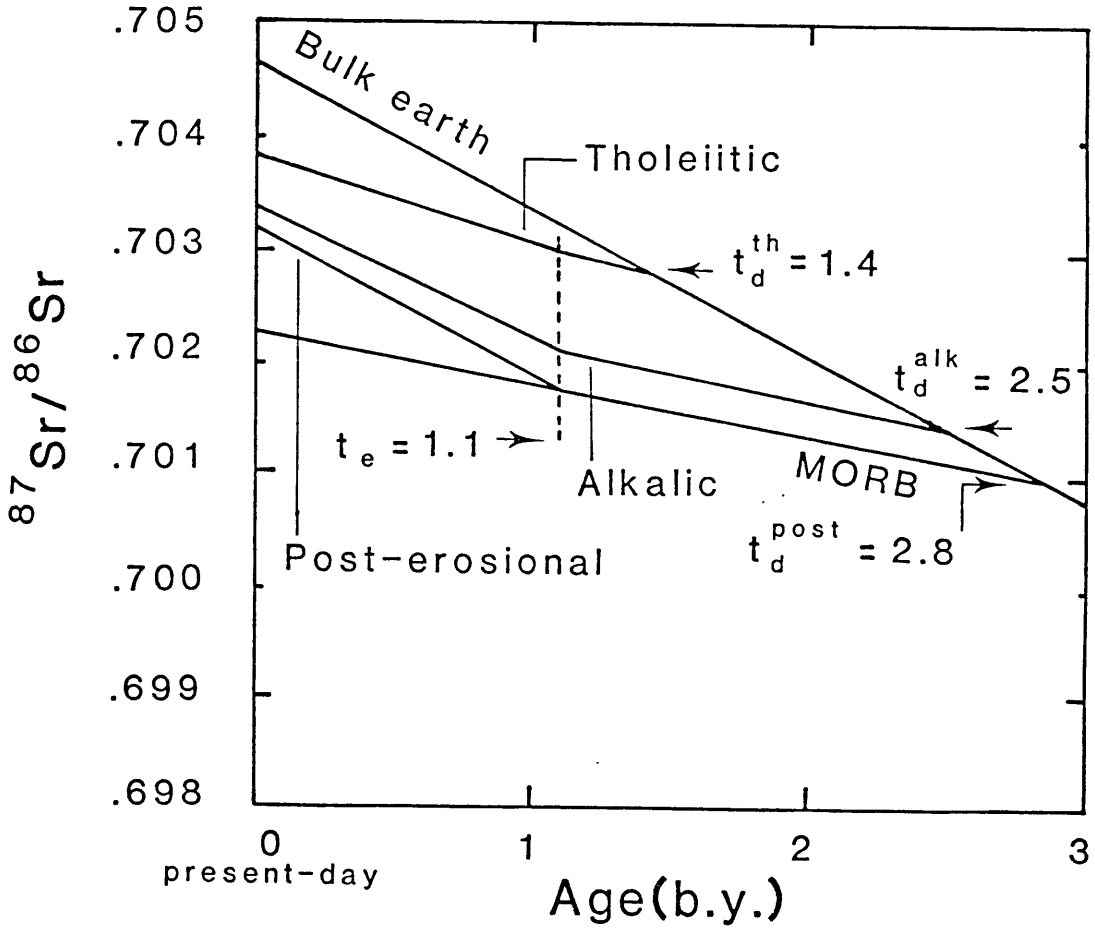

.705
.704
.703
.702
.701
.700
.699
.698
$^{87}Sr/^{86}Sr$
Bulk earth
Tholeiitic
$t_d^{th} = 1.4$
$t_d^{alk} = 2.5$
$t_e = 1.1$
Alkalic
MORB
Post-erosional
$t_d^{post} = 2.8$
0
present-day
1
2
3
Age(b.y.)

Figure 4-4(b)

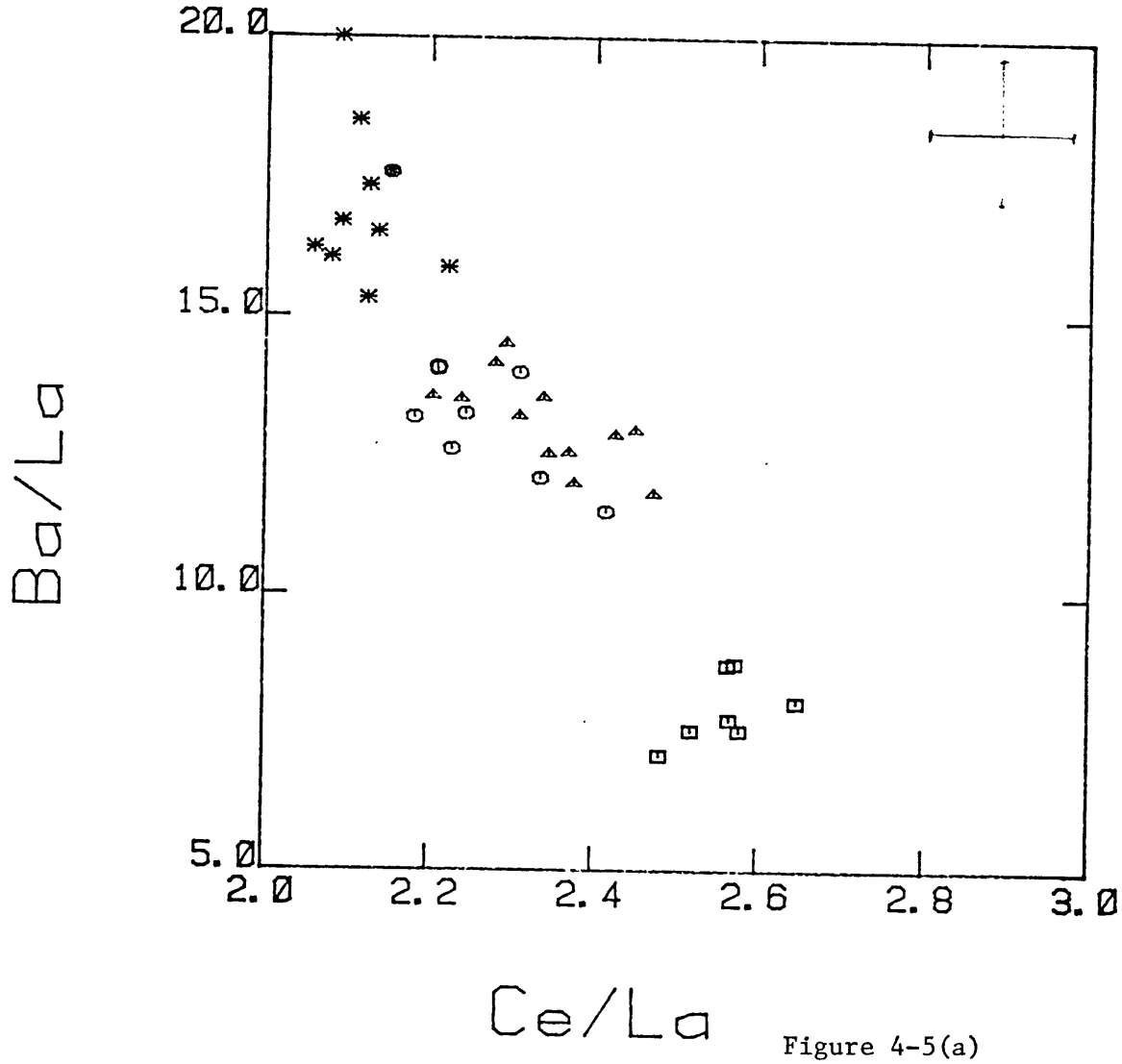


Figure 4-5(a)

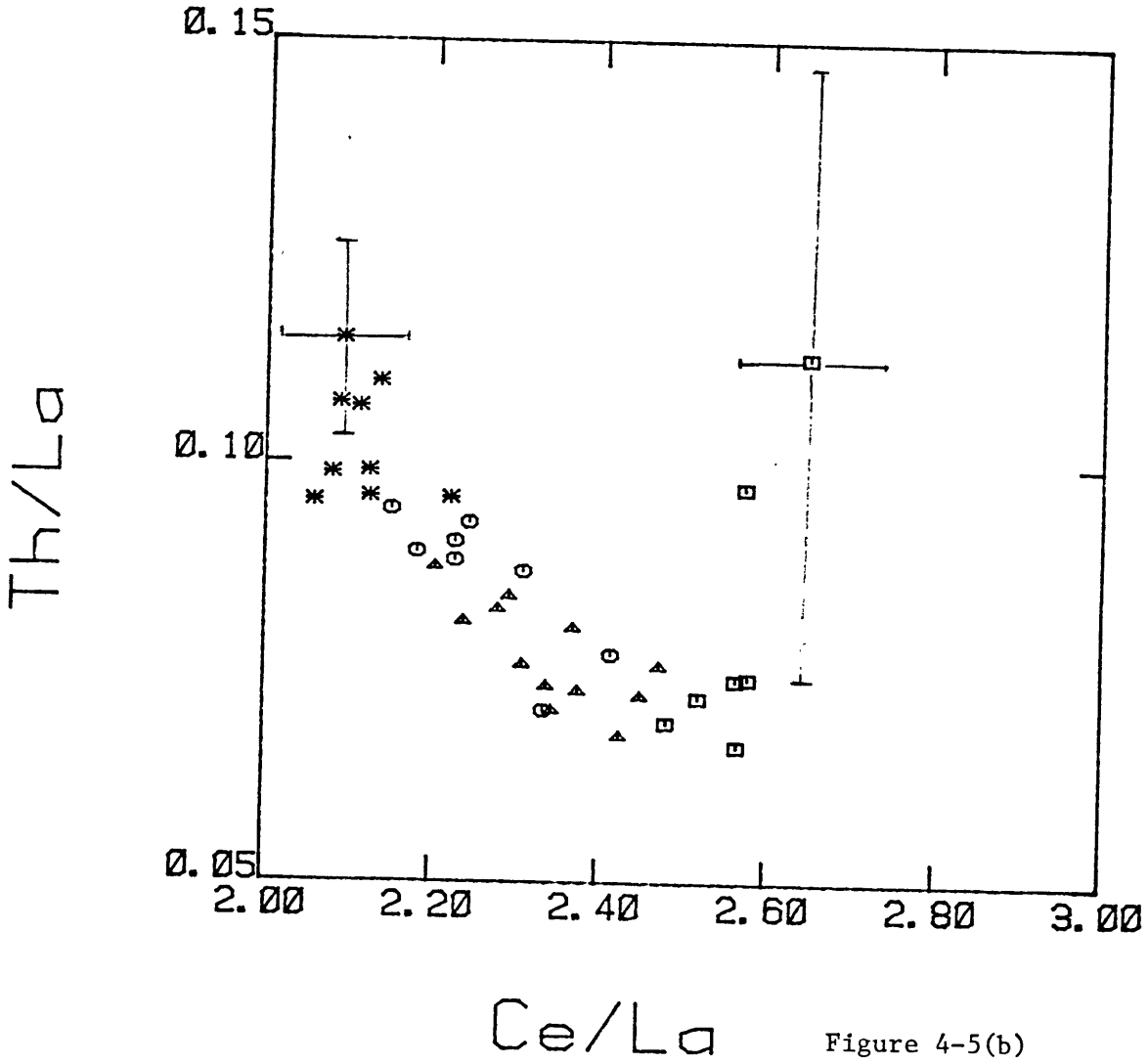


Figure 4-5(b)

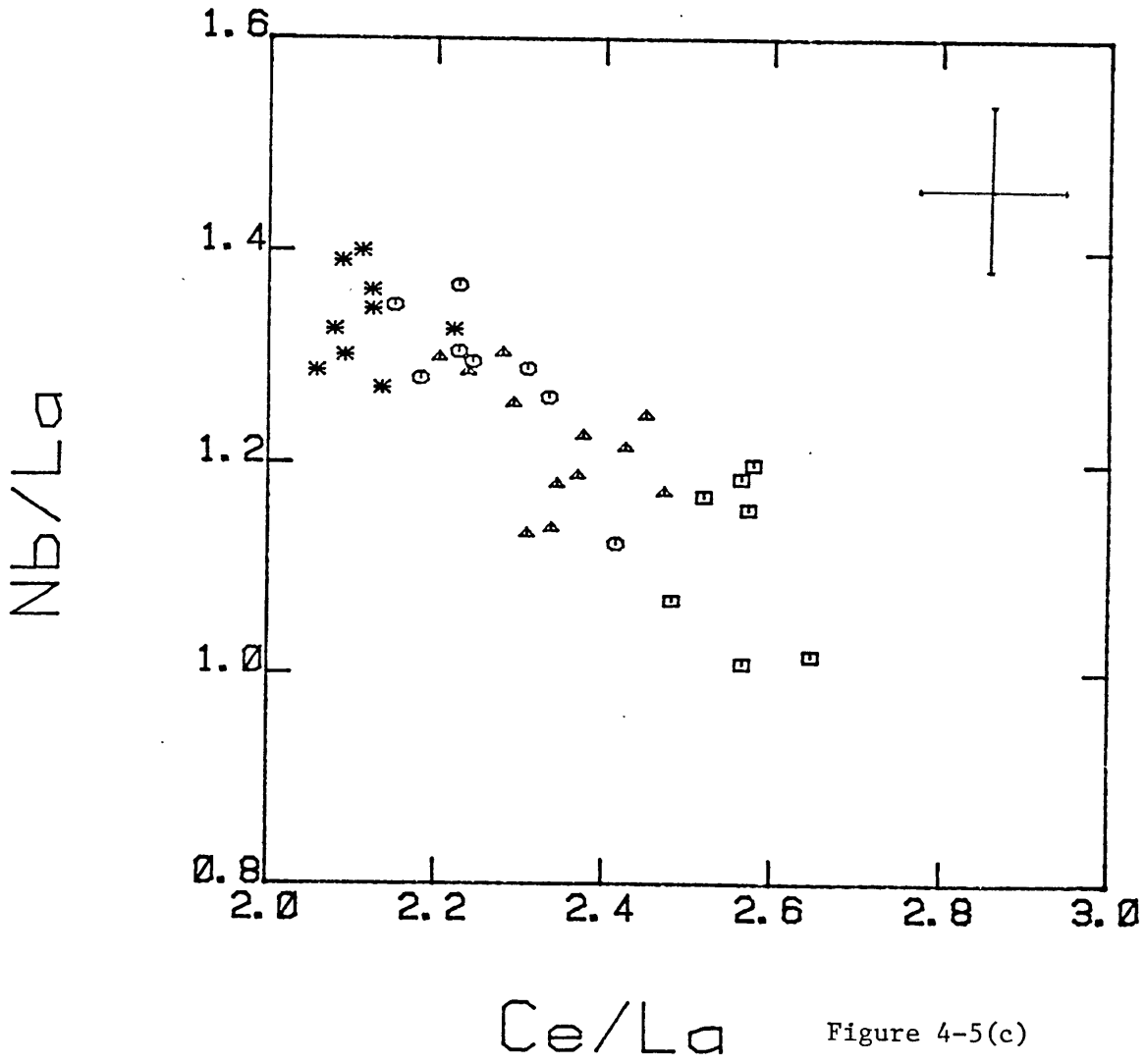


Figure 4-5(c)

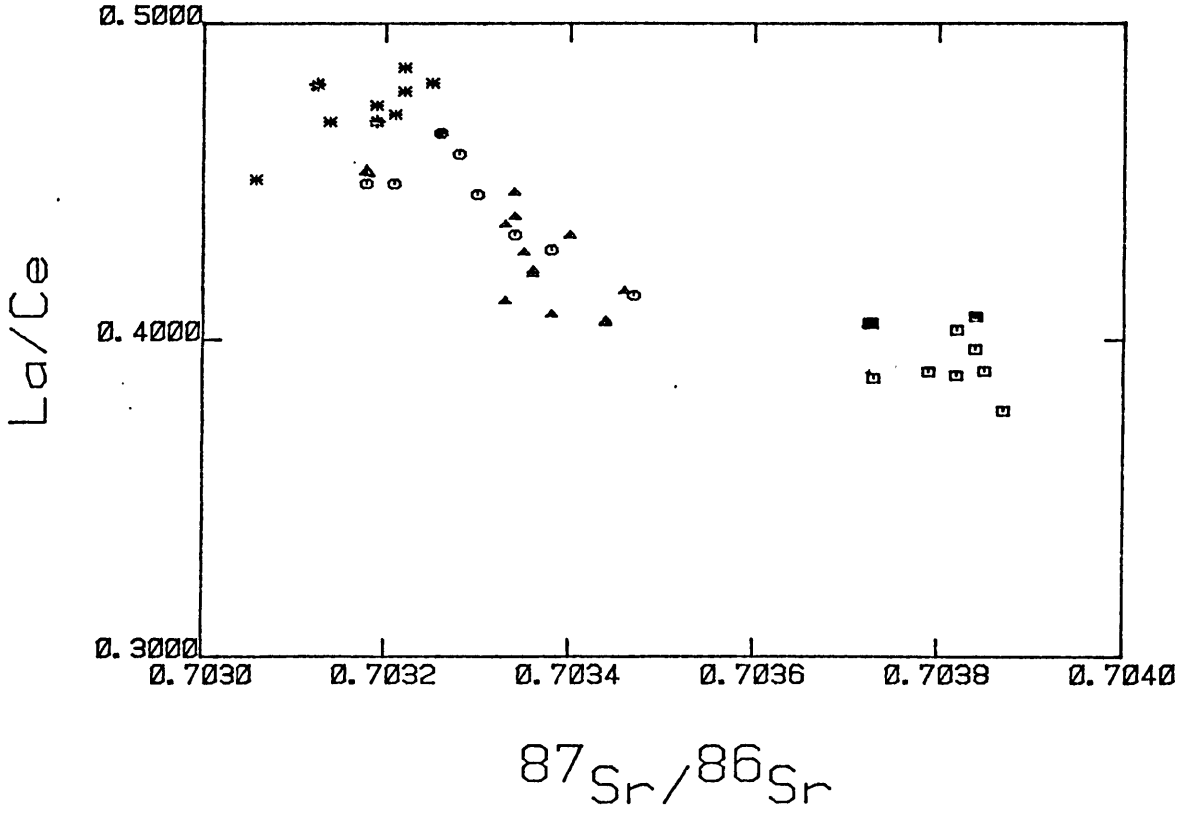

0.5000
0.4000
0.3000
La/Ce
0.7030
0.7032
0.7034
0.7036
0.7038
0.7040
87Sr/86Sr

Figure 4-6

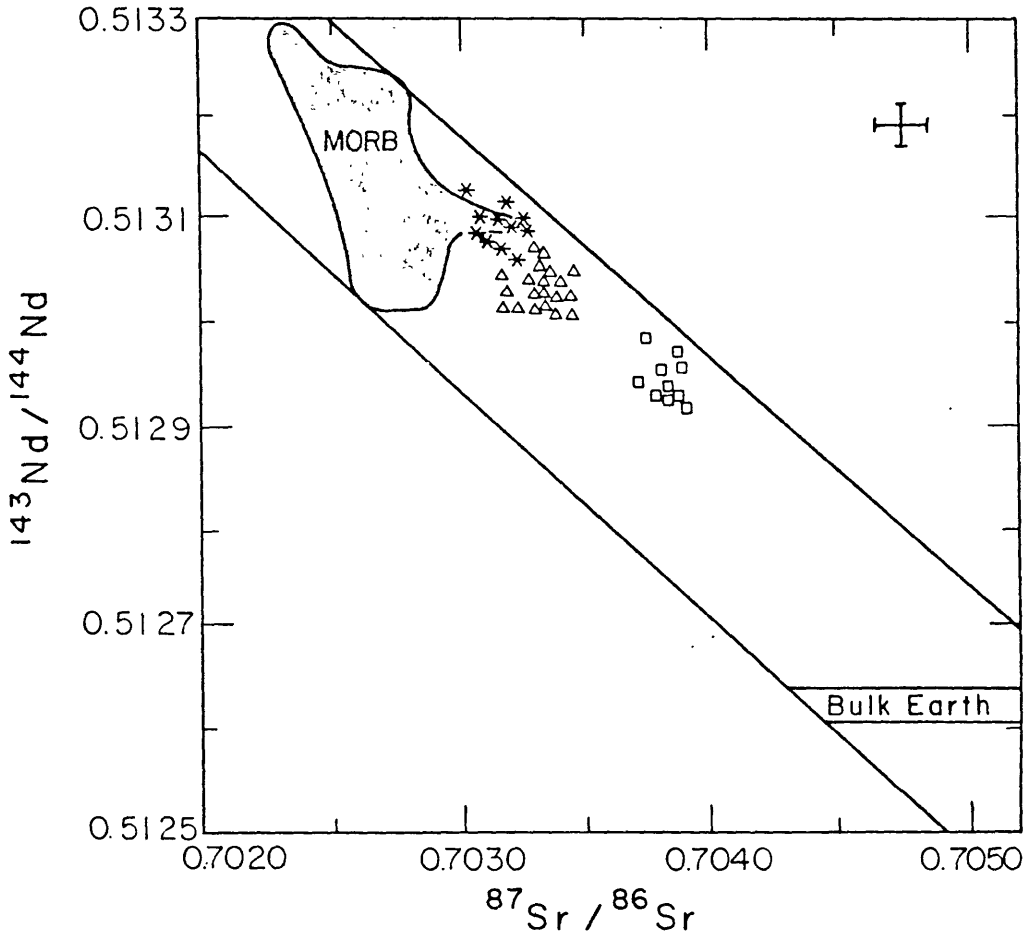

0.5133
0.5131
0.5129
0.5127
0.5125
$^{143}Nd/^{144}Nd$
MORB
Bulk Earth
0.7020
0.7030
0.7040
0.7050
$^{87}Sr/^{86}Sr$

Figure 4-7

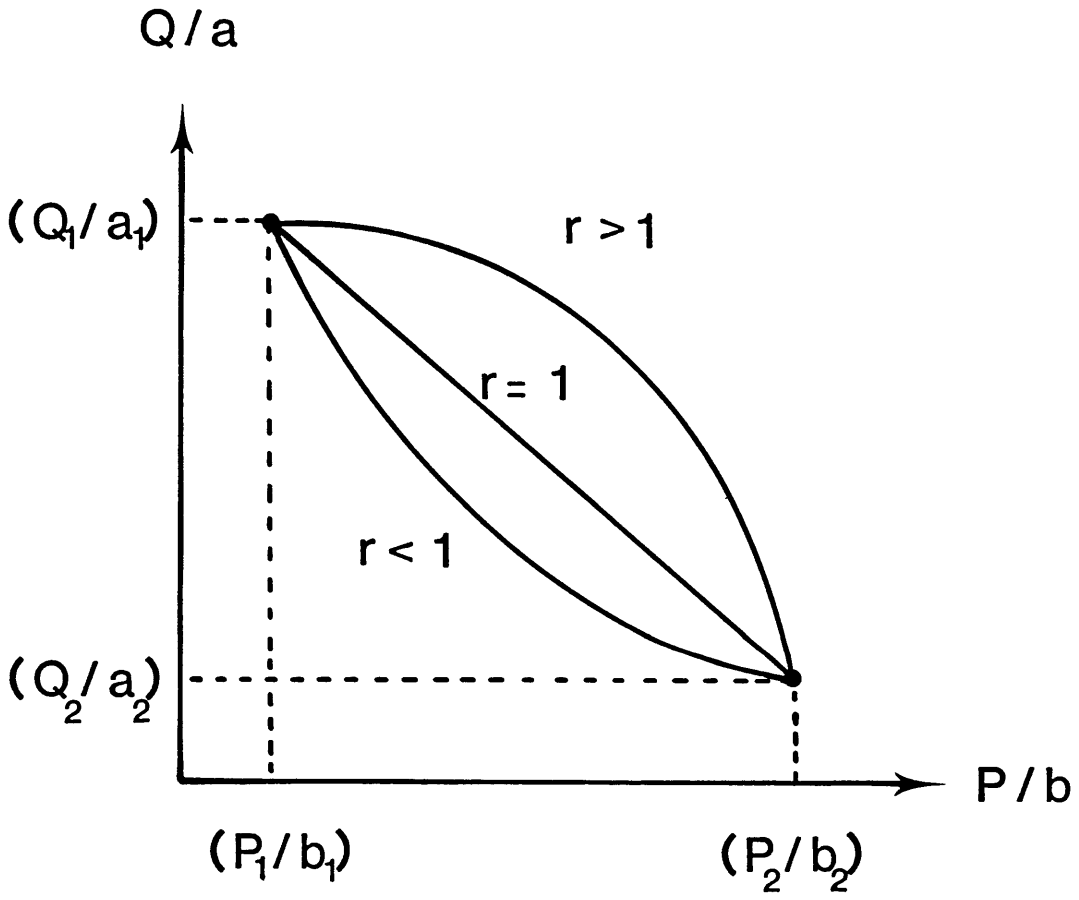


Figure 4-8

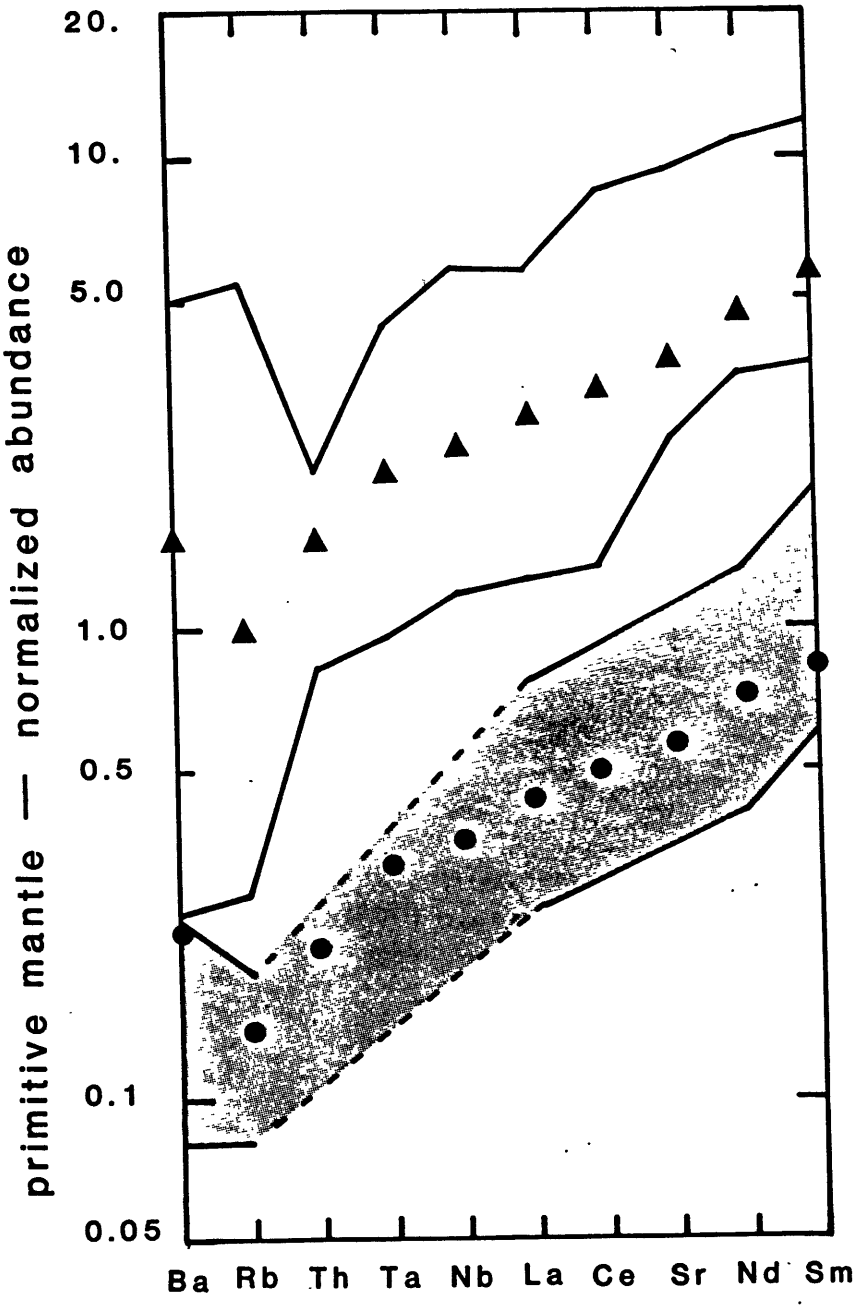

20.
10.
5.0
1.0
0.5
0.1
0.05
primitive mantle — normalized abundance
Ba Rb Th Ta Nb La Ce Sr Nd Sm

Figure 4-9

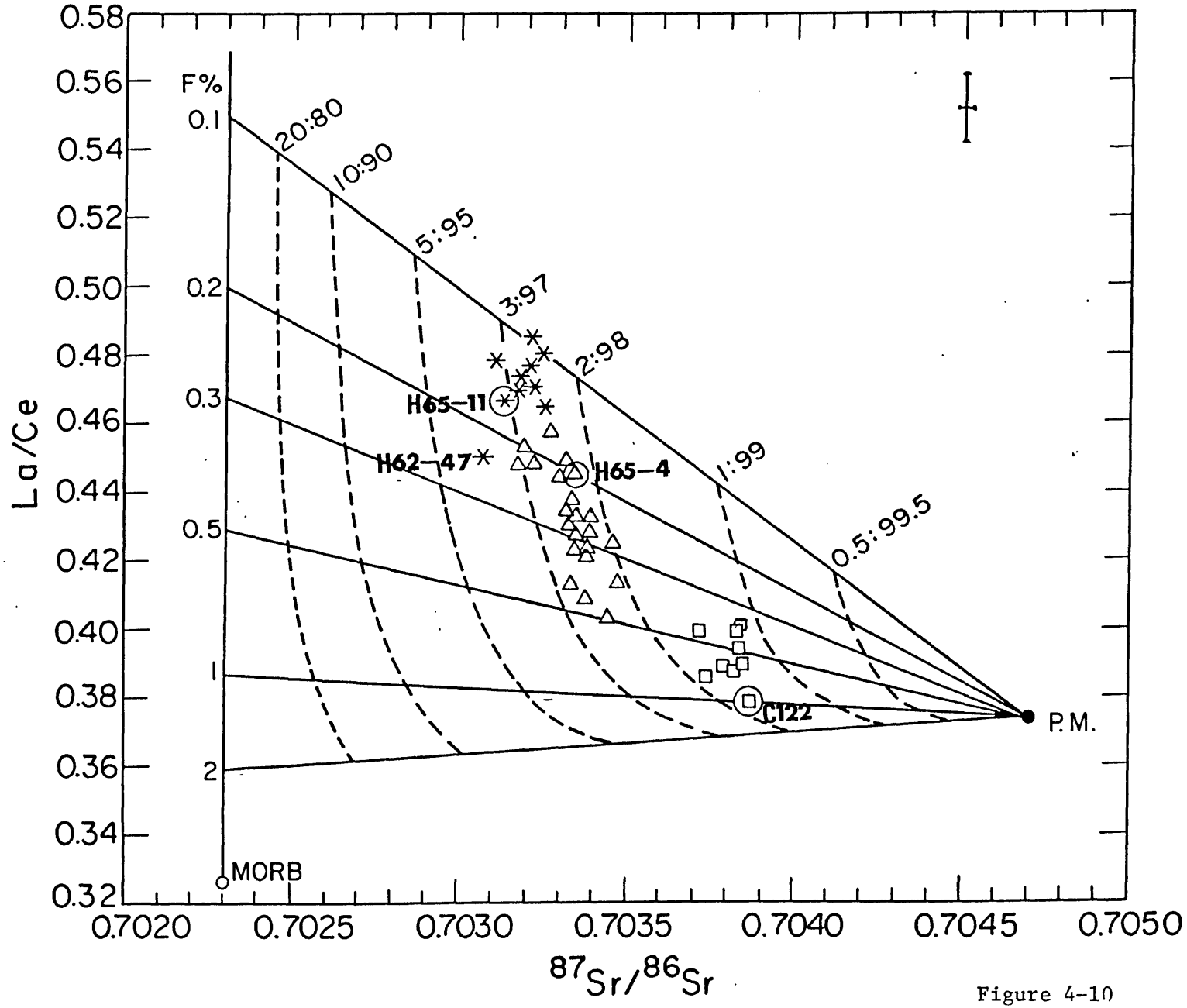

0.58
0.56
0.54
0.52
0.50
0.48
0.46
0.44
0.42
0.40
0.38
0.36
0.34
0.32
La/Ce
F%
0.1
0.2
0.3
0.5
1
2
20:80
10:90
5:95
3:97
2:98
1:99
0.5:99.5
H65-11
H62-47
H65-4
C122
P.M.
MORB
0.7020
0.7025
0.7030
0.7035
0.7040
0.7045
0.7050
87Sr/86Sr

Figure 4-10

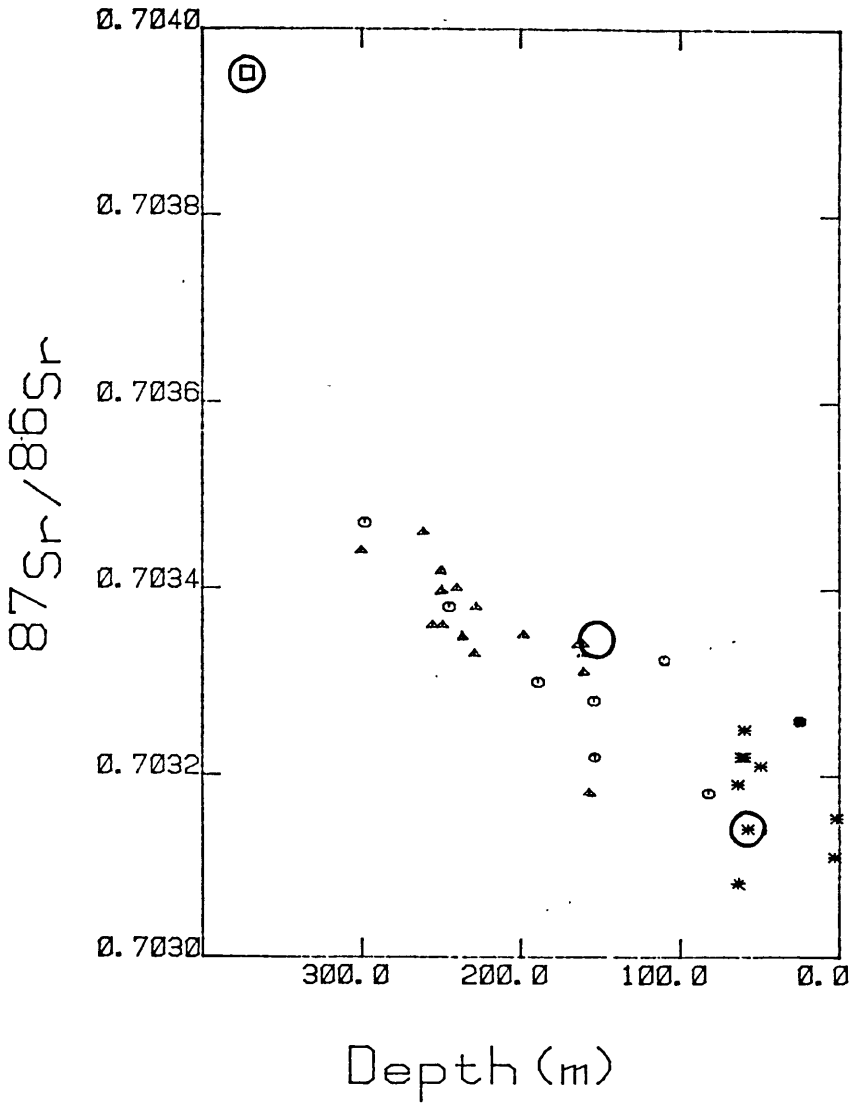

0.7040
0.7038
0.7036
0.7034
0.7032
0.7030
87Sr/86Sr
300.0
200.0
100.0
0.0
Depth (m)

Figure 4-11

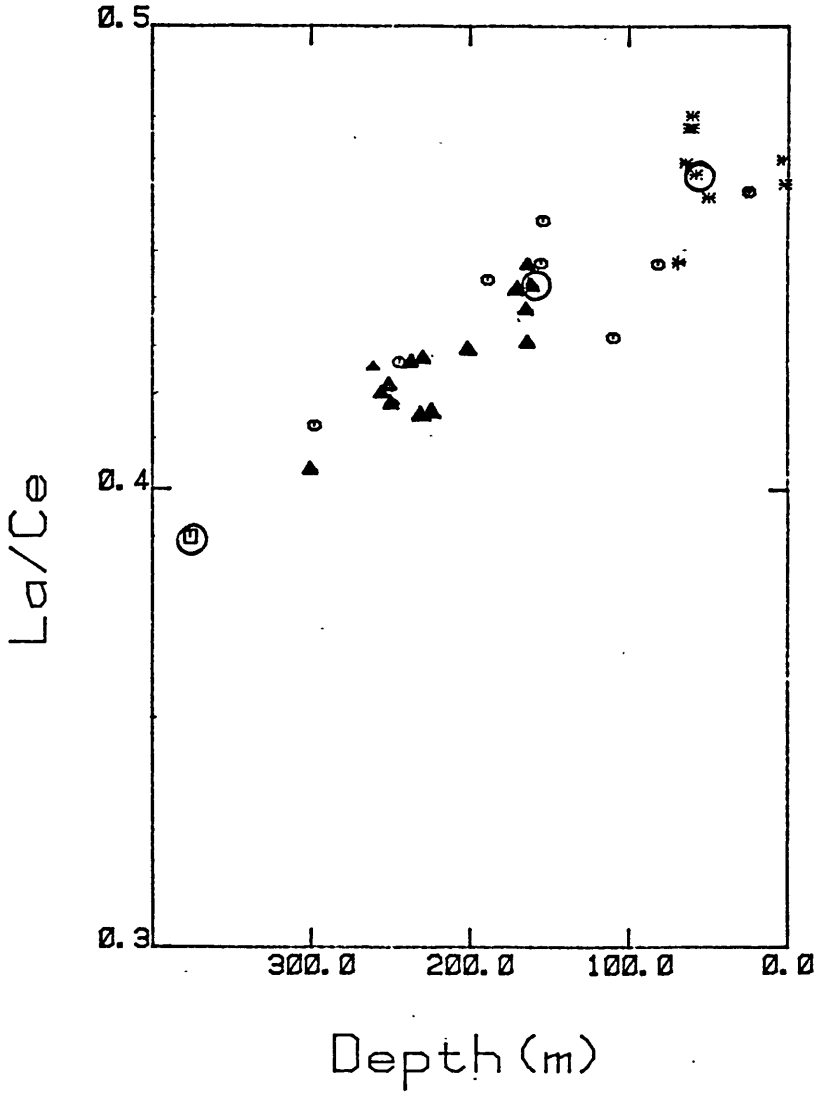


Figure 4-12

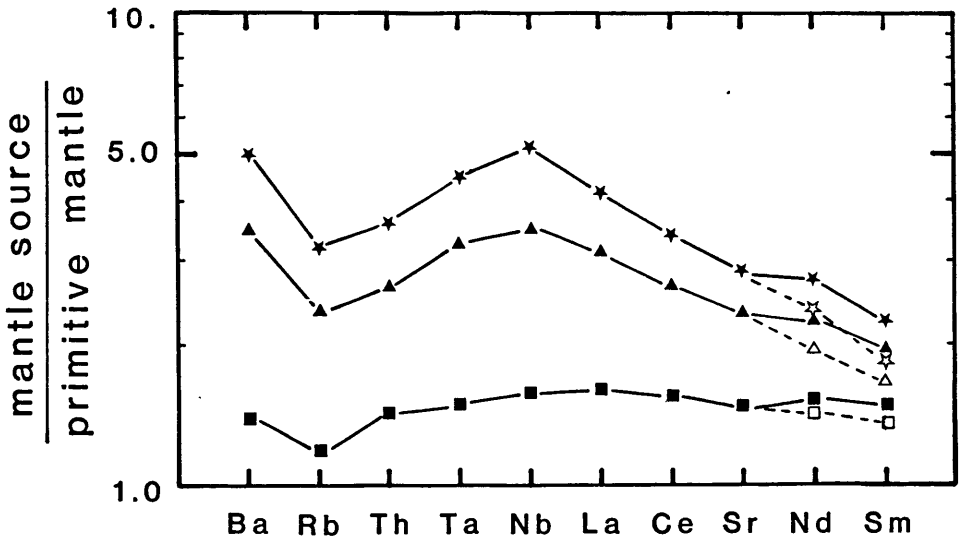

10.
5.0
1.0
mantle source / primitive mantle
Ba Rb Th Ta Nb La Ce Sr Nd Sm

Figure 4-13

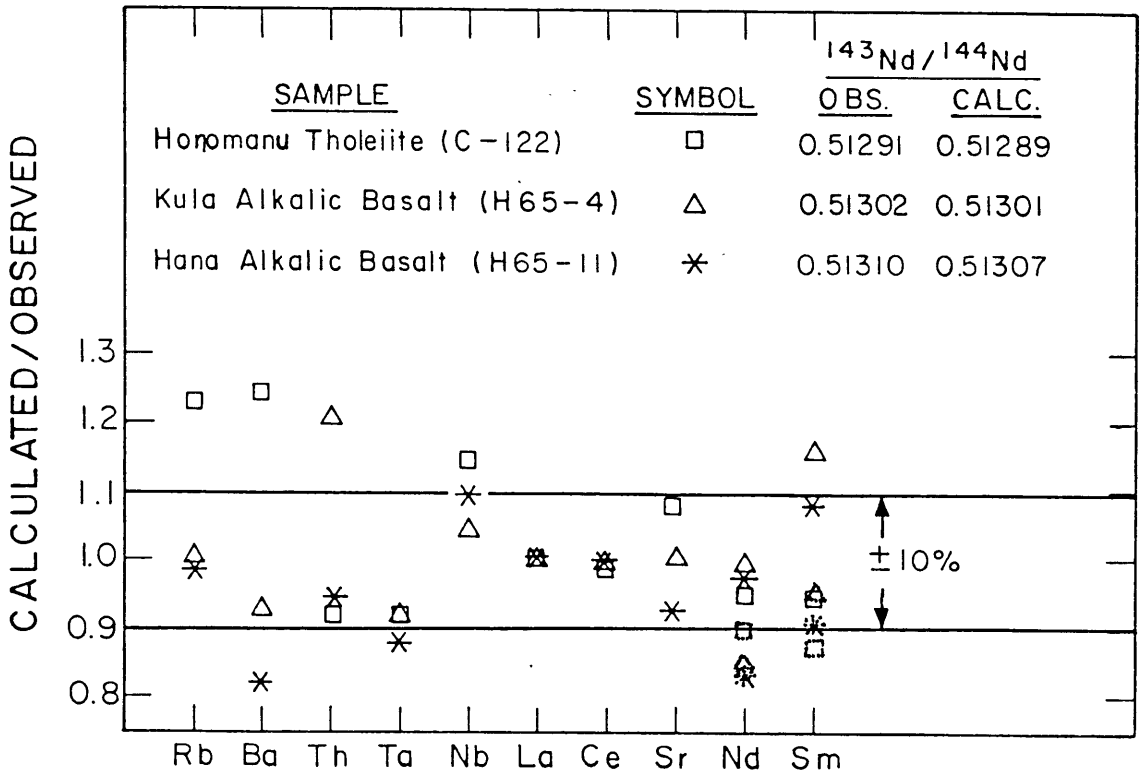

SAMPLE
SYMBOL
143Nd/144Nd
OBS.
CALC.
Honomanu Tholeiite (C-122)
0.51291
0.51289
Kula Alkalic Basalt (H65-4)
0.51302
0.51301
Hana Alkalic Basalt (H65-11)
0.51310
0.51307
CALCULATED/OBSERVED
1.3
1.2
1.1
1.0
0.9
0.8
±10%
Rb
Ba
Th
Ta
Nb
La
Ce
Sr
Nd
Sm

Figure 4-14

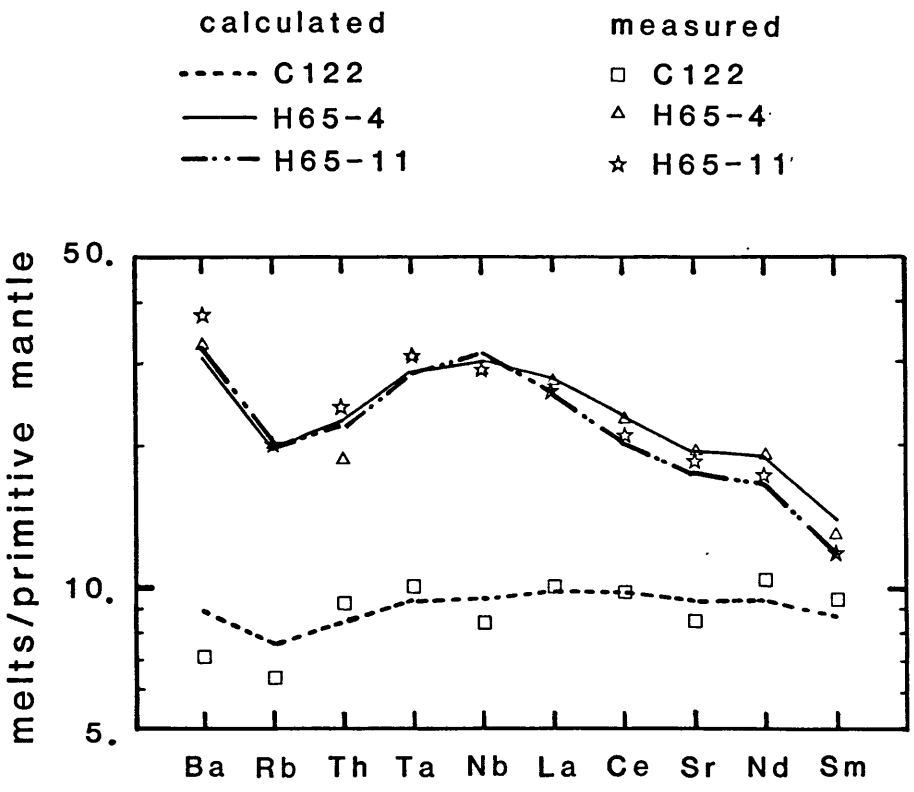

calculated
C122
H65-4
H65-11
measured
C122
H65-4
H65-11
melts/primitive mantle
50.
10.
5.
Ba Rb Th Ta Nb La Ce Sr Nd Sm

Figure 4-15

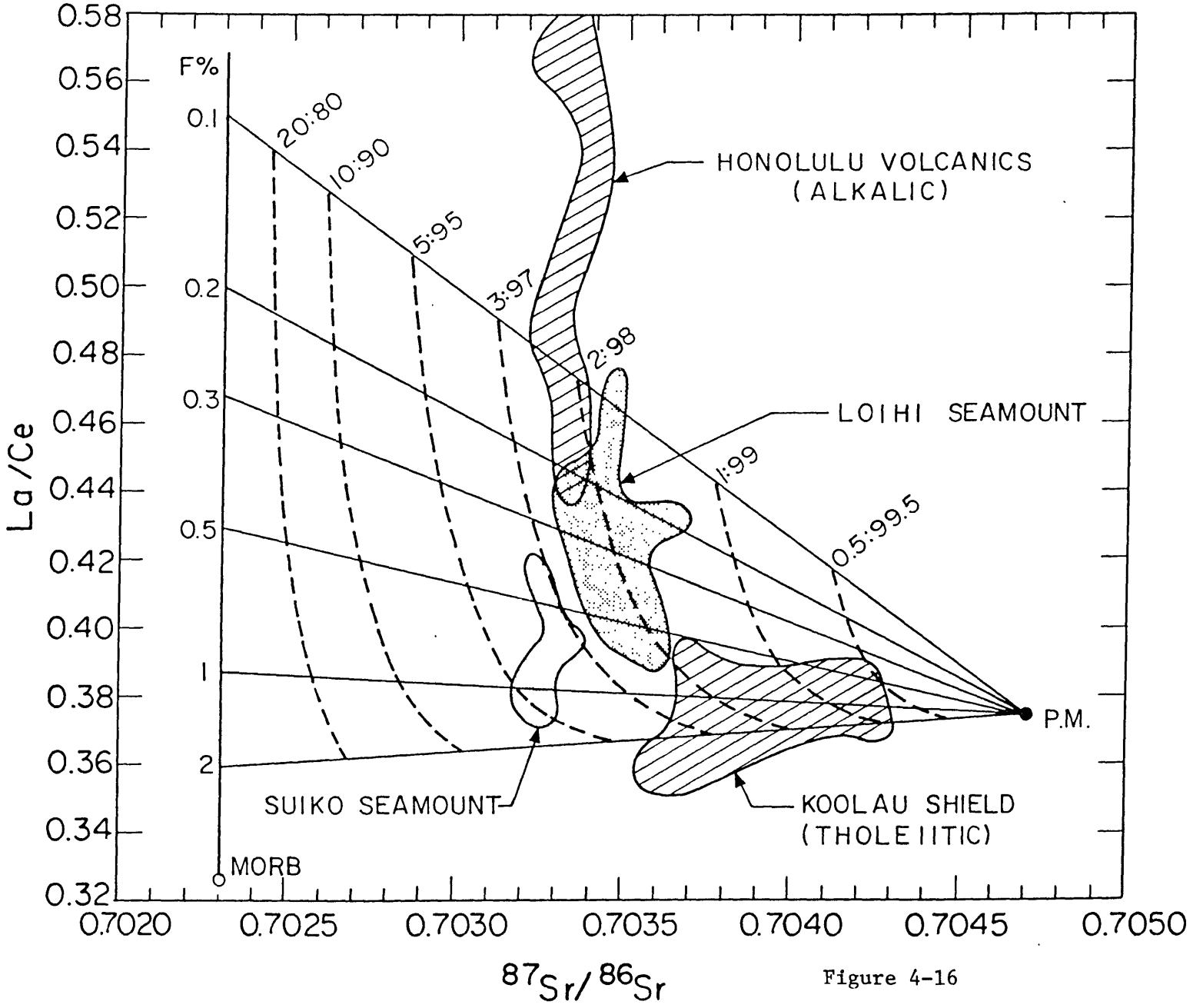

0.58
0.56
0.54
0.52
0.50
0.48
0.46
0.44
0.42
0.40
0.38
0.36
0.34
0.32
La/Ce
F%
0.1
0.2
0.3
0.5
1
2
20:80
10:90
5:95
3:97
2:98
1:99
0.5:99.5
HONOLULU VOLCANICS
(ALKALIC)
LOIHI SEAMOUNT
P.M.
SUIKO SEAMOUNT
KOOLAU SHIELD
(THOLEIITIC)
MORB
0.7020
0.7025
0.7030
0.7035
0.7040
0.7045
0.7050
87Sr/86Sr

Figure 4-16

References

Allegre, C.J., Ben Othman, D., Polve, M., and Richard, P., 1979, The Nd-Sr isotopic correlation in mantle materials, Phys. Earth Planet. Interiors, 19, 293-306.

Allegre, C.J., and Bottinga, Y., 1974, Tholeiite, alkali basalt and ascent velocity, Nature, 252, 31-32.

Allegre, C.J., Brevant, O., Dupre, B., and Minster, J.-F., 1980, Isotopic and chemical effects produced in a continuously differentiating convecting earth mantle, Phil. Trans. Roy. Soc. London, A297, 447-477.

Allegre, C.J., Hart, S.R., Minster, J-F., 1982, Inversion of the Rb-Sr, Sm-Nd and Lu-Hf mass balance equations: Structure and development of the mantle-continental crust system (abstract), EOS Trans. Amer. Geophys. Union, 63, 460.

Allegre, C.J., Treuil, M., Minster, J.-F., Minster, B., and Albarede, F., 1977, Systematic use of trace element in igneous process, Contr. Miner. Petrol., 60, 57-75.

Anderson, D.L., 1982, Isotopic evolution of the mantle: The role of magma mixing, Earth Planet. Sci. Lett., 57, 1-12.

Arndt, N.T., 1977, The separation of magmas from partially molten peridotite, Carnegie Inst. Wash. Yearbook 76, 424-428.

Arth, J.G., 1976, The behavior of trace elements during magmatic processes: A summary of theoretical models and their applications, J. Res., U.S. Geol. Survey, 4, 41-47.

Bailey, D.K., 1982, Mantle metasomatism - continuing chemical change within the Earth, Nature, 296, 525-530.

Barberi, F., Civetta, L., and Varet, J., 1980, Sr isotopic composition of Afar volcanics and its implication for mantle connection, Earth Planet. Sci. Lett, 50, 247-259.

Bargar, K.E., and Jackson, E.D., 1974, Calculated volumes of individual shield volcanoes along the Hawaiian-Emperor chain, J. Res. U.S. Geol. Survey, 2, 545-550.

Basaltic Volcanism Study Project, 1981, Oceanic intraplate volcanism, in Basaltic volcanism on the terrestrial planets, Chap. 1, Pergamon Press, N.Y., 1286 pp.

Beeson, M.H., 1976, Petrology, mineralogy, and geochemistry of the East Molokai volcanic series, Hawaii, U.S. Geol. Survey Prof. Paper 961, 53pp.

Bence, A.E., 1966, The differentiation history of the Earth by Rb-Sr isotopic relationships, Ph.D. Thesis, Mass. Inst. Tech. Cambridge, MA, 250 pp.

Bence, A.E., Taylor, S.R., and Fisk, M., 1980, Major- and trace-element geochemistry of basalts from Ōjin, Nintoku and Suiko seamounts of the Emperor seamount chain: DSDP-IPOD Leg 55, Initial Report Deep Drilling Project, 55, 599-605.

Bickle, M.J., Ford, C.E., and Nisbet, E.G., 1977, The petrogenesis of peridotitic komatiites: Evidence from high-pressure melting experiments, Earth Planet. Sci. Lett., 37, 97-106.

Biscaye, P.E., and Dasch, E.J., 1971, The rubidium, strontium, strontium-isotope system in deep-sea sediments: Argentine Basin, J. Geophys. Res., 76, 5087-5096.

Bougault, H., Joron, J.L., and Treuil, M., 1979, Alteration, fractional crystallization, partial melting; mantle properties from trace elements in basalts recovered from the North Atlantic, in Talwani, M., Harrison, C.G., and Hayes, D.E., eds., Deep Sea Drilling Results in the Atlantic Ocean: Ocean crust, 352-368, Amer. Geophys. Union, Washington, D.C.

Brey, G., 1978, Origin of olivine melilitites-chemical and experimental constraints, J. Volcanol. Geotherm. Res., 3, 61-88.

Brey, G., and Green, D.H., 1977, Systematic study of liquidus phase relations in olivine melilitite + H_2O + CO_2 at high pressures and petrogenesis of an olivine melilitite magma, Contr. Miner. Petrol., 61, 141-162.

Brooks, C., Hart, S.R., Hofmann, A.L., and James, D.E., 1976, Rb-Sr mantle isochrons from oceanic regions, Earth Planet. Sci. Lett., 32, 51-61.

Burwell, A.D.M., 1975, Rb-Sr isotope geochemistry of lherzolites and other constituent minerals from Victoria, Australia, Earth Planet. Sci. Lett., 28, 69-78.

Butler, R., 1982, The 1973 Hawaii earthquake: A double earthquake beneath the volcano Mauna Kea, Geophys. J. Roy. Astr. Soc., 69, 173-186.

Chase, C.G., 1978, Extension behind island arcs and motions relative to hot spots, J. Geophys. Res., 83, 5385-5387.

Chen, C.-Y., and Frey, F.A., 1980, Geochemistry of lherzolite inclusions from Mt. Leura, Victoria, Australia, (abstract) EOS Trans. Amer. Geophys. Union, 61, 413.

Chen, C.-Y., Frey, F.A., and Hart, S.R., 1981, The evolution of Haleakala volcano, East Maui: Evidence for heterogeneous mantle sources, (abstract), EOS Trans. Amer. Geophys. Union, 62, 1068-1069.

Church, S.E., 1971, Strontium isotope and alkali element geochemistry of selected sediments from the northeast Pacific Ocean, Geochim. Cosmochim. Acta, 35, 1300-1305.

Clague, D.A., 1974, The Hawaiian-Emperor seamount chain: Its origin, petrology, and implications for plate tectonics, Ph.D. Dissert., Univ. California, San Diego, 319 pp.

Clague, D.A. and M.H. Beeson, 1980, Trace element geochemistry of the East Molokai volcanic series, Hawaii, Amer. J. Sci., 280-A, 820-844.

Clague, D.A. and Frey, F.A., 1980, Trace element geochemistry of tholeiitic basalts from site 433C, Suiko Seamount, Initial Report Deep Sea Drilling Project, 55, 559-569, Washington, D.C.

Clague, D.A. and Frey, F.A., 1982, Petrology and trace element geochemistry of the Honolulu volcanics, Oahu: Implications for the oceanic mantle below Hawaii, J. Petrol., in press.

Clague, D.A., and Jarrard, R.D., 1973, Tertiary Pacific plate motion deduced from Hawaiian-Emperor chain, Geol. Soc. Amer. Bull., 84, 1135-1154.

Crough, S.T., 1978, Thermal origin of mid-plate hot-spot swells, Geophys. J. Roy. Astr. Soc., 55, 451-469.

Crough, S.T., Morgan, W.J., and Hargraves, R.B., 1980, Kimberlites: Their relation to mantle hot spots, Earth Planet. Sci. Lett., 50, 260-274.

Crough, S.T., and Thompson, G.A., 1976, Numerical and approximate solutions for lithospheric thickening and thinning, Earth Planet. Sci. Lett., 37, 107-116.

Crowley, J.C., and Giletti, B.J., 1982, A regional Rb/Sr isotopic and REE study of basalts from the Rio Grande Rift, N. Mex. and Colo., (abstract), EOS Trans. Amer. Geophys. Union, 63, 457.

Dalrymple, G.B., Lanphere, M.A., and Clague, D., 1980, Conventional and $^{40}Ar/^{39}Ar$ K-Ar ages of volcanic rocks from Ojin (site 430), Nintoku (site 432) and Suiko (site 433) seamounts and the chronology of volcanic propagation along the Hawaiian-Emperor chain, Initial Report Deep Sea Drilling Project, 55, 659-676.

Dasch, E.J., 1969, Sr isotopes in weathering profiles, deep-sea sediments and sedimentary rocks, Geochim. Cosmochim. Acta, 33, 1521-1552.

Davis, B.T.C., and Schairer, J.F., 1965, Melting relations in the join diopside-forsterite-pyrope at 40 kilobars and at one atmosphere, Carnegie Inst. Wash. Yearbook, 64, 123-134.

De Laeter, J.R., and Hosei, D.J., 1978, The abundance of Barium in stony meteorites, Earth Planet. Sci. Lett., 38, 416-420.

DePaolo, D.J., 1980, Crustal growth and mantle evolution: Inferences from models of element transport of Nd and Sr isotopes, Geochim. Cosmochim. Acta, 44, 1185-1196.

DePaolo, D.J., and Wasserburg, G.J., 1976a, Nd isotopic variations and petrogenetic models, Geophys. Res. Lett., 3, 249-252.

DePaolo, D.J., and Wasserburg, G.J., 1976b, Inferences about magma sources and mantle structure from variations of $^{143}Nd/^{144}Nd$, Geophys. Res. Lett., 3, 743-746.

DePaolo, D.J. and Wasserburg, G.J., 1977, The sources of island arcs as indicated by Nd and Sr isotopic studies, Geophys. Res. Lett., 4, 465-468.

Detrick, R.S. and S.T. Crough, 1978, Island subsidence, hot spots, and lithospheric thinning, J. Geophys. Res., 83, 1236-1244.

Dietz, R.S., and Menard, H.W., 1953, Hawaiian swell, deep, and arch and subsidence of the Hawaiian Islands, J. Geol., 61, 99-113.

Dosso, L. and Murthy, V.R., 1980, A Nd isotopic study of the Kerguelen islands: Inferences on enriched oceanic mantle sources, Earth Planet. Sci. Lett. 48, 268-276.

Duncan, R.A., and Compston, W., 1976, Sr-isotopic evidence for an old mantle source region for French Polynesian volcanism, Geology, 4, 728-732.

Easton, R.M., and Garcia, M.O., 1980, Petrology of the Hilina formation, Kilauea volcano, Hawaii, Bull. Volcanol., 43, 657-673.

Eaton, J.P., 1962, Crustal structure and volcanism in Hawaii, G.A. Macdonald and H. Kuno, eds., in The Crust of the Pacific Basin, Geophys. Monogr. 6, 13-29, Amer. Geophys. Union.

Eggler, D.H., 1978, The effect of CO_2 upon partial melting of peridotite in the system Na_2O-CaO-Al_2O_3-MgO-SiO_2-CO_2 to 35 Kb, with an analysis of melting in a peridotite-H_2O-CO_2 system, Amer. J. Sci., 278, 305-343.

Ellsworth, W.L., 1977, Three-dimensional structure of the crust and mantle beneath the island of Hawaii, Ph.D. Thesis, Mass. Inst. Tech., Cambridge, MA, 327 pp.

Eugster, O., Tera, F., and Wasserburg, G.J., 1969, Isotopic analyses of barium in meteorites and in terrestrial samples, J. Geophys. Res., 74, 3897-3908.

Feigenson, M.D., and Hofmann, A.W., 1980, Trace element geochemistry of Kohala volcano, Hawaii, Carnegie Inst. Wash. Yearbook 79, 472-476.

Feigenson, M.D., Hofmann, A.W., and Spera, F.J., 1982, Case studies on the origin of basalt II., The transition from tholeiitic to alkalic volcanism on Kohala volcano, Hawaii, Submitted to Cont. Miner. Petrol.

Feigenson, M.D., and Spera, F.J., 1980, Melt production by viscous dissipation: Role of heat advection by magma transport, Geophys. Res. Lett., 7, 145-148.

Feigenson, M.D., and Spera, F.J., 1981, Dynamical model for temporal variation in magma type and eruption interval at Kohala volcano, Hawaii, Geology, 9, 531-533.

Finnerty, T.A., 1977, Exchange of Mn, Ca, Mg and Al between synthetic garnet, orthopyroxene, clinopyroxene, and olivine, Carn. Inst. Wash. Yearbook, 76, 572-579.

Flanagan, F.J., 1973, 1972 values for international geochemical reference samples, Geochem. Cosmoch. Acta, 37, 1189-1200.

Flanagan, F.J., (ed.), 1976, Descriptions and analyses of eight new USGS rock standards, U.S. Geol. Survey Prof. Paper 840, 192 pp.

Fodor, R.V., and Keil, K., 1979, Review of the mineral chemistry of volcanic rocks from Maui, Hawaii, Hawaii Symposium on Intraplate Volcanism and Submarine Volcanism, abstract volume, 93-106.

Fodor, R.V., Keil, K., and Bunch, T.E., 1972, Mineral chemistry of volcanic rocks from Maui, Hawaii: Fe-Ti oxides (abstract), Geol. Soc. Amer. Abstract with program., 4, 507.

Fodor, R.V., Keil, K., and Bunch, T.E., 1975, Contributions to the mineral chemistry of Hawaiian rocks, IV., Pyroxenes in rocks from Haleakala and West Maui volcanoes, Maui, Hawaii, Contr. Miner. Petrol., 50, 173-195.

Fodor, R.V., Keil, K., and Bunch T.E., 1977, Contributions to the mineral chemistry of Hawaiian rocks, VI., Olivine in rocks from Haleakala and West Maui volcanoes, Maui, Hawaii, Pacific Sci., 31, 299-308.

Frey, F.A., 1980, The origin of pyroxenites and garnet pyroxenites from Salt Lake Crater, Oahu, Hawaii: Trace element evidence, Amer. J. Sci., 280-A, 427-449.

Frey, F.A., Bryan, W.B., and Thompson, G., 1974, Atlantic Ocean floor: Geochemistry and petrology of basalts from legs 2 and 3 of the Deep Sea Drilling Project, J. Geophys. Res., 79, 5507-5527.

Frey, F.A., and Clague, D.A., 1981, Minor and trace element geochemistry of basalt from Loihi seamount: Petrogenetic implications (abstract), EOS Trans. Amer. Geophys. Union, 62, 1082.

Frey, F.A., and Clague, D.A., 1982, Geochemistry of diverse basalt types from Loihi seamount, Hawaii, Earth Planet. Sci. Lett., submitted.

Frey, F.A., and Green, D.H., 1974, The mineralogy, geochemistry and origin of lherzolite inclusions in Victorian basanites, Geochim. Cosmochim. Acta, 38, 1023-1059.

Frey, F.A., Green, D.H., and Roy, S.D., 1978, Integrated models of basalt petrogenesis: A study of quartz tholeiites to olivine melilitites from southeastern Australia utilizing geochemical and experimental petrological data, J. Petrol., 19, 463-513.

Frey, F.A., and Prinz, M., 1978, Ultramafic inclusions from San Carlos, Arizona: Petrologic and geochemical data bearing on their petrogenesis, Earth Planet. Sci. Lett., 38, 129-176.

Furumoto, A.S., Wollard, G.P., Campbell, J.F., and Hussong, D.M., 1968, Variation in the thickness of the crust in the Hawaiian Archipelago, Geophys. Monogr. 12, 94-111, Amer. Geophys. Union.

Ganapathy, R., and Anders, E., 1974, Bulk composition of the Moon and Earth estimated from meteorites, Proc. Lunar Sci. Conf. 5th, 1181-1206.

Gast, P.W., 1968, Trace element fractionation and the origin of tholeiitic and alkaline magma types, Geochim. Cosmochim. Acta, 32, 1057-1086.

Goetze, C., 1978, The mechanisms of creep in olivine, Phil. Trans. Roy. Soc. London, A288, 99-119.

Green, D.H., and Ringwood, A.E., 1967, The genesis of basaltic magmas, Contr. Miner. Petrol., 15, 103-190.

Grove, T.L., and Bence, A.E., 1979, Crystallization kinetics in a multiply saturated basalt magma: An experimental study of Luna 24 ferrobasalt, Proc. Lunar Planet. Sci. Conf. 10th, 439-478.

Gunn, B.M., 1971, Trace element partition during olivine fractionation of Hawaiian basalts, Chem. Geol., 8, 1-13.

Hanson, G.N., 1977, Geochemical evolution of the suboceanic mantle, J. Geol. Soc. London, 134, 235-253.

Hanson, G.N., and Langmuir, C.H., 1978, Modeling of major elements in mantle-melt systems using trace element approaches, Geochim. Cosmochim. Acta, 42, 725-741.

Harrison, W.J., 1981, Partitioning of REE between minerals and coexisting melts during partial melting of a garnet lherzolite, Amer. Mineral. 66, 242-259.

Hart, R., 1970, Chemical exchange between seawater and deep ocean basalts, Earth Planet. Sci. Lett., 9, 269-279.

Hart, S.R., 1973, Submarine basalts from Kilauea rift, Hawaii: Nondependence of trace element composition on extrusion depth, Earth Planet. Sci. Lett., 20, 201-203.

Hart, S.R., 1976, LIL-element geochemistry, Leg 34 basalts, Initial Report Deep Sea Drilling Project, 34, 283-288, Washington, D.C.

Hart, S.R., and Brooks, C., 1974, Clinopyroxene-matrix partitioning of K, Rb, Cs, Sr and Ba, Geochim. Cosmochim. Acta, 38, 1799-1806.

Hart, S.R. and Brooks, C., 1977, The geochemistry of early Precambrian mantle, Contr. Miner. Petrol., 61, 109-128.

Hart, S.R., and Brooks, C., 1980, Sources of terrestrial basalts: An isotopic view point, in Basaltic Volcanism of the Terrestrial Planets, Chap. 7: Isotopic and trace element studies of basaltic volcanism; Basaltic volcanism study project, Lunar and Planetary Inst., Houston.

Hart, S.R., and Davis, K.E., 1978, Nickel partitioning between olivine and silicate melt, Earth Planet. Sci. Lett., 40, 203-219.

Hart, S.R., and Davis, K.E., 1979, Reply to D.B. Clarke and M.J. O'Hara, "Nickel and the existence of high-MgO liquids in nature", Earth Planet. Sci. Lett., 44, 159-161.

Hart, S.R., and A.J. Nawalk, 1970, K, Rb, Cs and Sr relationships in submarine basalts from the Puerto Rico trench, Geochim. Cosmochim. Acta, 34, 145-155.

Hart, S.R., Schilling, J.G., and Powell, J.L., 1973, Basalts from Iceland and along the Reykjanes Ridge: Sr isotope geochemistry, Nature, 246, 104-107.

Haskin, L.A., Frey, F.A., Schmitt, R.A., and Smith, R.H., 1968, Meteoritic, solar, and terrestrial rare-earth distributions, in L.H. Ahrens et al. (eds.), Physics and Chemistry of the Earth, 7, Pergamon Press, Oxford, 167-321.

Hawkesworth, C.J., O'Nions, R.K., Pankhurst, P.J., Hamilton, P.J., and Evensen, N.M., 1977, A geochemical study of island-arc and back-arc tholeiites from the Scotia Sea, Earth Planet. Sci. Lett., 36, 253-262.

Haxby, W.F., and Turcotte, D.L., 1978, On isostatic geoid anomalies, J. Geophys. Res., 83, 5473-5478.

Hedge, C.E., 1978, Strontium isotopes in basalts from the Pacific Ocean basin, Earth Planet. Sci. Lett., 38, 88-94.

Hofmann, A.W. and Hart, S.R., 1978, An assessment of local and regional isotopic equilibrium in the mantle, Earth Planet. Sci. Lett., 38, 44-62.

Hofmann, A.W., and White, W.M., 1982, Mantle plumes from ancient oceanic crust, Earth. Planet. Sci. Lett., 57, 421-436.

Hofmann, A.W., and Wright, T.L., 1979, Trace element fractionation and the nature of residual phases during tholeiite production in Hawaii, Carnegie Inst. Wash. Yearbook 78, 335-340.

Hofmann, A.W., White, W.M., and Whitford, D.J., 1978a, Geochemical constraints on mantle models: The case for a layered mantle, Carnegie Inst. Wash. Yearbook 77, 548-562.

Hofmann, A.W., T.L. Wright, and M. Feigenson, 1978b, Trace element and Sr isotope abundances in recent lavas from Kilauea, Hawaii, Carnegie Inst. Wash. Yearbook, 77, 590-596.

Irvine, T.N., 1977, Definition of primitive liquid compositions for basic magmas, Carnegie Inst. Wash. Yearbook, 76, 454-461.

Irvine, T.N., and Baragar, W.R.A., 1971, A guide to the chemical classification of the common volcanic rocks, Can. J. Earth Sci., 8, 523-548.

Ito, K., and Kennedy, G.C., 1968, Melting and phase relations in the plane tholeiite-lherzolite-nepheline basanite to 40 kilobars with geological implications, Contr. Miner. Petrol., 19, 177-211.

Jackson, E.D., 1968, The character of the lower crust and upper mantle beneath the Hawaiian Islands, Proc., 1, Internat. Geol. Cong., 23rd, Prague 1968, 135-150.

Jackson, E.D., and Shaw, H.R., 1975, Stress fields in central portions of the Pacific plate: Delineated in time by linear volcanic chains, J. Geophys. Res., 80, 1861-1874.

Jackson, E.D., and Wright, T.L., 1970, Xenoliths in the Honolulu volcanic series, Hawaii, J. Petrol., 11, 405-430.

Jacobsen, S.B. and Wasserburg, G.J., 1979, The mean age of mantle and crustal reservoirs, J. Geophys. Res., 84, 7411-7427.

Kaneoka, I., and Takaoka, N., 1980, Rare gas isotopes in Hawaiian ultramafic nodules and volcanic rocks, Science, 208, 1366-1368.

Kay, R.W., and Gast, P.W., 1973, The rare earth content and origin of alkali-rich basalts, J. Geol., 81, 653-682.

Kay, R.W., Hubbard, N.J., and Gast, P.W., 1970, Chemical characteristics and origin of oceanic ridge volcanic rocks, J. Geophys. Res., 75, 1585-1613.

Keil, K., Fodor, R.V., and Bunch, T.E., 1972, Contributions to the mineral chemistry of Hawaiian rock, II., Feldspars in rocks from Haleakala and West Maui volcanoes, Maui, Hawaii, Contr. Miner. Petrol., 37, 253-276.

Kennedy, W., 1933, Trends of differentiation in basaltic magmas, Amer. J. Sci., 25, 239-256.

Klerkx, J., Deutsch, S., and DePaepe, P., 1974, Rb, Sr content and Sr isotopic composition of strongly alkalic basaltic rocks from the Cape Verde Islands, Contr. Miner. Petrol., 45, 107-118.

Koyanagi, R.Y., and Endo, E.T., 1971, Hawaiian seismic events during 1969, U.S. Geol. Survey Prof. Paper 750-C, C158-C164.

Koyanagi, R.Y., Unger, J.D., Endo, E.T., and Okamura, A.T., 1976, Shallow earthquakes associated with inflation episodes at the summit of Kilauea volcano, Hawaii, O. Gonzales-Ferra ed., in Proceedings of the

Symposium on Andean and Antarctic Volcanology Problems, 621-631, Santiago, Chile, September 1974.

Kuno, H., 1969, Mafic and ultramafic nodules in basaltic rocks of Hawaii, Geol. Soc. Amer. Mem. 115, 189-234.

Kurz, M.D., Jenkins, W.J., and Hart, S.R., 1982a, Helium isotopic systematics of oceanic islands and mantle heterogeneity, Nature, 297, 43-47.

Kurz, M.D., Jenkins, W.J., Schilling, J.-G., and Hart, S.R., 1982b, Helium isotopic variations in the mantle beneath the central North Atlantic Ocean, Earth Planet. Sci. Lett., 58, 1- .

Kushiro, I., 1965, The liquidus relations in the system forsterite-$CaAl_2SiO_6$-silica and forsterite-nepheline-silica at high pressures, Carnegie Inst. Wash. Yearbook, 64, 103-109.

Kushiro, I., 1968, Compositions of magmas formed by partial zone melting of the earth's upper mantle, J. Geophys. Res., 73, 619-634.

Kushiro, I., 1969, Discussion of paper "The origin of basaltic and nephelinitic magmas in the earth's mantle," by D.H. Green, Tectonophys., 7, 427-436.

Kushiro, I., 1973, Origin of some magmas in oceanic and circumoceanic regions, Tectonophys., 17, 211-222.

Lanphere, M.A., 1982, $^{87}Sr/^{86}Sr$ ratios for basalt from Loihi seamount, Hawaii, Earth Planet. Sci. Lett., submitted.

Lanphere, M.A., and Dalrymple, G.B., 1980, Age and strontium isotopic composition of the Honolulu volcanic series, Oahu, Hawaii, Amer. J. Sci., 280-A, 736-751.

Lanphere, M.A., Dalrymple, G.B., and Clague, D.A., 1980, Rb-Sr systematics of basalts from the Hawaiian-Emperor volcanic chain, Initial Report Deep Sea Drilling Project, 55, 695-706.

Langmuir, C.H., and Hanson, G.N., 1980, An evaluation of major element heterogeneity in the mantle sources of basalts, Phil. Trans. Roy. Soc. London, A297, 383-407.

Langmuir, C.H., Vocke, Jr., R.D., Hanson, G.N., and Hart, S.R., 1978, A general mixing equation with applications to Icelandic basalts, Earth Planet. Sci. Lett., 18, 380-392.

Leeman, W.P., Budahn, J.R., Gerlach, D.C., Smith, D.R., and Powell, B.N., 1980, Origin of Hawaiian tholeiites: Trace element constraints, Amer. J. Sci., 280-A, 794-819.

Leeman, W.P., Murali, A.V., Ma, M.-S., and Schmitt, R.A., 1977, Mineral constitution of mantle source regions for Hawaiian basalts-rare earth element evidence for mantle heterogeneity, in Dick, H.J.B. (ed.), Magma Genesis, Bull. Oregon Dept. Geol. Miner. Ind. 96, 169-183.

Lipman, P.W., and Mehnert, H.H., 1975, Late Cenozoic basaltic volcanism and development of the Rio Grande depression in the southern Rocky Mountains, Geol. Soc. Amer. Mem., 144, 119-154.

Longhi, J., Walker, D., and Hays, J.F., 1978, The distribution of Fe and Mg between olivine and lunar basaltic liquids, Geochim. Cosmochim. Acta, 42, 1545-1558.

Lugmair, G.W., and Marti, K., 1977, Evolution of the lunar interior: Sm-Nd systematics of A15 green glass and the question of lunar initial $^{143}Nd/^{144}Nd$, Lunar Sci. Conf. 8th Abstract, 597-599.

Lugmair, G.W., Scheinin, N.B., and Marti, K., 1975, Search for extinct ^{146}Sm, 1. The isotopic abundance of ^{142}Nd in the Juvinas meteorite, Earth Planet. Sci. Lett., 27, 79-84.

Lussiaa-Berdou-Polve, M., and Vidal, P., 1973, Initial Sr Isotopic composition of volcanic rocks from Jan Mayen and Spitsbergen, Earth Planet. Sci. Lett., 18, 333-338.

Macdonald, G.A., 1949, Hawaiian petrographic province, Geol. Soc. Amer. Bull., 60, 1541-1596.

Macdonald, G.A., 1968, Composition and origin of Hawaiian lavas, Geol. Soc. Amer. Mem., 116, 477-522.

Macdonald, G.A., and T. Katsura, 1964, Chemical composition of Hawaiian lavas, J. Petrol., 5, 82-133.

Macdonald, G.A., and Powers, H.A., 1968, A further contribution to the petrology of Haleakala volcano, Hawaii, Bull. Geol. Soc. Amer., 79, 877-888.

MacGregor, I.D., 1965, Stability fields of spinel and garnet peridotites in the synthetic system $MgO-CaO-Al_2O_3-SiO_2$, Carnegie Inst. Wash. Yearbook 64, 126-134.

MacGregor, I.D., 1968, Mafic and ultramafic inclusions as indicators of the depth of origin of basaltic magmas, J. Geophys. Res., 73, 3737-3745.

Mason, B., 1979, Data of geochemistry, 6th Edition, Chapter B, Cosmochemistry, pt. 1, Meteorites, U.S. Geol. Survey Prof. Paper, 440-B-1.

McDougall, I., 1964, Potassium-argon ages from lavas of the Hawaiian Islands, Bull. Geol. Soc. Amer., 75, 107-128.

McDougall, I., 1971, Volcanic island chains and sea floor spreading, Nature, 231, 141-144.

Menzies, M., and Murthy, V.R., 1980a, Nd and Sr isotope geochemistry of hydrous mantle nodules and their host alkali basalts: Implications for local heterogeneities in metasomatically veined mantle, Earth Planet. Sci. Lett., 46, 323-334.

Menzies, M., and Murthy, V.R., 1980b, Mantle metasomatism as a precursor to the genesis of alkaline magmas - isotopic evidence, Amer. J. Sci., 280-A, 622-638.

Minster, J.B., Jorden, T.H., Molnar, P., and Haines, E., 1974, Numerical modeling of instantaneous plate tectonics, Geophys. J. Roy. Astr. Soc., 36, 541-576.

Minster, J.B., and Jorden, T.H., 1978, Present-day plate motions, J. Geophys. Res., 83, 5331-5354.

Minster, J-F., and Allegre, C.J., 1978, Systematic use of trace elements in igneous processes, Part III: Inverse problem of batch partial melting in volcanic suites, Contr. Miner. Petrol., 68, 37-52.

Minster, J-F., Minster, J.B., Treuil, M., and Allegre, C.J., 1977, Systematic use of trace elements in igneous processes. Part II: Inverse problem of the fractional crystallization process in volcanic suites, Contr. Miner. Petrol., 61, 49-77.

Minster, J.-F., Ricard, L.-P., and Allegre, C.J., 1979, ^{87}Rb-^{87}Sr chronology of enstatite meteorites, Earth Planet. Sci. Lett., 44, 420-440.

Molnar, P., and Atwater, T., 1973, Relative motion of hot-spots in the mantle, Nature, 246, 288-291.

Moore, J.G., 1966, Rate of palagonitization of submarine basalt adjacent to Hawaii, U.S. Geol. Survey Prof. Paper, 550-D, D163-D171.

Moore, J.G., Clague, D.A., and Normark, W.R., 1982, Diverse basalt types from Loihi seamount, Hawaii, Geology, 10, 88-92.

Morgan, W.J., 1971, Convection plumes in the lower mantle, Nature, 230, 42-43.

Morgan, W.J., 1972, Plate motions and deep mantle convection, Geol. Soc. Amer. Mem., 132, 7-22.

Nicolas, A., and Poirier, J.P., 1976, Crystalline plasticity and solid state flow in metamorphic rocks, Wiley, N.Y., 444 pp.

O'Hara, M.J., 1968, The bearing of phase equilibria studies in synthetic and natural systems on the origin and evolution of basic and ultrabasic rock, Earth Sci. Reviews, 4, 69-133.

O'Hara, M.J., Saunders, M.J., and Mercy, E.L.P., 1975, Garnet-peridotite, primary ultrabasic magma, and eclogite: Interpretation of upper mantle processes in kimberlite, Phys. Chem. Earth, 9, 571-604.

O'Hara, M.J., and Mathews, R.E., 1981, Geochemical evolution in an advancing, periodically replenished, periodically tapped, continuously fractionated magma chamber, J. Geol. Soc. London, 138, 237-277.

O'Neil, J.R., Hedge, C.E., and Jackson, E.D., 1970, Isotopic investigations of xenoliths and host basalts from the Honolulu volcanic series, Earth Planet. Sci. Lett., 8, 253-257.

O'Nions, R.K., and Pankhurst, R.J., 1974, Petrogenetic significance of isotope and trace element variations in volcanic rocks from the Mid-Atlantic, J. Petrol., 15, 603-634.

O'Nions, R.K., Hamilton, P.J., and Evensen, N.M., 1977, Variations in $^{143}Nd/^{144}Nd$ and $^{87}Sr/^{86}Sr$ ratios in oceanic basalts, Earth Planet. Sci. Lett., 34, 13-22.

O'Nions, R.K., Evensen, N.M., and Hamilton, P.J., 1980, Differentiation and evolution of the mantle, Phil. Trans. Royal Soc. London, A297, 479-493.

Oostdam, B.L., 1965, Age of lava flows on Haleakala, Maui, Hawaii, Bull. Geol. Soc. Amer., 76, 393-394.

Ottonello, G., 1980, Rare earth abundances and distribution in some spinel peridotite xenoliths from Assab (Ethiopia), Geochim. Cosmochim. Acta, 44, 1885-1901.

Parmentier, E.M., Turcotte, D.L., and Torrance, K.E., 1975, Numerical experiments on the structure of mantle plumes, J. Geophys. Res., 50, 4417-4424.

Pearce, J.A., and Norry, M.J., 1979, Petrogenetic implications of Ti, Zr, Y and Nb variations in volcanic rocks, Contr. Miner. Petrol., 69, 33-47.

Philpotts, J.A. and Schnetzler, C.C., 1970, Phenocryst-matrix partition coefficients for K, Rb, Sr, and Ba with applications to anorthosite and basalt genesis, Geochim. Cosmochim. Acta, 34, 307-322.

Philpotts, J.A., Schnetzler, C.C., and Thomas, H.H., 1972, Petrogenetic implications of some new geochemical data on ecologite and ultrabasic inclusions, Geochim. Cosmochim. Acta, 36, 1131-1166.

Powell, J.L., and Delong, S.E., 1966, Isotopic composition of strontium in volcanic rocks from Oahu, Science, 153, 1239-1242.

Powers, H.A., 1935, Differentiation of Hawaiian lavas, Amer. J. Sci., 30, 57-71.

Powers, H.A., 1955, Composition and origin of basaltic magma of the Hawaiian Islands, Geochim. Cosmochim. Acta, 7, 77-107.

Presnall, D.C., Dixon, J.R., O'Donnell, T.H., and Dixon, S.A., 1979, Generation of mid-ocean ridge tholeiites, J. Petrol., 20, 3-35.

Reid, J.B., and Frey, F.A., 1971, Rare earth distribution in lherzolite and garnet pyroxenite xenoliths and the constitution of the upper mantle, J. Geophys. Res., 76, 1184-1196.

Richard, P., Shimizu, N., and Allegre, C.J., 1976, $^{143}Nd/^{146}Nd$, a natural tracer: An application to oceanic basalts, Earth Planet. Sci. Lett., 31, 269-278.

Ringwood, A.E., 1975, Composition and petrology of the earth's mantle, McGraw-Hill, N.Y., 618 pp.

Roden, M.F., 1982, Geochemistry of the earth's mantle, Nunivak Island, Alaska and other areas: Evidence from xenolith studies, Ph.D. thesis, Mass. Inst. Tech., Cambridge, MA.

Roden, M.F., Frey, F.A., and Francis, D.M., 1980, REE, K, Rb, Sr and Sr isotopic geochemistry of peridotite xenoliths in basalt from Nunivax Island, Alaska, (abstract), EOS Trans. Amer. Geophys. Union, 61, 401.

Roden, M.F., Frey F.A. and Hart, S.R., 1981, The mantle source for the Honolulu volcanic series: Nd isotopic evidence (abstract), EOS, Trans. Amer. Geophys. Union, 62, 423.

Roeder, P.L., and Emslie, R.F., 1970, Olivine-liquid equilibrium, Contr. Miner. Petrol., 29, 275-289.

Ross, C.S., Foster, M.D., and Myers, A.T., 1954, Origin of dunites and of olivine-rich inclusions in basaltic rocks, Amer. Mineral., 39, 693-737.

Schilling, J.G., 1966, Rare-earth fractionation in Hawaiian volcanic rocks, Ph.D., thesis, Mass. Inst. of Tech., Cambridge, MA, 390 pp.

Schilling, J.G., 1973, Iceland mantle plume: Geochemical evidence along Reykjanes Ridge, Nature, 242, 565-571.

Schilling, J.G., 1975, Azores mantle blob: Rare earth evidence, Earth Planet. Sci. Lett., 25, 103-115.

Schilling, J.G., and Winchester, J.W., 1967, Rare-earth fractionation and magmatic processes, Runcorn, S.K. ed., in Mantles of earth and terrestrial planets, 267-283, Interscience.

Schnetzler, C.C., and Philpotts, J.A., 1970, Partition coefficients of rare-earth elements between igneous matrix mineral and rock forming phenocrysts - II, Geochem. Cosmochem. Acta, 34, 331-340.

Schroeder, B., Thompson, G., Sulanowska, M., and Ludden, J.N., 1980, Analysis of geologic materials using an automated X-ray fluorescence system, X-ray Spectrometry, 9, 198-205.

Sclater, J.G., Crowe, J., and Anderson, R.N., 1976, On the reliability of oceanic heat flow averages, J. Geophys. Res., 81, 2997-3006.

Sclater, J.G., Lawver, L.A., and Parsons, B., 1975, Comparison of long-wavelength residual elevation and free air gravity anomalies in the North Atlantic and possible implications for the thickness of the lithospheric plate, J. Geophys. Res., 80, 1031-1052.

Shaw, D.M., 1970a, Trace element fractionation during anatexis, Geochim. Cosmochim. Acta, 34, 237-243.

Shaw, H.R., 1969, Rheology of basalt in the melting range, J. Petrol., 10, 510-535.

Shaw, H.R., 1970b, Earth tides, global heat flow, and tectonics, Science, 168, 1084-1087.

Shaw, H.R., 1973, Mantle convection and volcanic periodicity in the Pacific: Evidence from Hawaii, Geol. Soc. Amer. Bull., 84, 1505-1526.

Shaw, H.R., 1980, The fracture mechanism of magma transport from the mantle to the surface, in Physics of Magmatic Processes, Hargraves, R.B., ed., Princeton University Press, Princeton, N.J., 201-264.

Shaw, H.R., and Jackson, E.D., 1973, Linear island chains in the Pacific: Result of thermal plumes or gravitational anchors?, J. Geophys. Res., 78, 8634-8652.

Shih, C.-Y., 1972, The rare earth geochemistry of oceanic igneous rocks, Ph.D. Thesis, Columbia University, N.Y.

Shimizu, N., 1974, An experimental study of the partitioning of K, Rb, Cs, Sr and Ba between clinopyroxene and liquid at high pressures, Geochim. Cosmochim. Acta, 38, 1789-1798.

Shimizu, N., 1975, Rare earth elements in garnets and clinopyroxenes from garnet lherzolite nodules in kimberlites, Earth Planet. Sci. Lett., 25, 26-32.

Shimizu, N., and Kushiro, I., 1975, The partitioning of rare earth elements between garnet and liquid at high pressures: Preliminary experiments, Geophys. Res. Lett., 2, 413-416.

Shor, G.G., Jr., and Pollard, D.D., 1964, Mohole site selection studies north of Maui, J. Geophys. Res., 69, 1627-1637.

Simkin, T., and Smith, J.V., 1970, Minor-element distribution in olivine, J. Geol., 78, 304-325.

Smith, E.L., and Stupak, W.A., 1978, A Fortran program for the classification of volcanic rocks using the Irvine and Baragar classification scheme, Computer and Geosciences, 4, 89-99.

Staudigel, H., Hart, S.R., Zindler, A., Lanphyre, M., Chen, C.Y., and Clague, D., 1981, Pb, Nd, Sr isotopes of Loihi Seamount, Hawaii, (abstract), EOS Trans. Amer. Geophys. Union, 62, 1083.

Stearns, H.T., and Macdonald, G.A., 1942, Geology and ground-water resources of the Island of Maui, Hawaii, Hawaii Div. Hydrography, Bull., 7, 344 pp.

Stosch, H.-G., Carlson, R.W., and Lugmair, G.W., 1980, Episodic mantle differentiation: Nd and Sr isotopic evidence, Earth Planet. Sci. Lett., 47, 263-271.

Stosch, H.-G. and Seck, H.A., 1980, Geochemistry and mineralogy of two spinel peridotite suites from Dreiser Weiher, West Germany, Geochim. Cosmochim. Acta, 44, 457-470.

Sun, S.-S., 1973, Lead isotope studies of young volcanic rocks from oceanic islands, mid-ocean ridges and island arcs, Ph.D. Thesis, Columbia University, New York.

Sun, S.-S., and Hanson, G.N., 1975, Origin of Ross Island basanitoids and limitations upon the heterogeneity of mantle sources for alkali basalts and nephelinites, Contr. Miner. Petrol., 52, 77-106.

Sun, S.-S. and Hanson, G.N., 1976, Evolution of the mantle: Geochemical evidence from alkali basalt: Reply, Geology, 4, 626-631.

Sun, S.-S., and Jahn, B.M., 1975, Lead and strontium isotopes in post glacial basalts from Iceland, Nature, 255, 527-530.

Sun, S.-S., and Nesbitt, R.W., 1977, Chemical heterogeneity of the Archean mantle, composition of the earth and mantle evolution, Earth Planet. Sci. Lett., 35, 429-448.

Sun, S.-S., Nesbitt, R.W., and Sharaskin, A. Ya., 1979, Geochemical characteristics of mid-ocean ridge basalts, Earth Planet. Sci. Lett., 44, 119-138.

Tatsumoto, M., 1978, Isotopic composition of lead in oceanic basalt and its implication to mantle evolution, Earth Planet. Sci. Lett., 38, 63-87.

Tatsumoto, M., Hedge, C.E., and Engel, A.E.J., 1965, Potassium, rubidium, strontium, thorium, uranium, and the ratio of strontium-87 to strontium-86 in oceanic tholeiitic basalt, Science, 150, 886-888.

Thompson, G., 1973, A geochemical study of the low-temperature interaction of seawater and oceanic igneous rocks, EOS Trans. Amer. Geophys. Union, 54, 1015-1019.

Tilley, C.E., 1950, Some aspects of magmatic evolution, Proc. Geol. Soc., London, 16, 37-71.

Tilley, C.E., and Scoon, J.H., 1961, Differentiation of Hawaiian basalts: Trends of Mauna Loa and Kilauea historic magma, Amer. J. Sci., 259, 60-68.

Unger, J.D., and Ward, P.L., 1979, A large deep Hawaiian earthquake - the Honomu, Hawaii event on April 16, 1973, Bull. Seism. Soc. Amer., 69, 1771-1781.

Walker, D., Shibata, T., and Delong, S.E., 1979, Abyssal tholeiites from the Oceanographer fracture zone, II. Phase equilibria and mixing, Contr. Miner. Petrol., 70, 111-125.

Watson, E.B., 1979, Calcium content of forsterite coexisting with silicate liquid in the system Na_2O-CaO-MgO-Al_2O_3-SiO_2, Amer. Mineral., 64, 824-829.

Watts, A.B., 1976, Gravity and bathymetry in the central Pacific Ocean, J. Geophys. Res., 81, 1533-1553.

White, R.W., 1966, Ultramafic inclusions in basaltic rocks from Hawaii, Contr. Miner. Petrol., 12, 245-314.

White, W.M., and Schilling, J.G., 1978, The nature and origin of geochemical variation of mid-Atlantic ridge basalts from central North Atlantic, Geochim. Cosmochim. Acta, 42, 1501-1516.

Wilshire, H.G., and Pike, J.E.N., 1975, Upper mantle diapirism: Evidence from analogous features in alpine peridotite and ultramafic inclusions in basalt, Geology, 3, 467-470.

Wilshire, H.G., and Shervais, J.W., 1975, Al-augite and Cr-diopside ultramafic xenoliths in basaltic rocks from western United States, Phys. Chem. Earth, 9, 257-272.

Wilson, J.T., 1963a, A possible origin of the Hawaiian Islands, Can. J. Phys., 41, 863-870.

Wilson, J.T., 1963b, Evidence from islands on the spreading of ocean floors, Nature, 197, 536-538.

Wood, D.A., Joron, J.-L., and Treuil, M., 1979a, A re-appraisal of the use of trace elements to classify and discriminate between magma series erupted in different tectonic settings, Earth Planet. Sci. Lett., 45, 326-336.

Wood, D.A., Joron, J.-L., Treuil, M., Norry, M., and Tarney, J., 1979b, Elemental and Sr isotope variations in basic lavas from Iceland and the surrounding ocean floor, Contr. Miner. Petrol., 70, 319-339.

Wood, D.A., Tarney, J., Varet, J., Saunders, A.D., Bougault, J., Joron, J.L., Treuil, M., and Cann, J.R., 1979c, Geochemistry of basalts drilled in the North Atlantic by IPOD, Leg 49: Implications for mantle heterogeneity, Earth Planet. Sci. Lett., 42, 77-97.

Wright, T.L., 1971, Chemistry of Kilauea and Mauna Loa lava in space and time, U.S. Geol. Survey Prof. Pap., 735.

Wright, T.L., 1981, Generation of Hawaiian tholeiite: A metasomatic model, (abstract), EOS Trans. Amer. Geophys. Union, 62, 1068.

Wright, T.L., and Doherty, P.C., 1970, A linear programming and least-squares method for solving petrologic mixing problems, Geol. Soc. Amer. Bull., 81, 1995-2008.

Yoder, H.S., and Tilley, C.E., 1962, Origin of basalt magmas: An experimental study of natural and synthetic systems, J. Petrol., 3, 342-352.

Zindler, A., 1980, Geochemical processes in the earth's mantle and the nature of crustal-mantle interactions: Evidence from studies of Nd and Sr isotope ratios in mantle derived igneous rocks and lherzolite nodules, Ph.D. Thesis, Mass. Inst. of Tech., Cambridge, MA, 263 pp.

Zindler, A., and Jagoutz, E., 1980, Isotope and trace element systematics in mantle derived peridotite nodules from San Carlos, (abstract), EOS Trans. Amer. Geophys. Union, 61, 374.

Zindler, A., Jagoutz, E., and Goldstein, S., 1982, Nd, Sr, and Pb isotopic systematics in a three-component mantle: A new perspective, Nature, 298, 519-523.

Zhou, X., and Armstrong, R.L., 1982, Cenozoic volcanic rocks of eastern China - secular and geographic trends in chemistry and strontium isotopic composition, Earth Planet. Sci. Lett., 58, 301-329.

Appendix 1 Sample Descriptions

HO-1: Tholeiite with common olivine phenocrysts, plagioclase microphenocrysts, and very rare clinopyroxene phenocrysts. The rims of olivine phenocrysts altered to brownish. Moderately vesicular.

HO-2: Tholeiite with common olivine phenocrysts and abundant plagioclase microphenocrysts. The rims of olivine altered. Highly vesicular.

HO-3: Tholeiite with rare olivine phenocrysts and common plagioclase phenocrysts. Rims of olivine altered slightly. Highly vesicular.

HO-4: Tholeiite with common olivine, rare clinopyroxene and rare plagioclase phenocrysts. Rims of olivine altered slightly. Moderate vesicular.

HO-5: Similar to HO-4 but with less olivine phenocrysts.

C121: Tholeiite with common olivine, rare clinopyroxene and rare plagioclase phenocrysts. Moderate iddingsite on rims of olivine.

C122: Tholeiite with abundant olivine phenocryst and very rare clinopyroxene phenocrysts. Fresh.

C123: Tholeiite with abundant olivine phenocrysts and rare clinopyroxene phenocrysts. Slightly altered.

C124: Alkalic basalt with common plagioclase phenocrysts. Moderately altered.

C125: Transitional basalt with common plagioclase phenocrysts. Highly altered.

C126: Transitional basalt with abundant plagioclase and common olivine phenocryst. Moderately altered.

H85-1: Alkalic basalt with rare plagioclase microphenocryst. Moderate vesicular.

H85-2: Hawaiite with rare plagioclase microphenocrysts and very rare biotite.

H85-3: Hawaiite with rare plagioclase microphenocrysts.

H85-4, H85-5 and H85-6: Hawaiite. Aphyric.

H85-7: Alkalic basalt with common clinopyroxene, common plagioclase phenocrysts and rare olivine phenocrysts.

H85-8: Alkalic basalt with rare plagioclase and clinopyroxene phenocrysts.

H85-9: Alkalic basalt with rare clinopyroxene phenocrysts and rare plagioclase microphenocrysts.

H85-10: Alkalic basalt with a few clinopyroxene megacrysts and rare plagioclase and rare olivine phenocrysts.

H85-11: Hawaiite with rare clinopyroxene microphenocrysts and rare plagioclase microphenocrysts.

H85-12: Alkalic basalt with rare olivine megacrysts, rare plagioclase microphenocrysts and rare clinopyroxene microphenocrysts.

H85-13: Alkalic basalt, aphyric.

H85-14: Alkalic basalt with common clinopyroxene phenocrysts, few olivine phenocrysts common plagioclase microphenocrysts and rare magnetite phenocrysts.

H85-15: Alkalic basalt with common olivine phenocrysts, common clinopyroxene phenocrysts, common plagioclase phenocrysts and microphenocrysts and rare magnetite phenocrysts. Moderately vesicular.

H85-16, H85-17, H85-18, H85-19, H85-20: Hawaiites. Aphyric.

H85-21: Alkalic basalt with common olivine phenocrysts, and a few clinopyroxene phenocrysts. Rims of olivine slightly altered. Slightly vesicular.

H85-22: Alkalic basalt. Aphyric. Slightly vesicular.

H85-23: Alkalic basalt. Aphyric. Slightly vesicular.

H85-24, H85-25, H85-26, H85-27, H85-28, H85-29, H85-30, H85-31: Mugearites. Aphyric.

H85-32, H85-33: Hawaiites with rare magnetite and rare olivine microphenocrysts. Slightly vesicular.

H65-1: Hawaiite. Aphyric.

H65-2: Mugearite with rare plagioclase microphenocryst.

H65-3: Mugearite. Aphyric.

H65-4: Alkalic basalt with common olivine phenocrysts and a few clinopyroxene phenocryst. Slightly vesicular.

H65-5, H65-6, H65-7: Hawaiites. Aphyric.

H65-8: Alkalic basalt with common clinopyroxene and common olivine phenocrysts.

H65-9, H65-10: Similar to H65-8.

H65-11: Alkalic basalt with common clinopyroxene, few olivine phenocrysts and rare plagioclase.

H65-12: Alkalic basalt with rare clinopyroxene phenocrysts. Slightly altered.

H65-13: Ankaramite with abundant clinopyroxene crystals, a few olivine crystals and rare plagioclase microphenocrysts.

H65-14: Similar to H65-13.

H62-47: Alkalic basalt with common olivine phenocrysts and few clinopyroxene phenocryst. Slightly vesicular.

H62-48: Similar to H62-47.

H62-49: Alkalic basalt with common olivine phenocrysts, common clinopyroxene phenocrysts and rare magnetite microphenocryst. Moderately vesicular.

H62-52: Hawaiite with rare olivine, clinopyroxene and magnetite microphenocrysts.

Appendix 2 Major Element Abundances[1] (wt%) of Haleakala Basalts

	BCR-1	BHVO-1	HO-1	HO-2	HO-3	HO-4	HO-5	C121	C122	C123
Rock[2]	Th	Th	Th	Th	Th	Th	Th	Th	Th	Th
SiO_2	55.37	49.98	47.97	47.24	48.53	48.22	48.19	48.38	48.96	46.62
Al_2O_3	13.83	13.89	15.69	15.75	13.29	14.00	13.93	14.09	10.35	12.03
FeO	12.30	11.84	13.31	13.85	13.13	12.89	13.16	12.83	12.53	13.11
MgO	3.52	7.02	8.39	7.74	10.44	9.57	10.12	9.31	16.46	15.67
CaO	7.03	11.87	9.85	9.55	10.27	10.82	10.29	10.66	7.94	8.06
Na_2O	3.33	2.20	2.53	2.06	2.02	2.17	2.18	1.92	1.31	1.65
K_2O	1.73	0.49	0.25	0.21	0.30	0.13	0.15	0.14	0.26	0.15
TiO_2	2.24	2.90	2.93	2.96	2.55	2.75	2.74	2.55	1.90	2.34
P_2O_5	0.37	0.15	0.27	0.27	0.27	0.24	0.27	0.20	0.28	0.40
total	99.72	100.54	101.19	99.63	100.80	100.78	101.03	100.08	99.99	100.03

	H62-1	H62-1*	H62-2	H62-2*	H62-3	H62-4	H62-5	H62-6	H62-7	H62-8
Rock[2]	AB	AB	AB	AB	AB	AB	ha	ha	ha	ha
Depth[3]	305	305	302	302	298	297	295	292	291	282
SiO_2	46.26	46.10	46.38	46.64	47.00	46.29	48.77	48.58	48.96	49.62
Al_2O_3	15.67	15.59	15.56	15.64	15.73	16.03	17.93	17.89	17.79	17.83
FeO	13.49	13.32	13.50	13.58	13.79	12.58	11.66	11.45	11.56	11.39
MgO	4.74	4.67	4.98	4.79	4.96	6.37	3.85	3.87	3.90	3.95
CaO	10.61	10.65	10.60	10.59	10.55	11.02	7.47	7.47	7.39	7.37
Na_2O	3.23	3.26	3.98	3.79	3.60	3.54	5.22	5.78	4.77	4.89
K_2O	1.12	1.12	1.14	1.14	1.15	0.99	1.77	1.81	1.81	1.79
TiO_2	3.87	3.87	3.87	3.90	3.92	3.51	3.03	3.04	3.05	2.92
P_2O_5	0.32	0.33	0.31	0.29	0.27	0.30	0.78	0.82	0.80	0.77
total	99.30	98.91	100.28	100.37	100.97	100.63	100.50	100.70	100.03	100.53

Appendix 2 (cont'd)

	H62-9	H62-10	H62-11	H62-12	H62-13	H62-14	H62-15	H62-15A	H62-16	H62-17
Rock	ha	ha	ha	AB	AB	AB	ha	ha	mu	mu
Depth	253	252	234	213	211	203	189	187	180	179
SiO_2	48.63	48.60	50.03	44.80	45.06	44.79	50.02	49.67	52.22	51.98
Al_2O_3	17.05	17.10	16.79	15.03	14.76	14.53	18.06	18.20	18.67	18.13
FeO	12.21	12.46	11.44	13.87	14.21	15.18	10.37	10.31	9.62	9.51
MgO	4.45	4.32	3.58	8.78	8.94	6.38	3.41	3.50	2.83	2.76
CaO	7.75	7.69	7.44	11.63	11.79	11.43	7.27	7.32	6.18	6.13
Na_2O	4.45	4.31	5.73	2.40	2.42	2.94	6.09	5.25	6.98	6.33
K_2O	1.42	1.42	1.73	0.68	0.68	0.95	1.95	1.94	2.37	2.35
TiO_2	3.48	3.55	3.03	3.00	3.00	3.51	2.67	2.69	2.10	2.11
P_2O_5	0.60	0.59	0.94	0.29	0.27	0.32	0.89	0.91	0.88	1.00
total	100.08	100.02	100.70	100.48	101.14	100.03	100.75	99.79	101.87	100.31

	H62-8	H62-19	H62-20	H62-21	H62-22	H62-23	H62-24	H62-25	H62-25*	H62-26
Rock	mu	ha	ha	ha	ha	ha	ha	mu	mu	mu
Depth	172	165	162	157	153	150	147	147	147	144
SiO_2	51.80	47.32	48.32	47.32	49.68	47.29	48.44	53.08	51.76	51.80
Al_2O_3	18.14	17.06	17.49	17.00	17.83	17.17	17.40	18.24	17.79	17.83
FeO	9.43	12.39	11.57	11.51	12.17	12.07	12.64	9.73	9.70	9.93
MgO	2.67	4.49	3.97	3.84	4.25	4.24	4.41	2.81	2.74	2.83
CaO	6.10	8.93	8.38	8.16	8.73	8.71	8.89	6.17	6.17	6.40
Na_2O	6.66	5.34	4.95	5.40	5.09	5.03	4.82	6.81	6.49	6.71
K_2O	2.39	1.43	1.59	1.62	1.58	1.47	1.40	2.25	2.28	2.19
TiO_2	2.09	3.87	3.39	3.34	3.53	3.71	3.74	2.18	2.22	2.33
P_2O_5	1.02	0.49	0.64	0.74	0.47	0.56	0.45	0.98	1.05	0.99
total	100.30	101.32	100.32	98.94	108.33	100.26	102.20	102.26	100.18	101.07

Appendix 2 (cont'd)

	H62-27	H62-28	H62-29	H62-30	H62-31	H62-32	H62-33	H62-34A	H62-35	H62-36
Rock[2]	ha	ha	ha	ha	ha	ha	ha	ha	ha	ha
Depth[3]	142	141	134	133	130	128	125	124	117	110
SiO_2	48.75	49.31	48.04	48.13	48.20	47.37	50.74	52.20	52.20	48.16
Al_2O_3	17.25	17.60	17.21	17.26	17.79	17.07	18.18	18.18	18.29	16.92
FeO	10.98	11.49	11.58	11.63	12.07	11.76	10.14	10.60	10.65	12.23
MgO	3.58	4.03	4.00	3.97	4.23	4.14	3.13	2.93	3.00	4.16
CaO	7.60	7.96	8.25	8.30	8.51	8.43	7.11	6.95	6.97	8.48
Na_2O	5.93	6.00	5.66	5.39	5.73	4.20	5.39	5.21	4.95	4.87
K_2O	1.82	1.69	1.58	1.55	1.55	1.47	2.12	1.97	2.07	1.54
TiO_2	3.02	3.26	3.50	3.50	3.60	3.60	2.64	2.28	2.28	3.31
P_2O_5	0.92	0.76	0.68	0.67	0.47	0.71	0.95	0.91	0.91	0.60
total	99.85	102.10	100.51	100.40	102.15	98.75	100.40	101.24	101.34	100.26

	H62-37	H62-38	H62-39	H62-40	H62-41	H62-42	H62-43	H62-44	H62-45	H62-46
Rock[2]	ha	ha	ha	ha	ha	ha	ha	AB	ha	ha
Depth[3]	109	105	91	90	83	80	74	73	72	71
SiO_2	48.41	48.06	47.10	46.99	47.50	46.81	46.86	44.97	46.50	46.15
Al_2O_3	17.06	17.04	17.93	18.04	18.63	18.40	18.29	15.21	18.15	17.94
FeO	12.05	12.10	12.02	12.06	11.17	11.36	11.69	14.20	11.78	11.84
MgO	4.11	4.19	4.38	4.47	4.08	4.18	4.38	9.03	4.46	4.38
CaO	8.54	8.53	8.43	8.46	8.66	8.71	8.86	11.43	8.76	8.95
Na_2O	4.58	4.82	5.27	5.10	6.19	6.17	5.46	2.39	5.88	5.10
K_2O	1.52	1.51	1.45	1.43	1.79	1.79	1.57	0.58	1.57	1.50
TiO_2	3.25	3.27	3.73	3.74	3.17	3.26	3.47	2.99	3.46	3.46
P_2O_5	0.59	0.58	0.49	0.49	0.65	0.67	0.54	0.31	0.56	0.57
total	100.12	100.13	100.81	100.79	101.83	101.36	101.12	101.10	101.14	99.89

Appendix 2 (cont'd)

	H62-47	H62-48	H62-49	H62-50	H62-51	H62-52	H62-53	H62-54A	H62-55	H62-56
Rock	AB	AB	AB	ha	ha	ha	ha	ha	ha	ha
Depth	67	62	50	44	34	25	23	17	16	11
SiO_2	45.31	45.55	45.53	44.75	44.21	44.94	44.31	45.46	45.21	47.80
Al_2O_3	15.04	14.62	13.98	16.75	16.68	16.17	16.08	17.32	17.30	18.15
FeO	14.07	14.07	14.08	13.76	13.81	14.38	13.78	13.29	12.96	11.77
MgO	7.89	8.35	9.58	5.13	5.23	6.02	5.95	05.10	5.21	4.52
CaO	10.48	10.64	11.28	9.51	9.61	10.30	10.10	09.19	9.14	7.86
Na_2O	3.74	3.42	3.02	4.74	4.36	4.48	4.13	05.10	4.75	5.43
K_2O	0.99	0.87	0.74	1.42	1.35	1.35	1.37	1.55	1.54	1.79
TiO_2	3.18	3.03	2.85	4.03	4.02	3.55	3.50	04.20	4.14	3.05
P_2O_5	0.38	0.35	0.30	0.43	0.45	0.42	0.48	00.43	0.45	0.64
total	101.09	100.91	101.38	100.52	99.72	101.63	99.71	101.64	100.71	101.02

	H62-57	H65-1	H65-2	H65-3	H65-4	H65-5	H65-6	H65-7	H65-8	H62-8*
Rock	ha	ha	mu	mu	AB	ha	ha	ha	AB	AB
Depth	5	171	158	149	145	132	115	71	64	64
SiO_2	46.15	47.20	51.58	51.30	44.37	49.84	49.35	51.53	45.14	44.83
Al_2O_3	16.54	16.54	17.01	17.14	14.42	18.35	18.07	17.80	15.17	14.78
FeO	15.27	13.10	10.38	10.85	14.56	10.80	11.38	10.70	14.39	14.45
MgO	5.98	4.88	3.09	3.30	8.49	3.59	3.89	2.71	8.32	8.29
CaO	9.97	8.59	6.58	6.89	11.55	7.52	7.80	6.58	10.77	10.61
Na_2O	3.99	4.37	5.93	6.00	3.26	6.37	5.74	5.28	3.02	3.27
K_2O	0.85	1.23	2.10	1.98	0.86	1.90	1.76	2.13	0.91	0.95
TiO_2	3.44	4.09	2.53	2.62	3.20	2.82	3.03	2.15	3.00	2.96
P_2O_5	0.26	0.41	0.12	0.95	0.23	0.74	0.71	1.13	0.28	0.34
total	102.44	100.41	100.30	100.02	100.94	101.92	101.72	100.01	101.00	100.48

Appendix 2 (cont'd)

	H65-9	H65-9*	H65-10	H65-10*	H65-11	H65-11*	H65-12	H65-13	H65-14	H65-14*
Rock	AB	AB	AB	AB	AB	AB	AB	Ank	Ank	Ank
Depth	62	62	60	60	58	58	56	3	2	2
SiO_2	45.12	45.05	45.24	44.93	44.97	44.85	45.28	44.10	44.18	44.24
Al_2O_3	15.20	15.15	14.96	14.88	14.91	14.67	15.03	13.86	13.73	13.64
FeO	14.26	14.37	14.21	14.14	14.26	14.28	14.62	14.09	14.06	13.82
MgO	8.27	8.27	8.22	8.19	8.54	8.74	9.00	9.67	9.53	9.99
CaO	10.80	10.79	10.77	10.75	10.77	10.81	10.33	12.60	12.32	12.46
Na_2O	2.82	2.88	3.12	3.29	2.77	2.89	1.97	1.97	2.36	2.57
K_2O	0.86	0.86	0.91	0.93	0.82	0.83	0.72	0.75	0.85	0.87
TiO_2	3.01	3.02	3.00	3.00	2.89	2.89	3.00	2.91	2.87	2.91
P_2O_5	0.30	0.30	0.30	0.34	0.32	0.32	0.32	0.28	0.30	0.28
total	100.64	100.70	100.73	100.45	100.24	100.28	100.28	100.23	100.20	100.78

	H83-1	H83-2	H83-3	H83-3*	H83-4	H83-5	H83-6	H83-7	H83-8	H83-9
Rock	AB	AB	AB	AB	AB	AB	ha	AB	ha	ha
Depth	240	223	216	216	209	198	166	145	134	80
SiO_2	47.76	46.74	47.96	47.12	47.79	46.18	49.88	45.62	50.23	45.08
Al_2O_3	14.70	14.84	15.74	15.37	13.26	15.85	17.61	15.16	18.17	17.59
FeO	14.02	14.62	13.68	13.74	11.74	12.91	11.86	14.00	10.84	11.78
MgO	5.26	4.33	6.90	6.80	9.86	6.57	4.33	8.59	3.77	4.33
CaO	10.78	9.97	11.67	11.67	10.21	10.96	7.39	11.44	7.63	8.29
Na_2O	3.23	3.19	2.92	3.01	3.26	3.72	4.90	3.21	6.21	6.00
K_2O	0.87	1.22	0.85	0.84	1.26	1.00	1.60	0.83	1.86	1.62
TiO_2	3.96	4.76	3.49	3.45	2.82	3.45	3.15	3.17	2.91	3.55
P_2O_5	0.23	0.29	0.15	0.20	0.54	0.31	0.66	0.31	0.76	0.56
total	100.81	99.96	103.36	102.19	100.74	100.94	101.38	102.34	102.39	101.81

Appendix 2 (cont'd)

	H85-1	H85-2	H85-3	H85-4	H85-5	H85-6	H85-7	H85-8	H85-9	H85-10
Rock	AB	ha	ha	ha	ha	ha	AB	AB	AB	AB
Depth	300	299	294	271	267	264	261	255	252	249
SiO_2	46.22	47.15	47.13	47.77	47.40	47.45	46.67	46.64	46.42	46.88
Al_2O_3	14.07	16.31	16.49	15.10	14.98	15.17	15.20	15.33	15.20	15.22
FeO	15.64	12.98	13.08	13.65	13.90	14.21	14.46	13.96	13.87	14.07
MgO	4.93	4.10	4.00	4.21	4.29	4.28	5.98	6.00	6.10	6.25
CaO	10.13	10.34	9.91	9.44	9.61	9.28	11.48	11.68	11.65	11.67
Na_2O	3.29	4.04	3.97	3.93	3.89	3.86	3.35	3.07	3.12	3.00
K_2O	0.98	1.07	1.07	1.50	1.43	1.41	0.89	0.86	0.85	0.85
TiO_2	5.22	4.18	4.17	4.42	4.61	4.56	3.74	3.66	3.60	3.63
P_2O_5	0.22	0.28	0.32	0.43	0.37	0.41	0.20	0.19	0.21	0.18
total	100.70	100.44	100.14	100.45	100.47	100.65	101.98	101.41	101.03	101.75

	H85-11	H85-12	H85-13	H85-14	H85-15	H85-16	H85-17	H85-18	H85-19	H85-21
Rock	ha	AB	AB	AB	AB	ha	ha	ha	ha	AB
Depth	245	240	229	228	198	189	179	175	174	164
SiO_2	46.20	46.69	46.33	46.42	46.42	49.93	47.49	51.06	51.37	44.99
Al_2O_3	16.33	15.33	15.02	15.91	16.00	17.82	16.86	16.94	17.13	14.84
FeO	14.55	14.24	14.76	13.11	12.55	11.98	13.59	11.18	11.11	14.47
MgO	4.99	5.14	4.55	6.26	7.75	4.29	4.84	3.34	3.37	8.41
CaO	8.98	10.51	10.56	11.09	11.57	7.44	8.66	7.04	7.17	11.50
Na_2O	3.90	3.63	3.58	3.42	2.82	4.92	4.42	5.68	5.55	1.79
K_2O	1.46	1.16	1.10	0.99	0.83	1.54	1.21	1.95	1.94	0.74
TiO_2	4.51	4.17	4.49	3.54	3.11	3.16	4.17	2.73	2.74	3.23
P_2O_5	0.44	0.28	0.24	0.27	0.27	0.61	0.37	1.11	1.05	0.31
total	101.37	101.15	100.62	101.01	101.32	101.70	101.61	101.03	101.43	100.28

Appendix 2 (cont'd)

	H85-22	H85-23	H85-24	H85-25	H85-26	H85-27	H85-28	H85-29	H85-30	H85-31
Rock	AB	AB	mu	mu	mu	mu	mu	mu	mu	mu
Depth	161	157	155	154	148	147	146	144	142	110
SiO_2	45.27	45.47	51.87	51.88	50.46	50.35	50.10	50.05	50.30	53.54
Al_2O_3	16.07	16.28	18.33	18.35	18.16	18.16	17.97	18.35	18.52	18.07
FeO	14.34	14.26	9.74	9.82	10.90	10.77	10.70	10.76	10.87	9.71
MgO	5.80	5.73	2.87	2.90	3.50	3.49	3.46	3.53	3.28	2.62
CaO	10.88	10.81	6.66	6.64	7.42	7.45	7.46	7.37	7.35	5.85
Na_2O	3.96	3.79	5.34	5.37	6.27	6.13	6.37	6.60	5.04	5.96
K_2O	0.99	0.97	2.19	2.20	1.94	1.93	1.97	1.94	1.84	2.39
TiO_2	3.70	3.67	2.27	2.27	2.76	2.78	2.78	2.76	2.85	1.99
P_2O_5	0.28	0.28	1.07	1.07	0.80	0.80	0.82	0.81	0.77	1.01
total	101.29	101.26	100.34	100.48	102.22	101.86	101.63	102.18	100.83	101.13

	H85-32	H85-33	H99-1	H99-2	H99-3	H99-4	H99-5	H99-6	H99-8	H99-10
Rock	ha	ha	ha	ha	ha	AB	mu	mu	mu	ha
Depth	88	82	312	288	240	226	204	189	131	70
SiO_2	48.99	46.75	48.96	48.73	48.52	45.12	51.95	50.29	50.59	47.18
Al_2O_3	17.10	17.40	17.66	17.96	17.02	14.54	18.26	18.25	17.63	18.33
FeO	11.89	12.99	11.84	11.75	12.51	13.99	9.57	10.69	10.69	11.28
MgO	4.08	4.49	4.24	4.48	4.46	8.69	2.90	3.55	3.31	3.92
CaO	8.32	8.89	8.11	7.66	7.85	11.25	6.67	7.01	7.07	8.61
Na_2O	5.73	4.21	4.42	4.48	3.96	3.24	6.08	6.22	6.18	6.23
K_2O	1.56	1.36	1.68	1.65	1.37	0.80	2.20	1.94	1.98	1.79
TiO_2	3.54	4.13	3.17	3.24	3.64	3.21	2.25	2.80	2.75	3.16
P_2O_5	0.64	0.42	0.64	0.63	0.53	0.36	1.02	0.86	0.94	0.69
total	101.55	100.64	100.72	100.60	99.88	101.20	100.90	101.61	101.13	101.18

[1] Major element analyses determined at Woods Hole Oceanographic Institute
[2] Th: tholeiite, AB: alkalic basalt, ha: hawaiite, mu: mugearite, ank: ankaramite
[3] Meters beneath ground surface
* Duplicate analyses